Technische Universität Braunschweig

Collaborative Research Centre SFB 578

From gene to product –

Development of biotechnological processes by integrating genetic and engineering methods

Edited by Dieter Jahn, Rainer Krull and Christoph Wittmann

Funded by the Deutsche Forschungsgemeinschaft

Cuvillier-Verlag

Collaborative Research Centre SFB 578
Technische Universität Braunschweig

Editors
Prof. Dr. Dieter Jahn
Prof. Dr. Rainer Krull
Prof. Dr. Christoph Wittmann

Cuvillier-Verlag
Göttingen, Deutschland

Herausgeber
Prof. Dr. Dieter Jahn, Prof. Dr. Rainer Krull, Prof. Dr. Christoph Wittmann
Sonderforschungsbereich SFB 578
Development of biotechnological processes by integrating genetic and engineering methods
- From gene to product -
TU Braunschweig
Gaußstraße 17, 38106 Braunschweig
www.sfb578.de

Bibliographische Informationen der Deutschen Nationalbibliothek
Die Deutsche Nationalbibliothek verzeichnet diese Publikation in der Deutschen Nationalbibliographie; detaillierte bibliographische Daten sind im Internet über *http://dnb.d-nb.de* abrufbar.
1. Aufl. – Göttingen: Cuvillier, 2012

Nonnenstieg 8, 37075 Göttingen
Telefon: 0551-54724-0
Telefax: 0551-54724-21
www.cuvillier.de

1. Auflage, 2012
Gedruckt auf säurefreiem Papier

ISBN 978-3-95404-135-0

Collaborative Research Centre 578

Concluding reports

Third funding period 2008 - 2012

Development of biotechnological processes by integrating genetic and engineering methods

- From gene to product -

Integration gen- und verfahrenstechnischer Methoden zur Entwicklung biotechnologischer Prozesse - Vom Gen zum Produkt -

Funded by the Deutsche Forschungsgemeinschaft

TECHNISCHE UNIVERSITÄT **CAROLO-WILHELMINA** zu Braunschweig

Content

			Page
Preface			*1*
Project area A: Molecular biology of product formation			*9*
A1	Production of recombinant glycosyltransferases using *Bacillus megaterium* and *Aspergillus niger*	D. Jahn / P. Dersch	*11*
A6	Systems biology of chaperones for the production of antibodies with *Bacillus megaterium*	S. Dübel / M. Hust	*29*
A7	Structural biology of glycosyltransferases for the optimization of biotechnical processes	D. W. Heinz / J. Seibel	*43*
Project area B: Systems biotechnology of product formation			*61*
B3	Influence of the environome on the morphology and productivity of filamentous fungi (*Aspergillus niger*)	R. Krull / D. C. Hempel	*63*
B4	Systems biology of product and pellet formation by *Aspergillus niger*	D. Jahn / B. Nörtemann / L. Jänsch	*81*
B7	Micromechanic properties of filamentous fungi	A. Kwade / I. Kampen	*99*
B8	Holistic bioprocess engineering of antibody fragment secreting *Bacillus megaterium*	E. Franco-Lara	*119*
B9	Integrative databases, bioinformatics tools, analysis and modeling for systems biology with *B. megaterium* and *A. niger*	R. Münch / D. Schomburg	*131*
B10	Systems biotechnology of glycosyltransferase production with *Bacillus megaterium*	D. Jahn / E. Franco-Lara	*147*
B11	Metabolic network dynamics for production of recombinant glycosyltransferases	C. Wittmann	*165*
Project area C: Process technique			*179*
C2	Continuous chromatographic separation of ternary and pseudo-ternary mixtures	A. Seidel-Morgenstern	*181*
C6	Nanoanalytics for protein production processes	M. Schilling / F. Ludwig	*195*
C7	Protein purification with functionalized magnetic nanoparticles	G. Garnweitner / M. Schilling	*211*
Project area D: Application technique			*227*
D1	Drug delivery systems for the controlled release of proteins	H. Menzel / H. Bunjes	*229*
D2	Microchips for protein analytics and diagnostics	S. Büttgenbach / S. Dübel	*247*

Preface

General goals, strategic approach and used methodology

Since 2001, the Collaborative Research Centre SFB 578, "*Development of biotechnological processes by integrating genetic and engineering methods - From gene to product*", has been dedicated to designing and implementing novel concepts and strategies for integrated strain and process development for industrial bio-production. Right from the beginning, research in SFB 578 employed a truly global and integrated approach for the optimization of production hosts and the corresponding production processes, a strategy which has meanwhile been coined systems biotechnology. For systems-wide strain and process engineering, disciplines from engineering and life sciences were integrated and combined to provide high-value biotechnological products in biologically active form at high titer and yield. This new integrated approach is now changing the way we design and develop industrial processes in biotechnology.

Strategically, we focused our research for the whole funding period on two model organisms and two product classes to achieve close cooperation and a synergistic interaction. The filamentous fungus *Aspergillus niger* and the bacterial host *Bacillus megaterium* were selected as work horses of SFB 578. Both microorganisms have a high industrial relevance. In addition, they share a substantial potential to produce and secrete recombinant proteins, thus promising that the obtained data and strategies will have broad relevance. Across different, closely interlinked research areas, high-value recombinant proteins were selected as relevant model products. These included biocatalysts involved in sugar metabolization and pharma proteins of the antibody and bone morphogenic factors. Among the products to be investigated, glycosyltransferases are receiving increasing interest for supplying pre-biotic sugars, which have been gaining more and more applications in the food and pharma sector. Moreover, recombinant antibodies for therapy and diagnostics represent the largest and most rapidly growing fraction of pharma proteins.

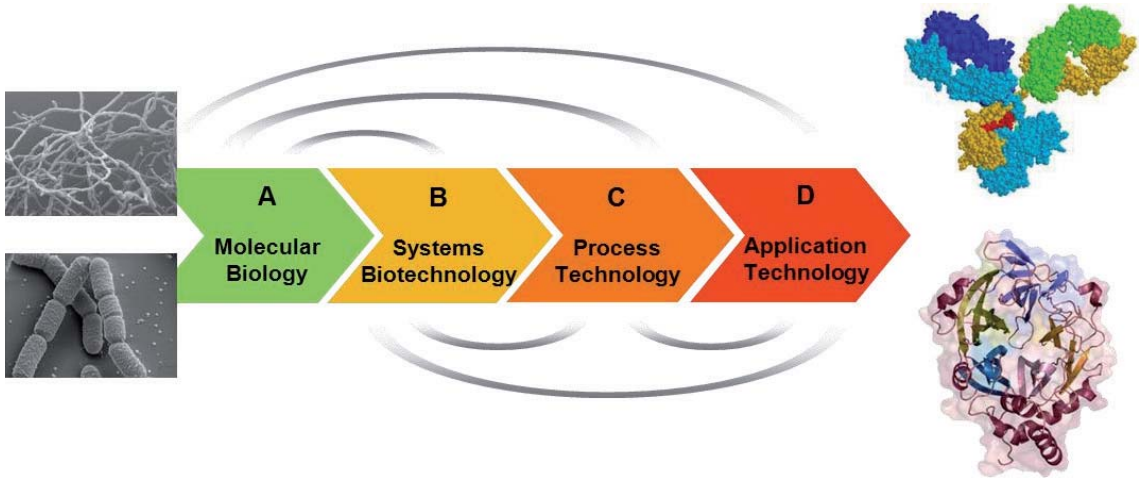

Development of Biotechnological Processes by Integrating Genetic and Engineering Methods - From Gene to Product.

Practically, results from quantitative physiology were complemented by information from an efficient omics technology platform, providing insights into metabolome, fluxome, transcriptome and proteome of the production host of interest. Bioinformatics was used to intelligently store, interpret and combine obtained results with literature data. Thus, a solid basis for regulatory and metabolic network modeling was generated. Model-based understanding of the underlying biological systems was used for prediction concerning the optimization of the overall production process, verified via experimentation and used for interative model optimization. Finally, obtained recombinant products were further developed with the goal of applying them in drug delivery, and for lab-on-the-chip and other diagnostic tools.

Research program and partners

The central overall aim of this SFB 578 was a holistic approach to analyze, quantify and model the biological and biochemical engineering processes for optimal product formation, purification and application of biotechnological cultivations. At the beginning of this last funding period, a solid basis of know-how from the last two funding periods of this SFB already exited. Genetically engineered production strains of both model systems, *A. niger* and *B. megaterium,* have been created for intra- and extracellular formation of antibodies and glycosyltransferases. A broad methodological repertoire for their analyses has been developed. Secreted target proteins can now be localized *in vivo* and characterized *in vitro* through biochemical and structural analysis. Modelling approaches have been established, and elaborated bioinformatics tools are at hand, the latter based on complete genome databases. The basis for quantitative determination of the transcriptome, proteome, metabolome and fluxome to characterize and optimize cultivation processes under different environmental conditions has been successfully established. Further, purification strategies for the target proteins as well as innovative strategies for their applications were developed. Thus, substantially all required methodological tools have been created. The central goal in the last funding period was to bring these pieces together, including data integration for the overall process and its optimization.

To attain the goals of SFB, a close and intensive collaboration between all partners was required. In this SFB, the core competence lay in the disciplines of Biochemical Engineering, Microbiology and Biotechnology of the Technische Universität Braunschweig. Furthermore, Institutes of Microtechnology, Technical Chemistry, Electrical and Pharmaceutical Engineering were involved. They were supported by working groups of the Helmholtz Centre for Infection Research (HZI), Braunschweig, and the Institute for Process Engineering, Otto-von-Guericke-University, Magdeburg. Overall, the SFB was divided into four project areas in 16 subprojects with 23 project managers and 27 PhD-students.

Project area A: Molecular biology of product formation

SFB 578 provided the basis for the establishment of a complete tool kit for recombinant intra- and extracellular protein production using *A. niger* and *B. megaterium*. To date, over 20 different expression vectors encoding various inducible systematically optimized

promoters, including those for phage RNA polymerases, in combination with perfect ribosome binding, are available for *B. megaterium*. Currently, 1.3 g per liter GFP model protein can be produced intracellularly. Various added affinity tags allow for fast affinity chromatographic purification. Furthermore, different high efficient signal sequences for protein export via the Sec system into the growth medium were added to the system, yielding up to 0.2 g per liter single chain antibody fragment and more than 1 g per liter of levansucrase exported into the growth medium. The system is commercialized with MoBiTec GmbH, Göttingen. High yield protein production was the result of a systematic systems biotechnological optimization strategy for both, *A. niger* and *B. megaterium*. This included transcriptome, proteome, metabolome and fluxome measurements and their bioinformatics based integration. Gene regulatory and metabolic modeling yielded predictions for process optimization. In this context, the genome of two *B. megaterium* strains was solved and annotated.

Furthermore, multiple sugar metabolizing enzymes were produced recombinantly by using *A. niger* and *B. megaterium,* and subsequently employed for the synthesis of high value sugars. The crystal structure of one central enzyme of interest was elucidated and used for designing substrate specificity changes.

Project area B: Systems biotechnology of product formation

Results obtained with *A. niger* and *B. megaterium* played a central role towards understanding the investigated cellular and bio-process systems and providing strategies for their tailor-made improvement. In this line, different projects were aimed at obtaining quantitative, highly informative data sets from genomics, transcriptomics, proteomics, metabolomics and fluxomics. In pioneering concepts, these should be integrated into the process environment on the level of shear stress, cellular morphology and fluid dynamics to provide the most comprehensive picture of the process to be optimized. Targets on the genetic as well as on the process level should be identified to be implemented by research groups from all other areas of SFB 578.

Project area C: Process technique

The downstream purification process of isolation, concentration and analytical detection of the target proteins from culture media was a further focus of this SFB 578. For protein produced by the recombinant *A. niger* and *B. megaterium* strains, a purification chromatographic method and functionalized nanoparticles were used and studied in depth. The purification of antibodies was performed by continuous chromatographic separation according to the simulated moving bed technology. The main task was the development of the theoretical basis for a simulation of the entire separation process. In addition, stabilized water-compatible functionalized iron oxide nanoparticles with covalently bound functionalization were developed for protein purification, prepared and applied for the purification of recombinantly produced antibody fragments and glycosyltransferases. The realization of a molecular functionalization was targeted, without large macromolecules such as polymers to shield the magnetic cores and reduce the active surface of the

system. Furthermore, the development of magnetic separation methods with homogenous gradient fields and thus homogenous adsorbance force was investigated to achieve highly specific separation and filtration of the protein-carrying magnetic particles. For a production-related on-line analysis of enzymes and antibodies, magnetorelaxometry was developed on the basis of a differential fluxgate setup. For the targeted bio-products sophisticated processing routines are available that allow generation of important, time-resolved analyses of data of high quality for complex systems biotechnological approaches.

Project area D: Application technique

The focus of this project area within this SFB 578 was the use of antibodies for different applications. The first example was the development of hydrogel drug delivery systems as attractive approaches for the administration of therapeutically relevant biomacromolecules such as antibodies. The main focus here was the engineering and delivery of the drug dosage precisely at the desired target and indicated dosing rate. The investigations were mainly based on biocompatible hydroxyethyl starch, modified with a crosslinkable side group (e.g. hydroxyethyl methacrylate). Single chain antibody fragment variables were incorporated in this hydrogel system. The application demonstrated a detailed realization of a drug delivery system involving synthesis characterization of the hydrogel and mobility of encapsulated substances, but also of *in vivo* studies and correlation of *in vitro* to *in vivo* release rates. Finally, this method allowed individual animals to be monitored over an extended period of time. This led to improved quality of data and, additionally, a much lower number of animals was required than that used in conventional animal studies.

The second application dealt with the development of a medical analysis laboratory in chip size (lab-on-chip) for point-of-care diagnostics as a tool for a much quicker diagnosis and the start of therapy. C-reactive protein (CRP) has been identified as a superior indicator for inflammatory diseases, but its analysis requires sophisticated and time consuming detection, which are not suitable for point-of-care applications. Consequently, CRP was used as a model molecule for the development towards a point-of-care analysis system. The developed method now provides different possibilities for application, since the detector antibody can be changed to measure a large variety of clinically relevant parameters. Furthermore, the microfluidic setup will allow facile parallelization in future setups to determine a larger number of samples or parameters simultaneously.

***Model system* Aspergillus niger**

During the years of funding, SFB 578 provided a range of innovations on systems biotechnology of *A. niger*. These included efficient genetics enabled the creation of production mutants for recombinant enzymes such as glucoamylase and fructofuranosidase, but also of GFP-based reporter strains. For systems-wide analysis of *A. niger*, a rich portfolio of experimental and computational methods was established. This allowed detailed investigations of gene expression and protein production and secretion, intracellular metabolite

levels or pathway fluxes. This was complemented by different methods to analyze morphological forms of *A. niger* under various process conditions. Coupled to automated image analyses, these studies allowed a precise estimation of morphological shape via newly derived dimensionless morphology numbers. All these tools are now available to the academic and industrial research. These could be exploited to fine tune morphology for bio-production. Novel approaches used the addition of inorganic micro particles to the culture to control the morphology of the fungus. Integrated with model-based medium design and process development, production of recombinant enzymes can be highly efficient. Exemplified for fructofuranosidase, SFB 578 created a production process for this valuable enzyme, which was more than tenfold more efficient than any other process reported to data, and perfectly underlining the great potential of systems biotechnology based strain and process engineering.

***Model system* Bacillus megaterium**

Multiple expression plasmids for the extra- and intracellular recombinant production of proteins in *B. megaterium* were constructed and commercialized in cooperation with the local company MoBiTec. These plasmids enable the gram per liter production of desired proteins, as well as their purification via affinity tags. In recent years, this productions system has been frequently employed world-wide by industrial companies. The described system was successfully developed to high productivity during bioreactor growth. For this purpose, novel integrated systems biology approaches were established. A genome database (MegaBac) and various novel bioinformatics tools for microarray and proteome data interpretation (JProGo, JVirGel), signal peptide prediction (PrediSi) and codon adaptation index calculation (JCat) were established and are now frequently utilized. Novel strategies for the inexpensive synthesis of high value sugar using recombinant enzymes and their variants were developed. The catalytic enzyme mechanisms that are involved were elucidated at the molecular level. Furthermore, high yield bioreactor based production processes for recombinant antibodies were implemented and optimized using the outlined systems biotechnological approach.

SFB key numbers

The last funding period of the SFB (2008 - 2012) involved 15 subprojects with 23 projects managers in four project areas. Additionally, in 2009 the SFB started the transfer project "*Recombinant production of new phytases by* Bacillus megaterium" (Jahn) together with the BASF AG, Ludwigshafen, developing methods, know-how and major new aspects of the SFB expertise into industrial application and ongoing fundamental research.

Within the projects of this SFB during the last funding period, approximately 125 publications were published in high-reputation journals (e.g. *Appl. Microbiol. Biotechnol., Appl. Environ. Microbiol., Bioinformatics, Biotechnol,. Biotechnol. Bioeng., ChemBioChem, Chem. Eng. Sci., Eng. Life Sci., J. Appl. Phys., J. Biotechnol., J. Chromatography, Lab on a Chip, Microb. Cell Fact., Nature Biotechnol.*). Additionally, 23 PhD-theses, which had been financed by SFB, were successfully completed, several more will follow soon. A vital

exchange with external research groups was established. Within the eleven-year-term of our SFB approximately 120 seminars with invited speakers from academia and industry were conducted. For the 100th colloquium anniversary in June 2010, two volumes of the renowned series of *Advances in Biochemical Engineering/Biotechnology* were published, nicely integrating the SFB research into the overall developments in systems biotechnology. Different status conferences with the entire SFB 578 community focused on project cooperations and on strengthening interdisciplinary efforts. Additionally, a vital and continuous exchange with direct team work between the PhD students developed that supported work in the different projects and areas. On the occasion of the completion of the SFB 578 the editorial board of the *Journal of Biotechnology* has invited the SFB 578 to provide a special issue dedicated to the "*Development of Biotechnological Processes by Integrating Genetic and Engineering Methods – From Gene to Product*", containing more than 20 scientific contributions of both research papers and review articles.

The SFB 578 initiated successful technology transfer from basic research to industrial application. The constructed vector systems for *Bacillus megaterium* were commercialized by the company MoBiTec GmbH, Göttingen. This expression system is now successfully used in several laboratories worldwide in academia as well as in industry for production and secretion of different kinds of recombinant proteins. A further industrial cooperation was established with Bayer Pharma AG, Bergkamen, on the development of indicators for the quality of filamentous seed cultures. Here, elaborated instrumental and experimental methods to evaluate spore quality are now established for routine use in industrial cultivation.

SFB 578 caused major structural changes at the Technische Universität Braunschweig

During the granting periods of SFB 578, a strong systems biology unit with a broad spectrum of Omics technologies in combination with various bioinformatics groups was established at our university. Due to its success, the university decided to focus its research strategy on systems biology in the Life Sciences. Consequently, the Faculties of Life Science and Mechanical Engineering adapted their hiring strategies to this research focus. Multiple professorships were filled with experts for example in proteomics (W2, Riedel), metabolomics and bioinformatics (W3, Schomburg), and fluxomics and bio-engineering (W3, Wittmann). In the next stage, the Technische Universität Braunschweig, in close cooperation with the local Helmholtz Center for Infection Research, is building a novel "*Braunschweig Integrated Center fo Systems Biology*" (BRICS) on the university campus close to the biocenter for 25 million Euro. The construction process will start in early 2013 and the center will host various groups (Wittmann, Jahn, Schomburg) involved in this SFB 578. The systems biology expertise of BRICS also constitutes a major component of the recently granted SFB-TR 51 ("*Ecology, Physiology and Molecular Biology of the Roseobacter Clade*"), the currently renewed DFG-Forschergruppe FOR 1220 ("*PROTRAIN - Prosthetic Groups: Transport and Insertion*") and the BMBF consortium UroGenOmics ("*Strain Specific Systems Biology of Uropathogenic Bacteria"*). Another

important offspring from SFB 578 is the new Pharma process engineering center (PVC) which will be built for 29 million Euro also on the campus of the university. Both centers, BRICS and PVC, are part of the local Translational Alliance in Niedersachsen (TRAIN), a joint venture of the Technische Universität Braunschweig, the local Helmholtz Center (HZI), the Medical School Hannover, the Leibniz Universität Hannover and the University of Veterinary Medicine Hannover.

Braunschweig, June 2012

Dieter Jahn (Speaker)
Christoph Wittmann (Deputy speaker)
Rainer Krull (Managing director)

Project area A: Molecular biology of product formation

Project-No.	Topic	Disciplines and field of work	Project manager, institution
A1	Production of recombinant glycosyltransferases using *Bacillus megaterium* and *Aspergillus niger*	Microbiology, Bacterial and fungal genetics, Recombinant protein production and secretion	D. Jahn and P. Dersch, Institute of Microbiology, TU BS
A6	Systems biology of chaperones for the production of antibodies with *Bacillus megaterium*	Biotechnology	S. Dübel and M. Hust, Department of Biotechnology, TU BS
A7	Structural biology of glycosyltransferases for the optimization of biotechnical processes	Organic chemistry, Structural biology, Biocatalysis, Glycobiology	D. Heinz, Department of Structural Biology HZI BS / J. Seibel, Institute of Organic Chemistry, University of Würzburg

3.1 General information on the completed project A1

3.1.1 Topic

***Production of recombinant glycosyltransferases using* Bacillus megaterium *and* Aspergillus niger**

3.1.2 Disciplines and field of work

Microbiology, bacterial and fungal genetics, recombinant protein production and secretion

3.1.3 Project manager

Prof. Dr. Dieter Jahn
(b.: 01.08.1959)
TU Braunschweig, Institute of Microbiology
Spielmannstraße 7
38106 Braunschweig
Phone: 0531/391-5801
Fax: 0531/391-5854
E-Mail: d.jahn@tu-bs.de

Prof. Dr. Petra Dersch
(b.: 22.05.1965)

Phone: 0531/6181-5700
Fax: 0531/6181-5709
E-Mail: p.dersch@tu-bs.de

3.2 Development of the subproject

3.2.1 Report

3.2.1.1 Current knowledge at the last application and initial question

The production, secretion and purification of recombinant proteins in eukaryotic as well as prokaryotic systems are major topics of industrial biotechnology. During the first application period (2001-2004) microbial expression systems for the filamentous nonpathogenic fungi *Aspergillus niger* as well for the Gram positive bacterium *Bacillus megaterium* were established. It has an efficient secretion systems which makes it applied in industrial production processes. The proteins produced by this organism possess posttranslational modifications. *B. megaterium* is nonpathogenic and able to metabolize numerous carbon sources. Further, it shows a great potential for protein secretion and, important for recombinant protein production, has a stable plasmid replication system. The major goal of the first funding period of SFB 578, the establishment of a system for the secretion of the recombinant proteins, which included different homologous and heterologous glycosyltransferases into the growth medium was reached.

During the second funding period (2004-2008) the expression systems for both organisms were further enhanced. This included the integration of different small affinity tags for purification of the intra- as well the extracellular produced recombinant proteins. Proteins could now be easily purified and used for different activity tests. Here, new glycosyltransferases recombinantly overproduced in *A. niger* and *B. megaterium* were characterized, respectively [*Homann et al., 2009, Zuccaro et al., 2008*]. New promoters and leader peptides were identified by secretome analysis for both hosts. These promoters could be induced using simple cheap carbon sources. For *B. megaterium* a further

promoter system based on a two vector system was developed. With this phage dependent system it was possible to produce recombinant proteins intracellularly.

Now, within the third application (2008-2012) the questions and requirements were phrased:

1. Enhancing and optimizing existing promoter systems using different strategies
2. Characterization of new promoter systems
3. Construction of strains coproducing rare tRNA
4. Sequencing and annotation of the genome of *B. megaterium* DSM319
5. Adaptation of the vector systems to the cloning host *E. coli* for cloning toxic genes
6. Establishment of microarray experiments

3.2.1.2 Results and applied methods

3.2.1.2.1 *Aspergillus niger*

Characterization of inducible promoters of *Aspergillus niger*

Suitable inducible promoter systems have fundamental impact for recombinant protein production using microorganisms. These systems are characterized by stringent control, cheap inducers and high inducibility. During the last application period different inducible promoters for recombinant protein production using *A. niger* were identified and further characterized using the green fluorescent protein Gfp as a model. These promoters include the sucrose inducible β-fructofuranosidase promoter P_{suc1} [*Zuccharo et al., 2008*], the promoter of the *phiA* gene which is induced by osmotic stress and the inducible gluco-amylase promoter P_{glaA} [*Ganzlin and Rinas, 2008*].

In this application period the promoter P_{suc1} was further characterized. For this, the strain ARAn1 (P_{suc1}-*gfp*) was constructed while the strain AB1.13 was used as a control. After verifying stringent inducibility of P_{suc1}, the influence of different carbon sources (maltose, xylose, fructose, sucrose, glucose) in minimal medium on growth and Gfp production was tested. Highest cell dry weight (CDW) was achieved if growing with maltose or sucrose (around 15 g L^{-1}). Further, the different carbon sources showed an influence on recombinant Gfp production (**Fig. 1**). While all strains showed fluorescent properties the production of Gfp with specific antibodies was only detected if grown with sucrose or with a mixture of sucrose and glucose. The specific fluorescence detected could be identified as background signal. These results clearly indicated that glucose did not cause catabolite repression.

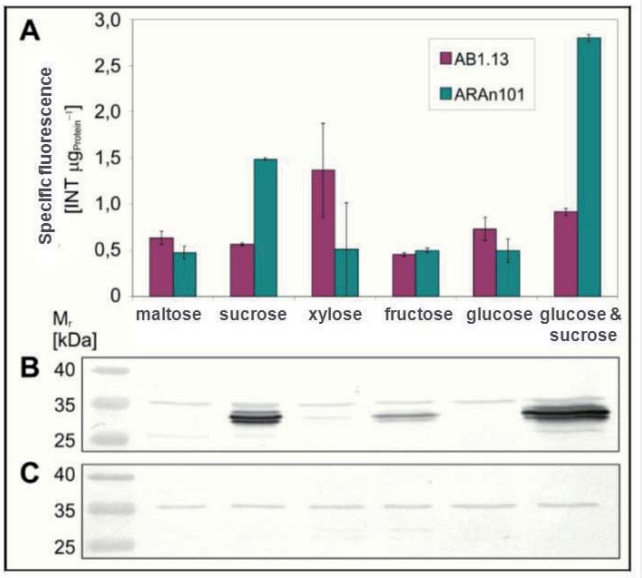

Fig. 1: Recombinant Gfp production in A. niger *under control of the β-fructofuranosidase promoter* P_{suc1}. A. niger *strains ARAn101 (*P_{suc1}-gfp*) and AB1.13 (control) were cultivated in minimal medium with the indicated sugars as carbon source (100 mM).* ***A:*** *Gfp fluorescence related to the total protein amount of the cell extract [INT* $\mu g_{protein}^{-1}$*].* ***B:*** *Immunoblot of the cell extract of* A. niger *ARAn101 using antibodies directed against Gfp.* ***C:*** *Immunoblot of the cell extract of* A. niger *AB1.13 using antibodies directed against Gfp.*

Next, different growth conditions were tested. Besides variations in the speed level of the shaker, the pH-values and the cultivation conditions were optimized. Based on these results, the standard conditions for all further cultivations were set to 140 rpm, to a pH of 5.5 and to a cultivation temperature of 37°C.

To get a more accurate view on the induction behavior of the *gfp* expression under control of the sucrose inducible promoter P_{suc1} *A. niger* strain ARAn101 (P_{suc1}-*gfp*) was cultivated using standard conditions for 48 h with glucose as single carbon source. The *gfp* expression was induced with sucrose. Microscopic pictures were taken before and 0.5, 1, 2, 3, 4 and 24 h after induction. The pictures show an increase of Gfp from 0 to 4 hours. Before induction with sucrose the promoter is repressed. After induction the Gfp production occurred in the whole complex mycelium structure of *A. niger.* Obviously, the Gfp amount did not differ much between 4 and 24 hours (**Fig. 2**) indicating that the highest Gfp amount is achieved between 4 and 24 hours. In summary, the new identified sucrose inducible P_{suc1} promoter is well suited for a controlled production of recombinant proteins in the eukaryotic *A. niger.*

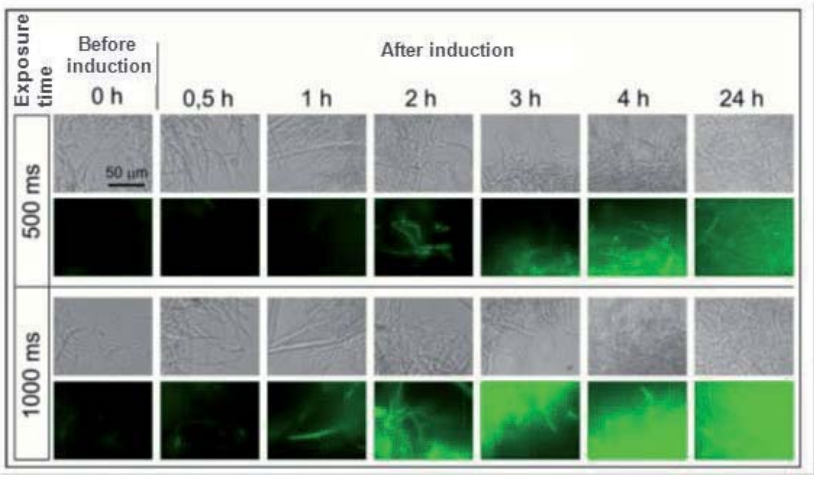

Fig. 2: Microscopic images of A. niger *strain ARAn101 (*P_{suc1}-gfp*) before (0 h) and after addi-tion (0.5, 1, 2, 3, 4 and 24 h) of sucrose. The cells were cultivated for 48 h under standard conditions with glucose as carbon source until the* gfp*-expression was induced with sucrose. The Gfp formation after induction is visible. Top row: bridge field; bottom row: fluorescence; exposure time: 500 and 1000 ms.*

Development of vector systems for production and purification of recombinant intracellular proteins in *A. niger*

To use *A. niger* for the product formation - recombinant fructosyltransferases and antibodies - suitable shuttle vector systems were necessary. These systems can vary in their promoters and in their tag sequences. Here, all vectors are equipped with the same multiple cloning site to allow for parallel cloning into all vectors. Further, they code for a His_6- or a StrepII-tag either N- or C-terminally located in the fusion protein. Also products without tags can be produced. The expression of a target gene can be controlled by the sucrose inducible P_{suc1} or by the constitutive P_{pkiA} (**Fig. 3**). The cloning steps in the host *E. coli* are sustained by *colE1-ori* and the ampicillin resistance gene of the vectors. The selection for positive clones in *A. niger* occurred via a uridine-auxotrophy and a complementary gene encoding the orotidine-5'-phosphate-decarboxylase (PyrG) located on the vector.

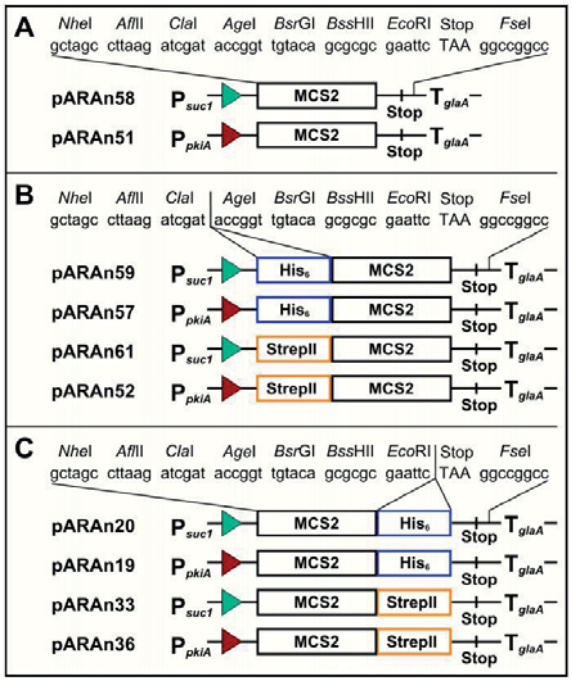

Fig. 3: New vector systems for the production of recombinant proteins in A. niger. *For the recombinant protein production two different promoters could be used: the sucrose inducible one P_{suc1} or the constitutive one P_{pkiA}. The restriction sides introduced into the multiple cloning site (MCS2) are indicated followed by the terminator sequence of* glaA *(T_{glaA}). (A) Basis vectors containing one of the two different promoters. (B) Vectors for the production of N-terminal tagged target proteins. (C) Vectors for the production of C-terminal tagged target proteins.*

The functionality of the new vector system was confirmed by testing established model proteins. For the recombinant over-production and purification Gfp and a hydrolase from *Thermobifida fusca* (Tfh) were tested (**Fig. 4**). Gfp was further successfully purified via His_6- as well as StrepII-tag (data not shown). The integration of the plasmids into the genome of the *A. niger* strain was found to be different for each plasmid. It varied between one and up to six integration events. But no correlation between integration events and concentration of the recombinant protein could be observed.

A. niger strains	Immuno blot with antibodies against His$_6$-*Tag*	StrepII-*Tag*	GFP	Activity GFP	Activity TFH
ARAn101 (P_{suc1}-*gfp*)	-	-		+	-
ARAn801 (P_{pkiA}-*gfp*)	-	-		+	-
ARAn55 (P_{suc1}-His$_6$-*gfp*)		-		+	-
ARAn27 (P_{pkiA}-His$_6$-*tfh*)		-	-	-	+
ARAn17 (P_{suc1}-*gfp*-His$_6$)		-		+	-
ARAn18 (P_{pkiA}-*gfp*-His$_6$)		-		+	-
ARAn15 (P_{pkiA}-*tfh*-His$_6$)		-	-	-	+
ARAn56 (P_{suc1}-StrepII-*gfp*)	-			+	-
ARAn50 (P_{pkiA}-StrepII-*gfp*)	-		n. v.	+	-
ARAn47 (P_{suc1}-*gfp*-StrepII)	-			+	-
ARAn60 (P_{pkiA}-*gfp*-StrepII)	-			+	-
ARAn63 (P_{pkiA}-*tfh*-StrepII)	-		-	-	+

Fig. 4: Summary of the immunoblots and the activity of recombinant proteins produced by the new vector systems. The recombinant A. niger *strains were cultivated for 48 h with sucrose (P_{suc1}) or glucose (P_{pkiA}) as carbon source. The intracellulare fractions of proteins were analyzed using specific antibodies against Gfp, His$_6$- and StrepII-tag, respectively. The activity was measured in the cell free extract.*

Vector system for secretion of recombinant proteins in *Aspergillus niger*

The export of recombinant proteins into the growth medium facilitates their purification. If the target protein is lacking an own secretion signal sequence, fusion to a homologous protein naturally secreted in *A. niger*can be used for the export into the growth medium. It was shown before that the fusion of an antibody or of Gfp to the glucoamylase of *A. niger* facilitate their secretion [*Gordon et al., 2000; Ward et al., 2004*].

If sucrose is added the β-fructofuranosidase (Suc1) of *A. niger* is strongly secreted. To use this feature for biotechnological applications a vector system encoding the P_{suc1} followed by 5' parts of the *suc1* gene was constructed. These fragments can be fused N-terminally as a leader sequence to the target protein to enable the fusion product to be secreted (**Fig. 5**).

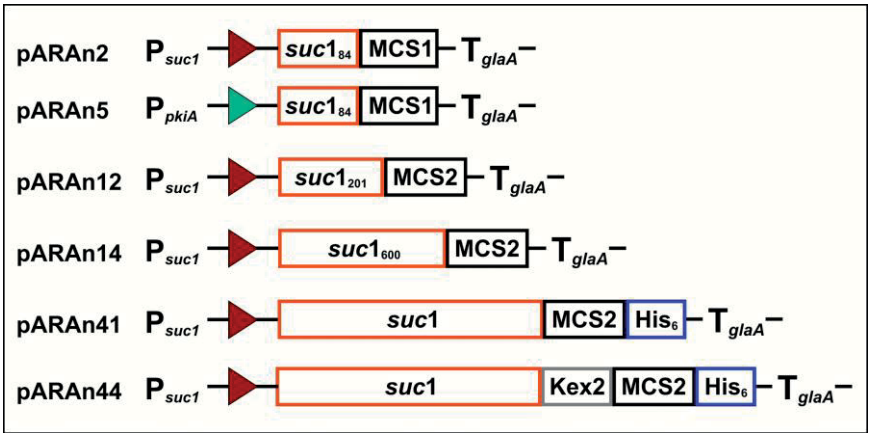

Fig. 5: Vectors for the secretion of recombinant fusion proteins mediated by N-terminal parts of different length of the Suc1. The fragments encoding different parts of Suc1 (84 bp, 201 bp, 600 bp, complete suc1*) are shown. Expression is under control of the promoters P_{suc1} or P_{pkiA}. MCS1 or MCS2 can be used for cloning genes of interest. The coding sequence for the His$_6$-tag could be used for purification of secreted proteins. Kex2: protease cleavage site. T_{glaA}: Terminator of* glaA.

The new constructs were tested using *gfp* and *tfh* as heterologous model genes. Different strains and growth conditions were tested. Although the intracellular recombinant production of these fusion proteins was successful (2 mg g_{CDW}^{-1}), so far neither Gfp nor

Tfh could be detected in the growth medium. In a cooperation project 3 g L^{-1} of vector encoded Suc1 were secreted into the growth medium [*Driouch et al., 2010*].

3.2.1.2.2 *Bacillus megaterium*

Optimizing the xylose inducible promoter system

The quantity of an intracellular protein formed by a microbial cell is mainly determined by several closely interconnected steps: transcription, mRNA stability and translation. Consequently, promoter sequences, mRNA signatures and ribosome binding site of the plasmid-borne P_{xylA}-controlled protein production system were target for directed genetic optimization approaches.

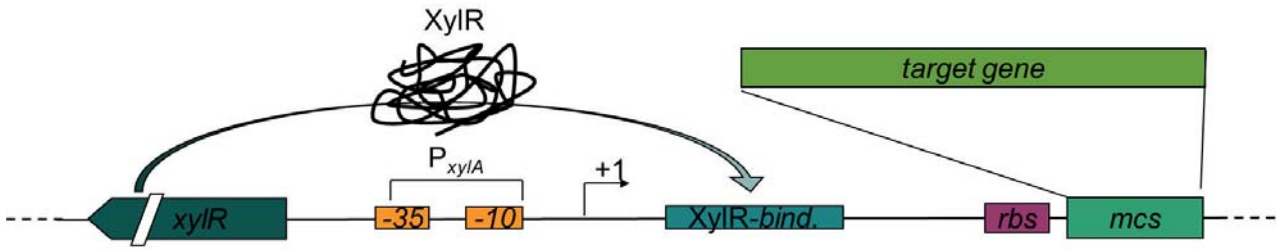

Fig. 6: Key features of the xylose-inducible promoter system of B. megaterium. *Ele-ments for regulated gene expression are the xylose-inducible promoter (P_{xylA}), the gene encoding the xylose repressor (XylR) and its DNA binding region (XylR-bind.). Addition of xylose leads to conformational changes of XylR resulting in its release from the binding re-gion and to transcription initiation. The multiple cloning site (*mcs*) for introduction of target genes is located downstream of the ribosome binding site (*rbs*).*

For increasing the amount of recombinant proteins produced in *B. megaterium* the xylose inducible promoter system (**Fig. 6**), which is used in all subprojects working with *B. megaterium* (A6, B8, B9, B10, B11, TF2) and meanwhile commercialized by the MoBiTec GmbH in Göttingen (Germany) was systematically optimized. Based on the vector pSTOP1622 [*Biedendieck et al., 2007b*] the -35 (-35^{+}) and the -10 (-10^{+}) region, the ribomsome binding site (rbs^{+}) as well as the 5' untranslated region including the XylR-binding site (utr^{+}) were individually changed to their optimal predicted sequences [*deHaseth et al., 1998; Malten et al., 2005*]. The production of our model Gfp, which can be easily detected via its fluorescent as well as in SDS PAGE gels, showed that all modification resulted in an increase compared to the native system of up to 11-fold (from 7.0 to 76.5 mg g_{CDW}^{-1}).

Further increasing protein yields were expected by a combination of the genetic elements enhancing target protein production. Therefore, a series of plasmids were constructed combining two or more of the optimized DNA elements. Again, the efficiency was proven using Gfp as model protein. First of all, the translation enhancing rbs^{+} was individually combined with the other optimized DNA sequences. Intracellular Gfp amounts showed

increase up to 62.9 mg g_{CDW}^{-1} (-10$^+$/*rbs*$^+$) and 75.0 mg g_{CDW}^{-1} (*utr*$^+$/*rbs*$^+$), respectively (**Fig. 7**). This increase was found to be significantly higher than an addition of the protein amounts produced by the strains carrying the plasmids with only a single modification (-10$^+$: 20.4 mg g_{CDW}^{-1}, *utr*$^+$: 26.6 mg g_{CDW}^{-1}, *rbs*$^+$: 14.8 mg g_{CDW}^{-1}). Obviously, a higher amount and a more stable mRNA represents an improved target for the ribosome which is attracted by the perfect *rbs*$^+$. In contrast, a third combination (-35$^+$/*rbs*$^+$) did not show this strong effect (80.6 mg g_{CDW}^{-1}) compared to cells employing only the optimized -35$^+$ (76.5 mg g_{CDW}^{-1}). Analogously, the combination of both consensus promoter elements (-35$^+$/-10$^+$) with the optimized *rbs*$^+$ did not yield the desired improvement (16.7 mg g_{CDW}^{-1}). In fact, a strong decrease in Gfp production was detected, when compared with cells employing -10$^+$/*rbs*$^+$ or -35$^+$/*rbs*$^+$ which encode a less conserved promoter. Further, under non-inducing conditions detectable amounts of Gfp were found within *B. megaterium* cells harboring the full consensus promoter (-35$^+$/-10$^+$/rbs$^+$) or optimized -35$^+$, *utr*$^+$ as well as *rbs*$^+$ indicating a loss of promoter controllability. Since the binding sequence for the XylR repressor is located just a few base pairs downstream of P_{xylA}, it seems to be probable, that the major repressing effect of XylR is caused by competitive binding to the promoter region as it was shown for the *lac* repressor of *E. coli* by Schlax et al. (1995).

Finally, in a collaboration project with B10 1.25 g Gfp per liter were recombinantly produced using the new optimized promoter system.

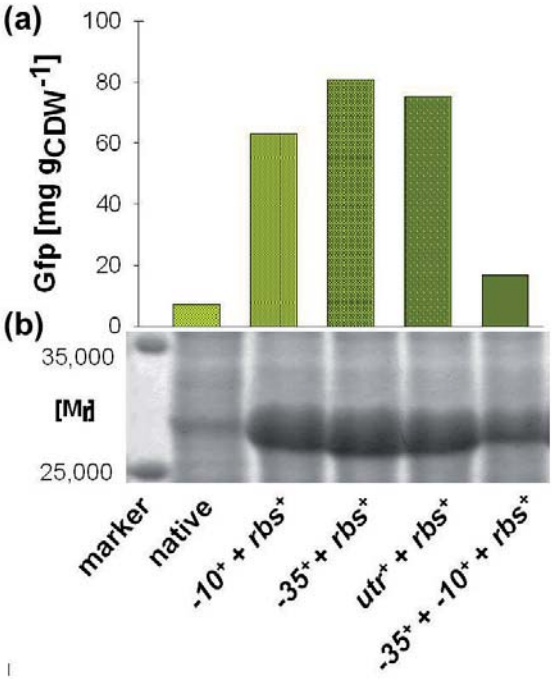

Fig. 7: Combinatory effect of optimized genetic elements. B. megaterium *cells were transformed with plasmids harboring* gfp *under control of the indicated optimized* P_{xylA}. *The nature of combined genetically optimized elements (-35*$^+$ *or -10*$^+$ *region, modified 5' utr*$^+$ *and optimized rbs*$^+$*) are outlined. Cells carrying the native expression vector were used as reference. (a) Gfp amounts per cell dry weight (CDW) were calculated using fluorescence measurement of whole cells. (b) Soluble proteins of cells taken from indicated cultures were separated on SDS PAGE gels and visualized by Coomassie Brilliant Blue staining.*

Recombinant protein export driven by novel signal peptides from *B. megaterium*

The signal peptides (SPs) for protein export via the Sec-pathway of *B. megaterium* were computationally predicted using the "PrediSi" software (http://www.predisi.de/) [*Hiller et al., 2004*]. During this process, all open reading frames (*orf*s) of the *B. megaterium* genome summarized in the database "MegaBac" (http://www.megabac.tu-bs.de/) were analyzed for

signal peptide-coding sequences. Most of the predicted signal peptides showed high similarity with the consensus sequence for type I signal peptides described for *B. subtilis* by Tjalsma et al. (*2000; 2004*). The three leader sequences originated from the proteins Vpr (serine protease), NprM (neutral protease) and YngK (hypothetical protein) showing a high signal peptide probability were chosen to be examined. These proteins were found to be efficiently secreted by *B. megaterium* before [*Wang et al., 2006*]. The signal peptide of YocH (hypothetical protein) was chosen from the list of predicted *B. megaterium* SPs due to its high similarity to the consensus signal peptide structure for Sec-dependent protein secretion described by Tjalsma et al. (*2000; 2004*). In addition to these native *B. megaterium* SPs, an artificial signal peptide (SP_{Asp}) was constructed. Two SPs already used in recombinant protein production and secretion in *B. megaterium* served as positive control. The signal peptides of penicillin amidase (SP_{Pac}) [*Panbangred et al., 2000; Yang et al., 2006*] and of the esterase LipA (SP_{LipA}) [*Ruiz et al., 2002*] were already tested to facilitate the secretion of a heterologous levansucrase LevΔ773 in *B. megaterium* [*Biedendieck et al., 2007a*].

Generally, *B. megaterium* cells employing the high performance (hp)-production system showed increased amounts of Tfh secreted into the growth medium compared to cells employing the corresponding basic expression systems (**Fig. 8**). Despite the use of the new hp-plamids and the testing of several novel signal peptides only a 16 % higher secretion of Tfh was detected (SP_{YocH} in hp-plasmid 7.7 mg L^{-1}) compared to the one mediated by SP_{LipA} used in combination with the non-optimized expression system (6.6 mg L^{-1}). These results clearly show limitations of the Sec-dependent secretion process since the intracellular protein production was drastically increased up to 18-fold (4.6 vs. 82.5 mg g_{CDW}^{-1}) as shown for Gfp production when employing the hp-production system.

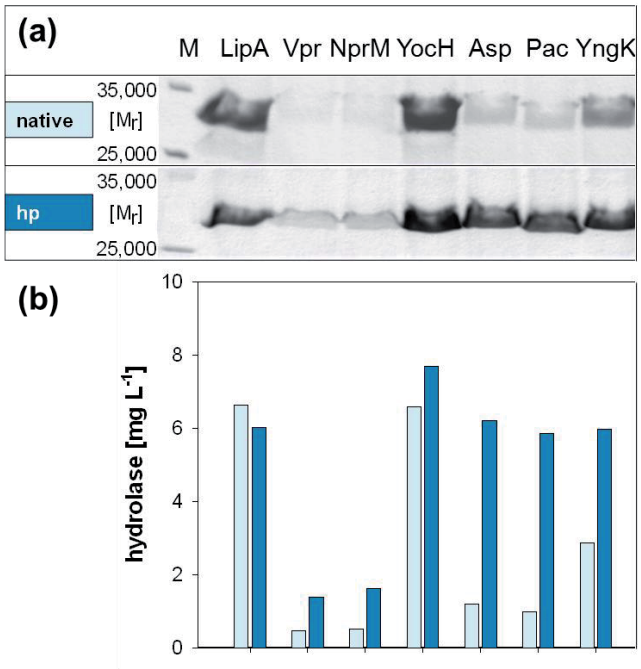

Fig. 8: Secretion of recombinant Tfh facilitated by new signal pepti-des. B. megaterium *cells were trans-formed with either the native or the optimized plasmids encoding the in-dicated SPs and Tfh-His_6. (a) Pro-teins from cell-free supernatant from indicated cultures were precipitated, separated by SDS PAGE gels and visualized by Coomassie Brilliant Blue staining. (b) Hydrolase activities were determined photometrically by an enzyme assay.*

Construction of the Ecoco system for the save cloning of *Bacillus megaterium* vectors in *Escherichia coli*

The productivity of xylose-dependent gene expression system was improved. Now, a broad plasmid toolbox enables the high yield production of both intra- and extracellular recombinant proteins. However sometimes cloning of target genes under control of P_{xylA} causes problems in *E. coli*. Major complications within the cloning host *E. coli* are supposed to base on the non-controllable transcription initiation at the P_{xylA} promoter although it is tightly controlled in *B. megaterium*. This leads to a constant basal production of the target protein in *E. coli*. If production of proteins has negative or even cytotoxic effect on *E. coli* growth this leads to negative selective pressure. Thus, even though the recombinant production is feasible in *B. megaterium* cloning already fails in *E. coli*.
To circumvent these problems a plasmid hybrid was constructed containing the approved optimized *Bacillus* elements in combination with *E. coli* elements of the pBAC / *oriV* [*Wild et al., 2002*]. These enable the maintenance of a plasmid in single-copy state intended for the use during the cloning procedure in *E. coli*. By reduction of the plasmid copy number the level of basal expression initiated at P_{xylA} and thus the amount of protein with potentially toxic effect on *E. coli* can be limited to a level enabling the growth of positive transformants. Short time before plasmid preparation, the inducible origin of replication (*oriV*) can be activated by TrfA and consequently the plasmid DNA yields increase.

The basis for the *Bacillus* parts of the new plasmid system named “Ecoco” (***E**. coli* **co**py **co**ntrol) was the optimized new xylose-dependent vector system without using the *E. coli* elements of this system. Instead, for maintenance in single-copy state in *E. coli* the *oriS* origin of replication, the *repE* gene and *parABC* partition determinants of the pBAC / *oriV* were inserted into the existing plasmid. Further, *oriV* for maintenance in multi-copy state and the β-lactamase gene for resistance-based selection in *E. coli* were used. At the end of this cloning procedure, a plasmid named pBmEcoco was generated (**Fig. 9**). It combined the highly functional elements for controlled protein production in *B. megaterium* with the elements for single-copy number maintenance. Further, it harbors the *oriV*, which is responsible for the amplification of pBmEcoco to multi-copy state in *E. coli*. The gene encoding the TrfA up-mutant necessary to induce the replication at *oriV* was placed on a second, auxiliary plasmid under control of the pBAD promoter. This additional vector is just necessary during the cloning and amplification phase of pBmEcoco in *E. coli*. *E. coli* cells harboring this new plasmid pEc-*trfA* produce TrfA if arabinose is present and induce the multi-copy state of the pBmEcoco plasmid.

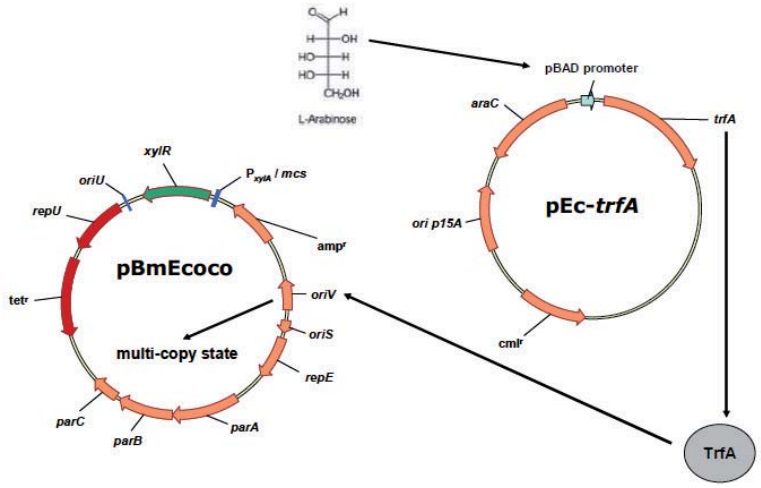

Fig. 9: Functionality of the Ecoco system in E. coli*. Both plasmids of the Ecoco system are present in* E. coli *during cloning and amplification. Functional elements in* E. coli *are colored in orange. The auxiliary plasmid pEc-*trfA *carries the* trfA *gene under control of the pBAD promoter (light blue). Further, the repressor of pBAD AraC is encoded divergently to* trfA*. Addition of arabinose leads to conformational changes of AraC and transcription of* trfA*. Plasmid maintenance is controlled by* ori p15A and *cml*^{r}*. Next to the elements functional in* Bacilli *(*P_{xylA}-mcs, xylR, oriU/repU, tet^r*) pBmEcoco contains genetic information for maintenance in single-copy state (*parABC, repE, oriS*) in* E. coli*. amp*^{r} *enables selection of plasmid containing cells. Induction of* oriV *by TrfA leads to the upregulation of the pBmEcoco copy number to multi-copy state.*

The functionality of the system was successfully proven using the model *gfp* (**Fig. 10**).

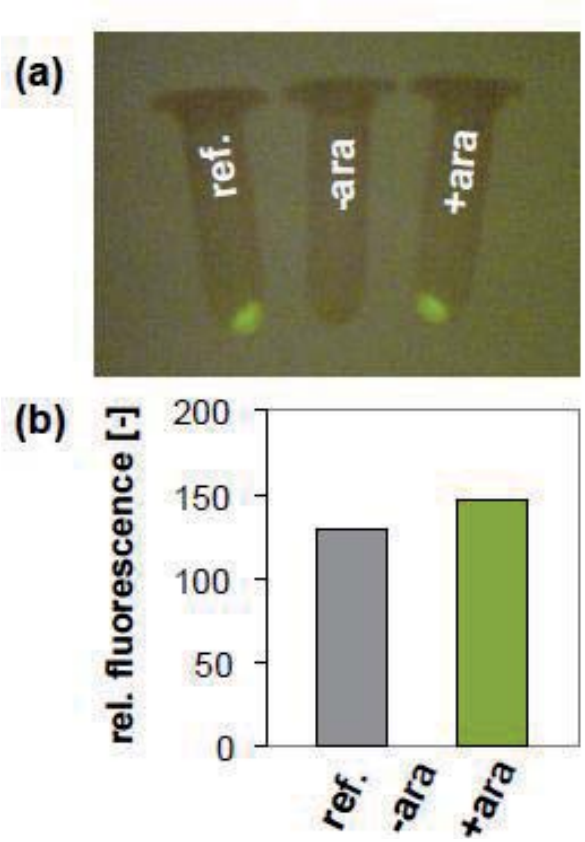

Fig. 10: Relative quantification of the plasmid copy number by Gfp fluorescence analysis. E. coli *cells were transformed either with the* gfp *carrying Ecoco system (pBmEcoco-gfp and pEc-trfA) or the gfp harboring optimized xylose-inducible system. Bacteria were cultivated aerobically. Either 0.02 % arabinose was (+ara) or was not added (-ara) to the media. Samples were taken approximately 8 hours after inoculation.* ***(a)*** *3 x 10*^{9} *cells were sedimented in reaction tubes by centrifugation and Gfp fluorescence was vi-sualized.* ***(b)*** *Relative Gfp fluorescence was measured in whole bacterial cells*.

Phage polymerase dependent gene expression

Only a limited number of phage RNA dependent polymerases (RNAP) are currently commercially available for *in vitro* and *in vivo* purposes. They differ in their modes of promoter recognition [*Jorgensen et al., 1991*], transcription initiation [*Chakraborty et al., 1977*] and enzymatic activity within the host cell, which may not always be compatible with the envisaged RNA or protein production process [*Stump and Hall, 1993*].

Here, new *in vivo* protein production systems for *B. megaterium* were developed employing T7, K1E and SP6 RNAP for target gene transcription. For this purpose, the corresponding RNAP genes *t7p, k1ep* and *sp6p* were cloned into a plasmid controlled by the homologous *B. megaterium* derived xylose-inducible promoter P_{xylA} (pT7-RNAP, pK1E-RNAP, pSP6-RNAP). A second compatible, stable maintained vector was equipped with the commonly used T7-, K1E- or SP6-promoters and appropriate terminators (**Fig. 11**).

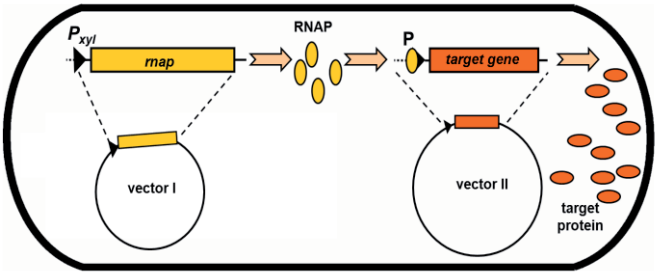

Fig. 11: B. megaterium *cell carrying two vectors. Both are functional in* B. megaterium*. Vector I is carrying the gene (yellow) encoding a RNA polymerase (RNAP-yellow) of the bacteriophage T7, K1E and SP6, respectively. Vector II is equiped with the corresponding phage RNAP dependent promoter regulating the expression of the target gene (orange).*

To evaluate the intracellular protein production achieved by this phage RNAP driven systems, the model gene *gfp* was cloned under control of the T7, K1E and SP6 phage RNAP promoters. *B. megaterium* cells were co-transformed with each of the phage RNAP encoding vectors individually and the corresponding plasmid which carried *gfp* under control of the phage RNAP promoters. Finally, Gfp production experiments were carried out with these two vector-harboring *B. megaterium* cells. Besides the natural combinations of T7 RNAP / P_{t7}, K1E RNAP / P_{k1e} and SP6 RNAP / P_{sp6}, the combination of K1E RNAP with the P_{sp6} was tested. It was shown that T7, SP6 as well as K1E RNAP were applicable for protein production in *B. megaterium* (**Fig. 12A**). Up to 60 mg of Gfp per g_{CDW} could be produced intracellularly while a Tfh activity of more than 6000 U L^{-1} was detected in the cell free growth medium with the phage RNAP dependent systems.

Besides the possibility of the production of high amounts of recombinant proteins, there is no basal activity of the promoter neither in *B. megaterium* nor in *E. coli*. This enables the system to even cope with toxic genes or genes encoding antibody fragments which provides problems if cloning in *E. coli* [*Jordan et al., 2007*].

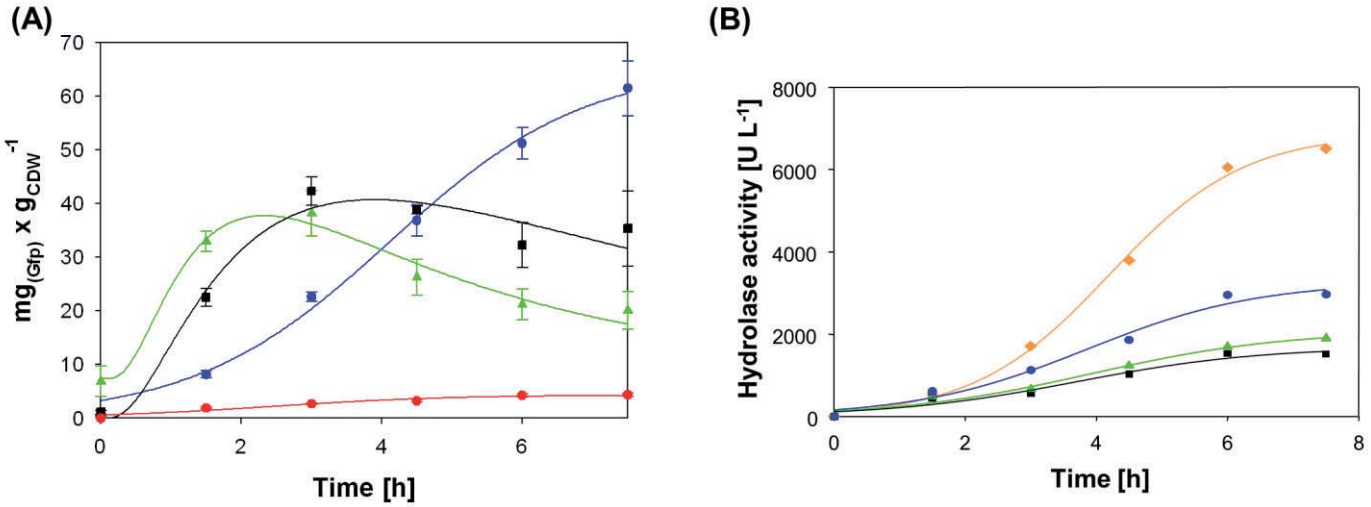

Fig. 12: Recombinant protein production in B. megaterium. B. megaterium *cells were cotransformed with two plasmids. One was carrying the gene encoding the phage RNAP, the second was harboring the* gfp *(A) or the* tfh *(B) gene under control of a phage RNAP promoter. Cultivated* B. megaterium *cells harbored*
- T7 RNAP and the T7 promoter
- K1E RNAP and the K1E promoter
- K1E RNAP and the SP6 promoter
- SP6 RNAP and the SP6 promoter
- optimized xylose system

Codon usage and recombinant gene expression in *Bacillus megaterium*

Besides this transcriptional activity achieved by optimizing the promoters for recombinant gene expression, the codon composition of a target gene for heterologous expression strongly influences the translational efficiency and thus the overall protein yield. This is caused by the degenerate nature of the genetic code meaning that more than 90 % of all amino acids are encoded by more than one codon. Most of the time synonymous codons just differ by one nucleotide in the third codon position. Synonymous codons are not used with equal frequencies and their usage varies between organisms and even between genes within the same genome. Experimental studies in *E. coli* revealed that mRNAs containing high portions of rare codons are less efficiently translated than mRNAs composed of preferred codons [*Sorensen et al., 1989*]. To overcome this problem the construction of codon optimized artificial genes is possible but still expensive. In *E. coli* such phenomenon is solved by overproducing rare tRNAs to enhance production of the corresponding protein.

The preference for distinct codons within a genome can be correlated with the abundance of tRNA species [*Ikemura, 1981*]. Based on the genome sequence of *B. megaterium* the relative abundance of codons encoding a particular amino acid within all predicted open reading frames was calculated. Especially, codons for the amino acids alanine (GCC), arginine (CGG, AGG), glycine (GGG), leucine (CUC), serine (UCC) and threonine (ACC) turned out to be of rare use. To evaluate the effect of these codons on the synthesis of recombinant proteins, a codon test system was established where four identical

consecutive codons of interest were 5‘-end fused to *gfp.* Fusion of rare codons compared to best codons coding for a specific amino acid clearly reduced the Gfp amounts.
Next, the effect of coproducing specific tRNAs rare in *B. megaterium* was analyzed. The tRNAs were encoded on the same vector under control of their native promoters as the *gfp* fusions. Coproduction of corresponding rare tRNAs (alanine, arginine) clearly increased

3.2.1.3 References to other works and collaborations in the SFB

The results of the here presented subproject A1 provided the basis for all subprojects in this SFB 578 working on recombinant protein production and secretion. The collaboration with A6 (Dübel/Hust) focused on the production and mainly secretion of antibody fragments with *A. niger* and *B. megaterium*. In subproject A7 (Heinz/Seibel) the glycosyltransferases SacB (*B. megaterium*) and Suc1 (*A. niger*) were characterized, modified and crystallized. Different publications arose from this collaboration within this funding period [*Beine et al, 2009; Strube et al., 2011; Zuccaro et al., 2008*]. In Driouch et al. (*2010, 2011*) the results of the exchange between subprojects B3 (Krull/Hempel) and A1 (Jahn/Dersch) are summarized. The collaboration with subprojects B8 (Franco-Lara) and B10 (Jahn/Franco-Lara) concentrated on the upscale of shaking flasks cultivations of *B. megaterium* done in A1. Here, first microarray analysis of the secretion process of antibodies (B8, Franco-Lara) and production of Gfp (B10, Jahn/Franco-Lara) were performed. Collaboration resulted in Stammen et al. (*2010*). Active exchange of ideas occurred with subproject B11 (Wittmann). Some results of the collaboration with the subproject B9 (Münch/Schomburg) are summarized in Eppinger et al. (*2011*) and Bunk et al. (*2010*). Further, the first design of custom-made Agilent-microarrays was performed with B9 (Münch/Schomburg).

3.2.1.4 Comparison with research outside the SFB

During the last few years raising interest in the production host *B. megaterium* was clearly visible in the three genome sequences now available. The genome of the host strain DSM319 used within this SFB578 was sequenced in parallel with that of the strain QM B1551 ending in a joint publication [*Eppinger et al., 2011*]. Now, a third *B. megaterium* genome sequence is available [*Liu et al., 2011*]. This group is focusing on the vitamin C where *B. megaterium* acts as is the companion strain for *Ketogulonigenium vulgare*.
The group of Prof. Friedhelm Meinhardt in Münster (Germany) is also working on secretion of recombinant proteins in *B. megaterium*. As these works supplemented the work within the SFB578 and vice versa an intensive exchange of knowledge occurred during the last years [*Biedendieck et al., 2011; Borgmeier et al., 2011*].

As the vector systems for *B. megaterium* constructed within this subproject A1 are commercialized by the small company MoBiTec GmbH, Göttingen (Germany) the expression system is successfully used in several laboratories worldwide in academia and industry for production and secretion of different kinds of recombinant proteins (personal communication).

The development of new expression systems is of great important for the production as well as secretion followed by purification of recombinant proteins. As was shown for *B. megaterium* the new expression systems will find users within research and industry. As an eukaryotic microorganism *A. niger* is mainly suitable in the production and secretion of eukaryotic proteins as they need special glycosylation patterns.

3.2.1.5 Literature

Beine, R.; Valente, A.R.; Biedendieck, R.; Jahn, D.; Seibel, J. (2009) Directed optimization of biocatalytic transglycosylation processes by the integration of genetic algorithms and fermentative approaches into a kinetic model. *Process Biochem.* 44, 1103-1114

Biedendieck, R.; Beine, R.; Gamer, M.; Jordan, E.; Buchholz, K.; Seibel, J.; Dijkhuizen, L.; Malten, M.; Jahn, D. (2007a) Export, purification and activities of affinity tagged *Lactobacillus reuteri* levansucrase produced by *Bacillus megaterium*. *Appl. Microbiol. Biotechnol* 74, 1062-1073

Biedendieck, R.; Yang, Y.; Deckwer, W.D.; Malten, M.; Jahn, D. (2007b) Plasmid system for the intracellular production and purification of affinity-tagged proteins in *Bacillus megaterium*. *Biotechnol. Bioeng.* 96, 525-537

Bunk, B.; Biedendieck, R.; Jahn, D.; Vary, P.S. (2010) *Bacillus megaterium* and other Bacilli: Industrial Applications. In Flickinger M. C. (Ed.) Encyclopedia of Industrial Biotechnology: Bioprocess, Bioseparation, and Cell Technology. Volume 1 pp 429-443. John Wiley & Sons. Inc., Hoboken, NJ

deHaseth, P. L.; Zupancic, M. L.; Record, M. T., Jr. (1998) RNA polymerase promoter interactions: the comings and goings of RNA polymerase. *J. Bacteriol.* 180, 3019-3025

Ganzlin, M.; Rinas, U. (2008) In-depth analysis of the *Aspergillus niger* glucoamylase (*glaA*) promoter performance using high-throughput screening and controlled bioreactor cultivation techniques. *J. Biotechnol.* 135, 266-271

Gordon, C.L.; Archer, D.B.; Jeenes, D.J.; Doonan, J.H.; Wells, B.; Trinci, A.P.; Robson, G.D. (2000) A glucoamylase: GFP gene fusion to study protein secretion by individual hyphae of *Aspergillus niger*. *J. Microbiol. Methods* 42, 39-48

Hiller, K.; Grote, A.; Scheer, M.; Münch, R.; Jahn, D. (2004) PrediSi: prediction of signal peptides and their cleavage positions. *Nucleic. Acids Res.* 32(Web Server issue), W375-379

Homann, A.; Biedendieck, R.; Götze, S.; Jahn, D.; Seibel, J. (2007) Switching from polymers to oligosaccharides - Functional modification of a novel levansucrase from *Bacillus megaterium* by site-directed mutagenesis. *Biochem. J.* 407, 189-198

Ikemura, T. (1981) Correlation between the abundance of *Escherichia coli* transfer RNAs and the occurrence of the respective codons in its protein genes: a proposal for a synonymous codon choice that is optimal for the *E. coli* translational system. *J. Mol. Biol.* 151, 389-409

Liu, L.; Li, Y.; Zhang. J.; Zou, W.; Zhou, Z.; Liu, J.; Li, X.; Wang, L.; Chen, J. (2011) Complete genome sequence of the industrial strain *Bacillus megaterium* WSH-002. *J. Bacteriol*. 193:6389-6390

Malten, M.; Hollmann, R.; Deckwer, W.D.; Jahn, D. (2005) Production and secretion of recombinant *Leuconostoc mesenteroides* dextransucrase DsrS in *Bacillus megaterium*. *Biotechnol. Bioeng.* 89, 206-218

Schlax, P.J.; Capp, M.W.; Record, M.T., Jr. (1995) Inhibition of transcription initiation by *lac* repressor. *J. Mol. Biol.* 245, 331-350

Sorensen, M.A.; Kurland, C.G.; Pedersen, S. (1989) Codon usage determines translation rate in *Escherichia coli*. *J. Mol. Biol.* 207, 365-377

Strube, C.P.; Homann, A.; Gamer, M.; Jahn, D., Seibel, J.; Heinz, D.W. (2011) Polysaccharide synthesis of the levansucrase SACB from *Bacillus megaterium* is controlled by distinct surface motifs. *J. Biol. Chem.* 286, 17593-17600

Tjalsma, H.; Bolhuis, A.; Jongbloed, J.D.; Bron, S.; van Dijl, J.M. (2000) Signal peptide-dependent protein transport in *Bacillus subtilis*: a genome-based survey of the secretome. *Microbiol. Mol. Biol. Rev.* 64, 515-547

Tjalsma, H.; Antelmann, H.; Jongbloed, J.D.; et al. (2004) Proteomics of protein secretion by *Bacillus subtilis*: separating the "secrets" of the secretome. *Microbiol. Mol. Biol. Rev.* 68, 207-233

Wang, W.; Hollmann, R.; Deckwer, W.D. (2006) Comparative proteomic analysis of high cell density cultivations with two recombinant *Bacillus megaterium* strains for the production of a heterologous dextransucrase. *Proteome Sci.* 4, 19

Ward, M.: Lin, C.; Victoria, D.C.; Fox, B.P.; Fox, J.A.; Wong, D.L.; et al. (2004) Characterization of humanized antibodies secreted by *Aspergillus niger*. *Appl. Environ. Microbiol.* 70, 2567-2576

Wild, J.; Hradecna, Z.; Szybalski, W. (2002) Conditionally amplifiable BACs: switching from single-copy to high-copy vectors and genomic clones. *Genome Res.* 12, 1434-1444

Yang, Y.; Biedendieck, R.; Wang, W.; Gamer, M.; Malten, M.; Jahn, D., Deckwer, W.D. (2006) High yield recombinant penicillin G amidase production and export into the growth medium using *Bacillus megaterium*. *Microb. Cell Fact.* 5, 36

Zuccaro, A.; Götze, S.; Kneip, S.; Dersch, P.; Seibel, J. (2008) Tailor-made fructooligosaccharides by a combination of substrate and genetic engineering. *Chembiochem.* 9, 143-149

3.2.2 Project relevant own publications

a) Works that have appeared in publications of a scientific quality assurance at the time of application or final adoption, and book publications

Biedendieck, R.; Bunk, B.; Fürch, T.; Franco-Lara, E.; Jahn, M.; Jahn, D. (2010) Systems biology of recombinant protein production in *Bacillus megaterium.* In "Advances in Biochemical Engineering / Biotechnology" (Scheper, T., Ed.); Biosystems Engineering (Wittmann, C., Ed.) *Springer, Berlin, Heidelberg* 120, 133-161

Biedendieck, R.; Borgmeier, C.; Bunk, B.; Stammen, S.; Scherling, C.; Meinhardt, F.; Wittmann, C.; Jahn, D. (2011) Systems biology of recombinant protein production using *Bacillus megaterium*. *Methods Enzymol.* 500, 165-195

Driouch, H.; Roth, A.; Dersch, P.; Wittmann, C. (2010) Optimized bioprocess for production of fructofuranosidase by recombinant *Aspergillus niger. Appl. Microbiol. Biotechnol.* 87, 2011-2024

Driouch, H.; Roth, A.; Dersch, P.; Wittmann, C. (2011) Filamentous fungi in good shape: Microparticles for tailor-made fungal morphology and enhanced enzyme production. *Bioeng. Bugs* 2:2, 1-5

Eppinger, M.; Bunk, B.; Johns, M.A.; Edirisinghe, J.N.; Kutumbaka, K.K.; Koenig, S.S.K.; Creasy, H.H.; Rosovitz, M.J.; Riley, D.R.; Daugherty, S.; Martin, M.; Elbourne, L.D.H.; Paulsen, I.; Biedendieck, R.; Braun, C.; Grayburn, S.; Dhingra, S., Lukyanchuk, V.; Ball, B.; ul-Qamar, R.; Seibel, J.; Bremer, E.; Jahn, D.; Ravel, J.; Vary, P.S. (2011) Genome sequences of the biotechnologically important *B. megaterium* strains QM B1551 and DSM319. *J. Bacteriol.* 193, 4199-4213

Gamer, M.; Fröde, D.; Biedendieck, R.; Stammen, S.; Jahn D. (2009) A T7 RNA polymerase-dependent gene expression system for *Bacillus megaterium*. *Appl. Microbiol. Biotechnol*. 82, 1195-1203

Roth, A.; Dersch, P. (2010) A novel expression system for intracellular production and purification of recombinant affinity-tagged proteins in *Aspergillus niger*. *Appl. Microbiol. Biotechnol.* 86, 659-670

Stammen, S.; Müller, B.K.; Korneli, C.; Biedendieck, R.; Gamer, M.; Franco-Lara, E.; Jahn, D. (2010) High yield intra- and extracellular protein production using *Bacillus megaterium. Appl. Environ. Microbiol.* 76, 4037-4046

Stammen, S.; Schuller, F.; Dietrich, S.; Gamer, M.; Biedendieck, R.; Jahn, D. (2010) Application of *Escherichia coli* phage K1E DNA-dependent RNA polymerase for *in vitro* RNA synthesis and *in vivo* protein production in *Bacillus megaterium. Appl. Microbiol. Biotechnol.* 88, 529-539

b) Other publications

Borgmeier, C.; Biedendieck, R.; Hoffmann, K.; Jahn, D.; Meinhardt, F. (2011) Transcriptome profiling of *degU* expression reveals unexpected regulatory patterns in *Bacillus megaterium* and discloses new targets for optimizing expression. *Appl. Microbiol. Biotechnol.* 92, 583-596

Bunk, B.; Schulz, A.; Stammen, S.; Münch, R.; Warren, M. J.; Rohde, M.; Jahn, D.; Biedendieck, R. (2010) A short story about a big magic bug. *Bioeng. Bugs* 1, 1-7

Fleißner, A.; Dersch, P. (2010) Expression and Export: Recombinant protein production systems for *Aspergillus*. *Appl. Microbiol. Biotechnol.* 87, 1255-1270

3.3 Looking back on the promotion

The project has been funded since July 2001 in the SFB 578. It was completed on June 2012 with the end of the program.

3.3.1 Employees in the project

	Name, acad. degree, service position	Narrower subject of the employee	Institute of university or non-university facility	Participation in the project in hours per week	Category
Basic staff					
Research associate (incl. auxiliary power)	1. D. Jahn, Prof. Dr. rer. nat.	Microbiology, Biochemistry	Institute of Microbiology	2	Professorship
	2. P. Dersch, Prof. Dr. rer. nat.	Microbiology Infection biology	Institute of Microbiology	2	Professorship
	3. R. Biedendieck, Dr. rer. nat.	Microbiology Biotechnology	Institute of Microbiology	15	Post doctoral
Supportive staff					
Research associate (incl. auxiliary power)	4. S. Stammen, Dipl. Biotechnol.	Microbiology, Biotechnology	Institute of Microbiology	40	PhD student
	5. A. Roth, Dipl. Biotechnol.	Microbiology, Biotechnology	Institute of Microbiology	40	PhD student
	6. T. Knuuti, M. Sc.	Microbiology	Institute of Microbiology	40	PhD student
	7. C. Finger, Dipl. Biol.	Microbiology	Institute of Microbiology	40	PhD student
Non-academic staff	8. N. N., Stud. assistant	Microbiology, Biotechnology	Institute of Microbiology	10	Students

Responsibilities of employees (basic staff)

Position 1: Prof. Dr. Dieter Jahn

Prof. Dr. Dieter Jahn was responsible for the supervision of the PhD-students and for scheduling the scientific work using the expression host *B. megaterium*. Further, he coordinated the collaboration with other subprojects involved in *B. megaterium* work within this SFB578.

Position 2: Prof. Dr. Petra Dersch

The scientific work on *A. niger* and the mentoring of the PhD-students was coordinated by Prof. Dr. Petra Dersch. She supported the students in project planning and in analysis of the results. Further, she was responsible for the coordination of team work within the *A. niger* group in this research consortium.

Position 3: Dr. Rebekka Biedendieck

Dr. Rebekka Biedendieck has supported the PhD-students in their microbiological and molecular biological problems, in coordination their scientific work as well as in the analysis and interpretation of data achieving from the field of systems biology as microarrays.

Responsibilities of employees (supportive staff)

Position 4: Dipl. Biotechnol. Simon Stammen

The optimization of the recombinant gene expression system in *B. megaterium* was one of the most important goals within this collaboration project. The system was finally used by all subprojects working on *B. megaterium* (A6, A7, B8, B9, B10) and also found broad application in research of academia and industry. Here, Simon Stammen optimized the xylose-inducible system by systematically changing different elements of the promoter. With this system more than 1.2 g GFP per liter cell culture were recombinantly produced in close collaboration with subproject B10.

To enlarge the expression system, Simon Stammen developed new phage dependent promoter systems. These systems were functional in *B. megaterium* and provided a clear alternative to the common used phage T7-RNA-polymerase dependent system which was also successfully adapted for the use in *B. megaterium*. Simon Stammen finished his PhD-thesis in 12/2010 and works now for Boehringer Ingelheim (Viennan).

Position 5: Dipl. Biotechnol. Andreas Roth

Starting in the last application period Andreas Roth continued his work on *A. niger*. He identified and characterized the sucrose inducible promoter P_{suc1}. Further, he established

the constitutive *pkiA*- and the inducible *glaA*-promoters for their use within this SFB (A6, B3, B4, B7).

Based on two of the successfully constructed and proved promoter systems for *A. niger*, P_{suc1} and P_{pkiA}, Andreas Roth developed a series of expression vectors suitable for the production of recombinant proteins fused to N- or C-terminal located small affinity tags (His_6, StrepII). Each construct was successfully proven using model proteins. Further, the system was enlarged by vectors enabling production followed by secretion of recombinant proteins with *A. niger*. Andreas Roth finished his PhD in 12/2010 and is now working at the Johann Heinrich von Thünen-Institut (Braunschweig).

Position 6: M. Sc. Tobias Knuuti

As the xylose-inducible promoter is not controlled in the cloning host *E. coli,* problems occurred if cloning difficult genes influencing growth of *E. coli* or especially genes encoding antibody fragments (A6). For this Tobias Knuuti who replaced Simon Stammen constructed the pBmEcoco system. With this system it was possible to control the gene expression in *E. coli* by influencing the copy number of the expression plasmid while it was still possible to use this system for the xylose inducible gene expression in *B. megaterium*. Further, Tobias Knuuti successfully showed that more than 10 different *B. megaterium* DSMZ-strains were also useful for recombinant protein production and secretion. This is of great importance as each strain shows different characteristics with respect to growth conditions, growth behavior and product specificity.

The initial works on constructing a codon plus *B. megaterium* strain were also planned and performed by Tobias Knuuti.

Position 7: Dipl. Biol. Constanze Finger

Constanze Finger replaced Andreas Roth. She mainly focused on the establishment of performing microarrays using the microarray reader funded by the DFG within the last application period. Besides the development of protocols for the RNA-preparation from *A. niger* and *B. megaterium* she was also involved in the performance of microarrays of both organisms. In collaboration with subproject B8 and collaboration projects outside the SFB she successfully performed first microarray chips. For the analysis and interpretation of the huge amount of data obtained after each run Constanze Finger was also supported by subproject B9.

Position 8: Stud. assistant

The student assistant supported the PhD-students especially in their cloning work as well as in doing the test cultivation in shaking flask scale. Further molecular biological analysis as gel electrophoresis, preparation of plasmids and transformation belonged to her/his field of activity.

3.1 General information on the completed project A6

3.1.1 Topic

***Systems biology of chaperones for the production of antibodies with* Bacillus megaterium**

3.1.2 Disciplines and field of work

Biotechnology

3.1.3 Project manager

Prof. Dr. Stefan Dübel
(b.: 13.01.1960)
PD Dr. Michael Hust
(b.: 22.10.1972)
Institute of Biotechnology, Biochemistry and Bioinformatics, TU Braunschweig
Spielmannstr. 7, 38106 Braunschweig
Phone: 0531/391-5732
Fax: 0531/391-5763
E-Mail: s.duebel@tu-bs.de
Phone: 0531/391-5760
Fax: 0531/391-5763
E-Mail: m.hust@tu-bs.de

3.2 Development of the subproject

3.2.1 Report

3.2.1.1 Current knowledge at the last application and initial question

During the first funding period, *Bacillus megaterium* was established as antibody production host. To obtain appreciable yields of functional scFvs, the production process had to be optimized [*Jordan et. al., 2007a*]. Therefore the influence of parameters such as cultivation time, temperature and media was examined.

The minimal media M9 and A5, and the complex media LB, 2x YT and TB were investigated referring to functional D1.3-scFv yields. The complex medium TB was identified as the most suited production medium for recombinant lysozyme specific D1.3-scFv in *B. megaterium*.

The production under the so far identified optimized conditions was further examined regarding cultivation time. Therefore samples between 0 and 48 hours after induction were analyzed for scFv secretion and a production time of 24 hour was found to be best acceptable for D1.3-scFv.

D1.3-scFv was produced at eight different cultivation temperatures between 23 and 45°C using LB medium. Although biomass was not optimal at 41°C, the most functional scFv was obtained at 41°C measured by ELISA. This result leads to the assumption that folding catalysts as chaperones play an important role during antibody production in *B. megaterium*. Especially heat shock proteins could improve folding of antibodies at elevated temperatures. Therefore the selection of chaperones improving antibody production should be examined in the second project period.

Furthermore, the yield of D1.3-scFv was compared between *Escherichia coli* and *B. megaterium*. The purification via IMAC resulted in 410 µg/L scFv from the culture

supernatant of *B. megaterium* compared to 290 µg/L from culture supernatant and periplasmatic preparation of *E. coli*. The specific activity of the scFvs produced in *B. megaterium* was higher than in *E. coli* measured by ELISA.

The production of the more complex antibody fragment D1.3-scFabdC was also investigated in *B. megaterium* using the former optimized production conditions [*Jordan et al., 2007b*]. The yield was lower if compared to the much smaller D1.3-scFv.

The production temperature found to be optimal for antibody production, differ from the conditions for the production of enzymes in *B. megaterium* or antibody production in *E. coli*. The elevated temperature for optimal antibody production is an indication for the involvement of heat shock proteins as chaperones.

One identified bottleneck in the production of recombinant protein in *B. megaterium* is the removal of the signal peptide from the precursor protein [*Malten et al., 2005*]. The production of *Leuconostoc mesenteroides* dextransucrase DsrS was increased 3.7-fold by coproduction of the SipM.

3.2.1.2 Results and applied methods

Construction of improved vectors for the antibody production

For the construction of improved vectors for antibody production in *B. megaterium*, strategies, that has improved recombinant production of the reporter protein Gfp or dextransucrase DsrS (A1, Jahn/Dersch) were used. The gene for the signal peptidase SipM and its promoter was introduced in the expression vector pEJBmD1.3-scFv. D1.3-scFv was produced with and without coexpression of the signal peptidase and the production supernatants were analyzed by ELISA (**Fig. 1**). The coproduction of SipM did not influence the D1.3-scFv-production, so removal of the signal peptide from the precursor protein doesn't seem to be a limiting step in D1.3-scFv production in *B. megaterium*.

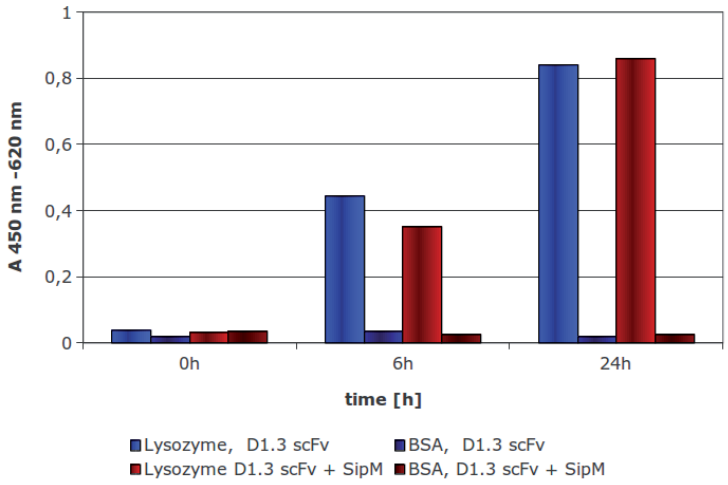

Fig. 1: Production of the signal peptidase SipM does not affect the production of functional D1.3-scFvs in B. megaterium*. A 450 nm – 620 nm: absorbance at 450 nm – absorbance at 620 nm*

Also, an alternative promoter system for the production of D1.3-scFv in *B. megaterium* was investigated. The plasmid pMiSBm10-D1.3-scFv contained the D1.3-scFv gene under the control of the phage polymerase promoter SP6. The production of the phage polymerase K1E encoded on the vector pSSBm73 [*Stammen et al., 2010*] is controlled by the Xylose inducible P_{XylA} promoter. For comparison D1.3 scFv was produced using the phage polymerase promoter and the Xylose inducible P_{XylA} promoter. Production supernatants were analysed by ELISA (**Fig. 2**).

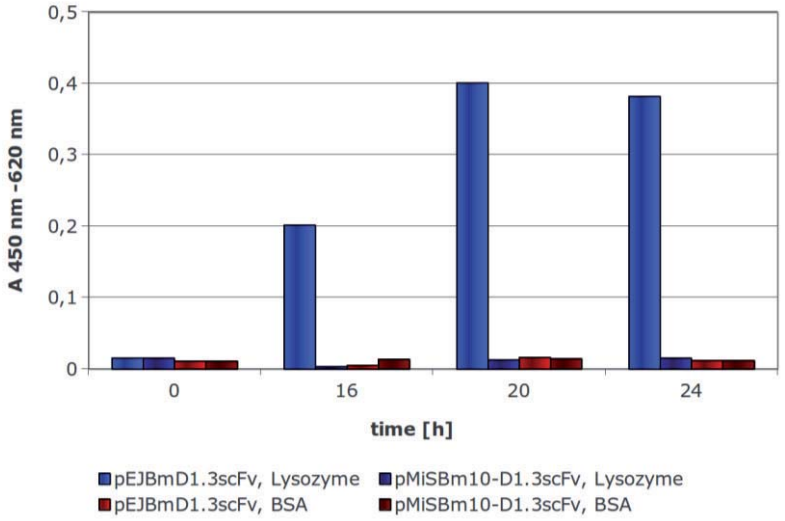

Fig. 2: Phage polymerase based expression is not suited for D1.3 scFv production in B. megaterium. *A 450 nm – 620 nm: absorbance at 450 nm – absorbance at 620 nm*

The strategies that were identified by others to improve production of recombinant proteins as Gfp and DsrS did not led to an increase in antibody production in *B. megaterium.* This correlates with the observation that the optimal production condition for antibodies compared to other recombinant proteins are found to be extremely different [*Jordan et al. 2007a*].

Phage display vectors for selection of chaperones

The optimal production temperature of 41°C lead to the hypothesis that heat shock proteins like chaperones could play an important role in antibody production in *B. megaterium*. We designed non-hypothesis-driven approach using a phage display technology based selection strategy to identify unknown beneficial factors.

Novel phage display vectors for selection of chaperones and other proteins which increase the yield of functional antibody were constructed within subproject A6. For this purpose, two recombinant proteins have to be encoded on vectors during phage display for chaperone selection. The first one is the antibody fused to the phage coat protein PIII, the second is the chaperone itself. These proteins could be encoded on one vector or on two different vectors. Both approaches have advantages and disadvantages.

In the first approach the antibody PIII fusion protein and the chaperone were encoded on the same plasmid pCHAP5-TOB5-D4 or pCHAP6-TOB5-D4 based on the phagemid pHAL14 for antibody selection (**Fig. 3**). A second ribosomal binding site and and a restriction site were inserted between the gene for the CRP specific scFv (single chain fragment variable) TOB5-D4 (derived from subproject D2 (Büttgenbach/Dübel) and the *lac* promoter. Here, fragments of genomic DNA of *B. megaterium* or for control genes for proteins with known chaperone function such as *dsbA, fkpA* and the reverse sequence of *fkpa* named *fkpa_r* as control were inserted in a bicistronic manner upstream the fusion protein. Both, the chaperone and the fusion protein were under the control of the *lac* promoter.

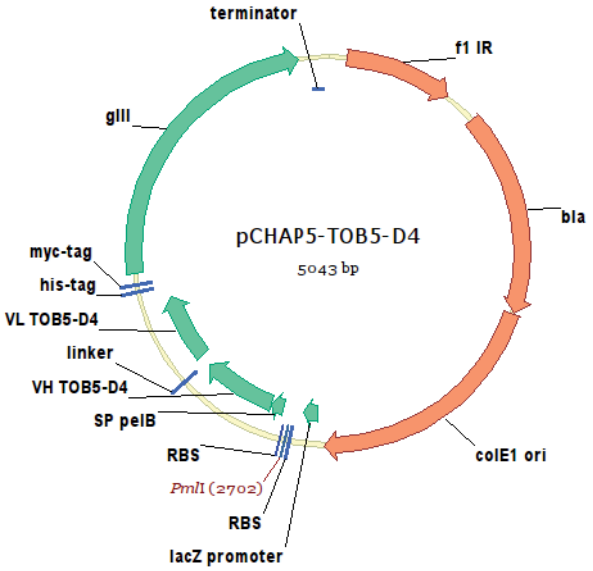

Fig. 3: Map of the phagemid pCHAP5-TOB5-D4. colE1 or*: origin of replication for* E. coli*,* bla: *gene for ß-lactamase as resistance marker against ampicillin*. f1 IR: *f1 intergenic region,* lacZ promoter*: inducible promoter of ß-galactosidase,* RBS*: ribosomal binding site,* SP pelB*: signal peptide of pectate lyase B of* Erwinia carotovora*.* VH TOB5-D4: *variable fragment of the heavy chain of TOB4-D4-scFv,* VL TOB5-D4: *variable fragment of the light chain of TOB4-D4-scFv,* linker: *polypeptide linker connecting V_H and V_L of TOB4-D4-scFv,* his tag: *polyhistidine-tag for detection and purification,* myc tag: *polypeptide tag derived from the transcription factor Myc,* gIII: *gene for the phage coat protein pIII,* terminator: *terminator for transcription,* PmlI: *restriction site recognized by the restriction enzyme* Pml*I.*

ScFv and scFv phage production were compared with and without chaperone coexpression by ELISA (**Fig. 4**) and Immunostain (**Fig. 5**).

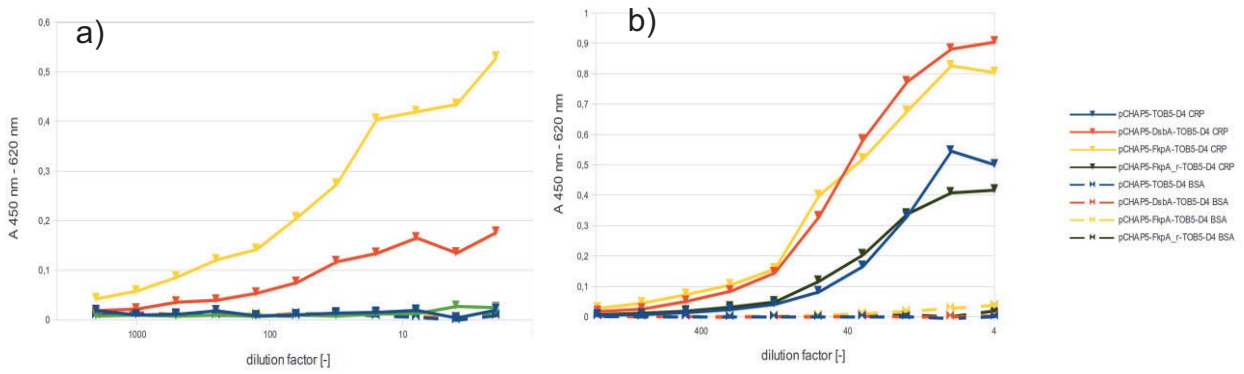

Fig. 4: Coproduction of the chaperones DsbA and FkpA enhances the production of functional TOB5-D4-scFvs and -phage in E. coli*; a): ELISA of TOB5-D4-scFv production supernatent, b): ELISA of TOB5-D4-scFv phage.*

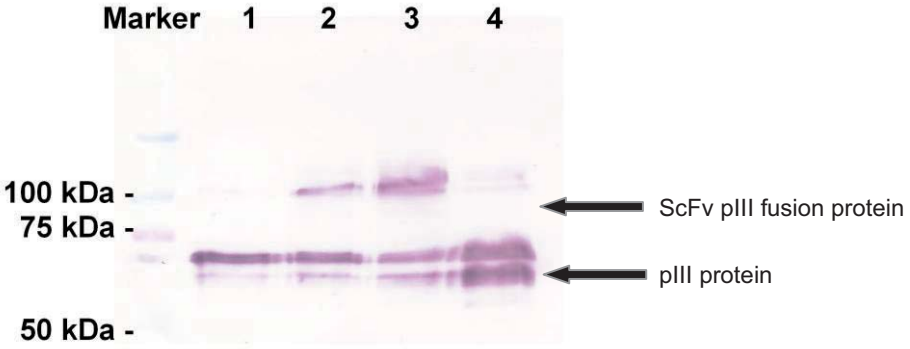

*Fig. 5: Coproduction of the chaperones DsbA and FkpA enhances the amount of scFv-pIII fusion protein of TOB5-D4-scFvs phage; 5*10^9 scFv phage produced in* E. coli *carring differnt phagemids were loaded per lane: 1) pCHAP5-TOB5-D4, 2) pCHAP5-dsba-TOB5-D4,3) pCHAP5-fkpa-TOB5-D4, 4) pCHAP5-fkpa_r-TOB5-D4; first detection antibody: mouse anti myc tag, second antibody: goat anti mouse Fc specific AP.*

Both assays showed that the amount of fusion protein presented on the phage was increased with chaperone coexpression. The production of soluble scFvs was only detectable if *fkpA* or *dsbA*, but not *fkpA_r* (control) were coexpressed. This indicated that a selection based on better production may be possible.

The second approach includes a two-vector-system, where the scFv and the chaperone are encoded on different plasmids (**Fig. 6**). The chaperone or the genomic DNA fragment is located on the phagemid pSOF4 including the f1 intergenic region, which is a signal for packaging DNA into the coat of phage particles. The second plasmid pHAL14-D1.3scFvdf1 encodes for the lysozyme specific scFv-D1.3 and theoretically should not be packaged into a phage particle, as it lacks a packaging signal. The great advantage of this system is, that once the library of genomic DNA fragments in pSOF4 is constructed, it can be combined with different antibodies and also antibody formats encoded on a second plasmid.

First experiments showed clearly that the packaging was not working very stringently as a significant amount of pHAL14-D1.3scFvdf1 lacking packaging signal (f1 intergenic region) was found to be packaged in phage particles as well. Different packaging conditions as various *E. coli* strains, helperphage and incubation time were investigated leading to a higher rate of pSOF4 packaged into phage particles rather than pHAL14-D1.3scFvdf1. However, the problem could not be completely solved.

The same experiments as shown above for the bicistronic phagemid system were performed for the two vector system. ScFvs and scFv phage were produced in the absence and presence of the two chaperones DsbA, FkpA and the control FkpA_r. This time, the coproduction of chaperones did not lead to an enhanced scFv and/or scFv phage production. Different production parameters including time and temperature were tested, but the coexpression of chaperones did not show a benefit on the production.

Further experiments were carried out using the single vector system pCHAP5-TOB5-D4.

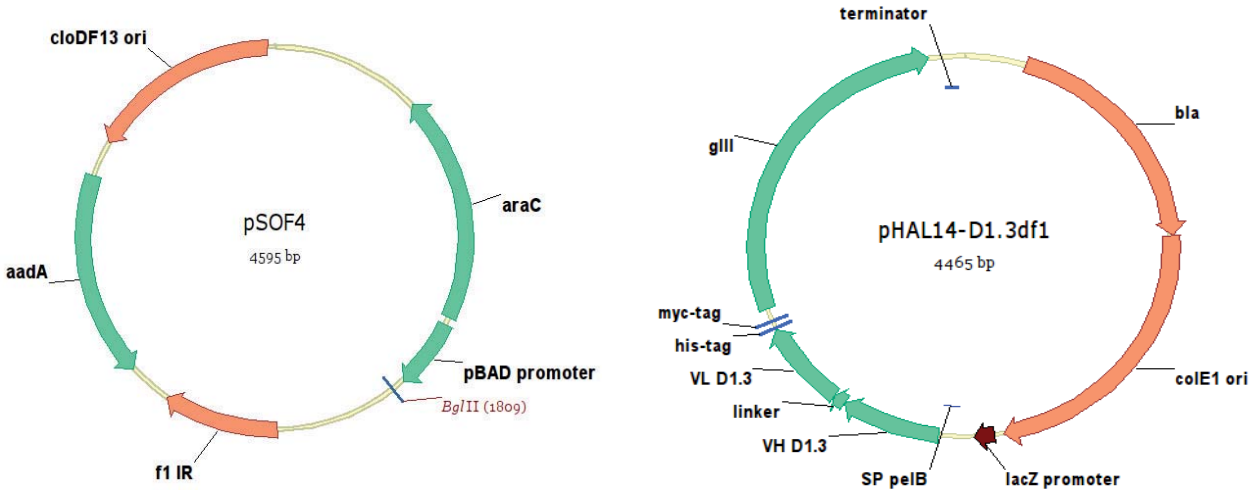

Fig. 6: Map of the pSOF4 (left) and pHAL14-D1.3df1 (right).
pSOF4: cloDF13 ori*: origin of replication for* E. coli*, aadA*: streptomycin/spectinomycin adenylyltransferase gene for streptomycin/spectinomycin resistance*.* f1 IR: *f1 intergenic region, pBAD promoter: L-arabinose inducible promoter of* araE*,* Bgl*II restriction site recognized by the restriction enzyme* Bgl*II,* araC*: encodes for positive regulatory protein required for L-arabinose utilization, pHAL14-D1.3df1:* colE1 ori*: origin of replication for* E. coli*,* bla: *gene for ß-lactamase as resistance marker for ampicillin,* lacZ promoter*: inducible promoter of ß-galactosidase,* SP pelB*: signal peptide of pectate lyase B of* E. carotovora*.* VH D1.3: *variable fragment of the heavy chain of D1.3-scFv,* VL D1.3: *variable fragment of the light chain of D1.3-scFv,* linker: *polypeptide linker connecting* V_H *and* V_L *of D1.3-scFv,* his-tag: *polyhistidine tag for detection and purification,* myc-tag: *polypeptide-tag derived from the transcription factor Myc,* gIII: *gene for the phage coat protein pIII,* terminator: *terminator for transcription.*

Panning of *B. megaterium* genomic DNA libraries

Genomic DNA (gDNA) of *B. megaterium* was isolated and fragmented by sonification. The obtained DNA fragments between 0.7 and 7 kb were cloned into pCHAP5-TOB5-D4 using the blunt end restriction site *Pml*I. The size of the library was $6.7x10^6$ clones. It was packaged into phage particles.

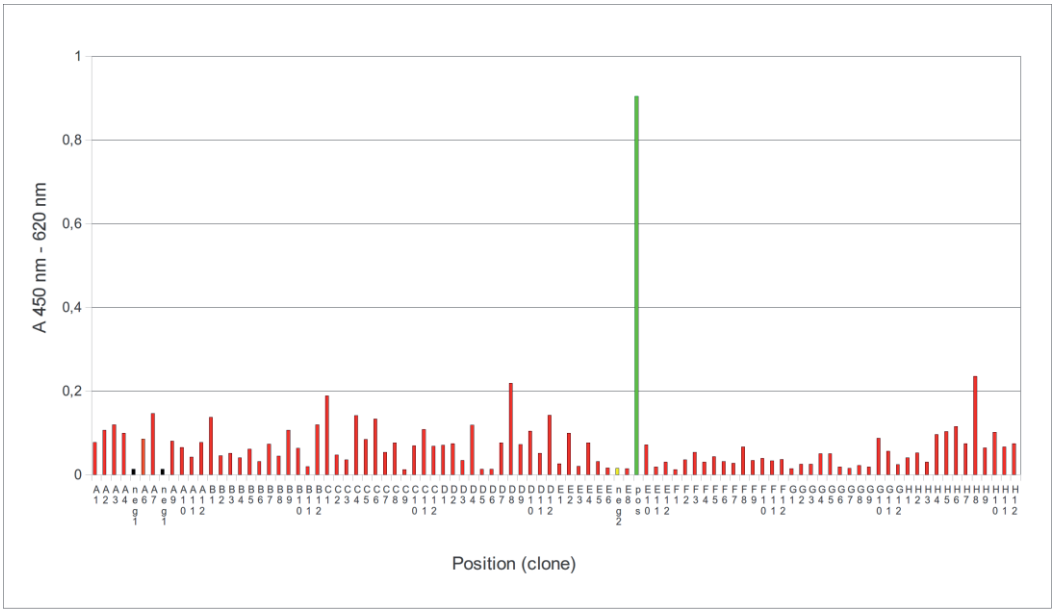

Fig. 7: Screening ELISA of the second panning round. neg 1 (blue): steril culture medium, neg 2 (yellow): production supernatant with E. coli *carrying pCHAP5-TOB5-D4, pos (green): production supernatant with* E. coli *carrying pCHAP5-dsba-TOB5-D4. A 450 nm – 620 nm: absorbance at 450 nm – absorbance at 620 nm*

The packaged library was used for panning to enrich helping factors like chaperones encoded on the inserted genomic DNA fragments and coproduced with the scFv pIII fusion protein. Individual clones from the panning were analyzed by screening ELISA (**Fig. 7**). The majority of clones lead to enhanced functional scFv production and therefore could encode for potential chaperones or helping factors. The selection procedure for clones with elevated scFv productivity was effective. But none of these clones resulted in higher scFv production than the clone encoding for the known chaperone FkpA.

The sequences of these clones were analyzed and compared to annotated genes of *B. megaterium* using the MEGABAC database of subproject B9 (http://megabac.tubs.de/websites/query_db.php) (**Tab. 1**). The genes that were found on the gDNA inserts were involved in metabolism, but no gene with known chaperone function was identified. The gDNA inserts of some clones had the wrong orientation in the vector.

Tab. 1: Analysis gDNA inserts of clones with enhanced scFv expression.

Name	Orientation in the vector	Length of gDNA insert [bp]	Part of the gene [%]	Physiological function
ArgH2 (Argininsuccinate lyase)	in frame	948	75	Energy metabolism
GbsA (Betaine aldehyde dehydrogenase	in frame	648	45	Amino acid metabolism
FeuB (Iron-uptake system permease protein)	reverse	98	10	Uptake of iron
RNR1 (Ribonucleoside-diphosphate reductase large chain)	reverse	220	28	dNTP synthesis
AtoE (Short-chain fatty acids transporter)	in frame	163	8	Uptake of fatty acids

Our Phage display approach is based on *E. coli* production/folding of antibody fragments. Presumably, *B. megaterium* chaperones do not work well in *E.coli* for folding antibody fragments. Further, the still unsolved problem of an efficient transformation system for *B. megaterium* makes it impractical to construct gDNA libraries in *B. megaterium* itself for similar approaches.

Despite of these problems, factors were identified which improve the antibody production. Significantly, these were not related to known folding helpers, indicating a possible role of the identified proteins as bottleneck factors in protein metabolism. Also interestingly, two gene fragments were in reverse orientation and only one gene fragment (ArgH2) covered more than 50% of gene lenght. One assumption is, that the gene fragments itself improve antibody gene expression. Both hypotheses have to be analyzed in further projects. The data demonstrate that the functional *in vivo* selection may be further evaluated to identify factors to increase antibody production/folding in *B. megaterium*.

3.2.1.3 References to other works and collaborations in the SFB

The SFB was instrumental to initiate a collaboration on the further development of production system for recombinant antibodies in *B. megaterium* together with the Fraunhofer-Institut für Toxikologie und Experimentelle Medizin (ITEM), Braunschweig. Here, robust protocols for the upscaling were developed, and the suitability of this production system was proven [*David et al., 2011*].

For the construction of improved vectors for the production of antibody fragments in *B. megaterium* vectors encoding for the signale peptidase SipM, and phage polymerase based vector system was delivered by subproject A1 (Jahn/Dersch). The experiments investigating the influence of chaperones on antibody and antibody phage production were performed with the scFv TOB5-D4 which was delivered by subproject D2 (Büttgenbach/Dübel). The analysis of the clones with elevated scFv production identified by ELISA was done with the MEGABAC database (B9, Münch/Schomburg). The production of different antibodies and antibody formats like the scIgG format were further examined in cooperation A1 (Jahn/Dersch) and B8 (Franco-Lara). These new antibodies were partly selected in subproject D2 (Büttgenbach/Dübel). Subproject C6 (Schilling/Ludwig) was provided with biotinylated peptid for examinations with streptavidin functionalized magnetic nanoparticles. Transcriptome analysis were performed in subproject A1 (Jahn/Dersch) from *B. megaterium* producing D1.3-scFv or Gfp. One candidate which was coproduced in D1.3scFv production was the chaperon PrsA. Coproduction of PrsA lead to enhanced D1.3-scFv-production in *B. megaterium* (B8, Franco-Lara). Recently, a cooperation on particle based separation of the produced antibodies from the cultivation supernatant of *B. megaterium* was initiated with the Karlsruher Institut für Technologie (KIT), Institut für Bio- und Lebensmitteltechnik.

3.2.1.4 Comparison with research outside the SFB

By using a phage display selection strategy of a genomic DNA library of *E. coli* the periplasmatic protein Skp was identified [*Bothmann and Plückthun, 1998*]. Here it was shown that Skp improves both, phage display and periplasmatic expression in *E. coli*. Later the selection was repeated using a genomic DNA library of a *skp* deficient *E. coli* strain [*Bothmann and Plückthun, 2000*]. In this attempt the periplasmatic peptidylprolyl *cis,trans*-isomerase (PPIase) FkpA was identified also to improve phage display and periplasmatic production. The vectors which were used here for selection do not contain any elements upstream the gDNA inserts as a promoter or a ribosomal binding site. Using *B .megaterium* gDNA, it was necessary to include these elements on the vector pCHAP5-TOB5-D4. Currently, no literature describing the selection of chaperones using phage display for other bacteria than *E. coli* exist.

Chaperone coproduction to enhance soluble recombinant protein production in *E. coli* is described using the helper plasmid pTUM4 [*Schlapschy et al., 2006*]. pTUM4 encodes for periplasmatic proteins which are known to act as chaperones or folding catalysts.

In another approach both, cytoplasmatic and/or periplasmatic chaperones were coproduced to enhance production of functional scFv [*Sonoda et al., 2011*]. Only the periplasmatic, not the cytoplasmatic chaperones increased the scFv production significantly, whereas coexpression of both types of chaperones decreased the yield of the scFv.

In the Gram positive bacterium *Bacillus subtilis* the secretory production of a scFv was also shown to be enhanced by the coproduction of chaperones [*Wu et al., 1998*]. The effect of cytoplasmatic and extracytoplasmatic chaperones was further analyzed on scFv production [*Wu et al., 2002*]. Here, the coproduction of either cytoplasmatic or extracytoplasmatic chaperones was only effective in the case of the extracytoplasmatic chaperones. This effect was enhanced with coproduction of both types of chaperones, which indicates, that the different chaperones act in sequential manner. In the same study the inactivation of the cell wall-bound protease WprA did further increase the yield of functional scFv.

In summary, the results demonstrate that a non-hypothesis-driven selection system based on randomly inserted cDNA influencing the production of an antibody necessary for selection provides a powerful tool to identify novel limiting steps in the metabolism of recombinant antibody production.

3.2.1.5 Literature

Biedendieck, R.; Beine, R.; Gamer, M.; Jordan, E.; Buchholz, K.; Seibel, J.; Dijkhuizen, L.; Malten, M.; Jahn, D. (2007) Export, purification and activities of affinity tagged *Lactobacillus reuteri* levansucrase produced by *Bacillus megaterium*. *Appl. Microbiol. Biotechnol.* 74, 1062-1073

Bothmann H.; Plückthun A. (1998) Selection for a periplasmic factor improving phage display and functional periplasmic expression. *Nat. Biotechnol.* 16, 376-380

Bothmann, H.; Plückthun A. (2000) The periplasmic *Escherichia coli* peptidylprolyl cis,trans-isomerase FkpA. I. Increased functional expression of antibody fragments with and without cis-prolines. *J. Biol. Chem*. 2, 275, 17100-17105

Malten, M.; Nahrstedt, H.; Meinhardt, F.; Jahn, D. (2005) Coexpression of the type I signal peptidase gene sipM increases recombinant protein production and export in *Bacillus megaterium* MS941. *Biotechnol. Bioeng.* 91, 616-621

Schlapschy, M.; Grimm, S.; Skerra, A. (2006) A system for concomitant overexpression of four periplasmic folding catalysts to improve secretory protein production in *Escherichia coli. Protein Engineering, Design & Selection* 19, 385-390

Sonoda, H.; Kumada, Y.; Katsuda, T.; Yamaji, H. (2011) Effects of cytoplasmic and periplasmic chaperones on secretory production of single-chain Fv antibody in *Escherichia coli. Biosci. Bioeng.* 111, 465-470

Stammen, S.; Schuller, F.; Dietrich, S.; Gamer, M.; Biedendieck, R.; Jahn, D. (2010) Application of *Escherichia coli* phage K1E DNA-dependent RNA polymerase for in vitro RNA synthesis and in vivo protein production in *Bacillus megaterium*. *Appl. Microbiol. Biotechnol.* 88, 529-539

Wu, S.C.; Ye, R.; Wu, X.C.; Ng, S.C.; Wong, S.L. (1998) Enhanced secretory production of a single-chain antibody fragment from *Bacillus subtilis* by coproduction of molecular chaperones. *J. Bacteriol.* 180, 2830-2835

Wu, S.C.; Yeung, J.C.; Duan, Y.; Ye, R.; Szarka, S.J.; Habibi, H.R.; Wong, S.L. (2002) Functional production and characterization of a fibrin-specific single-chain antibody fragment from *Bacillus subtilis*: effects of molecular chaperones and a wall-bound protease on antibody fragment production. *Appl. Environ. Microbiol.* 68, 3261-3269

3.2.2 Project relevant own publications

a) Works that have appeared in publications of a scientific quality assurance at the time of application or final adoption, and book publications

Steinwand, M.; Jordan, S.; Hust, M. (2010) Production of Antibody Fragments in the Gram-positive bacterium *Bacillus megaterium*. In: *Antibody engineering*, Ed: Kontermann, R. and Dübel, S., Springer-Verlag, 293-299

David, F.; Steinwand, M.; Hust, M.; Bohle, K.; Ross, A.; Dübel, S.; Franco-Lara, E. (2011) Antibody production in *Bacillus megaterium*: strategies and physiological implications of scaling from micro titer plates to industrial bioreactors. *Biotechnol. J.* 6,1516-1531

Lüders, S.; David, F.; Steinwand, M.; Jordan, E.; Hust, M.; Dübel, S.; Franco-Lara, E. (2011) Influence of the hydromechanical stress and temperature on growth and antibody fragment production with *Bacillus megaterium*. *Appl. Microbiol. Biotechnol.* 91, 81-90

b) Other publications

Dammeyer, T.; Steinwand, M.; Krüger, S.C.; Dübel, S.; Hust, M.; Timmis, K.N. (2011) Efficient production of soluble recombinant single chain Fv fragments by a *Pseudomonas putida* strain KT2440 cell factory. *Microb. Cell Fact.* 10, 11

Jordan, E., Hust, M., Roth, A., Biedendieck, R., Schirrmann, T., Jahn, D., Dübel, S. (2007). Production of recombinant antibody fragments in *Bacillus megaterium*. *Microb, Cell Fact.* 6, 2

Jordan, E.; Al-Halabi, L.; Schirrmann, T.; Hust, M.; Dübel, S. (2007) Production of single chain Fab (scFab) in *Bacillus megaterium*. *Microb. Cell Fact.* 6,38

Hust, M.; Steinwand, M.; Al-Halabi, L.; Helmsing, S.; Schirrmann, T.; Dübel, S. (2009) Improved microtitre plate production of single chain Fv fragments in *Escherichia coli*. *New Biotechnol.* 25, 424-428

3.3 Looking back on the promotion

The project has been funded since July 2004 in the SFB 578. It was completed on June 2012 with the end of the program.

3.3.1 Personnel in the project

	Name, acad. degree, service position	narrower subject of the employee	Institute of University or non-university facility	Participation in the project in hours per week	Category
Basic staff					
Research associate (incl. auxiliary power)	1. S. Dübel, Prof. Dr. rer. nat.	Biotechnology	Institute of Biochemistry, Biotechnology and Bioinformatics	4	Professorship
	2. M. Hust, PD Dr. rer. nat.	Biotechnology	Institute of Biochemistry, Biotechnology and Bioinformatics	20	Post-doctoral
Non academic staff	3. D. Meier, Technical Assistant	Molecular Biology	Institute of Biochemistry, Biotechnology and Bioinformatics	8	Technical staff
Supportive staff					
Research associate (incl. auxiliary power)	4. M. Steinwand, Dipl.-Biotechnol.	Biotechnology	Institute of Biochemistry, Biotechnology and Bioinformatics	40	PhD student
Non academic staff	5. N. N., Stud. assistant	Biotechnology	Institute of Biochemistry, Biotechnology and Bioinformatics	10	Students

Responsibilities of employees (basic staff)

Position 1 – 3: Prof . Dr. Stefan Dübel, PD Dr. Michael Hust, Doris Meier

The involved employees in the subproject A6 (Dübel/Hust) in the Institute of Biochemistry, Biotechnology and Bioinformatics worked together with the PhD-student in the development of phage display vectors for the selection of chaperones, coexpression of chaperones for antibody and antibody phage production as well as the construction of *B. megaterium* genomic libraries.

Responsibilities of employees (supportive staff)

Position 4: Dipl.-Biotechnol. Miriam Steinwand

To establish phage display for the identification of chaperones or other helping factors for antibody production Mrs Miriam Steinwand constructed different vectors that allow coexpression of other genes besides the antibody pIII fusion protein. For the validation of these vectors known chaperones were coexpressed with antibody fragments or antibody phage and analyzed by ELISA and Immunostain.

Furthermore *B. megaterium* genomic libraries were constructed, packaged into phage particles and used for the panning procedure. Then individual clones with enhanced antibody production were analyzed by sequence comparison.

Position 5: Stud. assistant

The student assistant supported the extensive experimental work. The key aspect was the production of antibody and antibody phage as well as helping with the biochemical analysis.

3.1 General information on the completed project A7

3.1.1 Topic

Structural biology of glycosyltransferases for the optimisation of biotechnical processes

3.1.2 Disciplines and field of work

Organic Chemistry, Structural Biology, Biocatalysis, Glycobiology

3.1.3 Project manager

Prof. Dr. Dirk Heinz
(b.: 01.08.1960)
Department of Structural Biology
Helmholtz Centre for Infection Biology
Inhoffenstraße 7, 38124 Braunschweig
Phone: 0531/6181-7000
Fax: 0531/6181-7098
E-Mail: dirk.heinz@helmholtz-hzi.de

Prof. Dr. Jürgen Seibel
(b.: 09.05.1971)
Institute of Organic Chemistry
University of Würzburg
Am Hubland, 97074 Würzburg
Phone: 0931/31-85326
Fax: 0931/31-84606
E-Mail: seibel@chemie.uni-wuerzburg.de

3.2 Development of the subproject

3.2.1 Report

3.2.1.1 Current knowledge at the last application and initial question

Carbohydrates represent one of the three major classes of biological macromolecules along with proteins and nucleic acids. Glycoconjugates play a functional role in numerous biological recognition processes, including bacterial or viral infection, inflammation and innate/adaptive immunity [*Dwek, 1996; Wong, 2005; Varki, 1993*]. Thus, there is a scientific and pharmaceutical interest in diverse oligosaccharides for developing new potential therapeutic agents, such as vaccines, glycoprotein therapeutics such as antibodies and glycosylated drugs [*Wong, 2003*]. Goal of the project was the structural- und functional analysis of selected glycosyltransferases. X-ray structures of glycosyltransferases should provide a deep understanding of their detailed reaction mechanisms. Such knowledge should pave the way for the design and redesign of tailor made biocatalysts by site-directed mutagenesis enabling the synthesis of unique oligosaccharides and glycosylated natural products.

During the previous funding period detailed structural information of the levansucrase SacB was obtained by X-ray crystallographic studies. In particular, we were able to identify the catalytic amino acids and determine their function during the progressive formation of the fructose-oligosaccharides (FOS) levan. Furthermore, Asn252 has been identified as a crucial amino acid regarding polymer- vs. oligomer synthesis [*Homann and Seibel, 2009a*].

Until this project including the last funding period despite the widespread biological function of carbohydrates, the polysaccharide synthesis mechanisms of glycosyltransferases remained largely unexplored. Thus goals of the recent funding period

were to further identify amino acids controlling the polymer- vs. oligomer synthesis. Based on biochemical analysis (sequence alignment with other fructosyl transferases and structural information of SacB we aimed to create novel variants of the enzyme located on the enzyme's surface remote from the active site on a rational basis. The obtained variants should then be subjected to biochemical and structural characterization (structure and function analysis relationship such as kinetic parameters, determination of product specificity, X-ray analysis) providing insights into structure and function relationship. These insights enable us to generate fructosyltransferases for the synthesis of specific oligosaccharides. Further studies with related and unrelated glycosyltransferases should led to "rules" for the rational protein redesign.

Despite bacterial glycosyltransferases we liked to explore eukaryotic glycosyltransferases (GT). In spite of the information concerning glycosylation disorders, the biochemical properties, as well as the structure-function relationship of the GTs involved in the glycosylation process are, however, hardly understood. A further goal of this project was to contribute to the understandings of the biochemical and structural features of human GTs through the recombinant production, characterization, mutagenesis and crystallization of sialyltransferases (STs) whose activity is induced in malignant cells as well as in other disease conditions.

3.2.1.2 Results and applied methods

Polysaccharide synthesis of the levansucrase SacB from *Bacillus megaterium* is controlled by distinct surface motifs

Bacterial levansucrases synthesize high molecular weight, β-(2,6) linked levan from sucrose by transfer of fructosyl units. We solved the structures of *Bacillus megaterium* levansucrase SacB variants Y247A, Y247W, N252A, D257A and K373A in resolutions between 1.75 and 2.0 Å. Kinetic and biochemical characterization of these variants reveal novel surface motifs outside the active site with distinct influence on the polysaccharide synthesis process. The wild-type activity (k_{cat}) and substrate affinity (K_m) is maintained by SacB variants with clearly distinguishable subsites for polysaccharide synthesis. These results lead to a new general understanding of carbohydrate transfer mechanisms. The newly identified surface motifs are discussed in the context of related glycosyltransferases.

Poly- and oligosaccharides are built by the linkage of activated monosaccharides and have remarkable structural variations. Their biological function depends on the extension, the type of linkage and the branching of the saccharide chain [*Varki, 1999*].

The biosynthesis of fructosyl polymers (fructan) is catalyzed by the action of enzymes called fructansucrases, also commonly referred to as fructosyltransferases. There are two types of fructansucrases known, levansucrases and inulosucrases. Levansucrases (EC 2.4.1.10) mainly form levan with β-(2,6)-linked fructosyl residues [*Chambert et al., 1974; Meng and Futterer, 2003*]. Inulosucrases (EC 2.4.1.9) synthesize fructans containing primarily β-(2,1)-linked fructosyl units which are referred to as inulins [*Ozimek et al., 2006; van Hijum et al., 2003*]. These enzymes cleave the glycosidic bond of their substrate sucrose and catalyze the transfer of a fructosyl unit from sucrose to a growing fructan

chain (polysaccharide formation) or to water (hydrolysis) [*Avigad et al., 1956a; Avigad et al., 1956b; van Hijum et al., 2006*]. Besides the synthesis of these biopolymers, fructansucrases are also capable of forming short-chain fructo-oligosaccharides in the presence of suitable acceptors or by mutagenesis in the active site [*Beine et al., 2008; Chambert and Petit-Glatron, 1991; Homann and Seibel, 2009b; Kralj et al., 2008*]. Each fructansucrase forms mainly one type of linkage in the synthesized fructo-oligosacharides. According to the database of Carbohydrate-Active enZYmes (CAZy) [*Henrissat and Davies, 1997*], bacterial fructansucrases have been included in the family 68 of Glycoside Hydrolases (GH). Clan GH-J comprises bacterial fructansucrases of GH 68 and the enzymes of family GH 32, mainly plant and fungal fructosyltransferases. These members share a β-propeller fold consisting of four antiparallel β-strands and a central negatively charged cavity, first discovered in tachylectin-2 [*Beisel et al., 1999*]. It was discovered by us that an amino acid not located in the active site of the fructosyltransferase SacB from *Bacillus megaterium* (Asn^{252}) abrogates its polysaccharide synthesis [*Homann et al., 2007*]. Analysis of the crystal structure of the homologous *Bacillus subtilis* levansucrase in complex with sucrose (pdb ID 1PT2) and raffinose (3BYN) provided insights into the functional role of Asn^{252} [*Meng and Futterer, 2003 and 2008*]. Nevertheless, it remained unclear if structural elements on the enzyme`s surface outside the active site take part in the transfructosylation process. In this project an extensive mutagenesis study combining biochemical analyses and structural information of the GH 68 levansucrase SacB from *Bacillus megaterium* was performed. Novel variants of amino acid residues located on the enzyme`s surface remote from the active site were rationally identified, characterized and crystallized. For the first time, five structures of SacB variants (Y247A, Y247W, N252A, D257A and K373A) in resolutions between 2.0 and 1.75 Å support a surface-modulated transfructosylation mechanism.

Polysaccharide synthesis is modulated by structural elements on the surface of SacB from Bacillus megaterium

Despite of thorough research during the recent years with many structures of sucrose-acting enzymes published, the polysaccharide synthesis mechanism remains unclear [*van Hijum et al., 2006*]. Even co-crystallizations with di- and trisaccharides did not lead to a detailed explanation of the transfructosylation process regarding oligo- and polysaccharide synthesis [*Meng and Futterer, 2003 and 2008*]. The previously described amino acids with impact on β-(2,6) linked levan- or β-(2,1) linked inulin formation were located in the active site. They interact with sucrose in the active site either catalyzing the cleavage of the glycosidic bond (Asp^{257}, Glu^{352}), stabilizing the enzyme-fructosyl complex (Asp^{95}) or stabilizing sucrose in the active site (Trp^{94}, Trp^{173}, Arg^{256}, Glu^{350}, Arg^{370}) (reviewed by van Hijum et al. (*2006*)). An asparagine residue in position 252 which is not located in the active site was identified by us as crucial for polysaccharide synthesis [*Homann et al., 2007*]. Hence, two questions arise: First, does a mutation of Asn^{252} have an impact on the

active site conformation? And second, are there other surface motifs influencing the polysaccharide synthesis and do their mutation influence the active site architecture?

We have shown for the first time that amino acids outside the active site of a polysaccharide-forming enzyme have a well-defined and rationally explainable effect on the polymer formation activity. Indirect effects on the position of other amino acids can be excluded due to the extensive structural data of SacB variants Y247A, Y247W, N252A and K373A. The structural data is consistent with the kinetic and biochemical analyses. Conformational analyses of variants Y247A, Y247W, N252A and K373A reveal an unchanged active site architecture (**Fig. 1**). Supporting the crystallographic data, the kinetic parameters of these variants are not significantly different compared to the wild-type SacB. Moreover, the structural data point towards a possible surface arrangement for the binding of an acceptor fructosyl chain. Residues Asn^{252}, Lys^{373} and Tyr^{247} form a platform for a possible stabilization of the acceptor fructan chain.

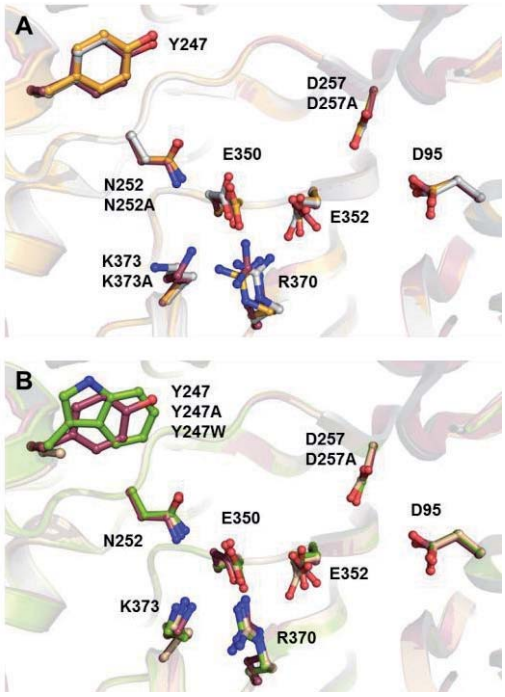

Fig. 1: Superposition of A) SacB variants D257A/N252A/K373A and B) D257A/Y247A/Y247W. The structures of the indicated SacB variants show a maintained active site architecture. The amino acid residues of the catalytic triad Asp^{95}/Asp^{257}/Glu^{352} do not change their conformation. Furthermore, also the amino acid residues in subsite +1 (Glu^{350}, Arg^{370}), +2 (Asn^{252}), +4/+5 (Lys^{373}) and +8/+9 (Tyr^{247}) do not change their conformation.

Clear subsites can be assigned to every exchanged amino acid (**Fig. 2**). The biochemical data along with the structural data show that Asn^{252} is located in subsite +2, whereas Lys^{373} (subsite +4/+5) and Tyr^{247} (+8/+9) are even further outside the active site. All exchanged amino acid residues are located on the surface of SacB thus must be interacting with the growing oligosaccharide chain. HPAEC analyses of the oligofructoside patterns show definite abrogations of the polymerization process depending on the location of the amino acid residue. Variants K373A, N252A and Y247A synthesize unique mixtures of oligosaccharides of different clearly distinguishable chain lengths correlating to their subsites on the surface of SacB. The exchange of lysine in position 373 to arginine leads to longer oligofructosides (9 fructosyl units) than its exchange to alanine (4-5

fructosyl units) (Fig. 2). Interactions between the functional amino groups of arginine in position 373 and the amino acid network as well as carbohydrate units are still possible although the interactions are reduced compared to the wild-type. This leads to an abrogated polymer formation. SacB variants Y247A and Y247I form oligosaccharides consisting of up to nine fructosyl units while variant Y247W forms the whole range of oligosaccharides compared to the wild-type spectrum. The reason may be that an unpolar favoured π-π-stacking mechanism is possible with tyrosine as well as tryptophan in this location but not with alanine or isoleucine. The superposition of Y247W with D257A shows the conserved conformation of tryptophan compared to tyrosine. The position of Tyr^{247} is supposed to be a key supporting location in an oligo- and polysaccharide-forming assembly line.

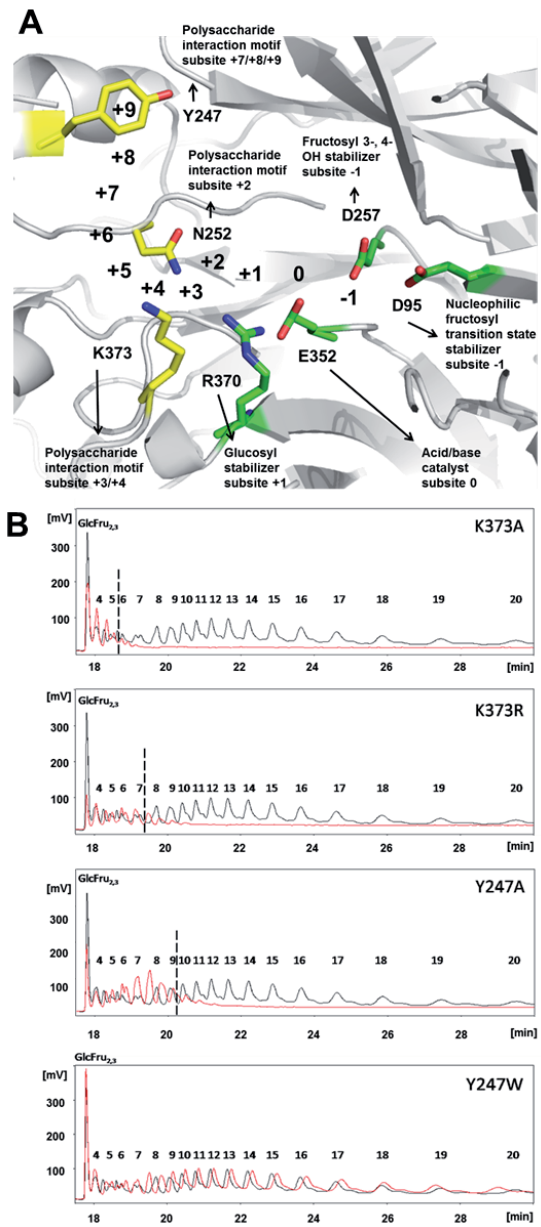

Fig. 2: The polysaccharide synthesis subsites of the levansucrase SacB from Bacillus megaterium*. The subsites indicated in A) are assigned according to the HPAEC analyses B). Black is the wild-type SacB, red is the indicated variant. The peaks are assigned according to previous carbohydrate standard measurements.*

Structural comparison of SacB from Bacillus megaterium *with other members of clan GH-J points towards a general mechanism of polysaccharide synthesis*

Structural comparison of the levansucrases SacB from *B. megaterium* and LsdA from *G. diazotrophicus* [*Martinez-Fleites et al., 2005*] enables insights into the functional role of Tyr^{247}. LsdA forms mainly the β-(2,1)-linked trisaccharide 1-kestose whereas the wild-type SacB forms mainly polysaccharides. One structural element on the surface of both levansucrases might influence this difference in oligo- *versus* polysaccharide synthesis. The conformation of Phe^{304} from LsdA might block the interaction of an oligofructosyl acceptor chain. These promising investigations may be a first step towards the implication on other enzymes of the structural related clan GH-J and beyond. Enzymes of clan GH-J include fungi and plant enzymes which act on sucrose or have an exclusively hydrolysis mechanism like the exo-inulinase from *Aspergillus awamori* (E.C. 3.2.1.80) [*Kulminskaya et al., 2003; Nagem et al., 2004*] or the invertase from *Thermotoga maritima* [*Alberto et al., 2004 and 2006*]. It remains to be investigated if similar surface structures influencing polysaccharide synthesis exist in these enzymes. A first indication towards hydrolysis *versus* polysaccharide synthesis mechanisms is the narrow and unpolar catalytic site architecture of the GH 68-related domain of the exo-inulinase from *A. awamori*, which does not bind any acceptor oligofructosides [*Kulminskaya et al., 2003; Nagem et al., 2004*]. Clearly, beneath other factors such as substrate concentration and reaction kinetics, the surface architecture of an enzyme is the key to its product spectrum.

Mechanism-orientated redesign of an isomaltulose synthase to an isomelezitose synthase by site-directed mutagenesis

Enzymes are highly efficient catalysts for stereoselective syntheses. However, the reactions are limited due to high substrate and product specificity. In order to overcome this limitation an approach for some enzymes could involve site-directed mutagenesis [*Strube et al., 2011*]. For this, incorporating the knowledge of structure and function of a given enzyme involving detailed data on the reaction mechanism is a basic requirement for the selection of target sites for site-directed mutations [*Lehmann et al., 2000*]. We liked to exam the possibility to redesign an enzyme for the specific synthesis of a given product. In the project we provided an example where an enzyme has been redesigned (enzyme engineering) for efficient synthesis of the trisaccharide isomelezitose (**Scheme 1**).

The trisaccharide isomelezitose (6-O^F-glucosylsucrose), recently found in honey [*Gómez Bárez et al., 1999*], has been identified as a potent nutraceutical candidate [*Munir, 1999*]. It is a substrate for bifidobacteria in the colon, thus providing probiotic properties [*Munir, 1999*]. It is not cleaved either by salivary enzymes or bacteria of the pharynx or in the small intestine. Isomelezitose is non-cariogenic, has a smaller calorie value in comparison to sucrose and is suitable for diabetic foods [*Munir, 1999*].

Using the α-glucosidase from *B. sp.* SAM1606 which forms isomelezitose 1 in small amounts as a starting point the following steps were performed to obtain an isomelezitose synthase:

- Identification of glucansucrases which exhibit high sequence identity to the α-glucosidase from *B. sp.* SAM1606 utilizing alignment tools (BLAST [*Altschul et al., 1997 and 2005*], ClustalW2 [*Chenna et al., 2003*])
- Narrowing down the query to enzymes within the PDB which show high transfer activity and perform the desired α-(1,6)-glycosidic coupling reaction (mechanism-based analysis)
- Selection of promising amino acids for site-directed mutagenesis by sequence and structural alignments in combination with docking studies (estimation of space requirement and possible interactions for the catalytic process)
- Site-directed mutagenesis to shift the product specificity to isomelezitose production

Alignments (BLAST [*Altschul et al., 1997 and 2005*], ClustalW2 [*Chenna et al., 2003*]) of the α-glucosidase from *B. sp.* SAM1606 revealed a large number of α-(1,6)-glucosidases from the GH13 family (a-amylase family, CAZy database [*Henrissat and Davies, 1997*]) to be most similar (>90% query coverage according to BLAST [*Altschul et al., 1997 and 2005*]). The query revealed the sucrose isomerases (SI, EC. 5.4.99.11, up to 99% transfer activity [*Nagai et al., 1994; Ravaud et al., 2009; Wu and Birch, 2005; Zhang et al., 2002*]) among which are SmuA from *Protaminobacter rubrum* and MutB from *Pseudomonas mesoacidophila* MX-45 (3D-Jury score: 365.00 and 361.33, respectively) to be most similar.

The SIs catalyze the isomerisation of sucrose to isomaltulose (D-fructofuranosyl-(6,1)-α-D-glucopyranoside) and trehalulose (D-fructofuranosyl-(1,1)-α-D-glucopyranoside). The formation of isomelezitose was not yet observed and the structural determinants enabling the synthesis of isomelezitose by α-glucosidases remain unknown. Implying the desired α-(1,6)-linkage into our query the sucrose isomerase from *P. rubrum* was finally identified.

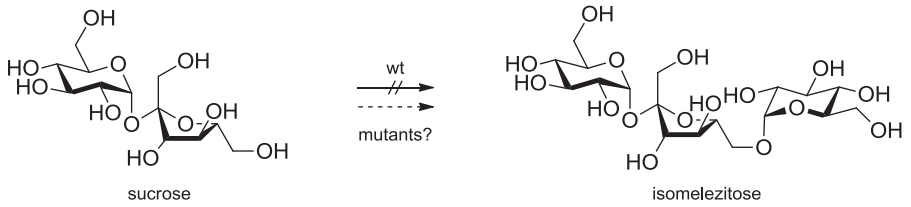

Scheme 1: Redesign of the isomaltulose synthase from P. rubrum *to an isomelezitose synthase by site-directed mutagenesis.*

Including the knowledge of previous studies [*Aroonnual et al., 2007; Lee et al., 2008; Ravaud et al., 2007; Veronese and Perlot, 1998; Wu and Birch, 2005; Zhang et al., 2003a and b*] we aimed to redesign (enzyme engineering) the isomaltulose synthase from *P. rubrum* to an isomelezitose synthase by site-directed mutagenesis. Comparison of the surface of the α-glucosidase (here: from *Bacillus cereus* A) and the SI SmuA points out that the α-glucosidase completely lacks the FBS (a characteristic domain of SIs which is made responsible for the isomerisation process) of SmuA. As a consequence the α-

glucosidase exhibits a widely open entrance to the active pocket favouring the hydrolysis, but enabling isomelezitose synthesis. In contrast the SmuA prevents hydrolysis due to its aromatic clamp, the FBS and a different loop/α-helix ^{257}QQQLKNFA^{265} (Na5, Lee et al. (*2008*)), but excludes trisaccharide formation.

In addition docking studies were performed to estimate the space requirement of sucrose as acceptor and to identify interactions between the enzyme (SI) and sucrose. According to the docking results sucrose fits in the active site of the glucopyranosyl-enzyme complex (**Fig. 3A**) and thus sucrose could act as an acceptor for the SI. The fructosyl-residue of sucrose (+1 sub-site, **Fig. 3A**) is able to occupy similar conformations compared to fructose sole (not shown) with C-6' in position for the nucleophilic attack of the glucopyranosyl-enzyme complex.

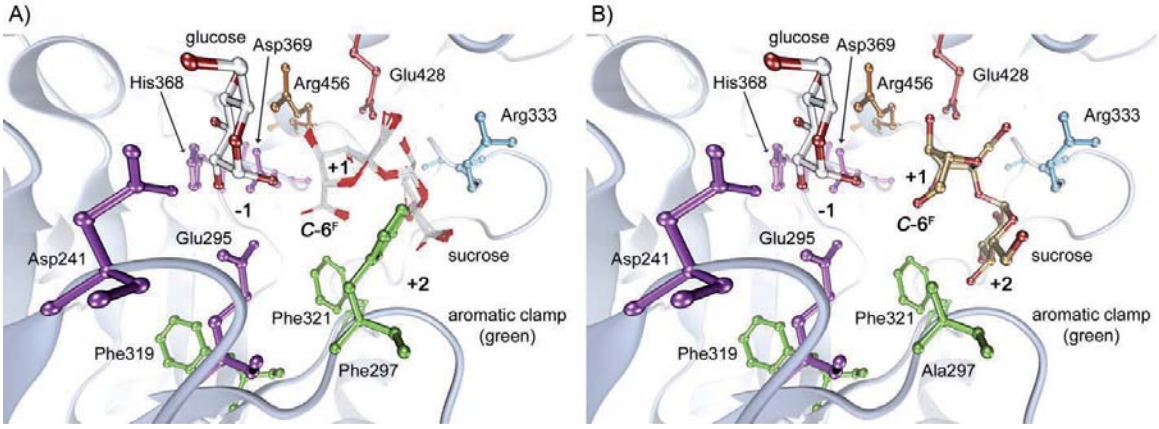

*Fig. 3: A) Docking of sucrose to the generated enzyme-substrate complex (visualization: VMD 1.9 [*Humphrey et al., 1996; Stone, 1998*]); B) Within cluster 4 the fructosyl-residue of sucrose is able to obtain new, more flexible conformations compared to the wild-type enzyme.*

Selection of targets for site-directed mutagenesis

Target sites for site-directed mutagenesis were chosen in proximity to the active site (+2 site, entrance). The -1 site and the FBS were not mutated since they are assumed to be critical for the reaction (previous mutations of the FBS lead to more hydrolysis supporting our suggestions [*Lee et al., 2008*]). We presumed that the bulky glucosyl-moiety of sucrose as acceptor may prohibit reactive conformations of the fructosyl-moiety. Therefore, we pursued to enlarge the +2 sub-site (**Fig. 3A**) while the polarity of the +2 sub-site was retained. In regard to previous studies, the alignments and the structural examinations the following target sites were identified.

The desired variants were created *in silico* (PyMOL Mutagenesis Tool) and similar AutoDock studies were carried out. As an example, **Fig. 3B** shows the docking of sucrose to the simulated ES-complex of variant F297A. In this docking experiment cluster 4 adapts new conformations for the fructosyl-residue. These conformations are probably caused by a different positioning of the glucosyl-moiety. Its calculated binding energy (−6.82 kcal/mol)

is higher than the binding energy of cluster 1 (−7.06 kcal/mol), but still exceeds the highest binding energy of the wild-type enzyme (−6.52 kcal/mol). Beside the influence of the mutation on the fructose binding and hydrolysis, this could reflect an increased possibility for the fructosyl-residue to occupy reactive conformations for isomelezitose synthesis.

Product specificity of the obtained variants and kinetic data

By site-directed mutagenesis we successfully generated multiple variants, which are able to a) synthesize isomelezitose with b) minor hydrolysis activity <5%. In particular, F297A and R333K still preserved 4 and 13% activity (calculated by the method of Vilozny et al. (*2009*) compared to isomaltulose formation by the wild-type enzyme. The mutations F297P und E428D as well as the combinations F297A_R333K and F321A_F319A lead to significant decrease in activity. For these variants the formation of the trisaccharide was observed and isomelezitose was isolated in similar yields (e. g. 70% for the variant F321A_F319A), but we were unable to receive reliable kinetic data. R456K showed nearly no activity, whereas only hydrolysis was observed for F321A. Interestingly, the Michaelis-Menten plots of the variants show linear regressions instead of hyperbolic slopes. This can either be explained by allosteric effects or a switch in the reaction mechanism [*Hehre et al., 1979*]. Since two molecules of sucrose are needed for synthesis of the isomelezitose, the kinetic reaction order can differ strongly from the facilitated Michaelis-Menten plot [*Zhao et al., 2008*].

Similar to some variants of the α-glucosidase from *B. sp.* SAM1606, the formation of isomelezitose was fast at the beginning with no detectable production of isomaltulose, trehalulose or monosaccharides (hydrolysis). Isomelezitose can be obtained in a preparative scale in 70% yield based on sucrose consumed (200 mM sucrose, 50 mM Sorensen buffer pH 6.0, 25 °C, 17 h). After long time the reaction proceeds with the formation of isomaltulose. To optimize the process, isomelezitose has to be continuously isolated.

In conclusion the scope of an enzyme was enhanced by site-directed mutagenesis. We succeeded with one single amino acid exchange, R333K, to yield up to 70% isomelezitose, far above the previous, not observed activity. Sequence and structure alignments as well as mechanism-based computational docking studies were utilized to create an isomelezitose synthase out of the sucrose isomerase from *P. rubrum*. An industrial process by using this enzyme as an immobilized catalyst could be envisaged.

A structure-function study of human glycosyltransferases

Modified cell surfaces through deglycosylation or by a false-escorted recognition processes can also lead to an increased risk of bacterial and viral infections [*Chen and Fukuda, 2006; Nilsson et al., 2006*]. Glycosylation processes include mannosyl-, fucosyl-, galactosyl- and sialyltransferases [*Holgersson and Lofling, 2006*] that transfer monosaccharides from an activated nucleotide sugars to hydroxyl groups of an appropriate carbohydrate and exhibit remarkable regio- and stereoselectivity [*Gerber-Lemaire and Juillerat-Jeanneret, 2006*]. In spite of the information concerning glycosylation disorders, the biochemical properties, as well as the structure-function relationship of the sialyltransferases (STs) involved in the glycosylation process are, were studied. The aim of this project was to evaluate substrate selectivity of STs.

Sialyltrasferases expression and activity

The enzymes selected for this study, ST3Gal1, ST3Gal4 and ST6Gal1 transfer sialic acid (Sia) from CMP-Sia onto a terminal β-D-galactose residue linked to glycoproteins or glycolipids resulting in α2-3 or α2-6 linkages. Although ST3Gal1 and ST3Gal4 form the same linkage (α2-3), they have different acceptor specificity regarding the molecule bound to the galactose acceptor moiety. STs are type II transmembrane glycoproteins which results in highly insoluble proteins after heterologous production of full-length enzymes in *Escherichia coli*. Thus vectors bearing either the maltose binding protein (MBD) or galectin1 (**Fig. 4**) were used for cloning the genes encoding the STs. About 15 mg/L of soluble target proteins were obtained when expressing the target enzymes as fusions (**Fig. 5**), which represents around 20 % of the *E. coli* soluble proteins.

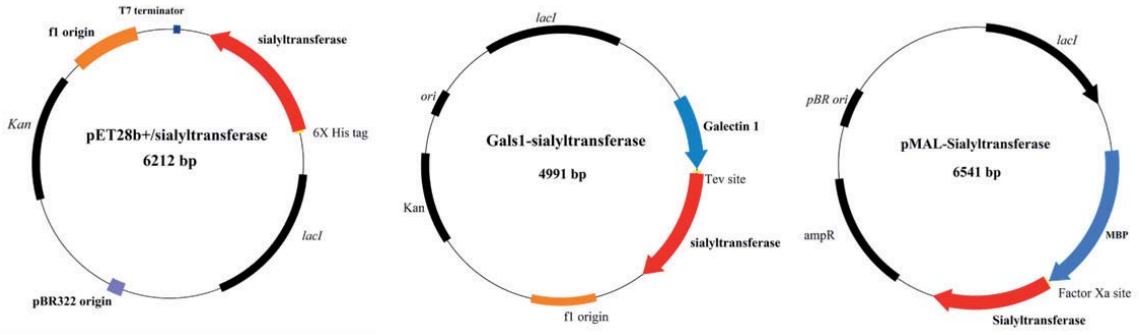

Fig. 4: Vectors used for STs production.

For activity assays, reactions with CMP-Sia as donor and LacNAc as acceptors were carried out using recombinant α2,3-(N)-ST, α2,3-(O)-ST and α2,6-ST as positive controls, whereas a reaction without enzyme was used as negative controls. All STs showed to be active at pH 7.5 when using LacNAc as acceptor (**Fig. 5**). The reaction products were analyzed by mass spectroscopy.

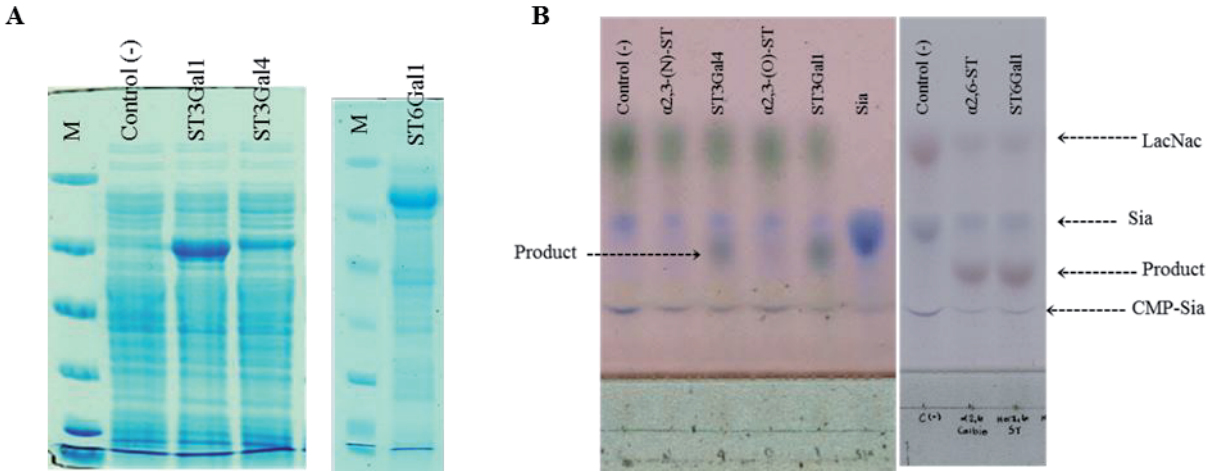

Fig. 5: Sialyltransferases expression and activity. A) SDS-PAGE: M: Molecular weight standard; Control (-): Soluble E. coli *extract without induction. B) Activity assay: Control (-): Reaction without enzyme; α2,3-(N)-ST, α2,3-(O)-ST and α2,6-ST: commercial enzymes; ST3Gal1, ST3Gal4 and ST6Gal1: recombinant human sialyltransferases.*

It was demonstrated that human STs can be produced as soluble and active proteins in *E. coli* even though they are not glycosylated in this expression system.

Structure-Function studies

To define the structural bases of STs specificity structural models of human STs were built using the structure of the only mammalian ST (ST3Gal1) crystalized up to now [*Rao et al., 2009*]. Six mutants were constructed from hST3Gal1 and hST3Gal4, which are believed to be crucial for substrate specificity. Amino acids were chosen based both on the reported contacts between pST3Gal1 and a β1,3-linked acceptor and based on the differences observed in the catalytic sites from the generated models. The mutants were well expressed and are currently being analyzed for specificity.

3.2.1.3 References to other works and collaborations in the SFB

The research collaborations interacted with the subprojects A1 (Jahn/Dersch), A3 (Buchholz/Hofer), B4 (Jahn/Nörtemann/Jänsch) and B11 (Wittmann) of the SFB. Cooperations were carried out with subproject A1 (Jahn/Dersch) on the transfer and the development of the fructofuranosidase producing strain *A. niger* SKAn1015 and also with the levansucrase of *Bacillus megaterium* including variants of this enzyme [*Homann et al., 2009a,b; Beine et al. 2009, Strube et al. 2011*]. The objective was to gain a better understanding in molecular mechanisms of such enzymes in order to optimize production and the catalysis of glycosyl-transfer reactions. Industrial cooperations on the development of enzymes for industrial reactions were established with BRAIN.

3.2.1.4 Comparison with research outside the SFB

Carbohydrate structures have been identified in eukaryotic and prokaryotic cells as glycoconjugates with communication skills. Their recently discussed role in various diseases has attracted high attention in the development of simple and convenient methods for oligosaccharide synthesis. Many investigations regarding their synthesis have been followed [*Homann et al., 2009a*]. Due to their complex structures the organic chemical synthesis seemed for a long time the only way to succeed. However, even there has been progress achieved as many chemical glycosylation methods are now developed academia and industry is still confronted with the need of convenient and large-scale synthesis [*Buchholz, Seibel, 2010*]. The first automation of the oligosaccharide assembling with very selected example demonstrated its possibility but also the limitations of this approach [*Plante et. al, 2001*]. Many years oligosaccharide synthesis by enzymes has been followed successfully by some prominent groups. [*Van Hjium et al., 2006; Homann et al., 2009b*]. In this project, we expanded nature's power for the design of tailor made biocatalysts by x-ray data in combination with detailed understanding of their mechanisms for enzyme engineering. In example we were able to solve longstanding questions like how is the polymer synthesis of carbohydrates regulated, where does the selectivity (chemo-, regio- and stereoselectivity) may come from? Our strategies lead to highly efficient and selective glycosylation reactions. The introduced concept shall be a first step in the direction to a glycosylation toolbox, which paves the way for the tailor-made synthesis of designed carbohydrate structures.

3.2.1.5 Literature

Alberto, F.; Bignon, C.; Sulzenbacher, G.; Henrissat, B.; Czjzek, M. (2004), The Three-dimensional Structure of Invertase (β-Fructosidase) from Thermotoga maritima Reveals a Bimodular Arrangement and an Evolutionary Relationship between Retaining and Inverting Glycosidases, *J. Biol. Chem.* 279, 18903-18910

Alberto, F.; Jordi, E.; Henrissat, B.; Czjzek, M. (2006), Crystal structure of inactivated Thermotoga maritima invertase in complex with the trisaccharide substrate raffinose, *Biochem. J.* 395, 457-462

Altschul, S. F.; Madden, T. L.; Schaffer, A. A.; Zhang, J.; Zhang, Z.; Miller, W.; Lipman, D. J. (1997), Gapped BLAST and PSI-BLAST: a new generation of protein database search programs, *Nucleic Acids Res.* 25, 3389-3402

Altschul, S. F.; Wootton, J. C.; Gertz, E. M.; Agarwala, R.; Morgulis, A.; Schaffer, A. A.; Yu, Y. K. (2005), Protein database searches using compositionally adjusted substitution matrices, *FEBS J.* 272, 5101-5109

Aroonnual, A.; Nihira, T.; Seki, T.; Panbangred, W. (2007), Role of several key residues in the catalytic activity of sucrose isomerase from *Klebsiella pneumoniae* NK33-98-8, *Enzym. Microb. Technol.* 40, 1221-1227

Avigad, G.; Feingold, D. S.; Hestrin, S. (1956a), The mechanism of polysaccharide production from sucrose. 4. Isolation and probable structures of oligosaccharides formed from sucrose by a levansucrase system, *Biochem. J.* 64, 351-361

Avigad, G.; Feingold, D. S.; Hestrin, S. (1956b), The mechanism of polysaccharide production from sucrose. 3. Donor–acceptor specificity of levansucrase from *Aerobacter levanicum*, *Biochem. J.* 64, 340-351

Beine, R.; Moraru, R.; Nimtz, M.; Na'amnieh, S.; Pawlowski, A.; Buchholz, K.; Seibel, J. (2008), Synthesis of novel fructooligosaccharides by substrate and enzyme engineering, *J. Biotechnol.* 138, 33-41

Beisel, H. G.; Kawabata, S.; Iwanaga, S.; Huber, R.; Bode, W. (1999), Tachylectin-2: crystal structure of a specific GlcNAc/GalNAc-binding lectin involved in the innate immunity host defense of the Japanese horseshoe crab Tachypleus tridentatus, *EMBO J.* 18, 2313-2322

Chambert, R.; Treboul, G.; Dedonder, R. (1974), Kinetic Studies of Levansucrase of *Bacillus subtilis*, *Eur. J. Biochem.* 41, 285-300

Chambert, R.; Petit-Glatron, M. F. (1991), Polymerase and hydrolase activities of Bacillus subtilis levansucrase can be separately modulated by site-directed mutagenesis, *Biochem. J.* 279 (Pt 1), 35-41

Chen, S.; Fukuda, M. (2006), Cell Type–Specific Roles of Carbohydrates in Tumor Metastasis, *Methods Enzymol.* 416, 371-380

Chenna, R.; Sugawara, H.; Koike, T.; Lopez, R.; Gibson, T. J.; Higgins, D. G.; Thompson, J. D. (2003), Multiple sequence alignment with the Clustal series of programs, *Nucleic Acids Res.* 31, 3497-3500

Dwek, R. A. (1996), Glycobiology: toward understanding the function of sugars, *Chem. Rev.* 96, 683-720

Gerber-Lemaire, S., and Juillerat-Jeanneret, L. (2006), Glycosylation Pathways as Drug Targets for Cancer: Glycosidase Inhibitors, *Mini-Reviews in Medicinal Chemistry* 6, 1043-1052

Gómez Bárez, J.; Garcia-Villanova, R.; Elvira Garcia, S.; González Paramás, A. (1999), Optimization of the capillary gas chromatographic analysis of mono-and oligosaccharides in honeys, *Chromatographia* 50, 461-469

Hehre, E. J.; Brewer, C. F.; Genghof, D. S. (1979), Scope and mechanism of carbohydrase action. Hydrolytic and nonhydrolytic actions of beta-amylase on alpha-and beta-maltosyl fluoride, *J. Biol. Chem.* 254, 5942-5950

Henrissat, B.; Davies, G. (1997), Structural and sequence-based classification of glycoside hydrolases, *Curr. Opin. Struct. Biol.* 7, 637-644

Holgersson, J.; Lofling, J. (2006), Glycosyltransferases involved in type 1 chain and Lewis antigen biosynthesis exhibit glycan and core chain specificity, *Glycobiology* 16, 584-593

Homann, A.; Biedendieck, R.; Gotze, S.; Jahn, D.; Seibel, J. (2007), Insights into polymer versus oligosaccharide synthesis: mutagenesis and mechanistic studies of a novel levansucrase from *Bacillus megaterium*, *Biochem. J.* 407, 189-198

Homann, A.; Seibel, J. (2009a), Chemo-enzymatic synthesis and functional analysis of natural and modified glycostructures, *Nat. Prod. Rep.* 26, 1555-1571

Homann, A.; Seibel, J. (2009b), Towards tailor-made oligosaccharides—chemo-enzymatic approaches by enzyme and substrate engineering, *Appl. Microbiol. Biotechnol.* 83, 209-216

Humphrey, W.; Dalke, A.; Schulten, K. (1996), VMD: visual molecular dynamics, *J. Mol. Graph.* 14, 33-38

Kralj, S.; van Leeuwen, S. S.; Valk, V.; Eeuwema, W.; Kamerling, J. P.; Dijkhuizen, L. (2008), Hybrid reuteransucrase enzymes reveal regions important for glucosidic linkage specificity and the transglucosylation/hydrolysis ratio, *FEBS J.* 275, 6002-6010

Kulminskaya, A. A.; Arand, M.; Eneyskaya, E. V.; Ivanen, D. R.; Shabalin, K. A.; Shishlyannikov, S. M.; Saveliev, A. N.; Korneeva, O. S.; Neustroev, K. N. (2003), Biochemical characterization of *Aspergillus awamori* exoinulinase: substrate binding characteristics and regioselectivity of hydrolysis, *Biochim. Biophys. Acta* 1650, 22-29

Lee, H. C.; Kim, J. H.; Kim, S. Y.; Lee, J. K. (2008), Isomaltose Production by Modification of the Fructose-Binding Site on the Basis of the Predicted Structure of Sucrose Isomerase from *Protaminobacter rubrum*, *Appl. Environ. Microbiol.* 74, 5183-5194

Lehmann, M.; Pasamontes, L.; Lassen, S. F.; Wyss, M. (2000), The consensus concept for thermostability engineering of proteins, *Biochim. Biophys. Acta* 1543, 408-415

Martinez-Fleites, C.; Ortiz-Lombardia, M.; Pons, T.; Tarbouriech, N.; Taylor, E. J.; Arrieta, J. G.; Hernandez, L.; Davies, G. J. (2005), Crystal structure of levansucrase from the Gram-negative bacterium *Gluconacetobacter diazotrophicus*, *Biochem. J.* 390, 19-27

Meng, G.; Fütterer, K. (2003), Structural framework of fructosyl transfer in *Bacillus subtilis* levansucrase, *Nat. Struct. Biol.* 10, 935-941

Meng, G.; Futterer, K. (2008), Donor substrate recognition in the raffinose-bound E342A mutant of fructosyltransferase *Bacillus subtilis* levansucrase, *BMC Struct. Biol.* 8, 16

Munir, M. V. M. (1999) Method for producing isomelezitose and sweetining agents containing isomelezitose. Suedzucker AG Mannheim/Ochsenfurt, M. M., Vogel M. (ed.), Europe

Nagai, Y.; Sugitani, T.; Tsuyuki, K. (1994), Characterization of alpha-glucosyltransferase from Pseudomonas mesoacidophila MX-45, *Biosci. Biotechnol. Biochem.* 58, 1789-1793

Nagem, R. A.; Rojas, A. L.; Golubev, A. M.; Korneeva, O. S.; Eneyskaya, E. V.; Kulminskaya, A. A.; Neustroev, K. N.; Polikarpov, I. (2004), Crystal Structure of Exo-inulinase from *Aspergillus awamori*: The Enzyme Fold and Structural Determinants of Substrate Recognition, *J. Mol. Biol.* 344, 471-480

Nilsson, C.; Skoglund, A.; Moran, A. P.; Annuk, H.; Engstrand, L.; Normark, S. (2006), An enzymatic ruler modulates Lewis antigen glycosylation of *Helicobacter pylori* LPS during persistent infection, *Proc. Natl. Acad. Sci. USA* 103, 2863-2868

Ozimek, L. K.; Kralj, S.; van der Maarel, M. J.; Dijkhuizen, L. (2006), The levansucrase and inulosucrase enzymes of *Lactobacillus reuteri* 121 catalyse processive and non-processive transglycosylation reactions, *Microbiology* 152, 1187-1196

Plante, J.P., Palmacci, E.R., Seeberger, P.H. (2001), Automated Solid-Phase Synthesis of Oligosaccharides, *Science*, 291, 1523-1527

Rao, F. V.; Rich, J. R.; Rakic, B.; Buddai, S.; Schwartz, M. F.; Johnson, K.; Bowe, C.; Wakarchuk, W. W.; DeFrees, S.; Withers, S. G.; Strynadka, N. C. J. (2009), Structural insight into mammalian sialyltransferases, *Nat. Struct. Mol. Biol.* 16, 1186-1188

Ravaud, S.; Robert, X.; Watzlawick, H.; Haser, R.; Mattes, R.; Aghajari, N. (2007), Trehalulose synthase native and carbohydrate complexed structures provide insights into sucrose isomerization, *J. Biol. Chem.* 282, 28126-28136

Ravaud, S.; Robert, X.; Watzlawick, H.; Haser, R.; Mattes, R.; Aghajari, N. (2009), Structural determinants of product specificity of sucrose isomerases, *FEBS Lett.* 583, 1964-Stone, J. E.

Strube, C. P.; Homann, A.; Gamer, M.; Jahn, D.; Seibel, J.; Heinz, D. W. (2011), Polysaccharide synthesis of the levansucrase SACB from *Bacillus Megaterium* is controlled by distinct surface motifs, *J. Biol. Chem.* 286, 17593-17600

Varki, A. (1993), Biological roles of oligosaccharides: all of the theories are correct, *Glycobiology* 3, 97-130

van Hijum, S. A.; van der Maarel, M. J.; Dijkhuizen, L. (2003), Kinetic properties of an inulosucrase from *Lactobacillus reuteri* 121, *FEBS Lett.* 534, 207-210

van Hijum, S. A.; Kralj, S.; Ozimek, L. K.; Dijkhuizen, L.; van Geel-Schutten, I. G. (2006), Structure-function relationships of glucansucrase and fructansucrase enzymes from lactic acid bacteria, *Microbiol. Mol. Biol. Rev.* 70, 157-176

Varki, A. (1999) *Essentials of glycobiology*, Cold Spring Harbor Laboratory Press, Cold Spring Harbor, NY

Veronese, T.; Perlot, P. (1998), Proposition for the biochemical mechanism occurring in the sucrose isomerase active site, *FEBS Lett.* 441, 348-352

Vilozny, B.; Schiller, A.; Wessling, R. A.; Singaram, B. (2009), Enzyme assays with boronic acid appended bipyridinium salts, *Anal. Chim. Acta.* 649, 246-251

Wong, C. H. (2005), Protein glycosylation: new challenges and opportunities, *J. Org. Chem.* 70, 4219-4225

Wong, C.-H. (2003) *Carbohydrate-based drug discovery*, Wiley-VCH, Weinheim, New York

Wu, L.; Birch, R. G. (2005), Characterization of the highly efficient sucrose isomerase from *Pantoea dispersa* UQ68J and cloning of the sucrose isomerase gene, *Appl. Environ. Microbiol.* 71, 1581-1590

Zhang, D.; Li, X.; Zhang, L. H. (2002), Isomaltulose Synthase from Klebsiella sp. Strain LX3: Gene Cloning and Characterization and Engineering of Thermostability, *Appl. Environ. Microbiol.* 68, 2676-2682

Zhang, D.; Li, N.; Lok, S. M.; Zhang, L. H.; Swaminathan, K. (2003a), Isomaltulose synthase (PalI) of Klebsiella sp. LX3, *J. Biol. Chem.* 278, 35428-35434

Zhang, D.; Li, N.; Swaminathan, K.; Zhang, L. H. (2003b), A motif rich in charged residues determines product specificity in isomaltulose synthase, *FEBS Lett.* 534, 151-155

Zhao, Y. Y.; Takahashi, M.; Gu, J. G.; Miyoshi, E.; Matsumoto, A.; Kitazume, S.; Taniguchi, N. (2008), Functional roles of N-glycans in cell signaling and cell adhesion in cancer, *Cancer Sci.* 99, 1304-1310

3.2.2 Project relevant own publications

a) Works that have appeared in publications of a scientific quality assurance at the time of application or final adoption, and book publications

Beine, R.; Rocas Valente, A.; Biedendieck R.; Jahn, D.; Seibel J. (2009) Directed optimization of biocatalytic transglycosylation processes by the integration of genetic algorithms and fermentative approaches into a kinetic model. *Proc, Biochem.* 44, 1103-1114

Buchholz, K.; Seibel, J. (2010) Industrial applications of carbohydrates. In: Encyclopedia of Industrial Biotechnology (Flickinger, M. C., Ed.) Wiley

Homann, A.; ul-Qamar, R.; Serim, S.; Dersch, P.; Seibel, J. (2010) Bioorthogonal metabolic glycoengineering of human larynx carcinoma (HEp-2) cells targeting sialic acid. *Beilstein J. Org. Chem.* 6, 1-7

Homann, A.; Seibel J. (2009a) Chemo-enzymatic synthesis and functional analysis of natural and modified glycostructures. *Nat. Prod. Rep.* 26, 1555-1571

Homann, A. Seibel J. (2009b) Towards tailor-made oligosaccharides-chemo-enzymatic approaches by enzyme and substrate engineering. *Appl. Microbiol. Biotechnol.* 83, 209-216.

Görl, J.; Timm, M.; Seibel J. (2012) Mechanism-oriented redesign of an isomaltulose synthase to an isomelezitose synthase by site-directed mutagenesis. *Chembiochem.* 13, 149-156

Seibel, J.; Jördening H.J.; Buchholz, K. (2010) Extending Synthetic Routes for Oligosaccharides by Enzyme, Substrate and Reaction Engineering. *Adv. Biochem. Eng. Biotechnol.* 120,163-193

Strube, C. P. Homann, A. Gamer M., Jahn, D. Seibel, J. Heinz, D.W. (2011) Polysaccharide synthesis of the levansucrase SACB from *Bacillus Megaterium* is controlled by distinct surface motifs. *J. Biol. Chem.* 286, 17593-17600

3.3 Looking back on the promotion

The project has been funded since July 2004 in the SFB 578. It was completed on June 2012 with the end of the program.

3.3.1 Employees in the project

	Name, acad. degree, service position	narrower subject of the employee	Institute of University or non-university facility	Participation in the project in hours per week	Category
Basic staff					
Research associate (incl. auxiliary power)	1. J. Seibel, Prof. Dr. rer. nat.	Organic Chemistry	University of Würzburg, Institute of Organic Chemistry	10	Professorship
	2. D. Heinz, Prof. Dr. rer. Nat.	Structural Biology	HZI, Department of Structural Biology	4	Professorship
	3. M. Ortiz-Soto, PhD	Microbiology	University of Würzburg, Institute of Organic Chemistry	10	Post-doctoral
Non academic staff	4. S. Schmidt, BTA	Biotechnology	HZI, Department of Structural Biology	8	Technical staff
	5. D. Simon, CTA	Chemistry	University of Würzburg, Institute of Organic Chemistry	8	Technical staff
Supportive staff					
Research associate (incl. auxiliary power)	6. C. Strube, Dr. rer. nat.	Biology	HZI, Department of Structural Biology	40	PhD student
	7. A. Homann Dr. rer. nat.	Biotechnology	University of Würzburg, Institute of Organic Chemistry	40	PhD student
	8. M. Timm, Dipl.-Biotechnol.	Biotechnology	University of Würzburg, Institute of Organic Chemistry	40	PhD student
	9. J. Görl Dipl. Chem	Chemistry	University of Würzburg, Institute of Organic Chemistry	40	PhD student
Non academic staff	10. N. N., Stud. assistant	Biochemical Engineering, Biotechnology		10	Students

Responsibilities of employees (basic staff)

Position 1-2, 4-5: Prof. Dr. Seibel, Prof. Dr. Heinz, S. Schmidt, D. Simon

The involved employees in the subproject A7 (Heinz/Seibel) of the Department of Structural Biology, HZI, and the Institute of Organic Chemistry, Universität Würzburg, will support the PhD-students in their synthetic chemistry and structural biology problems as well as in the development of biocatalysts models, the implementation of cultivation and analysis and the construction of experimental facilities.

Responsibilities of employees (supportive staff)

Position 3: Dr. Maria Ortiz Soto

Dr. Soto investigated cloning and expression of a human sialyltransferases in *E. coli*. Successful expression by developing a vector system with fusion proteins, correct folding of the human protein and solubility of the protein were studied. New methods will be provided which can now address such problems. She performed further amino acid substitutions in order to change substrate and product specificity of such enzymes.

Position 6: Dr. Christian Strube

Dr. Strube was in charge of structural analysis of the proteins. For high resolution he used synchrotron sources in Germany (DESY) and France (ESRF Grenoble). He solved phase problems with the multiwavelength anomalous dispersion (MAD) and molecular displacement (MOLREP). He analyzed structures and refined them. He also performed expression and purification of proteins. He succeeded in crystallization and X-ray analysis of different levansucrase structures and additional glycosyltransferases.

Position 7: Dr. Arne Homann

Dr. Homann produced glycosyltransferases, purified and and characterized them kinetically. In combination with the x-ray structures he interpreted the mechanism of the levansucrase.

Position 8: Dipl. Biotechnol. Malte Timm

Mr. Timm performed site-directed mutagenisis of glycosyltransferases and evaluated structure-function relations of family 13, family 68 and family 70 enzymes. He discovered principles of such enzyme family leading also to anchor answers of their origins.

Position 9: Dipl.-Chem. J. Görl

Investigated for the first time a glycosyltransferase (a isomelizitose synthase) by rational redesign combining structural insights of enzymes with the good understanding of reaction mechanism.

Position 10: Stud. assistant

The student assistant supported the extensive experimental work in the implementation and evaluation of cultivations as well as in the routine of biotechnological and molecular biological studies.

Project area B: Systems biotechnology of product formation

Project-No.	Topic	Disciplines and field of work	Project manager, institution
B3	Influence of the environome on the morphology and productivity of filamentous fungi (*Aspergillus niger*)	Biochemical engineering, Morphology engineering, Fluid dynamics	R. Krull and D. C. Hempel, Institute of Biochemical Engineering, TU BS
B4	Systems biology of product and pellet formation by *Aspergillus niger*	Microbiology, Molecular biology, Mycology, Biotechnology, Systems biology	D. Jahn, Institute of Microbiology, TU BS / B. Nörtemann, Institute of Biochemical Engineering, TU BS / L. Jänsch, Cellular Proteom Research, HZI BS
B7	Micromechanic properties of filamentous fungi	Process engineering, Materials science, Biotechnology	A. Kwade and I. Kampen, Institute for Particle Technology, TU BS
B8	Holistic bioprocess engineering of antibody fragment secreting *Bacillus megaterium*	Bioprocess Engineering, Single cell analysis, Transcriptomics	E. Franco-Lara, Institute of Biochemical Engineering, TU BS
B9	Integrative databases, bioinformatics tools, analysis and modeling for systems biology with *B. megaterium* and *A. niger*	Bioinformatics, Systems biology	R. Münch, Institute of Microbiology, TU BS / D. Schomburg, Institute of Biochemistry and Biotechnology, TU BS
B10	Systems biotechnology of glycosyltransferase production with *Bacillus megaterium*	Biochemical engineering, Systems biotechnology	D. Jahn, Institute of Microbiology, TU BS / E. Franco-Lara, Institute of Biochemical Engineering, TU BS
B11	Metabolic network dynamics for production of recombinant glycosyltransferases	Biochemical engineering, Systems biotechnology	C. Wittmann, Institute of Biochemical Engineering; TU BS

3.1 General information on the completed project B3

3.1.1 Topic

Influence of the environome on the morphology and productivity of filamentous fungi (*Aspergillus niger*)

3.1.2 Disciplines and field of work

Biochemical Engineering, Morphology Engineering, Fluid Dynamics

3.1.3 Project manager

apl. Prof. Dr. Rainer Krull
(b.: 20.4.1961)
Institute of Biochemical Engineering, TU Braunschweig
Gaußstraße 17, 38106 Braunschweig
Telefon: 0531/391-7653
Telefax: 0531/391-7652
E-Mail: r.krull@tu-bs.de

Prof. Dr.-Ing. Dietmar C. Hempel
(b.: 22.12.1943)
Telefon: 0531/391-7657
Telefax: 0531/391-7652
E-Mail: d.hempel@tu-bs.de

3.2 Development of the subproject

3.2.1 Report

3.2.1.1 Current knowledge at the last application and initial question

Due to their metabolic diversity, high production capacity, secretion efficiency, and capability of carrying out post-translational modifications, filamentous fungi like *Aspergillus niger* are widely exploited as efficient cell-factories in the production of metabolites, bioactive substances, native and heterologous proteins, respectively [*Archer, 2000; Lubertozzi and Keasling, 2009; Meyer, 2008; Papagianni, 2004*]. One of the most sensitive process parameters is the complex fungal morphology. **Fig. 1** shows different morphological forms of *Aspergillus*. Mycelial growth can be differentiated into micro- and macroscopic morphology [*Krull et al., 2010*]. In submerged cultivations, the observed macroscopic morphology of filamentous fungi varies from freely dispersed mycelium over loose mycelial clumps to dense pellets [*Casas López et al., 2005; Papagianni, 2004*].

Pellets are spherical aggregates consisting of a more or less dense, branched and partially intertwined network of hyphae [*Berovič et al., 1991*]. At times, the pellet type of morphology causes advantages in downstream processing because of the Newtonian flow behavior [*Atkinson and Daoud, 1976; Zhou et al., 2000*]. Pellet growth seems favourable for production of citric acid [*Gomez et al., 1988; Papagianni, 2004*], glucoamylase [*Lin et al., 2010*] or polygalacturonidase [*Hemmersdorfer et al., 1987*]. In these cultivations the mass transfer of oxygen and nutrients is considerably better and the subsequent separation of the pellets from the cultivation broth is simpler than in mycelia cultivations [*Reichl et al., 1992*]. However, concentration gradients within the pellet results in a depletion of nutrients, especially oxygen is limited in the central regions of the pellets [*Hille et al., 2005*].

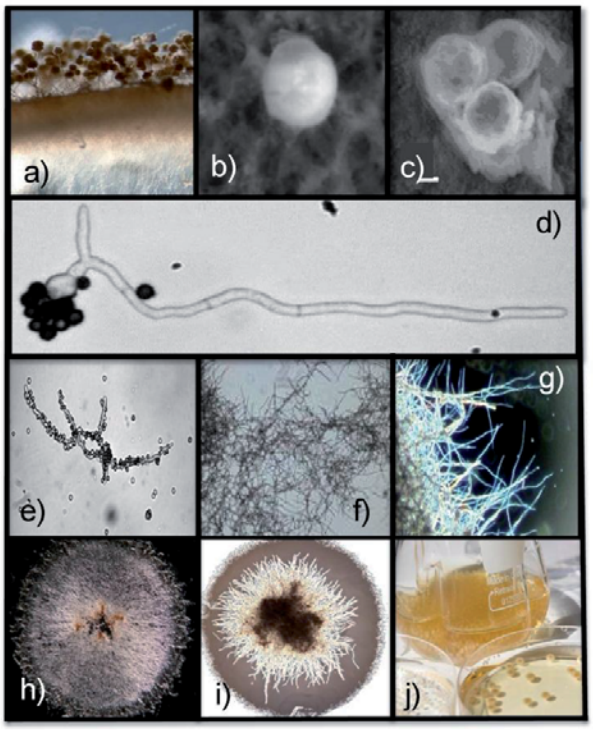

Fig. 1: Morphological forms of Aspergillus sp.: *a) profile view of conidiophores on solid agar medium, b) single spore (spore diameter approx. 5 µm), c) spore package, d) germinated tube, e) coagulated type of mycel, in which single ungerminated spores adhere to germinated hyphal tubes, f) dispersed mycel, g) exposed hyphae of a pellet ("pellet hair"), h) pellet slice (pellet diameter approx. 300 µm), i) hairy biopellet, and j) submerged biopellets.*

However, the use of freely dispersed mycelium in submerged cultures of fungi has found more application recently, due to the fact that this morphology enhances growth and production of several products. Mycelial growth is preferred for the formation of fumaric acid or amylase [*Gibbs et al., 2000*].

Recently, studies have demonstrated interesting biotechnological activities of fungal secondary metabolites, including antitumor, anti-inflammatory and cytotoxicic effects [*Liu et al., 2007*]. Filamentous microorgansims are also in focus for biotransformation of steroids, where free mycelium facilitates downstream processing, the production of enzymes such as amylase, neo-fructosyltransferase and phytase [*Teng et al., 2009*] or penicillin [*Vecht-Lifshitz et al., 1990*]. Filamentous growth increases the viscosity of the cultivation broth which results in temperature and concentration gradients within the bioreactor as a result of transfer limitations [*Kossen, 2000; Papagianni, 2004; Znidarsic and Pavko, 2001*].

Depending on the desired product, the suitable morphology for a given bioprocess varies and cannot be generalized. Because the optimal productivity correlates with a specific morphological form [*Kaup et al., 2008*], the advantages and disadvantages of mycelial or pellet cultivation should be carefully balanced for each biological system.

The morphological type and related physiology of fungal systems strongly depend on the environmental conditions in the bioreactor, i.e., the environome [*Krull et al., 2010*]. Among other factors, the variable environmental cultivation conditions such as the inoculum concentration, spore viability, pH-value, cultivation temperature, dissolved oxygen concentration, medium composition, mechanical stress and the process mode are mentioned [*Deckwer et al., 2006; Papagianni, 2004*].

Fig. 2 illustrates a biotechnological process with the morphology of the biological system influenced by the environome [*Wucherpfennig et al., 2010*]. Morphology and environome as main process parameters are located in the center of the triangle, as they have an influence on the overall process performance. Productivity is placed on the top of the triangle because it is the central parameter to be optimized. Broth rheology and biomass growth form the base of the triangle. Broth rheology causes mixing problems, which may inhibit cell growth. Product formation is closely related to the form of biomass growth as the product is mainly expressed at the tips of the hyphae. Optimized growth leads to extensive product formation and therefore to high productivity. Furthermore, the rheology of the broth has an impact on the purification of the product as high viscosities complicate its recovery. A laborious and expensive purification procedure in turn leads to an overall uneconomical production.

In this regard, the task of subproject B3 was to show the influence of the environome on the fungal morphology of *A. niger* and to generate process tools to control morphology shape for optimal productivity.

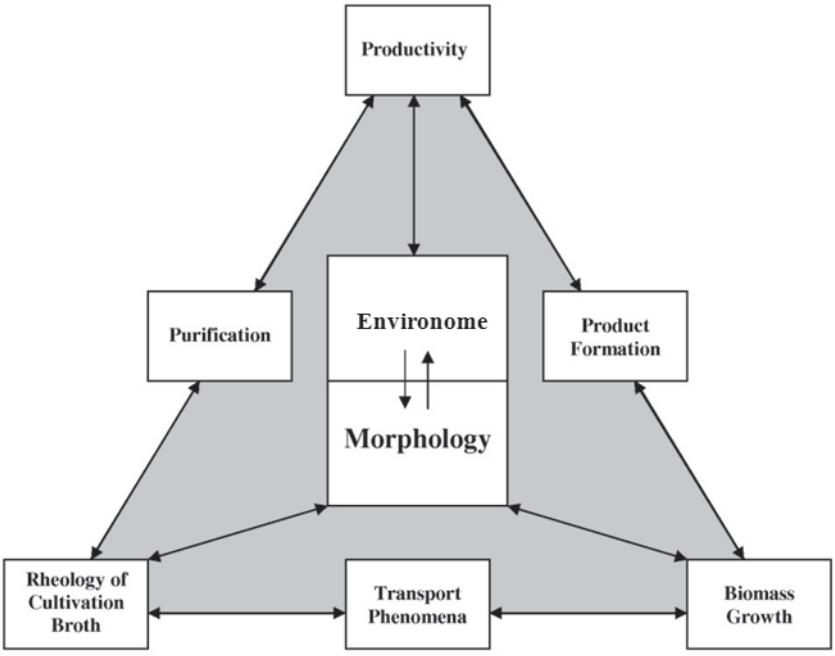

*Fig. 2: Schematic illustration of a biotechnological process with filamentous microorganisms [*Wucherpfennig et al., 2010*].*

3.2.1.2 Results and applied methods

Effect of volumetric power input on pellet morphology

The different impact of volumetric power input by aeration and by agitation, respectively, on pellet morphological developments and on product formation *A. niger* AB1.13 was examined for a constant total volumetric power input by combination of the induced power input by aeration and agitation by Lin et al. (*2010*). To investigate the internal pellet structure, pellet slicing was applied. The images of *A. niger* pellets slices (thickness of

70 µm) from the equatorial region, cultivated at different mechanical stresses of stirring and aeration, are shown in **Fig. 3**.

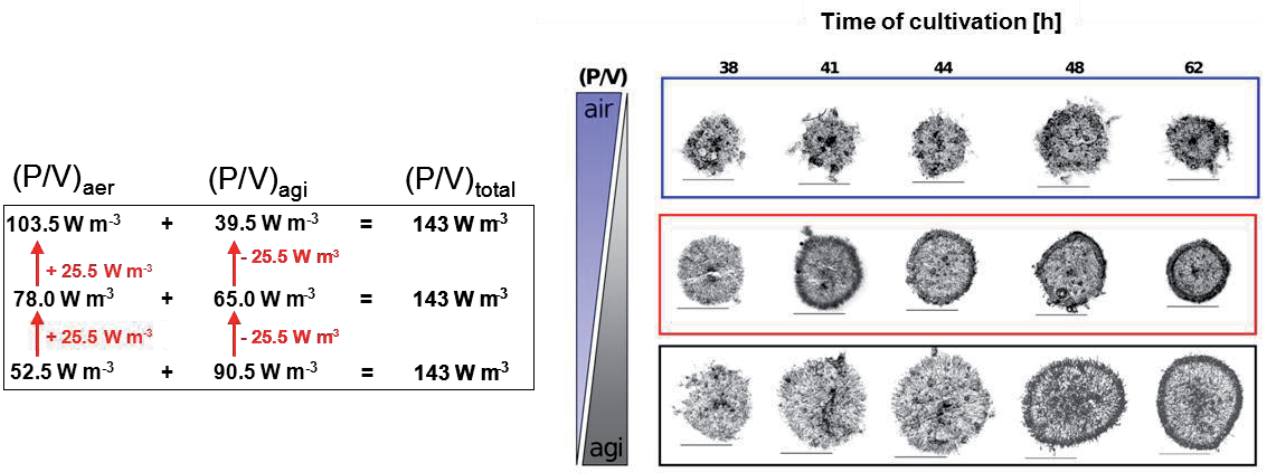

Fig. 3: Microscopic images of pellet slices over the cultivation time of A. niger *AB1.13 in a stirred bioreactor at different combinations of volumetric power input P/V (aeration [aer] and agitation [agi]) of the total volumetric power input of 143 W m^{-3} (bottom row: 52 [aer] + 91 [agi] W m^{-3}, middle row: 78 [aer] + 65 [agi] W m^{-3}, upper row: 103 [aer] + 40 [agi] W m^{-3}), scale bar: 500 µm [*Lin et al., 2010*].*

Biopellets at the highest aeration were relatively unstructured and irregular at the periphery and had a much larger structure overall. In contrast, those pellets that were treated with increased agitation ratios were rather circular and have a more compact pellet surface structure.

To determine the influence of volumetric power input on pellet micro morphology in more detail, sedimentation velocities were measured and correlated graphically with the theoretically calculated sedimentation velocities of ideal smooth spheres of the same diameter and mean density (**Fig. 4**). Depending on the pellet surface structure, the trend lines exhibit different slopes. The slope of the trend line is proportional to the compactness of the pellet surface structure [*Hille, 2008*]. Thus, a larger slope value can be interpreted as a higher compactness of the pellet periphery. The diagonal line has a slope of one, which indicates that the pellets have a perfectly spherical and compact shape. The periphery of the pellets which were treated with the highest share of aeration was the least compact, whereas the pellets treated with a lower share of the aeration showed much more compact pellet surface structures.

The resulting pellet sizes revealed important aspects of the different impacts of the volumetric power input on pellet macro morphology. A decrease in aeration could not be compensated by an increase in agitation of the same amount. The increase in the share in the aeration-induced volumetric power input led to greater mechanical stress and therefore to smaller pellets and a higher pellet concentration. The volumetric power input by aeration was thus proven to have a more distinct effect on pellet macro morphology than the volumetric power input by agitation. This finding was in good agreement with the investigations of mechanical stress based on an inorganic clay polymer floc system where

the volumetric power input by aeration was shown to generate higher mechanical stress than the agitation-induced volumetric power input [*Stintzing et al., 2008*].

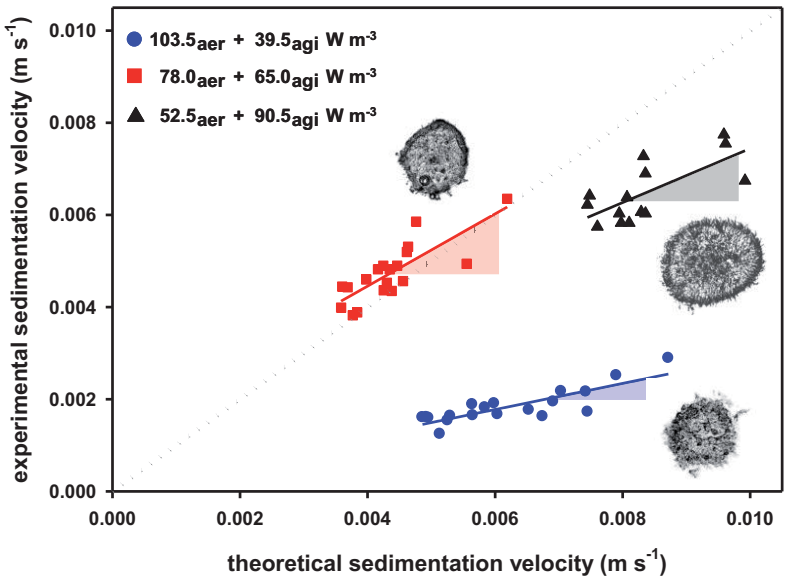

Fig. 4: Correlation between experimentally determined and theoretically calculated sedimentation velocity of A. niger AB1.13 *pellets after 48 h of cultivation at different combinations of the total volumetric power input of 143 W m^{-3} (aer: aeration; agi: agitation) [*Lin et al., 2010*].*

Effect of osmolality on *A. niger* productivity

A sophisticated way to tailor-make fungal morphology was investigated by manipulation of osmolality within the culture medium. Increased NaCl concentrations led to mycelial growth and enhanced productivity for *A. niger* AB1.13 and SKAn1015 [*Wucherpfennig et al., 2011*]. The morphology and productivity of both strains was shown to be considerably influenced by osmotic pressure. In all cases, the increased osmolality led to stronger mycelial growth.

The specific productivity of the fructofuranosidase-producing strain *A. niger* SKAn1015 could be increased approximately 18-fold from 0.5 to 9 U mg^{-1} h^{-1} (**Fig. 5**). The specific productivity of the glucoamylase-producing strain *A. niger* AB1.13 could be elevated using the same procedure. However, the observed changes in productivity might not be due to the change in morphology alone. The external parameter of osmolality might have affected the fungal physiology which could in turn affect the morphology independently. The increase in the observed productivity was shown to correlate with the active surface area. This approach is a nice complementation of the microparticle based morphology engineering developed in cooperation with subproject B11 (Wittmann).

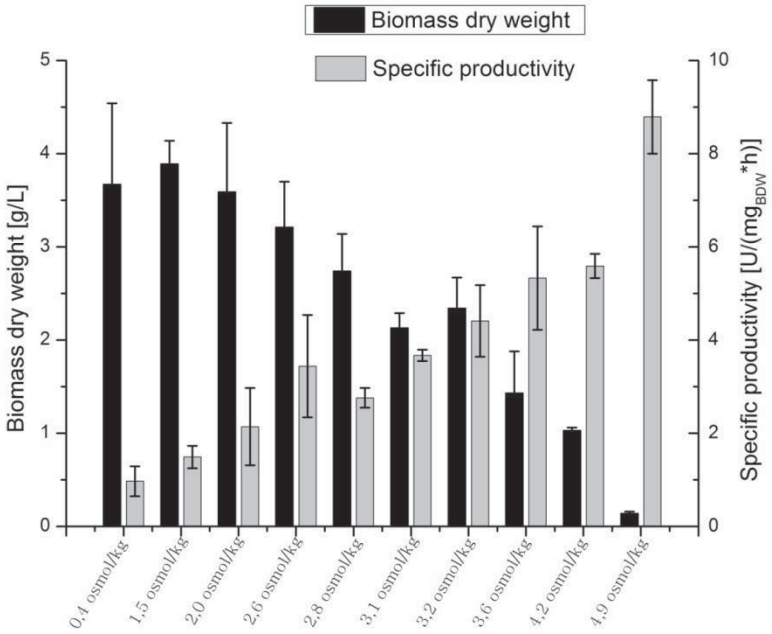

Fig. 5: Influence of osmolality on A. niger *SKAn1015 productivity: Biomass dry weight (black) and specific productivity (grey) after 72 h of cultivation are depicted at different culture broth osmolalities [*Wucherpfennig et al., 2011*].*

Characterization of fungal morphology

A macro morphologic approach was chosen for characterization of fungal morphology. Since mycelial morphology as investigated was in clumps or pellets, parameters of particle size and shape, like projected area, perimeter, circularity, solidity and aspect ratio were applied. Circularity is a parameter to quantify the closeness to a perfect circle. It is calculated as $4\pi \times [\text{area}] \times [\text{perimeter}]^{-2}$, with a value of 1.0 indicating a perfect circle and an irregular object having a value close to 0. Solidity is a measure of the surface of a particle, also known as roughness. It is calculated by dividing the projected area through the convex area. The convex area being the area enveloped by the convex hull perimeter which can be illustrated as an elastic band placed around the particle determined by the software. A smooth shape has solidity of 1.0. Irregular objects tend to have a much lower value for solidity. Solidity is a good approximation of the surface area of the fungal pellet being available for mass transport. Aspect ratio is defined as major axis divided by minor axis and is a measure of elongation of a particle. A shape symmetrical in all axes such as a circle or square will have an elongation value of 1.0 whereas elongated particles will possess considerably larger values.

Fig. 6A reveals an influence of osmolality on pellets size. The projected area of *A. niger* SKAn1015 declined with an increase in osmolality up to 4.2 osmol kg^{-1}. The standard deviation between the measured particles decreased, confirming the culture to be more homogenous at higher osmolalities. At an osmolality of 4.9 osmol kg^{-1} a perfect mycelial morphology was found. In **Fig. 6B**, the influence of osmolality on parameters of particle shape is depicted. Aspect ratio and solidity correlate well with osmolality. The parameter

circularity is not significantly influenced by the raised osmotic pressure. Fungal particles get more elongated and their surface tends to be rougher at higher osmolality. The parameter solidity describes the particle roughness, and therefore the active surface of the clump or pellet. At higher concentrations of NaCl fungal particles have considerably more active area. At 4.2 osmol kg^{-1} loose mycelial clumps were observed. An osmolality beyond that led to a pure mycelial morphology without any clumps or pellets.

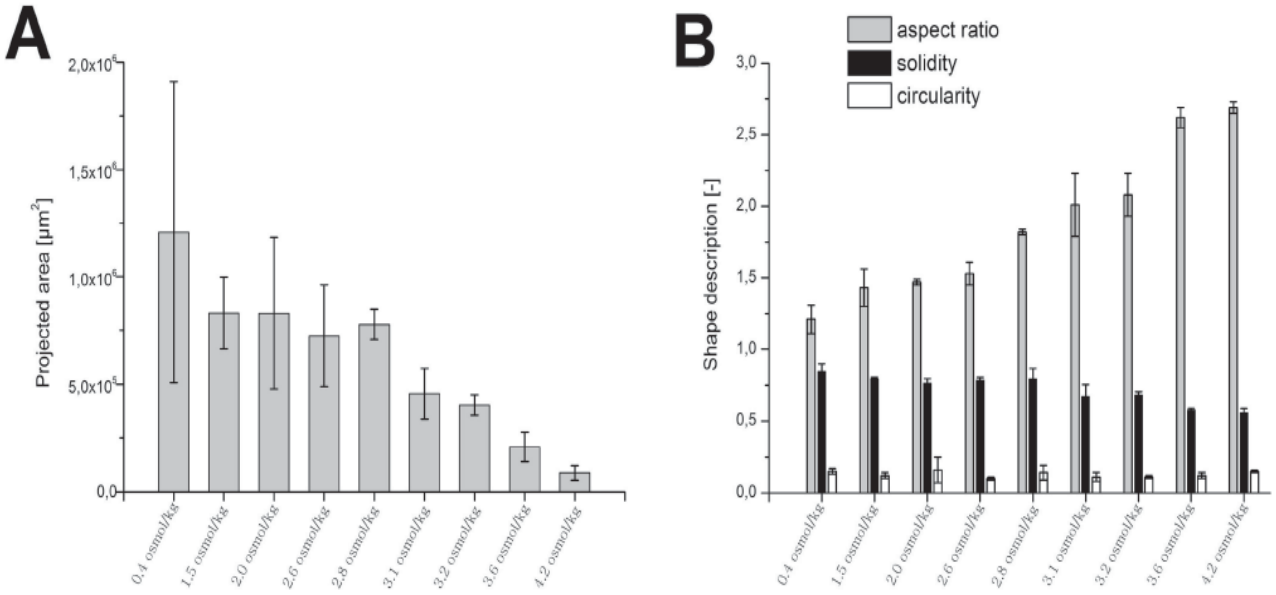

Fig. 6: Morphological change of A. niger *SKAn1015 induced by osmolality: (A) Projected area as determined by automatic image analysis is shown at different culture broth osmolalities. (B) Display of aspect ratio (grey), solidity (black) and circularity (white) as measured by automated image analysis with ImageJ 1.44m [*Wucherpfennig et al., 2011*].*

Correlation of fungal morphology and productivity

Since earlier results suggested an obvious correlation between fungal morphology and protein secretion, it was an objective in this project to link productivity to morphologic appearance. Several parameters obtained by automatic image analysis as projected area, solidity and aspect ratio changed significantly with increased osmolality. However, too many parameters make quick assessment of fungal morphology complicated. Therefore, an effort was undergone to combine parameters from image analysis to a dimensionless morphology number (MN) which can be used for a holistic characterization of morphology. Filamentous fungi can either grow as pellets or as mycelia. Between these extremes there is a whole span of intermediates as elongated irregular pellets or clumps. Accordingly, the following formula was introduced to combine the relevant morphological parameters observed

$$Morphology\ Number \equiv \frac{2 \cdot \sqrt{Projected\ area} \cdot Solidity}{\sqrt{\pi} \cdot D_{max} \cdot Aspect\ ratio}$$

with D_{max} as the maximal pellet diameter. Perfectly round and smooth pellets will in microscopic images appear as perfect circles. For such particles MN has a value of 1.0. The smallest fragment of mycelial morphology can be simplified as a one-dimensional line

yielding a MN of zero. All intermediate morphological forms will therefore have values between 0 and 1.0. A good correlation (R^2 = 0.9) is obtained when plotting the specific productivity of all *A. niger* SKAn1015 cultivations versus MN (**Fig. 7**).

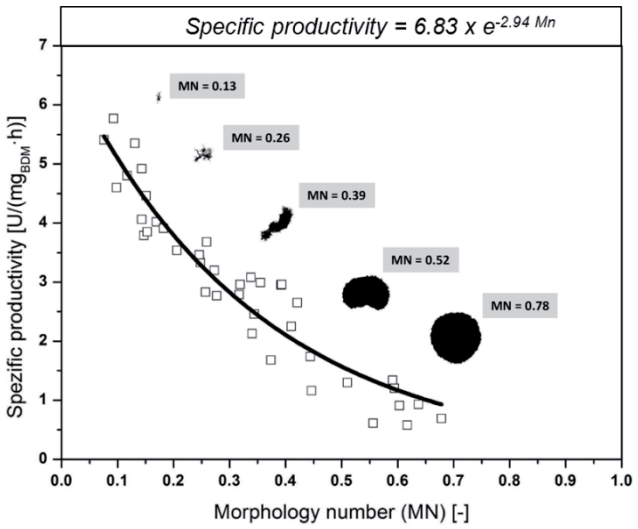

Fig. 7: Correlation of specific productivity and fungal morphology using the morphology number (MN) of the fructofuranosidase producing strain A. niger *SKAn1015 (redrawn from* Wucherpfennig et al. (2011)*).*

Correlation of fungal morphology, rheology and productivity

To investigate the influence of fungal morphology on rheological parameters independent from biomass, culture broth from different cultivations after 65 h of cultivation with pellet, mycelial and intermediate morphology was collected. Subsamples with differing biomass between 0.3 and 9 g L^{-1} bio dry weight (BDW) but equal morphology were created. The rheology and mycelial morphology of each subsample were determined. The rheological parameters of the consistency index K and the flow index n were determined using the Ostwald-de Waele model and correlated with the BDW concentration (**Fig. 8**).

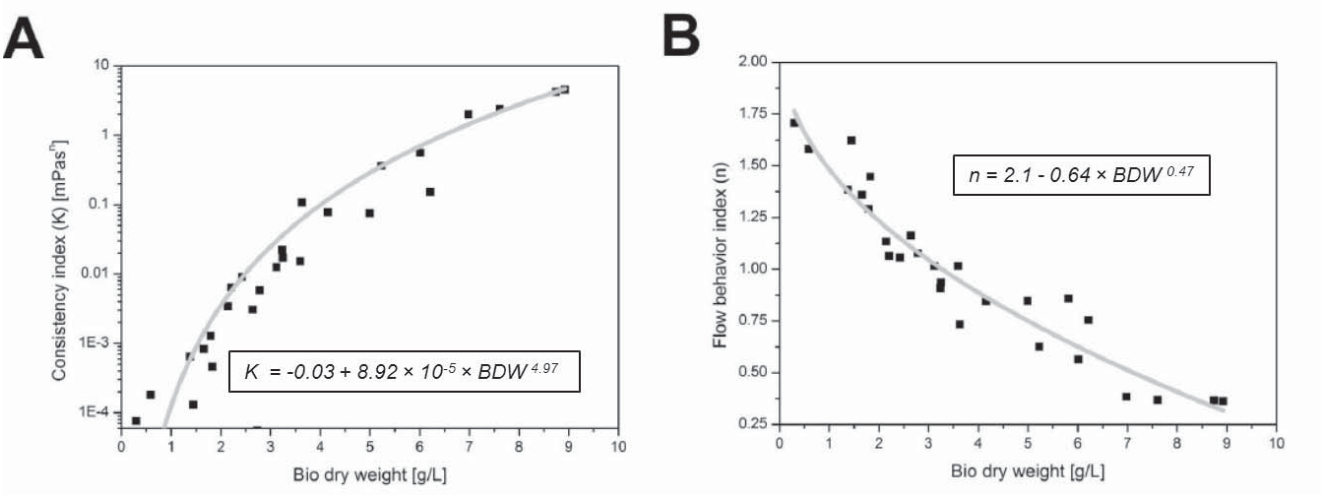

Fig. 8: Influence of biomass dry weight concentration on rheological parameters derived from the Ostwald-de Waele model of strain A. niger *SKAn1015: (A) Consistency index K and (B) Flow behavior index n vs. bio dry weight.*

Through these correlations a theoretical rheological parameter set for every BDW concentration can be calculated. A similar correlation for both rheological parameters was found in the study of Ruohang and Webb (*1995*). The quotient of the measured rheological parameter (K or n) divided by the corresponding theoretical rheological parameter, gained by correlation, is subsequently displayed with a subscript BDW. The rheological K_{BDW} and n_{BDW} can be used to examine the influence of morphology independent of biomass (**Fig. 9**).

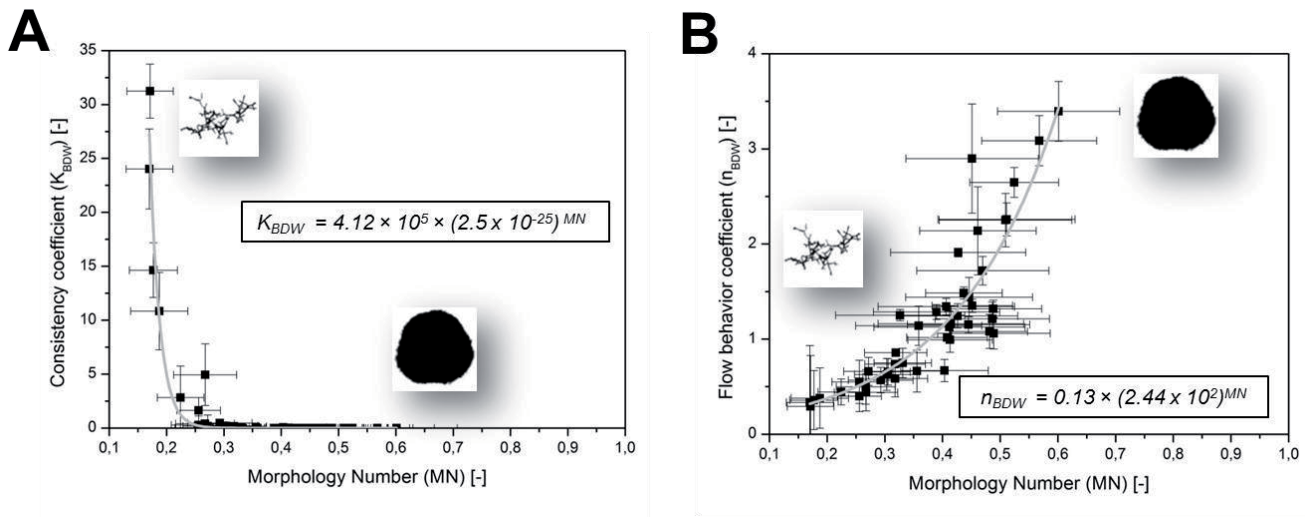

Fig. 9: Consistency coefficient K_{BDW} (A) and flow behavior coefficient n_{BDW} (B) are depicted over morphology number MN.

While specific productivity most commonly is the parameter which is strived to be improved during process development, the total productivity with consideration of product purification is equally important and should be taken into account. In the case of filamentous fungi a dispersed morphology leads to an increased specific productivity while impairing transport properties through increased culture broth viscosity. Therefore, it is beneficial to have one model for estimation of both, productivity and flow behavior of culture broth. Thus, the introduced parameter MN is used to assess the rheological coefficients K_{BDW} and n_{BDW}.

Through comparison of morphological and rheological data it becomes evident that a filamentous morphology of *A. niger* is most productive but also exhibits the highest culture broth viscosity. Since both traits fructofuranosidase activity and viscosity seem to change in conjunction it seems feasible to estimate fructofuranosidase activity from rheological data. In **Fig. 10** specific fructofuranosidase activity is plotted over n_{BDW}. Predicted and actual values of fructofuranosidase activity show a good conformance for this correlation.

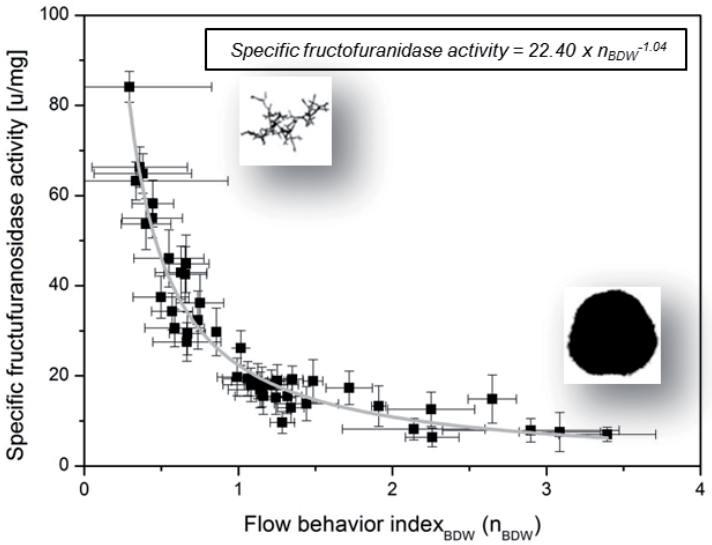

Fig. 10: Specific fructofuranosidase activity correlated with flow behavior coefficient n_{BDW}.

Numerical simulation of mechanical stress

One of important parameters which influences the morphology is the mechanical stress induced by either stirring or aeration. Computational Fluid Dynamics (CFD) facilitates the quantification of the stress due to turbulent fluctuations, namely the Reynolds stress, and characterization of flow pattern throughout the reactor by using appropriate turbulence models (Reynolds Stress Model, RSM) [*Eslahpazir et al., 2010*]. To refer the numerical simulation to the cultivation process in stirred tank reactor (STR) parallel investigations have been undertaken concerning disintegration kinetics of a shear sensitive inorganic polymer floc system [*Stintzing et al., 2008*] and with pellets of *A. niger*.

The local kinetic energy dissipation rate ε and the Reynolds normal and shear stresses were investigated for a 2 L STR with a double Rushton turbine at an agitation rate of 400 min^{-1}. The mean bubble diameter was set equal to 3 mm. An unstructured grid for both single- and multi-phase flows with approximately 700,000 grid cells was applied and the convergence criteria were set for all RMS-residues less than 10^{-4}. The ANSYS CFX solver was used to obtain the results. The Speziale, Sarkar and Gatski (SSG) Reynolds Stress Model (RSM) [*Speziale et al., 1991*] and the SST-Reynolds Transport turbulence model [*Wilcox, 2000*] were chosen for single- and multi-phase simulations, respectively.

As depicted in **Fig. 11**, the maximum value of kinetic energy dissipation rate was much higher in the binary (water/air) system in comparison to the single-phase system (water). The maximum in the binary flow occurs right at the air inlet where the liquid phase instantaneously incurs a high momentum leading to rapid loss of kinetic energy. The main reason for this behavior is the larger inertial forces of water and compared with air preventing the water flow of being fully affected by low gassing rate. However, the higher maxima of ε in binary flow influenced the volume integral of kinetic energy dissipation only in a marginal manner. The volume integral of the binary system is approximately 70 % lower in comparison to the single-phase system with 0.113 m^2 s^{-3} confirming the fact that less energy is needed to stir the water/air-system.

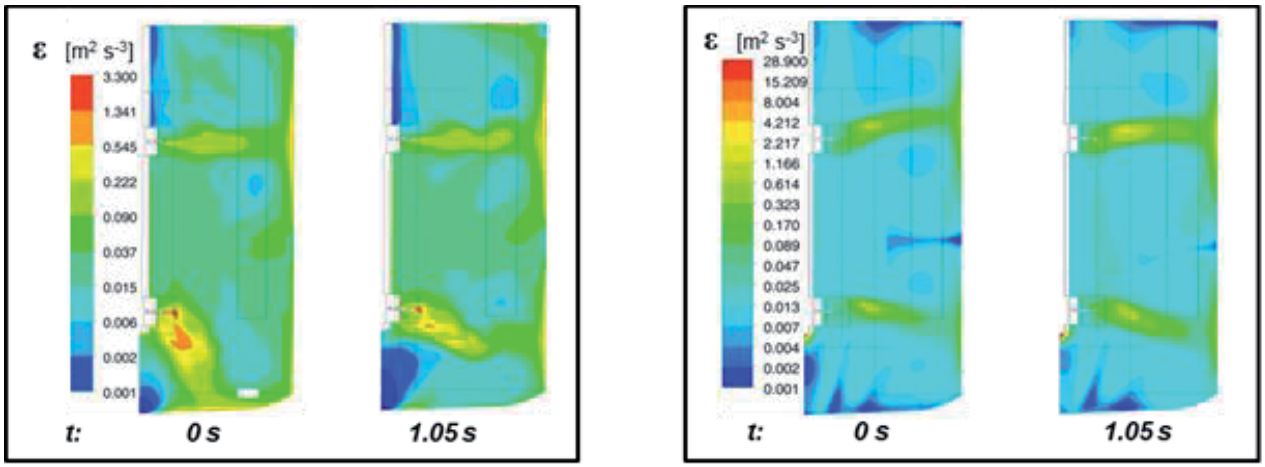

Fig. 11: Kinetic energy dissipation rate ε (left box: single-phase, right box: multi-phase, 0 s: steady-state, 1.05 s: transient flow)

Furthermore, the normal- (τ_{yy}) and shear Reynolds stresses (τ_{yz}) are depicted in **Fig. 12.** The maxima and minima are much larger at the air inclusion region right underneath the shaft which implies a high gradient region in terms of velocity and energy dissipation rate. Apart from this, in the bulk flow, the absolute values of both stress components are higher in the single-phase system and this is consistent with the dissipated kinetic energy.

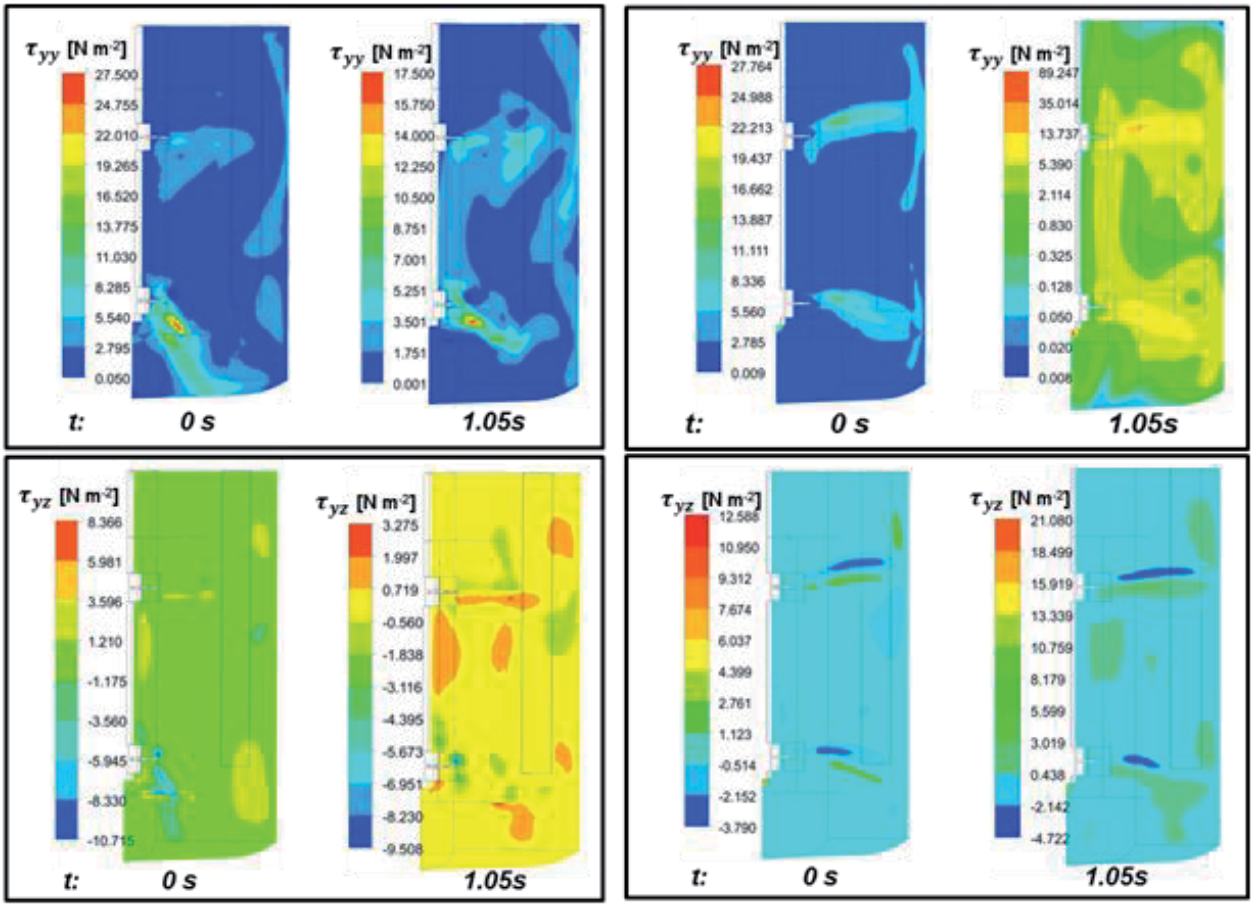

Fig. 12: left box: Reynolds stresses in single-phase system (water); right box: Reynolds stresses in binary system (water/air).

Mechanical stress in stirred tank reactor

The experimental mechanical stress in stirred tank reactor was previously determined according to Stintzing et al. (*2008*) based on floc size distribution and its time dependence at certain volumetric power inputs with focused beam reflectance measurement (FBRM) using a shear sensitive inorganic polymer floc system. These results were now compared by a floc size reduction under defined mechanical stress in a Couette shear gap device. **Fig. 13** compares the experimental mechanical stress data with calculated results of applying the mean normal stress based on volumetric mean of turbulent kinetic energy in a single-phase (water) STR-system [*Appel, 2010*]. The measured stress in the STR comprises all stress components and hence differs from the calculated one. At lower volumetric power inputs the shear forces are significantly higher than normal forces implying a higher difference between measured and calculated stresses. The main cause of this difference is mainly the fact that, if the stirrer speed is relatively low, i.e. the fluid velocity is low, then it is similar to the case that the shear forces act like friction in normal motion. The lower the velocity, the higher are the friction forces. If the fluid moves more rapidly the shear forces are less influential and the gap between normal and total stresses are less significant.

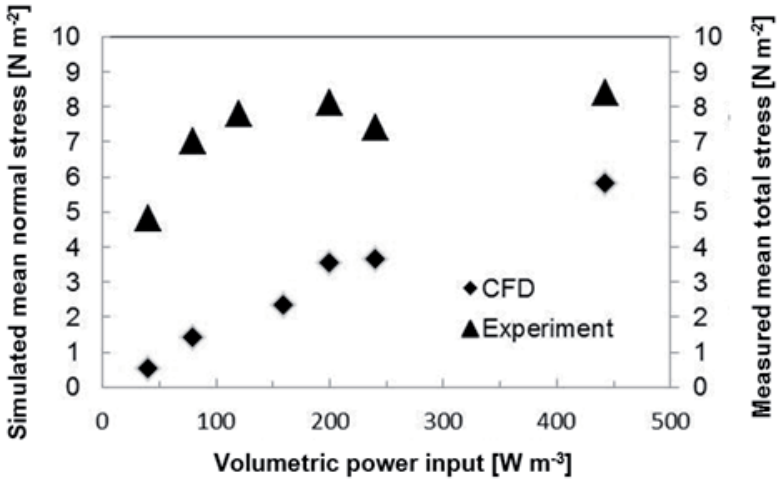

Figure 13: Simulated mean normal stress and measured mean total stress over the volumetric power input.

The analysis of the results also allows a hypothetical explanation of size reduction mechanisms: apparently, the cells are first deformed by normal tension forces and subsequently the shear stresses accomplish the size reduction by their erosive effects.

3.2.1.3 References to other works and collaborations in the SFB

The research collaborations interacted with the subprojects A1 (Jahn/Dersch), B4 (Jahn/Nörtemann/Jänsch), B7 (Kwade/Kampen) and B11 (Wittmann) of the SFB. A cooperation was carried out with subprojects A1 (Jahn/Dersch) on the transfer of the fructofuranosidase producing strain *A. niger* SKAn1015, with B4 (Jahn/Nörtemann/ Jänsch) to gain a better understanding of the molecular and cell biology of the filamentous microorganisms [*Krull et al., 2010*], with B7 (Kwade/Kampen) on characterization of fungal

growth conditions, morphology, mechanical behavior and product formation [*Priegnitz et al., 2012; Krull et al., 2010*] and with B11 (Wittmann) on analysis and engineering of fungal morphology [*Driouch et al., 2012; Eslahpazir et al., 2011; Wucherpfennig et al., 2010 and 2012*]. An industrial cooperation on the development of indicators for the production and quality of filamentous seed cultures and the influence of the sporulation conditions was established with Bayer Pharma AG, Bergkamen.

3.2.1.4 Comparison with research outside the SFB

Due to their high industrial relevance the past years have seen a substantial development of tools and techniques to characterize the growth of fungi and obtain quantitative estimates on their morphological properties. Advances in particle and image analysis and in micromechanical devices have provided quantitative morphological data. Wucherpfennig et al. (*2010*) described the current state on morphology and growth of filamentous fungi with special attention given to specific problems as they arise from fungal growth forms and the mass transfer in fungal bio-pellets. To emphasize the importance of the flow behavior of filamentous cultivation broths the most important rheological models and recent studies concerning rheological parameters were reviewed. Furthermore, current knowledge on morphology and productivity in relation to the environome was outlined.

From the engineering point of view, a distinct fungal morphology has to be controlled by defined environmental conditions. There are several experimental approaches in the literature, which focus on variations in the environome, changing the most important operating parameters such as the spore concentration (e.g., *Bizukojc and Ledakowicz, 2010; Liu et al., 2008; Papagianni and Mattey, 2006*), pH value and pH shifting (e.g., *Bizukojc and Ledakowicz, 2009; Papagianni, 2004*) and mechanical stress due to power input by agitation and/or aeration (e.g., *Amanullah et al., 2002; Casas López et al., 2005; Nielsen and Krabben, 1995; Wang et al., 2003; Henzler, 2000*), cultivation temperature (e.g., *Liu et al., 2008*) or medium composition (e.g., *Liu et al., 2008; Papagianni and Mattey, 2004; Znidarsic et al., 2000*). A pioneering contribution towards the customization of filamentous morphology was the addition of KCl to increase the protein secretion of *A. niger* mycelia by Bobowicz-Lassociska et al. (*1995*). In addition, Fiedurek (*1997*) was able to increase the activity of *A. niger* produced glucose oxidase 2-fold by adding NaCl to centrifuged mycelia, thereby administering an osmotic shock to the fungus.

3.2.1.5 Literature

Amanullah, A.; Christensen, L.H.; Hansen, K.; Nienow, A.W.; Thomas, C.R. (2002) Dependence of morphology on agitation intensity in fed-batch cultures of *Aspergillus oryzae* and its implications for recombinant protein production. *Biotechnol. Bioeng.* 77, 815-826

Archer, D.B. (2000) Filamentous fungi as microbial cell factories for food use. *Curr. Opin. Biotechnol.* 11, 478-483

Atkinson, B.; Daoud, I. (1976) Microbial floes and flocculation in fermentation process engineering. *Adv. Biochem. Eng./Biotechnol.* 4, 41-124

Berovič, M.; Cimerman, A.; Steiner W.; Koloini T. (1991) Submerged citric acid fermentation: rheological properties of *Aspergillus niger* broth in a stirred tank reactor. *Appl. Microbiol. Biotechnol.* 34, 579-581

Bizukojc, M.; Ledakowicz, S. (2009) Physiological, morphological and kinetic aspects of lovastatin biosynthesis by *Aspergillus terreus*. *Biotechnol. J.* 4, 647-664

Bizukojc, M.; Ledakowicz, S. (2010) The morphological and physiological evolution of *Aspergillus terreus* mycelium in the submerged culture and its relation to the formation of secondary metabolites. *World J. Microb. Biot.* 26, 41-54

Bobowicz-Lassociska, T.; Grajek, W. (1995) Changes in protein secretion of *Aspergillus niger* caused by the reduction of the water activity by potassium chloride. *Acta Biotechnol.* 15, 277-287

Casas López, J.L.; Sánchez Pérez, J.A.; Fernández Sevilla, J.M.; Rodríguez Porcel, E.M.; Chisti, Y. (2005) Pellet morphology, culture rheology and lovastatin production in cultures of *Aspergillus terreus*. *J. Biotechnol.* 116, 61-77

Deckwer, W.D.; Jahn, D.; Hempel, S.C.; Zeng, A.P. (2006) System biology approach to bioprocess development. *Life Sci. Eng.* 6, 455-469

Fiedurek, J. (1998) Effect of osmotic stress on glucose oxidase production and secretion by *Aspergillus niger*. *J. Basic Microbiol.* 38, 107-112

Gibbs, P.A.; Seviour, R.J.; Schmid, F. (2000) Growth of filamentous fungi in submerged culture: Problems and possible solutions. *Crit. Rev. Biotechnol.* 20, 17-48

Hemmersdorfer, H.; Leuchtenberger, A.; Wardsack, C.; Ruttloff, H. (1987) Influence of culture conditions on mycelial structure and polygalactorunidase synthesis of *Aspergillus niger*. *J. Basic Microbiol.* 27, 309-315

Henzler, H.-J. (2000) Particle stress in bioreactors. In: Influence on Stress on Cell Growth and Product Formation, Series: Scheper, T. (ed.), *Adv. Biochem. Eng./Biotechnol.* 67, 35-82

Hille, A.; Neu, T.R.; Hempel, D.C.; Horn, H. (2005) Oxygen profiles and biomass distribution in biopellets of *Aspergillus niger*. *Biotechnol. Bioeng.* 92, 614-623

Hille, A. (2008) Stofftransport- und Stoffumsatzprozesse in filamentösen Pilzpellets. In: ibvt-Schriftenreihe, Band 32, Hempel, D.C. (Hrsg.), *FIT-Verlag für Innovation und Technologietransfer*, Paderborn, ISBN 978-3-932252-38-9, zgl. Dissertation TU Braunschweig

Kaup, B.A.; Ehrich, K.; Pescheck, M.; Schrader, J. (2008) Microparticle-enhanced cultivation of filamentous microorganisms: Increased chloroperoxidase formation by *Caldariomyces fumago* as an example. *Biotechnol. Bioeng.* 99, 491-498

Kossen, N.W. (2000) The morphology of filamentous fungi. *Adv. Biochem. Eng./Biotechnol.* 70, 1-33

Liu, J.; Shimizu, K.; Konishi, F.; Noda, K.; Kumamoto, S.; Kurashiki, K.; Kondo, R. (2007) Antiandrogenic activities of the triterpenoids fraction of *Ganoderma lucidum*. *Food Chem.* 100, 1691-1696

Liu, Y., Liao, W., Chenet, S., (2008) Study of pellet formation of filamentous fungi *Rhizopus oryzae* using a multiple logistic regression model. *Biotechnol. Bioeng.* 99, 117-128

Lubertozzi, D.; Keasling, J.D. (2009) Developing *Aspergillus* as a host for heterologous expression. *Biotechnol. Adv.* 27, 53-75

Meyer, V. (2008) Genetic engineering of filamentous fungi – Progress, obstacles and future trends. *Biotechnol. Adv.* 26, 177-185

Nielsen, J., Krabben, P., (1995) Hyphal growth and fragmentation of *Penicillium chrysogenum* in submerged cultures. *Biotechnol. Bioeng.* 46, 588-598

Oncu, S.; Tari, C.; Unluturk, S. (2007) Effect of Various Process Parameters on Morphology, Rheology, and Polygalacturonase Production by *Aspergillus sojae* in a Batch Bioreactor. *Biotechnol. Progr.* 23, 836-845

Papagianni, M., (2004) Fungal morphology and metabolite production in submerged mycelial processes. *Biotechnol. Adv.* 22, 189-259

Papagianni, M.; Mattey, M. (2004) Physiological aspects of free and immobilized *Aspergillus niger* cultures producing citric acid under various glucose concentrations. *Process. Biochem.* 39, 1963-1970

Reichl, U., King; R.; Gilles, E.D. (1992) Characterization of pellet morphology during submerged *Streptomyces tendae* by image analysis. *Biotechnol. Bioeng.* 39, 164-170

Ruohang, W.; Webb, C. (1995) Effect of Cell Concentration on the Rheology of Glucoamylase Fermentation Broth. *Biotechnol. Tech.* 9, 55-58

Speziale, C.G.; Sarkar, S., Gatski, T. (1991) Modeling the pressure-strain correlation of turbulence: an invariant dynamical systems approach. *J. Fluid Mech.* 227, 245-272

Teng, Y.; Xu, Y.; Wang, D. (2009) Changes in morphology of *Rhizopus chinensis* in submerged fermentation and their effect on production of mycelium-bound lipase. *Bioprocess Biosyst. Eng.* 32, 397-405

Vecht-Lifshitz, S.E.; Magdassi, S.; Braun, S. (1990) Pellet formation and cellular aggregation in *Streptomyces tendae*. *Biotechnol. Bioeng.* 35, 890-896

Wang, L.; Ridgway, D.; Gu, T.; Moo-Young, M. (2003) Effects of process parameters on heterologous protein production in *Aspergillus niger* fermentation. *J. Chem. Technol. Biotechnol.* 78, 1259-1266

Wilcox, D.C. (1988) Reassessment of the scale-determining equation for advanced turbulence models. *AIAA J.* 26, 1299-1310

Zhang, Z.; Jin, B.; Kelly, J (2007) Effects of cultivation parameters on the morphology of *Rhizopus arrhizus* and the lactic acid production in a bubble column reactor. *Eng. Life Sci.* 7, 490-496

Zhou, Y.; Du, J.X.; Tsao, G.T. (2000) Mycelial pellet formation by *Rhizopus oryzae* ATCC20344. *Appl. Biochem. Biotechnol.* 84-86, 779-789

Znidarsic, P.; Pavko, A. (2001) The morphology of filamentous fungi in submerged cultivations as a bioprocess parameter. *Food Technol. Biotechnol.* 39, 237-252

3.2.2 Project relevant own publications

a) Works that have appeared in publications of a scientific quality assurance at the time of application or final adoption, and book publications

Driouch, H.; Hänsch, R.; Wucherpfennig, T.; Krull, R.; Wittmann, C. (2012) Improved enzyme production bysuperior bio-pellets of *Aspergillus niger* - Targeted morphology engineering using titanate micro particles. *Biotech. Bioeng*. 109, 462-471

Eslahpazir Esfandabadi, M.; Hempel, D. C.; Krull, R. (2010) CFD-Anwendungen für Rührkesselreaktoren in der Bioverfahrenstechnik. *Chem. Ing. Tech.* 82, 229-241

Lin, P.-J.; Scholz, A.; Krull, R.(2010) Effect of volumetric power input by aeration and agitation on pellet morphology and product formation of *Aspergillus niger. Biochem. Eng. J.* 49, 213-220

Priegnitz, B.-E.; Wargenau, A.; Brandt, U.; Rohde, M.; Dietrich, S.; Krull, R.; Fleißner, A. (2012) The role of initial spore adhesion in pellet and biofilm formation in *Aspergillus niger. Fung. Genet. Biol.* 23, 23-34

Stintzing. A.; Pilz, R.; Hempel, D. C.; Krull, R. (2008) Mechanische Beanspruchungen in Mehrphasen-reaktoren. *Chem. Ing. Tech.* 80, 1837-1842

Wucherpfennig, T., Hestler, T., Krull, R. (2011) Morphology engineering – Osmolality and its effect on*Aspergillus niger* morphology and productivity. *Microb. Cell Fact.* 10, 323-348

Wucherpfennig, T.; Lakowitz, A.; Driouch, H.; Krull, R.; Wittmann, C. (2012) Customization of *Aspergillus niger* morphology through addition of talc microparticles. *J. Vis. Exp.,* in press, e4023, DOI: 10.3791/4023

b) Other publications

Appel, C. (2010) Numerische Simulation der Strömung in Bioreaktoren. In: ibvt-Schriftenreihe, Band 44, Hempel, D.C. (Hrsg.), *FIT-Verlag für Innovation und Technologietransfer*, Paderborn, ISBN 978-3-932252-53-2, also PhD-thesis TU Braunschweig

Eslahpazir, M.; Wittmann, C.; Krull, R. (2011) Computational Fluid Dynamics. In: *Comprehensive Biotechnology*, Second Edition (Moo-Young, M.; ed. in chief), Vol. 2, 1027-1038, Elsevier

Kiep, K.A. (2010) Einfluss des Environoms auf die Morphologie und Produktbildung von *Aspergillus niger.* In: ibvt-Schriftenreihe, Band 53, Wittmann, C. (Hrsg.), Cuvillier-Verlag Göttingen, ISBN 978-3-86955-679-6, also PhD-thesis TU Braunschweig

Krull, R.; Cordes, C.; Horn, H.; Kampen, I.; Kwade, A.; Neu, T.R.; Nörtemann, B. (2010) Morphology of filamentous fungi - Linking cellular biology to process engineering using *Aspergillus niger*. In: Biosystems Engineering II – Linking Cellular Networks and Bioprocesses, Series: *Adv. Biochem. Eng./ Biotechnol.*, Vol. 121, Scheper, T. (Series Ed.), Wittmann, C.; Krull, R. (Vol. Eds.), ISBN 978-3-642-13865-2,1-21, Springer Verlag, Heidelberg

Wucherpfennig, T.; Kiep, K.A.; Driouch, H.; Wittmann, C.; Krull, R. (2010) Morphology and rheology in filamentous cultivations. In: *Adv. Appl. Microbiol*., Vol. 72, Chapter 4, Laskin, A. I.; Sariaslani, S.; Gadd, G. M. (eds.), ISBN: 978-0-12-380989-6, Academic Press 72, 89-133, Elsevier

3.3 Looking back on the promotion

The project has been funded since July 2001 in the SFB 578. It was completed on June 2012 with the end of the program.

3.3.1 Personnel in the project

	Name, acad. degree, service position	narrower subject of the employee	Institute of University or non-university facility	Participation in the project in hours per week	Category
Basic staff					
Research associate (incl. auxiliary power)	1. R. Krull, apl. Prof. Dr. rer. nat.	Biochemical Engineering	Institute of Biochemical Engineering	10	Professorship
	2. D. C. Hempel, Prof. Dr.-Ing.	Biochemical Engineering	Institute of Biochemical Engineering	4	Professorship
	3. B. Nörtemann, Dr. rer. nat.	Microbiology, Biochemical Engineering	Institute of Biochemical Engineering	2	Post-doctoral
Non academic staff	4. Y. Göcke, BTA	Biotechnology	Institute of Biochemical Engineering	8	Technical staff
	5. D. Rasch, CTA	Biochemical Engineering	Institute of Biochemical Engineering	8	Technical staff
Supportive staff					
Research associate (incl. auxiliary power)	6. M. Eslahpazir, Dipl.-Ing.	Biochemical Engineering	Institute of Biochemical Engineering	40	PhD student
	7. K. Kiep, Dipl.-Biotechnol.	Biotechnology	Institute of Biochemical Engineering	40	PhD student
	8. P.-J. Lin, Dipl.-Biotechnol.	Biotechnology	Institute of Biochemical Engineering	40	PhD student
	9. T. Wucherpfennig, Dipl.-Biotechnol.	Biotechnology	Institute of Biochemical Engineering	40	PhD student
Non academic staff	10. N. N., Stud. assistant	Biochemical Engineering, Biotechnology		10	Students

Responsibilities of employees (basic staff)

Position 1 - 5:

The involved employees in the subproject B3 (Krull/Hempel) of the Institute of Biochemical Engineering, TU Braunschweig supported the PhD-students in their bioprocess and molecular biological work as well as in the development of reaction models, the implementation of cultivation and analysis and the construction of experimental facilities.

Responsibilities of employees (supportive staff)

Position 6: Dipl.-Ing. Manely Eslahpazir

To elucidate the aspects of fluid mechanics with respect to mechanical stress induced by stirring and aeration, Mr. Dipl.-Ing. Eslahpazir carried out the CFD simulations. Morphological disintegration studies were conducted together with the PhD-student (position 9) to quantify and correlate the resulting particle size distribution to fluid dynamical patterns and give an image of the stress phenomena which lead to a change in morphology.

Position 7: Dipl.-Biotechnol. K. Kiep

Mrs. Dipl.-Biotechnol. Kiep characterized the influence of the environome on morphology and productivity in batch cultivations of the homologous-recombinant β-fructofuranosidase (SUCA, EC 3.2.1.26) producing filamentous fungus *A. niger* SKAn1015. As result of her methodical investigation of the complex processes targets for improving, optimizing and controlling the production process of filamentous microorganisms were found.

Position 8: Dipl.-Biotechnol. P.-J. Lin

Mrs. Dipl-Biotechnol. Lin investigated the influence of different volumetric power input by agitation and aeration on the growth on pellets of the glucoamylase producing strain *A. niger* AB1.13. The quantification of the pellet morphology was accomplished by digital image analysis and laser diffraction technique. The qualification of the pellet surface structure was determined by the microscopic image analysis of the pellet slices and verified by sedimentation velocity measurements.

Position 9: Dipl.-Biotechnol. T. Wucherpfennig

Mr. Dipl.-Biotechnol. Wucherpfennig developed the automatic image analysis to generate conventional and fractal parameters for a holistic description of the whole range of fungal morphology. Ultimately, Mr. Wucherpfennig linked fructofuranosidase activity directly to rheological parameters of the cultivation broth establishing an easy reproducible method for productivity estimation.

Position 10: Stud. assistant

The student assistant supported the extensive experimental work in the implementation and evaluation of fungal cultivations as well as in the routine of biotechnological and molecular biological studies.

3.1 General information on the completed project B4

3.1.1 Topic

***Systems biology of product and pellet formation by* Aspergillus niger**

3.1.2 Disciplines and field of work

Microbiology, Molecular Biology, Mycology, Biotechnology, Systems Biology

3.2 Project manager

Prof. Dr. Dieter Jahn
(b.: 1.8.1959)
Institute of Microbiology
TU Braunschweig
Spielmannstr. 7
38106 Braunschweig
Phone: 0531-391-5801
Fax: 0531-391-5854
E-Mail: d.jahn@tu-bs.de

Dr. Bernd Nörtemann
(b.: 24.5.1957)
Institute of Biochemical Engineering,
TU Braunschweig
Gaußstraße 17
38106 Braunschweig
Phone: 0531-391-7654
Fax: 0531-391-7652
E-Mail: b.noertemann@tu-bs.de

Prof. Dr. Lothar Jänsch
(b.: 8.11.1967)
Helmholtz Centre for Infection Research
Cellular Proteom Research
Inhoffenstraße 7
38124 Braunschweig
Phone: 0531-6181-3030
Fax: 0531-6181-7099
E-Mail: Lothar.Jaensch@helmholtz-hzi.de

3.2 Development of the subproject

3.2.1 Report

3.2.1.1 Current knowledge at the last application and initial question

This project was focused on the optimization of recombinant protein production in the fungi *Aspergillus niger* using a systems biology approach. For this purpose the production of the model protein fructofuranosidase was characterized by transcriptome, proteome and metabolome analyses. To obtain reproducible quantitative data the fungus was grown in bioreactors under standardized conditions with automated time-resolved sampling. Obtained results were integrated with literature data into regulatory and metabolic models. Model based predictions were employed to iteratively optimize the production process. Thus, fructofuranosidase was produced under the control of a strong constitutive promoter. Glucose as carbon and nitrate as nitrogen source in combination with sufficient Fe^{2+} and Mn^{2+} amounts were the major components of the synthetic medium for robust and reproducible bioreactor based protein production. Transcriptome and proteome analysis revealed a significant adaptation of the energy metabolism, the cellular stress responses and of the protein synthesis machinery to recombinant protein production. Quantitative metabolome analysis showed the drastic changes of the central metabolism, especially of the TCA cycle, for the adaptation to fructofuranosidase formation. Metabolic modelling in concert with obtained data allowed for the prediction of optimization strategies.

The basis of all systems biology is an easy accessible, well annotated genome sequence. In the previous application period until 2008, a reliable and robust database (*ANiger DB*)

for all three available genome sequences of *A. niger* was implemented [*Grote 2008*]. It became an important tool for the evaluation of DNA microarray and proteome data. The used genome sequences were from the *A. niger* ATCC1015 (Joint Genome Institute, USA), *A. niger* CBS 513.88 (DSM, NL) as well as from *A. niger* NRRL 3 / ATCC9029 (Integrated Genomics, this consortium). A web interface was developed for the database and for predicted metabolic networks which were based on the genome sequences.

Reproducible cultivation conditions as continuous and batch culture were established for strain *A. niger* AB 1.13 in stirred tanks. Hereby, significant influences of growth rate, pH value and carbon sources of cultivation medium on the morphology of the fungus and its productivity for glucoamylase were identified. DNA microarray studies of *A. niger* gene expression revealed significant differences between *A. niger* grown as pellets and mycelia as well as between *A. niger* from the exponential and stationary phase. The stationary phase was characterized by the induction of genes responsible for catabolic processes, and for the protection against various stresses resulting from oxygen and nutrition deficiency. In contrast, exponential phase showed induction of genes responsible for anabolism including multiple loci involved in cell wall formation. The utilization of custom made Agilent microarrays in the last period allowed for an improved understanding of gene regulatory phenomena of interest.

The proteome analysis was originally based on a classical 2D gel electrophoreses approach. Around 200 differentially produced proteins were identified for *A. niger* grown under glucoamylase producing conditions. Furthermore, significant differences of the proteome were identified for *A. niger* with different morphology, e.g. coming from pelleted and mycelial growth.

Additionally, metabolome studies were applied to study the metabolic adaptation of *A. niger* during protein production. In agreement with the transcriptome and proteome analyses significant differences of the metabolism during different growth stages as well as between different morphologies were observed. In particular, a broad spectrum of metabolites of the central carbon metabolism, various amino acid biosynthetic pathways and the organic acid metabolism were detected with high reproducibility and quantified using GC-EI-MS. The overall handling of the probes, including the sampling methods and the further processing of samples were optimized. Up to 75 metabolites could be routinely identified and analyzed in parallel. In this context bioinformatics tools for quantitative metabolomics were developed. The total quantification using non-linear regression using signals from GC-EI-MS chromatograms were enabled by the newly developed bioinformatics tool MetaQuant [*Bunk et al., 2006*]. As discussed for proteome and transcriptome analyses, metabolome analyses also revealed significant differences of the central metabolism between different growth stages and morphologies. First metabolic modelling approaches using metabolic flux and elementary flux mode analyses and different metabolic scenarios were investigated under small scale network conditions [*Melzer et al., 2007*].

However, to model gene regulatory and metabolic adaptation processes at a broader range, under multiple physiological conditions comparing target protein production and non-producing conditions, genome basedlarge scale metabolic network analyses using innovative MATLAB based computational tool were required to facilitate desired predictions.

3.2.1.2 Results and applied methods

Outline and Summary

Based on the results of the previous funding periods our aim was to employ the established transcriptome, proteome and metabolome technologies for the thorough, systematic qualitative and quantitative characterization of the fructofuranosidase production process by *A. niger*. For this purpose a robust batch-fermentation process including the optimization of the sampling technique had to be established and systematically optimized. Obtained data in combination with available literature should be used for the generation, optimization and integration of gene regulatory and advanced metabolic model. Obtained model should provide the basis for predictions, their testing and thus for an iterative optimization process of knowledge based production process improvement.

Systematic growth medium optimization for recombinant fructofuranosidase production by *A. niger* in bioreactors

At first, the production medium was systematically optimized using a modelling-based statistical approach in collaboration with project B11 (Wittmann). Among various carbon sources tested, glucose allowed for the fastest growth and also resulted in the highest enzyme production [*Driouch et al., 2010*]. Previous fructofuranosidase production processes are almost exclusively based on sucrose and require high substrate concentration of typically more than 200 g/L. This is obviously due to the fact that these high sucrose levels are needed to induce fructofuranosidase gene expression in the *A. niger* wild type strains [*Chen and Liu, 1996*]. Accordingly, other sugars including glucose typically enable fast growth of the wild type strain but resulting in low enzyme production due to the missing induction of gene expression [*Zuccaro et al., 2008*]. This was not observed for the recombinant strain *A. niger* SKAn1015 which expresses the fructofuranosidase gene under the control of the strong constitutive *pkiA* promoter which is independent from endogenous transcriptional control mechanisms. Now, the superior efficiency of glucose dependent growth could be fully exploited for fructofuranosidase production which seems a major advantage.

Recent studies revealed interesting effects of the chosen nitrogen source on production properties and the morphology of the cells [*Balasubramaniem et al., 2001*]. Accordingly, sodium nitrate was tested to the most efficient nitrogen source. It should be noticed that

also complex nitrogen sources, such as peptone or yeast extract, enabled efficient production. However, since we aimed at a fully defined medium for a robust, reproducible production process avoiding batch-to-batch variation which are typical for complex nutrients, these complex nitrogen sources were prevented.

Among the microelements, Fe^{2+} and Mn^{2+} were identified as key nutrients. It is interesting to note that both trace elements had to be supplied in limited concentration for efficient production of citric acid by *A. niger* [*Papagianni, 2007*]. The production of this organic acid demands for a down-regulation of the tricarboxylic acid (TCA) cycle at the level of citric acid.

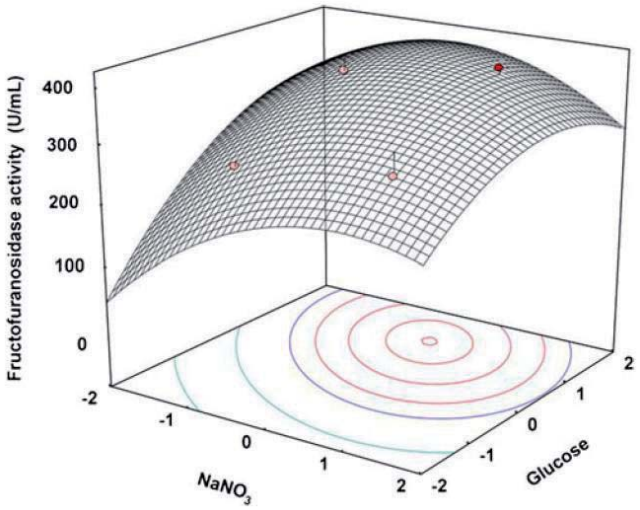

Fig. 1: Influence of glucose and $NaNO_3$ on fructofuranosidase production as predicted by the model. The interaction is visualized by a response surface plot.

This was achieved by the low Fe^{2+} and Mn^{2+} concentrations limiting the cofactor production required for various TCA cycle enzymes. Here, the stimulating role of the two metals in the fructofuranosidase production indicated that an actively operating TCA cycle, supplying energy and building blocks, is absolutely essential to obtain high enzyme titers in *A. niger* SKAn1015.

The subsequent optimization of the level of glucose and nitrate (**Fig. 1**) as well as Fe2+ and Mn2+ using central composite design allowed a threefold increase in fructofuranosidase production in shake flask cultivation. Subsequently, the process was transferred from shake flask to bioreactor for further optimization. Already in batch operation, this allowed a higher enzyme production (**Tab. 1**). Starting from the basic medium in batch operated shake flasks (fructofuranosidase activity = 92 U/mL), the product levels were increased by a factor of 7 using optimized medium in the bioreactor. The presented bioprocess strategy served as robust and reliable basis for systems biological approach.

Tab. 1: Production of extracellular fructofuranosidase by A. niger *SKAn1015 using different processes in flasks and in bioreactor with basic and optimized medium.*

Process (cultivation time)	**Batch (100 h)**			
	Shake flasks		**Bioreactor**	
Medium	**Basic**	**Opt.**	**Basic**	**Opt.**
Cell dry weight [g/L]	5.6±0.6	8.5±0.4	8.2±0.4	5.3±0.1
Protein [mg/mL]	0.8±0.1	1.3±0.2	0.9±0.0	2.0±0.1
Volumetric activity [U/mL]	92±6	400±20	160±10	750±20
Productivity [U/Lh]	920	4000	1600	7500
Specific activity [$U/mg_{protein}$]	115	310	180	380

Transcriptome analyses of fructofuranosidase production by *A. niger*

Based on the robust bioreactor growth and protein production protocol a novel genome wide transcriptome analysis using Agilent technology was successfully established for *A. niger*. The Agilent technology allows for the custom design of the array. In our case we included all known *A. niger* genes from the various genome projects. Moreover, appropriate replicates and background controls were included in the design. The array was applied for the investigation of specific gene regulation based on protein overproduction. First, the effect of fructofuranosidase overproduction on the gene expression of two strains, the wild type and the recombinant SKAn1015 variant, was determined and compared. For this purpose batch cultivations of the strains in stirred bioreactors with optimized medium in combination with transcriptome analyses using Agilent microarrays were performed. Next, an intensive evaluation of different sampling times (15, 20, 25, 30 and 35 h) followed. A cultivation time of 30 h turned out to be the optimal for visualization of significant differences between both strains at transcriptomic levels.

Cy3-labeled for non-overproducing and Cy5-labeled RNA for overproducing conditions were used for transcriptome analysis. The processing of the resulting microarray data was done using the *marray* package of Bioconductor (www.bioconductor.org). Interestingly, statistical analysis showed, that only about 400 of the tested 14,000 genes were found significantly differentially expressed (adj. p-value < 0.09), with an almost equal number of 200 genes up-regulated in the wild type and the SKAn1015 variant.

An unusual number of genes encoding hypothetical proteins was found induced. A strong up-regulation of genes for sugar and amino acid transporter, for exoenzymes including lipases, peptidases, DNases and various sugar metabolizing enzymes in the fructofuranosidase overproducing strain was observed (**Tab. 2**). Since the specific growth rates of the two tested strains were similar an increase of the demand for carbon and nitrogen sources for fructofuranosidase overproduction was concluded. All that was accompanied by a distinct gene regulatory scenario which included the induction of various genes for transcriptional regulators of RNA polymerase II and signal transduction

proteins. A detailed analysis of the observed up-regulation of transcriptional regulatory proteins revealed the strategy for the required transcriptional adaptation process.

Tab. 2: Selection of up- and down-regulated genes in A. niger *SKAn1015 compared to wild type.*

	GeneName	Median logFC	Fold change	Description	adj. P values
up regulated genes in SKAn1015	Aspni1_171113	1.29	2.4	Phosphatidylcholine desaturase (1.3.1.35)	0.09
	Aspni1_119995	1.1	2.1	Glycosyl transferase, family 28 (IPR004276)	0.01
	Aspni1_41877	0.84	1.79	Glycosyl hydrolase, family 88 (IPR010905)	0
	Aspni1_50977	2.41	5.3	Glycoside hydrolase, family 10 (IPR001000)	0.07
	Aspni1_44614	2.06	4.16	Fungal transcriptional regulatory protein, N-terminal (IPR001138)	0.07
	Aspni1_57188	1.02	2.02	DNA-directed RNA polymerase (2.7.7.6)	0
	Aspni1_128818	2.77	6.82	ABC transporter (IPR003439)	0.07
down regulated genes in SKAn1015	Aspni1_49258	-1.31	2.47	Succinate-semialdehyde dehydrogenase (NAD(P)+) (1.2.1.16)	0.04
	Aspni1_181280	-0.92	1.89	Peptidase M24 (IPR000994)	0.01
	Aspni1_140567	-0.85	1.80	Alpha amylase, catalytic region (IPR006047)	0.01
	Aspni1_42017	-0.91	1.88	Alcohol dehydrogenase (1.1.1.1)	0

Interestingly, a down-regulation of various genes which gene products are involved in stress response (glutathione-S-transferase, heat shock proteins, chaperones, peptidyl-prolyl cis-trans-isomerase, etc.) was observed for the recombinant fructofuranosidase producing strain. Clearly, the ribosome was restructured indicated by the formation of different ribosomal components for the two analyzed conditions. Finally, a down-regulation of succinate dehydrogenase indicates a distinct decreasing of TCA cycle activity under protein overproducing conditions, which is in good agreement with data from metabolic flux analysis (B11 (Wittmann)) and *in silico* studies as discussed in the following chapter. Again, the down-regulation process was coordinated by a significant change in transcription factor gene expression.

Proteome analyses of fructofuranosidase production by *A. niger*

Simultaneously, the influence of recombinant protein production was studied at the proteome level using the DIGE (differential gel electrophoresis) technique and was finally

integrated into the holistic systems biological approach. Two different protein extracts from biomass of *A. niger* SKAn1015 and wild type, respectively, were labelled separately with the dyes Cy2 and Cy3 and separated together on one acrylamide gel (**Fig. 2**).

Results showed that up to 10,000 protein species could be resolved using 2D gel electrophoresis. Time resolved batch experiments using optimized medium revealed significant differences between non- and overproducing cells. Obtained results were found in good agreement with the transcriptome analyses.

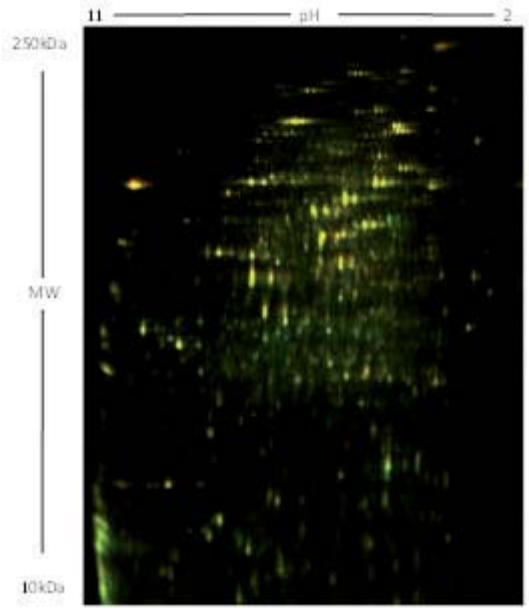

Fig. 2: 2D gel based proteomics approach using DIGE technology. Red: proteins induced during fructofuranosidase over-production, green: abundant proteins in non-overproducing cells, yellow: common proteins in both strains, all cultivated in stirred bioreactor under optimized conditions.

Quantitative metabolome analyses of fructofuranosidase production by *A. niger*

Next, time-resolved quantitative GC-MS-based metabolome analyses continued our efforts for a thorough investigation of the genetic and metabolic changes underlying the recombinant production of sugar metabolizing enzymes in *A. niger*. The glucoamylase as well as the fructofuranosidase production which acquires important metabolic and physiological functions in the cells caused significant effects in the quantities of metabolites of the central carbon metabolism. The most significant effects are depicted in **Fig. 3**.

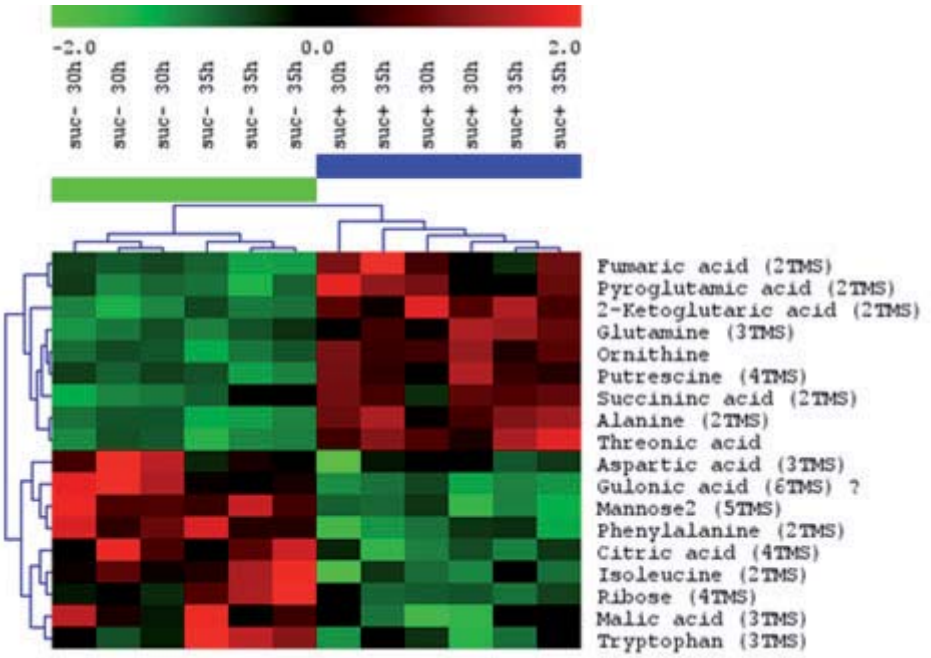

Fig. 3: Time resolved cluster map of metabolites of central carbon metabolism. Overproduction of fructofuranosidase leads to 2 - 15 fold up-regulation (red) of some amino acids and glutamic acid derivatives which are directly connected to a down-regulation (green) of the TCA.

The overproduction of fructofuranosidase lead to a 2 - 15 fold up-regulation of various amino acids and glutamic acid derivatives which are directly connected to a down-regulation of the oxidative TCA. Besides oxalic acid, gluconic acid was one of the most frequent organic acids found during cultivations with glucose as sole carbon source.

An overproduction of fructofuranosidase revealed a significant decrease of side product formation which was in agreement with the network simulation studies (see below). The considerable metabolic response caused by protein overproduction can be visualized by statistical analysis (Partial component analysis (PCA)) using partial component analysis where a clear response was identified at 25 - 35 h of cultivation (**Fig. 4**).

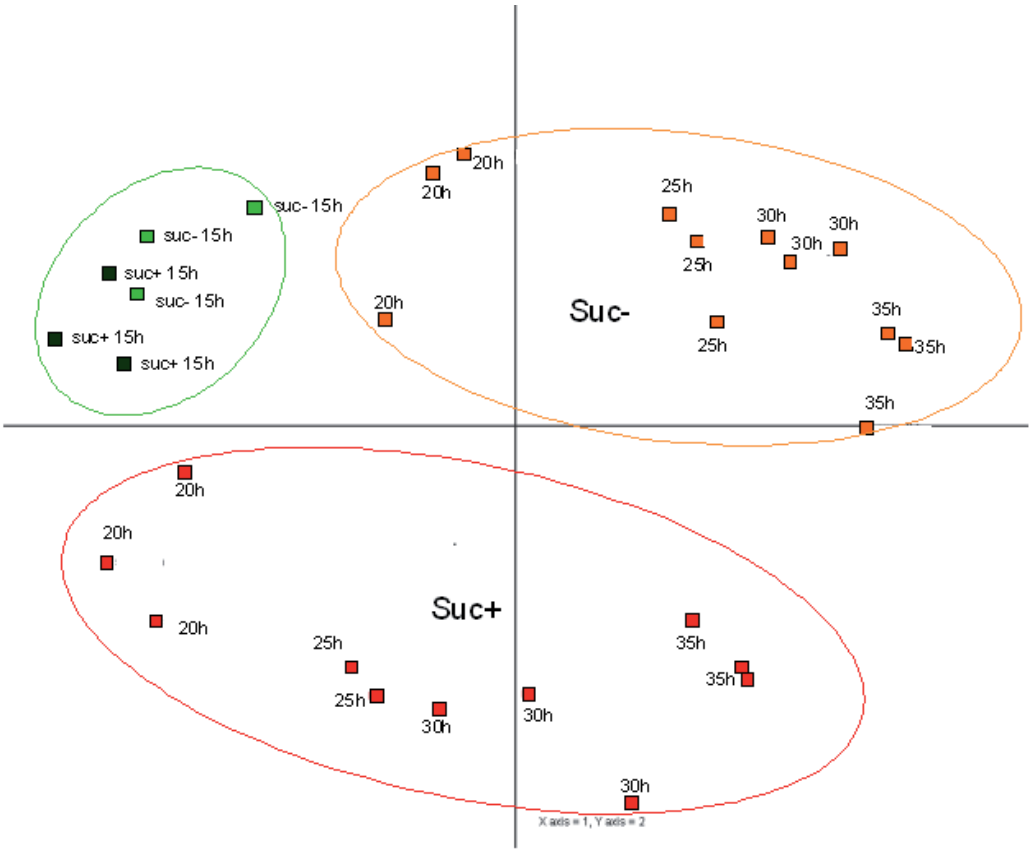

Fig. 4: Partial component analysis (PCA) plot of metabolic response during different cultivation times (15 h, 20 h, 25 h, 30 h, 35 h) as well as during overproducing (Suc+) and non producing conditions (Suc-) in A. niger *cultivated in stirred bioreactor using optimized conditions.*

Metabolic modelling for fructofuranosidase production during growth on glucose

Elementary mode analysis provided a rigorous basis to systematically characterize cellular phenotypes, metabolic flexibility and robustness for the thorough understanding of cell physiology [*Papin et al., 2004; Schuster, 2002*]. In the last period, this pathway analysis tool was applied and systematically extended to predict system-wide optimization targets for metabolic engineering approaches towards improved production in systems with optimally designed fluxes [*Melzer et al., 2009*].

A condensed genome based metabolic network of *A. niger* was used for the modelling studies in this work (in cooperation with B11 (Wittmann)). Overall, about 21,000 modes were obtained for growth on glucose and ammonium. The modes differed substantially in the corresponding for the enzyme and biomass yields (**Fig. 5**). Only 0.8% of all modes allowed maximum enzyme yield, all at zero growth. The reduced substrate glycerol revealed an optimal production of 0.83 c-mol/c-mol and was the best carbon source (Fig. 5B). Oleic acid (0.72 c-mol/mol) and xylose (0.73 c-mol/c-mol) were slightly less efficient (Fig. 5C, D).

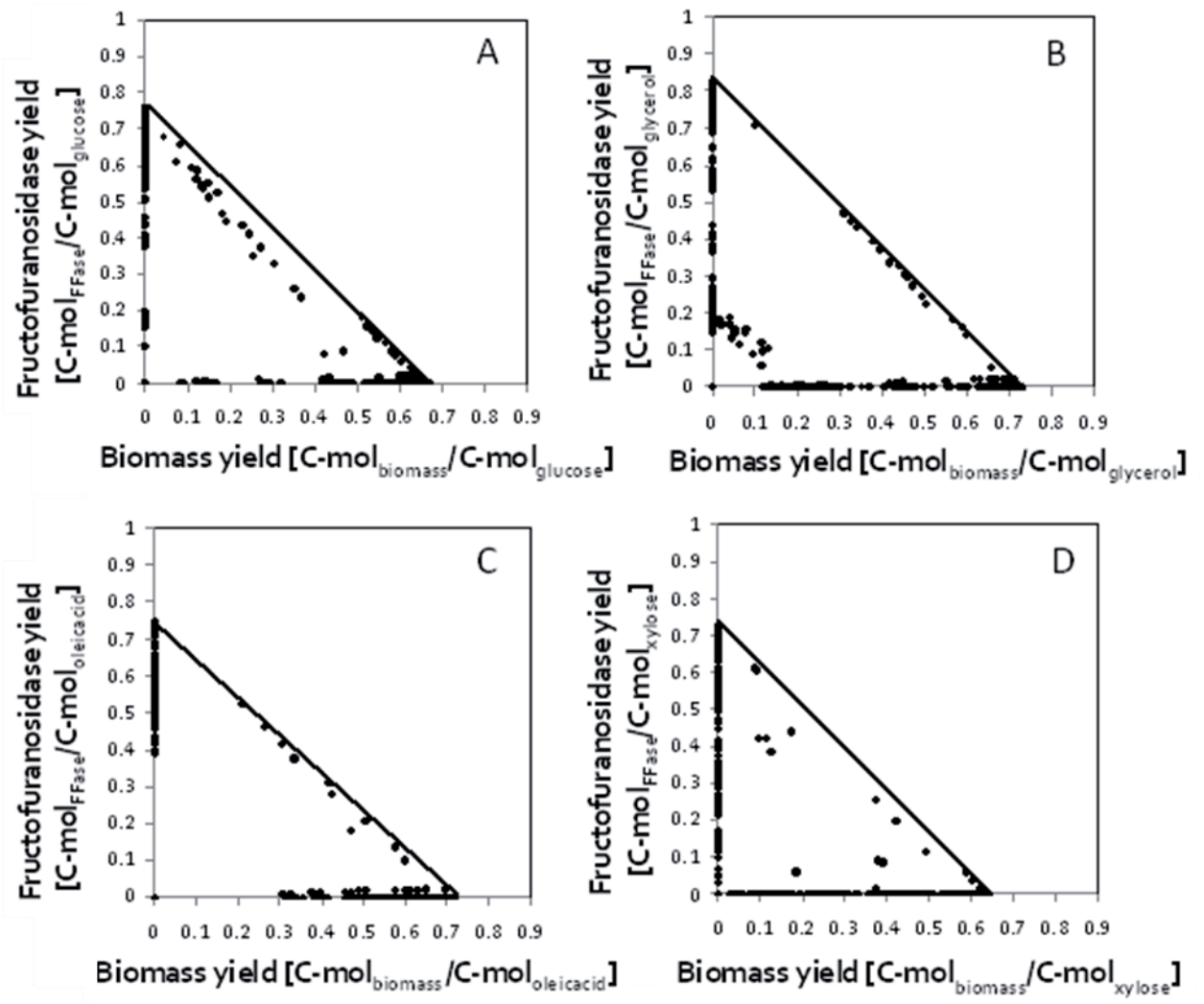

Fig. 5: Comparison of elementary modes for fructofuranosidase versus biomass production in A. niger *grown on different carbon sources. A: glucose, B: glycerol, C: oleic acid, D: xylose. The solution space of the elementary modes, represented by the black dots, is marked through the interior as well as the sides of the rectangular triangle. The modes on the axes represent extreme modes exclusively linked to production of either biomass or fructofuranosidase (FFase).*

The dominating fraction of modes was linked to exclusive production of either fructofuranosidase or biomass. The maximal carbon yield was 0.76 c-mol/c-mol for fructofuranosidase and 0.67 c-mol/c-mol for biomass (**Tab. 3**). In comparison, 1,986 elementary modes (9%), located within the interior of the triangular solution space, exhibited simultaneous formation of both compounds.

Tab. 3: Elementary flux mode analysis (EFM) of fructofuranosidase production by A. niger *on different carbon and nitrogen sources.*

Maximum carbon yield [C-mol/C-mol]			**Number of elementary modes**		
Carbon / Nitrogen Source	FFase	Biomass	total	Modes linked to FFase production (% of total EFM)	Modes linked to Biomass and FFase production (% of total EFM)
Glucose / NH_3	0.76	0.67	21,147	7,045 (33)	1,986 (9)
Glycerol / NH_3	0.83	0.73	21,122	8,070 (38)	2,267 (11)
Oelic acid / NH_3	0.75	0.72	20,895	9,071 (43)	1,702 (8)
Xylose / NH_3	0.73	0.64	13,364	3,896 (29)	187 (1)
Mannitol / NH_3	0.80	0.70	20,507	7,422 (36)	1,926 (9)
Sucrose / NH_3	0.76	0.67	52,926	16,046 (30)	5,190 (10)
Fructose / NH_3	0.76	0.67	17,680	5,033 (28)	1,810 (10)
Mannose / NH_3	0.76	0.67	13,196	4,536 (34)	1,313 (10)
Glucose / NH_3	0.61	0.54	29,435	13,160 (45)	1,425 (5)
Glycerol / NH_3	0.67	0.59	33,462	14,090 (42)	2,984 (9)
Oelic acid / NH_3	0.65	0.59	27,753	12,652 (46)	1,724 (6)
Xylose / NH_3	0.59	0.52	24,098	8,443 (35)	249 (5)
Mannitol / NH_3	0.64	0.57	40,751	17,816 (44)	2,755 (7)
Sucrose / NH_3	0.61	0.54	82,812	31,684 (38)	5,268 (6)
Fructose / NH_3	0.61	0.54	27,365	10,321 (38)	2,009 (7)
Mannose / NH_3	0.61	0.54	22,207	9,804 (44)	1,489 (7)

The average flux distribution deduced from the modes with maximum enzyme yield provided a detailed picture on the reactions involved (**Fig. 6**). The contribution of non-oxidative pentose phosphate pathway (PPP), the glycolysis, the fructofuranosidase synthesis as well as transport processes was rather constant as indicated by the low deviation of corresponding fluxes. Other reactions showed a higher flexibility suggesting that key functions of the network under optimal production conditions can be realized by different flux states.

Interestingly, this included a number of cytosolic enzymes which are all involved in the supply of NADPH, i.e. the oxidative PPP, malic enzyme and isocitrate dehydrogenase as well as mannitol 2-phosphate dehydrogenase. Furthermore, maximum production was linked to zero by-product formation. The entire ATP formed was completely recruited for fructofuranosidase production.

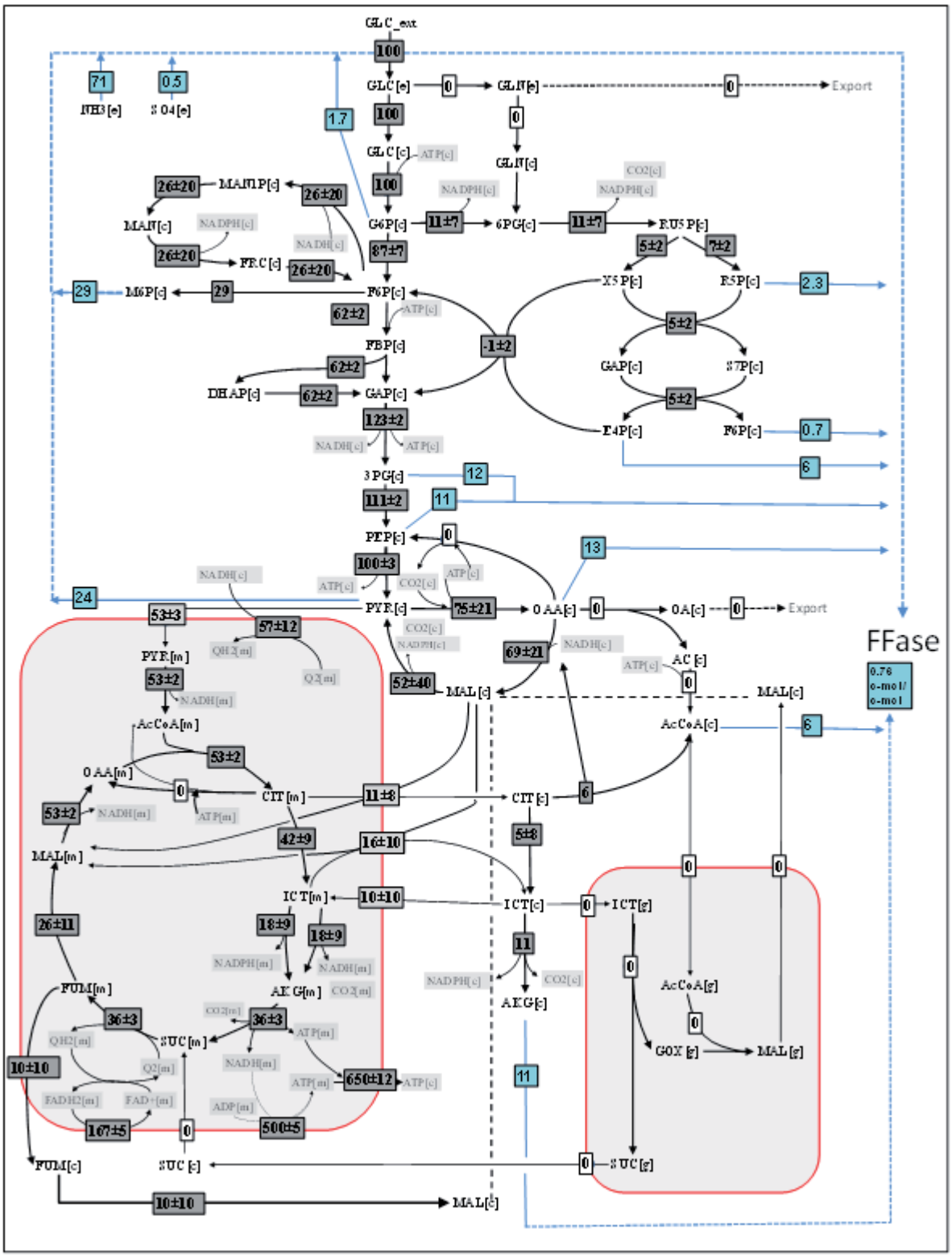

Fig. 6: Flux distribution for theoretical maximum of fructofuranosidase (FFase) production by A. niger *using glucose and ammonium. The relative flux coefficients are averaged from 160 elementary flux modes for maximum production obtained. All fluxes are given as relative molar flux normalized to 1 mol of glucose unit [mol (mol glucose)$^{-1}$ 100] [*Melzer, 2010*].*

Metabolic modelling for fructofuranosidase production during growth on glycerol

Glycerol was metabolized by simultaneous involvement of the NADH-dependent glycerol-dehydrogenase and the FAD-dependent glycerol 3-phosphate dehydrogenase. Due to this, reducing equivalents were released into the cytosol and mitochondria, respectively. This caused an increased flux through the NADH-ubiquinone oxidoreductase, counterbalancing the NADH excess in the cytosol. Probably linked to the different entry point of glycerol into metabolism, the supply of NADPH differed for this carbon source with respect to the reactions involved.

Here, the oxidative PPP played only a minor role whereas the mannitol cycle and the malic enzyme were recruited. For oleic acid the flux distribution differed drastically. For optimal production degradation involved two parallel routes, that in mitochondria as well as that in the glyoxysomes resulting in a large relative flux through the glyoxylate shunt and reactions of the TCA cycle with the corresponding mitochondrial shuttle systems [*Melzer et al., 2009; Melzer, 2010*]. Additionally, the high supply of NADH by the degradation of the reduced fatty acids was obviously utilized by the mannitol cycle to form NADPH. The oxidative PPP was not involved in NADPH supply. Production on xylose demanded for increased NADPH supply as indicated by average flux through the oxidative PPP, the mannitol cycle and the malic enzyme. This at least partly attributed to the NADPH demand linked to the xylose uptake system [*Prathumpai et al., 2003*]. As for glucose, by-product formation was not observed for the alternative carbon sources under maximal production. The degree of reduction also played a role for the nitrogen source. The optimum yield decreased by about 18% for all carbon sources when nitrate instead of ammonia as nitrogen source was used.

Prediction of metabolic targets for the optimization of fructofuranosidase production

We proposed a strategy for improved biotechnological production strains through optimally designed fluxes (with project B11 (Wittmann)). The bioinformatics approach, we named FluxDesign, computes elementary modes. It searches through the modes, identifies targets to be amplified (positive correlation) or down-regulated (negative correlation). Evidence that the predicted optimization strategies open realistic chances for improvement were obtained from recent studies [*Melzer et al., 2009 and 2010*]. Our flux balance analysis and also stoichiometric flux analysis indicate the importance of sufficient NADPH supply for protein production in *A. niger* [*Melzer et al., 2007; Pedersen et al., 2000*] and *A. oryzae* [*Riedel et al., 2001*] whereby the PPP plays an important role which was also found in the present study [*Melzer, 2010*].

3.2.1.3 References to other works and collaborations in the SFB

The development and characterization of *A. niger* producing strains and mutants was performed in close collaboration with the subproject A1 (Jahn/Dersch). Between this subproject B4 and B3 (Krull/Hempel) the impact of cultivation experiments using optimized medium and variation of parameters was strongly discussed. As in the subprojects B8 (Franco-Lara) and B10 (Jahn/Franco-Lara) also worked on microarray analysis (*B. megaterium*) the development and establishment of Agilent transcriptome technologies was done together with these two projects. The establishment of modeling tools for improved network analysis was done in co-work with B9 (Münch/Schomburg) and B11 (Wittmann) while medium optimization and GC/MS analysis were also performed in collaboration with B11 (Wittmann).

3.2.1.4 Comparison with research outside the SFB

Optimization of bioprocesses for glycosyltransferase production: A number of studies have previously aimed at the isolation of fructofuranosidase producing strains from nature [*Cuervo et al., 2007*] or the screening for suitable production media [*Balasubramaniem et al., 2001*]. Most of these studies, however, resulted in relatively low production efficiency which might be attributed to the fact that wild type strains were employed and processes were performed in shake flask cultures. Subsequently, the process was transferred from shake flask into bioreactor for further optimization. This step appears especially important since for the production of fructofuranosidase such investigations are quite rare [*Maiorano et al., 2008*].

Only few groups have been applied metabolome studies using filamentous fungi during the last years whereas the focus is often directed to secondary metabolism [*Nasution 2006*]. However, strong progress was made in the group of *Kluyver Centre for Genomics of Industrial Fermentation* in Delft (Peter Punt and Mariet J. van der Werf) regarding using GC-MS technologies investigating metabolomics as a tool for target identification in strain improvement with *A. niger* [*Braaksma et al., 2011*]. However, since metabolome data are often acquired semi-quantitative, a fully quantitative approach was developed and used in the present work within the last application period.

Modelling approaches: In comparison to alternative methods such as linear programing elementary flux mode analysis enables the investigation of all possible physiological states in the cell and can identify all existing metabolic flux vectors without any a priori knowledge or assumption on measured fluxes [*Trinh et al., 2008*]. Elementary flux mode analysis has been applied to predict promising gene deletion strategies as shown for rational design of L-methionine production in bacteria [*Krömer et al., 2007*], the identification of genetically independent pathways in recombinant yeast [*Carlson et al., 2002*] or the construction of a minimal *E. coli* cell for high yield ethanol production [*Trinh et al., 2008*]. Recent modelling studies showed that such a coupling of fluxes is an important behaviour of biological systems e.g. with respect to co-regulation of genes [*Notebaart et al., 2008*]. However, a

direct application towards target identification and superior production strains has not been considered so far.

3.2.1.5 Literature

Balasubramaniem, A.K.; Nagarajan, K.V.; Paramasamy, G. (2001) Optimization of media for fructofuranosidase production by *Aspergillus niger* in submerged and solid state. *Process Biochem.* 36, 1241-1247

Braaksma, M.; Bijlsma, S.; Coulier, L.; Punt, P.J.; Van der Werf, M.J. (2011) Metabolomics as a tool for target identification in strain improvement: the influence of phenotype definition. *Microbiology* 157, 147-159

van den Brink, H.J., Petersen, S.G.; Rahbek-Nielsen, H.; Hellmuth, K.; Harboe, M. (2006) Increased production of chymosin by glycosylation. *J. Biotechnol.* 125, 304-310

Bunk, B.; Kucklick, M.; Jonas, R.; Münch, R.; Schobert, M.; Jahn, D.; Hiller, K. (2006) MetaQuant: a tool for the automatic quantification of GC/MS-based metabolome data. *Bioinformatics* 22, 2962-2965

Carlson, R.; Fell, D.; Srienc, F. (2002) Metabolic pathway analysis of a recombinant yeast for rational strain development. *Biotechnol. Bioeng.* 79, 121-134

Chen, W.; Liu, C. (1996) Production of β-fructofuranosidase by *Aspergillus japonicas Enzyme Microb. Technol.* 18, 153-160

Cuervo, R.F.; Ottoni, C.A.; Silva, E.S.; Matsubara, R.S.; Carter, J.M.; Magossi, L.R.; Wada, M.A.A.; Rodrigues, M.F.A.; Guilarte, B.M.; Maiorano, A.E. (2007) Screening of β-fructofuranosidase producing microorganisms and effect of pH and temperature on enzymatic rate. *Appl. Microbiol. Biotechnol.* 75, 87-93

Jacobs, D.I.; Olsthoorn, M.M.; Maillet, I., Akeroyd, M.; Breestraat, S.; Donkers, S.; van der Hoeven, R.A.; van den Hondel, C.A.; Kooistra, R.; Lapointe, T. (2008) Effective lead selection for improved protein production in *Aspergillus niger* based on integrated genomics. *Fungal Genet. Biol.* 46, S141-152

Kim, H.U.; Kim, T.Y.; Lee, S.Y. (2008) Metabolic flux analysis and metabolic engineering of microorganisms. *Mol. Biosyst.* 2, 113-120

Krömer, J.O.; Wittmann, C.; Schröder, H.; Heinzle, E. (2006) Metabolic pathway analysis for rational design of L-methionine production by *Escherichia coli* and *Corynebacterium glutamicum*. *Metab. Eng.* 8, 353-369

Maiorano, A.E.; Piccoli, R.M.; Sabino da Silva, E.; Rodrigues, M.F.A. (2008) Microbial production of fructosyltransferases for synthesis of prebiotics. *Biotechnol. Lett.* 30, 1867-1877

Melzer, G.; Dalpiaz, A.; Grote, A.; Kucklick, M.; Göcke, Y.; Jonas, R.; Dersch, P.; Franco-Lara, E.; Nörtemann, B.; Hempel, D.C. (2007) Metabolic flux analysis using stoichiometric models for *Aspergillus niger*: comparison under glucoamylase-producing and non-producing conditions. *J. Biotechnol.* 132, 405-417

Moralejo, F.J.; Cardoza, R.E.; Gutierrez, S.; Martin, J.F. (1999) Thaumatin production in *Aspergillus awamori* by use of expression cassettes with strong fungal promoters and high gene dosage. *Appl. Environ. Microbiol.* 65, 1168-1174

Nasution, U.; Van Gulik, W.M.; Kleijn, R.J.; Van Winden, W.A.; Proell, A.; Heijnen, J.J. (2006). Measurement of intracellular metabolites of primary metabolism and adenine nucleotides in chemostat cultivated *Penicillium chrysogenum*. *Biotechnol. Bioeng.* 94, 159-166

Notebaart, R.A.; Teusink, B.; Siezen, R.J.; Papp, B. (2008) Co-regulation of metabolic genes is better explained by flux coupling than by network distance. *PLoS Comput Biol.* 4:e26

Papagianni, M. (2007) Advances in citric acid fermentation by *Aspergillus niger*: biochemical aspects, membrane transport and modelling. *Biotechnol. Adv.* 5, 244-263

Papin JA, Stelling J, Price ND, Klamt S, Schuster S, Palsson BO (2004). Comparison of network-based pathway analysis methods. Trends Biotechnol. 22, 400-405

Patil, K.R.; Rocha, I.; Forster, J.; Nielsen, J. (2005) Evolutionary programming as a platform for *in silico* metabolic engineering. *BMC Bioinform.* 6, 308

Pedersen, H., Christensen, B.; Hjort, C.; Nielsen, J. (2000) Construction and characterization of an oxalic acid nonproducing strain of *Aspergillus niger*. *Metab. Eng.* 2, 34-41

Prathumpai, W.; Gabelgaard, J.B.; Wanchanthuek, P.; van de Vondervoort, P.J.; de Groot, M.J.; McIntyre, M.; Nielsen, J. (2003) Metabolic control analysis of xylose catabolism in *Aspergillus*. *Biotechnol. Prog.* 19, 1136-1141

Riedel, C.; Rittmann, D.; Dangel, P.; Mockel, B.; Petersen, S.; Sahm, H.; Eikmanns, B.J. (2001) Characterization of the phosphoenolpyruvate carboxykinase gene from *Corynebacterium glutamicum* and significance of the enzyme for growth and amino acid production. *J. Mol. Microbiol. Biotechnol.* 3, 573-583

Schuster, S.; Hilgetag, C.; Woods, J.H.; Fell, D.A. (2002) Reaction routes in biochemical reaction systems: algebraic properties, validated calculation procedure and example from nucleotide metabolism. *J. Math. Biol.* 45, 153-181

Trinh, C.T.; Unrean, P.; Srienc, F. (2008) Minimal *Escherichia coli* cell for the most efficient production of ethanol from hexoses and pentoses. *Appl. Environ. Microbiol.* 74, 3634-3643

Zuccaro, A.; Götze, S.; Kneip, S.; Dersch, P.; Seibel, J. (2008) Tailor-made fructooligosaccharides by a combination of substrate and genetic engineering. *Chem. Bio. Chem.* 9, 143-149

3.2.2 Project relevant own publications

a) Works that have appeared in publications of a scientific quality assurance at the time of application or final adoption, and book publications

Driouch, H.; Roth, A.; Dersch, P.; Wittmann, C. (2010) Optimized bioprocess for production of fructofuranosidase by recombinant *Aspergillus niger*. *App. Microbiol. Biotechnol.* 87, 2011-2024

Driouch, H.; Roth, A.; Dersch, P.; Wittmann, C. (2011) Filamentous fungi in good shape: Microparticles for tailor-made fungal morphology and enhanced enzyme production. *Bioeng. Bugs* 2:2, 1-5

Driouch, H.; Melzer, G.; Wittmann, C. (2012) Integration of *in vivo* and *in silico* metabolic fluxes for improvement of recombinant protein production. *Metab. Eng.* 14, 47-58

Grote, A.G. (2008) Datenbanksysteme und bioinformatische Werkzeuge zur Optimierung biotechnologischer Prozesse mit Pilzen. Dissertation. Technische Universität Braunschweig

Melzer, G.; Eslahpazir Esfandabadi, M.; Franco-Lara, E.; Wittmann, C. (2009) Flux design: *In silico* design of cell factories based on correlation of pathway fluxes to desired properties. *BMC Syst. Biol.* 25, 120 (**highly accessed paper)**

Melzer, G. (2010). Metabolic Network Analysis of the Cell Factory *Aspergillus niger*. *Cuvillier-Verlag, Göttingen*, ISBN-10: 3869554568

b) Other publications

Melzer, G.; Eslahpazir, M.; Franco-Lara, E.; Nörtemann, B.; Hempel, D.C.; Wittmann, C. (2009) Elementary mode analysis of *Aspergillus niger* metabolic network for optimization of recombinant sucrase production. *Chem. Eng. Tech.* 81, 1253

3.3 Looking back on the promotion

The project has been funded since July 2004 in the SFB 578. It was completed on June 2012 with the end of the program.

3.3.1 Personnel in the project

	Name, akad. degree, service position	narrower subject of the employee	Institute of University or non-university facility	Participation in the project in hours per week	Category
Basic staff					
Research associate (incl. auxiliary power)	1. D. Jahn, Prof. Dr. rer. nat.	Microbiology, Systems Biology	Institute of Microbiology	5	Professorship
	2. B. Nörtemann, Dr. rer. Nat.	Biochemical Engineering	Institute of Biochemical Engineering	5	Post-doctoral
	3. L. Jänsch, Prof. Dr. rer. nat.	Proteomic Research Group, HZI	HZI, Helmholtz Zentrum for Infection Research	5	Professorship
	4. P. Dersch, Prof. Dr. rer. nat.	Molecular Infections Biology, HZI	HZI, Helmholtz Zentrum for Infection Research	5	Professorship
	5. G. Melzer, Dr.-Ing.	Biochemical Engineering	Institute of Biochemical Engineering	15	Post-doctoral
	6. J. Melzer, Dr. rer. nat.	Microbiology, Systems Biology	Institute of Microbiology	5	Post-doctoral
Non academic staff	7. Y. Göcke, BTA	Biochemical Engineering	Institute of Biochemical Engineering	5	Technical staff
Supportive staff					
Research associate (incl. auxiliary power)	8. E. Berger, Dipl. Biotechnol.	Proteomic Research Group, HZI	HZI, Helmholtz Centre for Infection Research	40	PhD student
	9. T. Stolz, BTA	Microbiology, Systems Biology	Institute of Microbiology	40	Technical staff
Non academic staff	10. N. N., Stud. assistant	Biochemical Engineering, Biotechnology		10	Students

Responsibilities of employees (basic staff)

Position 1 - 7:

The involved employees in the subproject B4 (Jahn / Nörtemann / Jänsch) of the Institute of Microbiology, Institute of Biochemical Engineering and Helmholtz Centre of Infection Research have supported the involved staff in their bioprocess and molecular biological problems as well as in the development of reaction models, the implementation and the performance of cultivation and analysis and the construction of experimental facilities as well as the development of modeling tools.

Responsibilities of employees (supportive staff)

Position 8: Dipl. Biotechnol. Evelin Berger

The characterization of physiological response by sucrase overproduction on proteomic level was investigated using DIGE technology and 2D gel electrophoreses. To elucidate the several aspects of production influenced by different parameters e.g. sampling time of cultivation Mrs. Dipl. Biotechnol. Evelin Berger has been carried out development and implementation of the described proteomic technologies. The main characteristics of the results are elucidation of the functionality and usefulness of the described methods to apply for systems biology issues.

Position 9: BTA Tatjana Stolz

Mrs. Stolz characterized the influence of the environome on productivity in batch cultivations with the homologous recombinant β-fructofuranosidase producing filamentous fungus *A. niger* SKAn1015. As example, the formation of the homologous-recombinant β-fructofuranosidase (EC 3.2.1.26), produced under the control of the constitutive promoter of pyruvate kinase (P_{pki}), was investigated. Within the cultivation process, the growth was optimized in collaboration with B11 (Dr.-Ing. Habib Driouch) and samples were investigated using microarray technologies together with Dr. Jana Melzer (Institute of Microbiology). Results of varying sampling times were described on transcriptomic level and biomass growth. Furthermore metabolic pathways as well as the expression of genes, which are associated with biomass growth, metabolism, signal transduction pathways or secretion, were determined to rate the physiological status of the biomass during cultivation. Finally, targets for improving, optimizing and controlling the production process of filamentous microorganisms were investigated in strong collaboration with B11 (Dr.-Ing. Guido Melzer) using *in silico* tools.

Position10: Stud. assistant

The student assistant supported the extensive experimental work in the implementation and evaluation of fungal cultivations as well as in the routine of biotechnological and molecular biological studies.

3.1 General information on the completed project B7

3.1.1 Topic

Micromechanic properties of filamentous fungi

3.1.2 Disciplines and field of work

Process Engineering, Materials Science, Biotechnology

3.1.3 Project Manager

Prof. Dr.-Ing. Arno Kwade
(b.: 7.1.1965)
Institute for Particle Technology, TU Braunschweig
Volkmaroder Str. 5, 38104 Braunschweig
Phone: 0531/391-9610
Fax: 0531/391-9633
E-Mail: a.kwade@tu-bs.de

Dr.-Ing Ingo Kampen
(b.: 3.3.1972)
Phone: 0531/391-7095
Fax: 0531/391-8146
E-Mail: i.kampen@tu-bs.de

3.2 Development of the subproject

3.2.1 Report

3.2.1.1 Current knowledge at the last application and initial questions

The filamentous ascomycete fungus *Aspergillus niger* is used in various biotechnological processes. Its productivity within these processes is closely linked to its complex morphological development. Generally two different types can be distinguished: pellets and free dispersed mycelia. The morphology is determined by cultivation parameters such as pH value, salt concentration and shear stress [*Papagianni et al., 1998*]. In subproject B3 (Krull/Hempel) the influence of the hydrodynamic properties and the composition of the media on the pellet morphology was investigated. In this context Grimm et al. postulated a spore aggregation model, in which the morphogenesis is divided into two basic steps [*Grimm et al., 2005a*]. The first step is the agglomeration of spores right after inoculation. Depending on the initial spore concentration, shear stress and adhesion forces, an equilibrium between aggregation and disaggregation is developed [*Elmayergi et al., 1973; Tucker und Thomas, 1992; Fujita et al., 1994; Ryoo und Choi, 1999*]. The second step in the morphogenesis is the agglomeration of spores and young hyphae which are formed by the first germinating spores. The model predicted a pellet-morphology in case of a strong aggregation. The shape of these pellets should be significantly influenced by the size of the spore aggregates and thus also by the initial spore concentration [*Elmayergi et al., 1973; Suijdam und Metz, 1981b; Ryoo und Choi, 1999*]. For this reason, the microscopic investigation of the first and the second aggregation process was the main target in this subproject.

Nevertheless the underlying effects of the spore aggregation were mostly unknown. Ryoo and Choi (*1999*) calculated Gibbs free energy via contact angle measurements in aqueous media. They obtained a negative value and concluded that hydrophobic interactions may play an important role. In contrast Fujita et al. assume a linear connection between the

number of spores in a pellet and the van der Waals forces between the spores [*Fujita et al., 1994*]. Furthermore, specific chemical bonds like those observed between polysaccharides might be responsible for observed aggregation [*Gerin et al., 1993; Tronchin et al., 1995; Ryoo und Choi, 1999*]. These forces are generally attractive; in colloidal systems they are superimposed by repulsive electrostatic forces, resulting from the pH dependent surface potential. As reported in literature the zeta potential and the electrophoretic mobility are often measured to characterize these interactions and have already been determined for spores of *A. niger* and other filamentous growing fungi [*Gerin et al., 1993; Jones, 1994; Dynesen and Nielsen, 2003*]. Measurements of agglomeration kinetics in a bioreactor by Grimm et al. (*2005b*) (B3 Krull/Hempel) showed an increased spore aggregation at high pH values although the absolute zeta potential increased. A suggested explanation for this unexpected result was a stabilization of the aggregates due to a thicker boundary.

During growth the hyphae form a complex dense pellet structure with many physical merges [*Galbraith und Smith, 1968; Gerin et al., 1993; El-Enshasy et al., 1999; Amanullah et al., 2001*]. However at the same time fluid dynamic forces lead to a reduction of the pellet size by breakage of whole pellets or by erosion of the pellet edges. For a better description of this process it is often correlated with the energy dissipation into the reactor [*Suijdam and Metz, 1981a; Fujita et al., 1994*]. The tensile strength of the pellets against the forces that occur by the interactions between small vortexes and fungal pellets is calculated. In contrast, Cui et al. derived from the observation of only few small pellet fragments in an *Aspergillus awamori* cultivation, that breakage of hyphae at the edge of the pellet is responsible for the erosion [*Cui et al., 1997*]. For these models it is essential to suppose values for the elastic behavior and the Young's modulus, which are not directly available by cultivation experiments. Therefore it must be remembered that theoretically derived parameters are compared with experimental data. Merely, Stocks and Thomas (*2001*) performed micromanipulation experiments to obtain values for the breaking force and Young´s modulus of the filamentous bacteria *Saccharopolyspora erythraea*. They studied the direct connection between the breaking force and factors like the thickness of the cell wall or the diameter of the hyphae under nitrate and glucose limited conditions during cultivation. To identify the hyphae breakage mechanisms the determination of mechanical properties as well as shear experiments were another main target in this subproject.

3.2.1.2 Results and applied methods

Spore-spore adhesion force determination

In this subproject adhesion forces between single spores and between spores and hyphae of the filamentous growing, uridin auxotrophic fungus *Aspergillus niger* strain AB 1.13 were investigated. The spore cultivation and harvesting were conducted batch wise on potato dextrose agar supplemented with uridin according to the methods developed in subproject B3 (Krull/Hempel).

All adhesion force measurements were carried out using an atomic force microscope (AFM). For this purpose it was necessary to enhance the immobilization of single spores to a substrate. It was found that spores adhere 3 to 6 times better to a silicon carrier which was treated with a solution of 5% (v/v) dimethyldichlorosilane in toluene than to other spores. In the previous funding period an immobilization technique of single spores to a tipless cantilever was developed. The immobilization was achieved with a light-activated, solvent-free epoxy resin. To characterize the main interactions between two spores and a spore and hyphae several measurements under different environmental conditions were performed. In particular the dependencies between the adhesion forces and the pH value, the salt concentration and the contact time were investigated. In addition a statistical evaluation was elaborated, which describes the adhesion force data by a continuous distribution. This model allows the identification of significant differences between the measurements even though directly measured adhesion forces are, for practical reasons, not stochastically independent and show due to a high deviation overlapping force distributions.

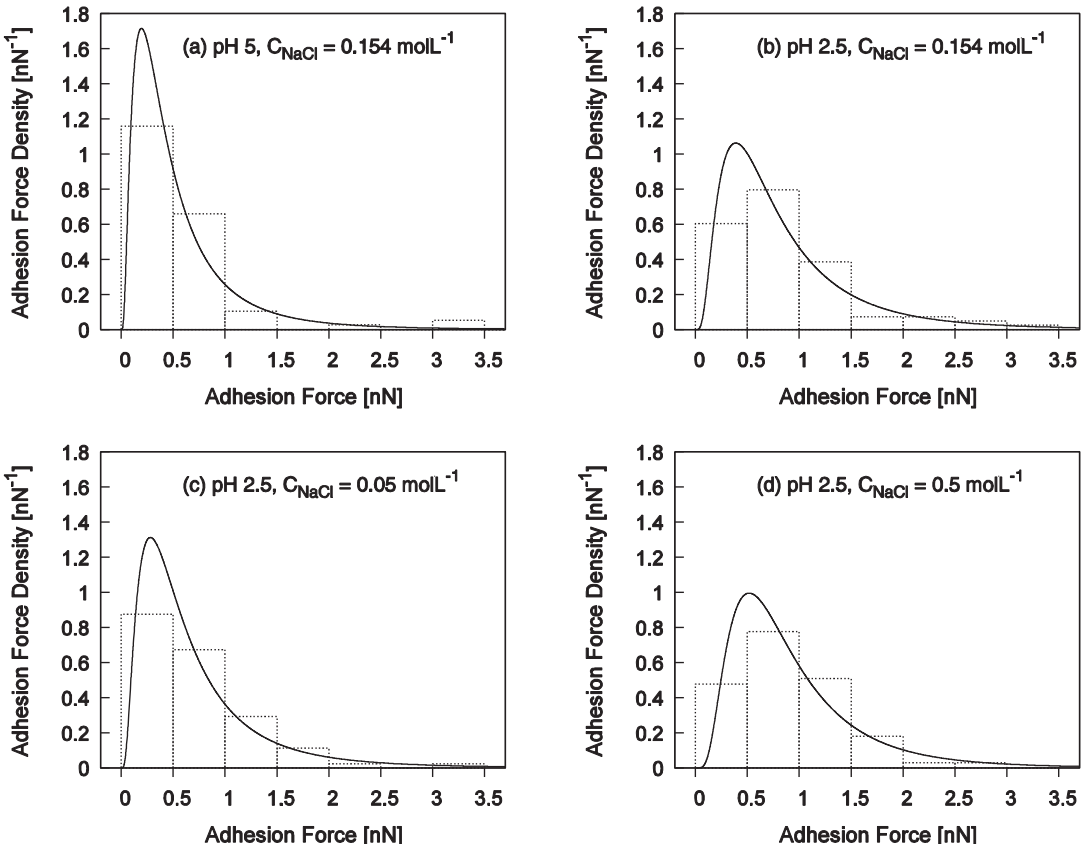

Fig. 1: Histograms and estimated distributions of adhesion force between two single spores in different solutions. The area of one bar represents the relative de-adhesion events within this class. Each distribution is the result of 100 force-distance curves recorded between 10 cantilever-immobilized spores and 100 different substrate-immobilized spores.

Fig. 1 shows the influence of ionic strength and pH value on the adhesion force measurements between two single spores. With increasing pH values, a statistically significant shift to smaller adhesion forces can be observed. Moreover, a shift towards higher adhesion forces with increasing ionic strength can be detected. These findings can be attributed to a change in the electrostatic interactions. Zeta potential measurements have shown a negative surface potential within a wide range of pH values [Grimm et al., *2005a; Wargenau et al., 2011*]. Because of the absence of an isoelectric point down to pH values smaller than 3, it is unlikely that surface charge is essentially induced by proteins [*Hannan, 1961*]. In fact the spore is coated with a distinct layer of melanin on top of the spare wall, which seems to be arbitrative for the electrostatic surface potential.

In addition the influence of the contact time on the adhesion force distribution was examined. **Fig. 2** shows the effect of an extension of the contact time from 1 s to 10 s. It can be seen that in this dimension a longer contact time is linked with higher adhesion forces. A prolongation beyond 10 s did not result in any further increase of adhesion forces (data not shown). Besides this an interesting difference in the retraction curves could be observed. Usually they show one sharp adhesion peak with only few measurements differing from the typical pattern by two or more de-adhesion events. This number increases along with the contact time. Together these findings suggest that besides the electrostatic forces, discrete molecular interactions like polysaccharide bridging as described by [*Gerin et al., 1993*] for *Phanerochaete chrysosporium* play a certain role especially during the germination process. To investigate if there is a change in surface properties of germinating spores as reported by Dague et al. [*Dague et al., 2008*], numerous single cell-cell force measurements were conducted in cultivation media for at least 8 h. However, no significant change could be detected within this time. Only one spore showed a significantly increased adhesion force after 5 h of in the cultivation media, but this effect could not be reproduced.

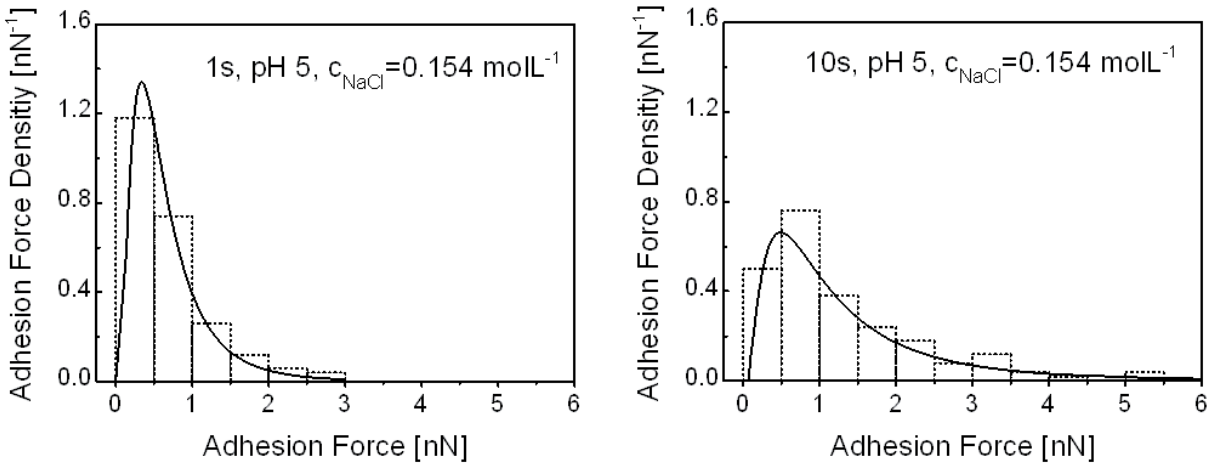

Fig. 2: Histograms and estimated distributions of adhesion forces between spores at different contact times and at constant ionic strength and pH values. The area of one bar represents the relative de-adhesion events within this class. Each distribution is the result of 100 force-distance curves recorded between 10 cantilever-immobilized spores and 100 different substrate-immobilized spores.

Aggregation measurements

In order to estimate the influence of the adhesion forces on the aggregation behavior, aggregation experiments at different NaCl concentrations and pH values were performed in a baffled blade-stirred vessel with a defined, constant volumetric power input. The results in **Fig. 3** show the equilibrium fraction of agglomerated spores. With increasing pH the aggregation tendency of spores decreases. In fact a slightly negative mean value at pH 5 implies that hardly any spores aggregate. These findings are in good agreement with the expectations by the zeta potential measurements. In contrast the relation between salt concentration and spore aggregation seems to be more complex. Firstly, an increase of the NaCl concentration from 0.01 to 0.154 molL^{-1} causes more aggregation, but a further raise has an opposite effect. An explanation requires a more intensive investigation of the potential profile which was carried out by a numerical approach taking the variable melanin coating into account.

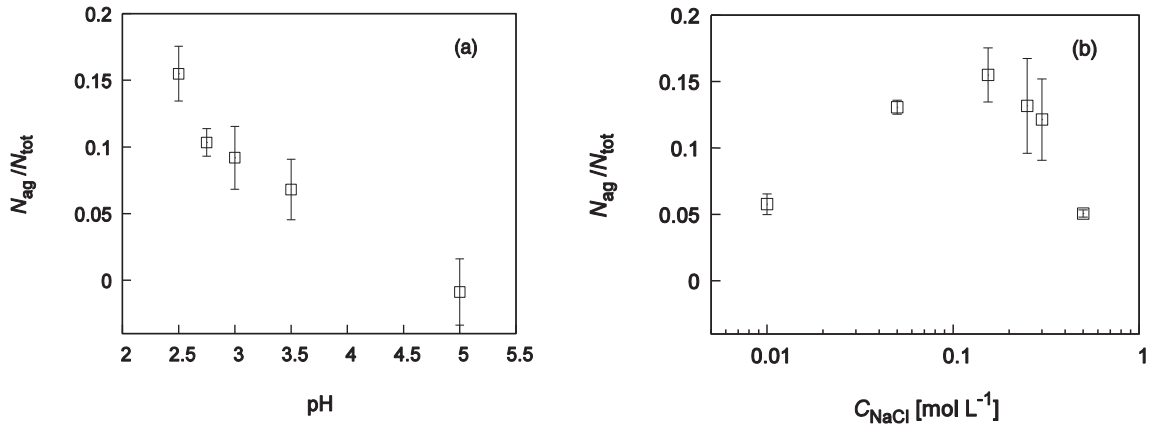

Fig. 3: Degree of spore aggregation in stirred suspensions of different pH values (a) and sodium chloride concentrations (b). Diagrams show means (□) and standard deviations of estimated relative amounts of spores present in aggregates after 80 min of stirring. pH-dependent data refer to a sodium chloride concentration of 0.154 molL^{-1}, data determined as a function of salt concentration to a pH of 2.5.

Electrostatic surface potential and aggregation behavior

The fact of the negative zeta potentials, which could be found even at pH values of 2 were interesting, because they reveal strong negative charged groups at the surface which are supposed to have a big influence on the aggregation behavior. To characterize the spore surface, the alkali-soluble wall material and in particular the melanin coating of the spores was subject of a thorough examination. Earlier studies [Wheeler und Bell, 1988] revealed that the melanin of *A. niger* can generally be regarded as water soluble and is isolated by alkaline treatment [*Koroleva et al., 2007*]. Moreover it was shown, that *A. niger* melanin contains ionizable groups [*Zavgorodnyaya et al., 2002*].

For more detailed information the extraction behavior of the melanin coating was investigated. **Fig. 4** shows the pH-dependent degree of melanin extraction based on a

comparison with the maximal extraction in 0.1 M NaOH [*Wargenau et al., 2011*]. Surprisingly, it is partially extracted even under acidic conditions.

The extraction curve shows a plateau between pH 5 and 6 suggesting a two-stage process. Under the simplified assumption that the amount of the released pigment is proportional to the degree of dissociation of the mentioned ionizable groups (shown by a least square fit for a pK_a value of 4.3), a fast protonation of carboxyl groups can be assumed to be responsible for the increase of the extracted melanin at higher pH values. Conductometric titration experiments of a defined amount of the alkali-soluble wall material between pH 3.5 and 7 with 0.1 M NaOH support this assumption [*Wargenau et al., 2011*]. In order to exclude the responsibility of protein carboxyl groups from the total amount of titratable groups, first an amino acid hydrolysis with 6 M HCl and proteinase K and second a HPLC amino acid analysis were carried out, with the result that almost no protein could be found in the wall material. Furthermore, the measured mass fraction of carbohydrates determined by the phenol-sulfuric acid method [*Swan, 1974*] with glucose as a standard, was about 4 % whereby the melanin associated amount of carbohydrates seemed to be low. Therefore it is most likely that the melanin molecule itself contains carboxyl groups.

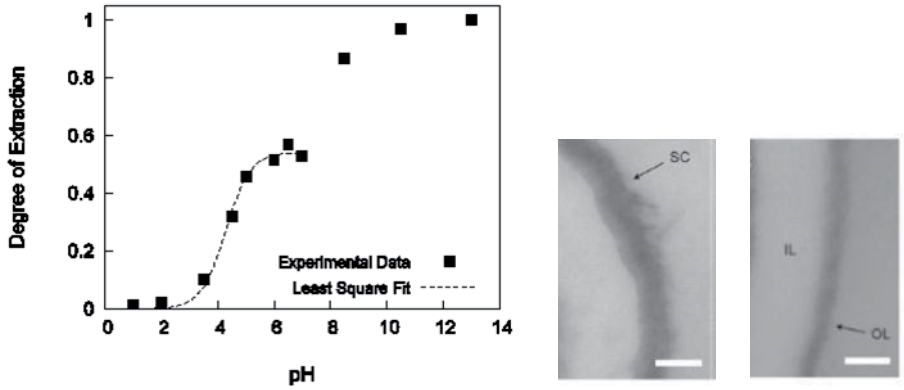

Fig. 4: Left: pH-dependent degree of extraction determined from absorbance measurements. Middle: TEM image of A. niger *spore without alkali treatment (SC: Surface coating). Right: TEM image of* A. niger *spore after alkali treatment (IL: Inner Wall Layer, OL: Outer Wall Layer). Scale bar: 100 nm [Wargenau et al., 2011].*

Generally the zeta potential can be used for a prediction of the stability of an aggregate. As already investigated by Hannan (*1961*), *A. niger* spores show a generally negative zeta potential, but with this finding alone the complex spore aggregation under different conditions could not be satisfactorily explained. So with the target of characterizing and modeling the spore aggregation the zeta potential at different pH values and salt concentrations was investigated, keeping the pH depending melanin extraction in mind. The zeta potential was calculated by the Smolukowski equation [*Lyklema, 2003*] from electrophoretic mobility measurements in buffer solutions with pH values from 2 to 6. The results are depicted in **Fig. 5**. The figure shows that the zeta potential decreases with increasing pH value. Additionally, increasing salt concentrations also lead to higher zeta potential. These findings are in good agreement with the partial release of melanin at different pH values. At pH 6 more melanin is released from the spore surface than at lower

pH values leading to less shielding of the positive charged spore wall by the negatively charged melanin. Experiments with albino spores, which completely lack of melanin showed an isoelectroc point at pH 3.5 [*Priegnitz et al., 2012*]. This fact demonstrates the influence of the melanin on the Zeta potential.

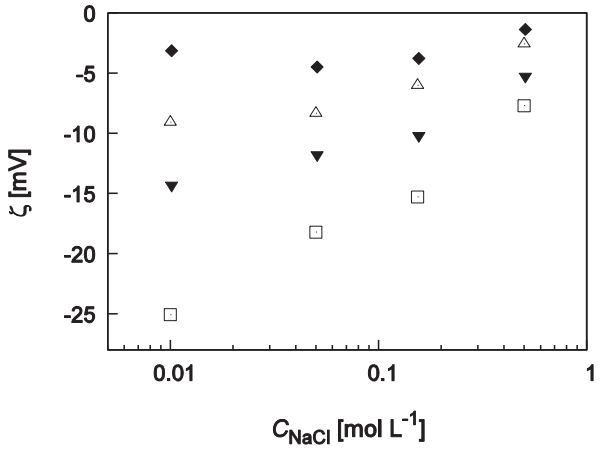

Fig. 5: Zeta potential of A. niger *spores as a function of sodium chloride concentration, determined at pH 2.5 (♦), pH 3 (△), pH 3.5 (▼) and pH 5 (□).*

Theoretical approach of the spore aggregation

Investigating the agglomeration behavior of particles, their electrostatic properties are supposed to play a key role in the agglomeration. In the case of *A. niger* spores, the surface shows due to its melanin coating a much more complex behavior than anorganic particles. For the description of this behavior a Poisson-Boltzmann model was proposed. With the help of this model the potential profiles across the spore solution or between two spores were calculated, assuming different spore surface potentials, melanin layer thicknesses and charges. In this model the potential profile arises from three sources. First of all the charge density at the surface of the spore (σ). Second: the charge density of the ionized carboxyl groups in the melanin containing layer. Third: The charge densities of mobile ions from the solution which are assumed to obey Boltzmann's distribution. These ions are able to penetrate the melanin containing layer, but not the spore wall. They derive from salt, which is added to the medium as well as from dissociations processes due to the pH value. A schematic of the model is shown in **Fig. 6**.

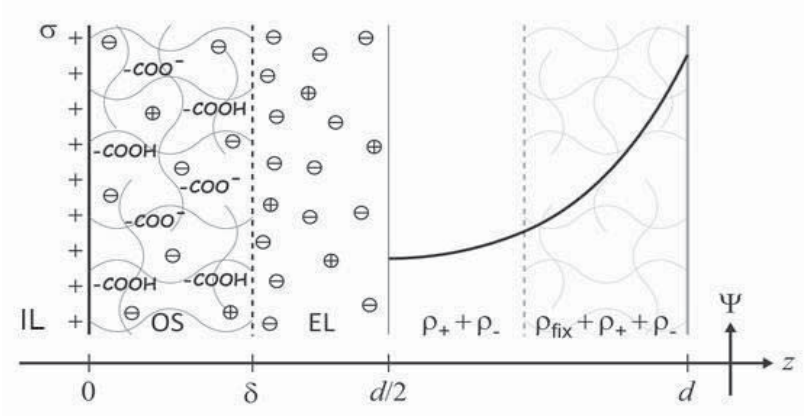

Fig. 6: Schematic of the Poisson-Boltzmann model for the calculation of the potential profiles Ψ(z). On the left side the positively charged spore surface is shown (IL). It is followed by an ion-penetrable melanin layer of the thickness δ (OS) and the ion containing solution (EL). On the right side a second spore in a distance of d is denoted.

Using this model, a sensitivity analysis was performed regarding the parameters thickness of the melanin containing layer, surface potential, pH, bulk ion concentration, ion solubility in the melanin containing layer, interaction with another spore surface and a compression of the melanin layers between these interacting spores. As an example the electrostatic potential profiles for different bulk ion concentrations are shown in **Fig. 7** (left). The calculated values at the surface of the melanin containing layer, which is assumed to be identical to the zeta potential, are close to zero. Higher salt concentrations show smaller absolute Zeta potentials. This is in agreement with zeta potential measurements. But calculating the electrostatic pressure between the spores at different distances and ion concentrations, a minimum or a maximum at an ion concentration of 0.1 molL^{-1} can be achieved (Fig. 7, right). A minimum in the electrostatic pressure is a reasonable explanation for the aggregation maximum which was measured during aggregation experiments (shown in Fig. 3). The Poisson-Boltzmann model turned out to be a potent tool for the interpretation of electrostatic interactions between particles.

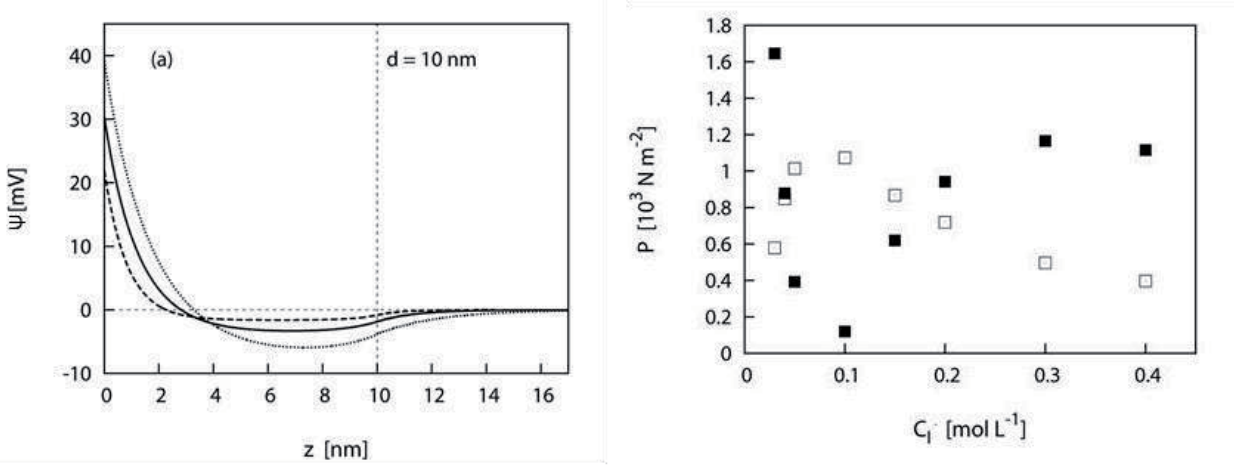

Fig. 7: Left: Potential profiles of different bulk ion concentrations. Calculation conditions: σ= 0.02 Cm^{-2}, δ=10 nm, pH= 2.5, c$_l$= 0.02 molL^{-1}(·····), c$_l$= 0.05 molL^{-1}(——), c$_l$= 0.12 molL^{-1}(----). Right: Electrostatic pressure between two spore surfaces as a function of bulk ion concentration. Calculation conditions: σ= 0.02 Cm^{-2}, δ= 5 nm, pH= 2.5, d= 5 nm (■), d= 10 nm (□).

Spore-hyphae adhesion force determination

According to the initial aims of this research also the adhesion forces between single spores and hyphae were object of further investigations. To this end the same approach as in the spore-spore adhesion experiments was used, except that hyphae were immobilized on a substrate instead of spores. It turned out that the silicon carriers treated with dimethyldichlorosilane were well-suited for the immobilization of the hyphae.

Fig. 8 shows the distributions of the measured adhesion forces. Each distribution is the result of 100 force-distance curves recorded between 10 spores and 10 different hyphae. They were cultured directly on the silicon carrier in a defined minimal medium for at least 8 h. Altogether, the estimated adhesion force distributions are similar to each other. For testing in NaCl solution with two single spores at two different pH values no significant

change in the adhesion force distributions can be confirmed. The same trend observed here is also exhibited in measurements in the cultivation medium at a pH value of 5. In contrast at a pH value of 2.5 the adhesion forces are significantly higher. These findings can be partly explained by the fact that the zeta potential of spores in the cultivation medium at a pH value of 2.5 is supposed to be close to zero. The resulting low electrostatic repulsion leads to higher adhesion forces.

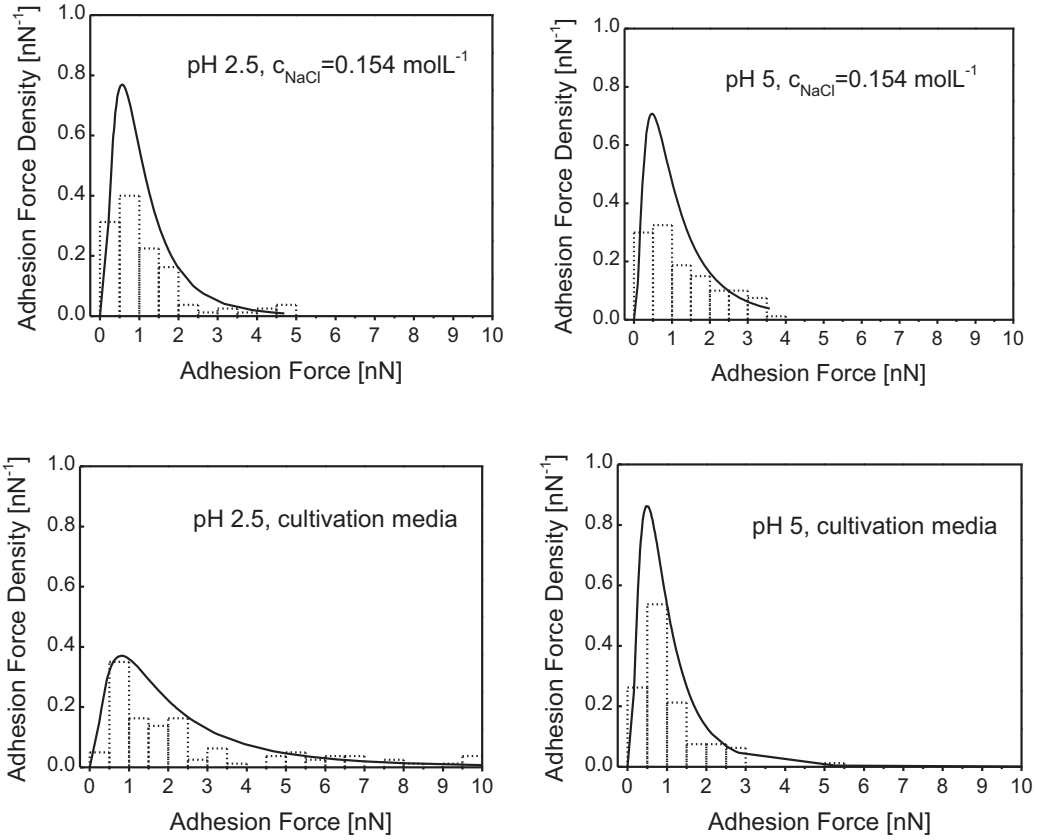

Fig. 8: Histograms and estimated distributions of adhesion force between a single spore and different hyphae, measured in NaCl solution and in cultivation media at different pH values. The area of one bar represents the relative de-adhesion events within this class.

Nevertheless Grimm et al. (*2005b*) (subproject B3 (Krull/Hempel)) found a deviant behavior in which low pH values cause a morphological differentiation to mycelia that is associated with little spore aggregation and hence with smaller adhesion forces. Recent studies on the aggregation of germinating *Aspergillus fumigatus* conidia [Fontaine et al., 2010] have shown that α1-3 glucans become visible after the loss of the outer spore wall. Also Dague et al. (*2008*) detected by dynamic chemical force spectroscopy major changes on the spore surface, the behavior being inversed from being mostly hydrophobic towards showing a purely hydrophilic characteristic. This indicates that in *A. niger* as well as in *A. fumigatus* a modification of the spore surface leads to different adhesion forces for which reason the different findings in the subprojects B3 (Krull/Hempel) and this subproject are quite consistent.

Micromechanical characterization of *A. niger* hyphae

For the micromechanical characterization of *A. niger* hyphae a method for the investigation of single hyphae in defined aqueous solutions with an atomic force microscope (AFM) had to be established. In the microscopic regime frequently indentations with the tip of a cantilever are used to measure mechanical properties. The main challenge was the immobilization of hyphae towards a substrate. This was done by combining the germination and immobilization process. The spores were cultivated in the presence of hydrophobized silicon carriers. After 15 h of cultivation the growing hyphae were already attached to the surface. Further growth and branching of the hyphae during force spectroscopic measurements were avoided by changing the culture medium to physiological NaCl-solution. Based on AFM-images of the hypha surface force distance curves on defined positions of the sample surface were performed.

The initial contact between hypha and cantilever showed a nonlinear behavior. This section of the curve is often used for the calculation of the Young's Modulus by the Hertzian theorie [*Touhami et al., 2003; Zhao et al., 2005*]. The application of this model requires several boundary conditions. For instance knowledge's of the exact tip geometry, elastic deformation behavior of the cell surface and a plane surface. Since these boundary conditions could not met in this case, the microbiological spring constant was used instead. It is a frequently used value for the description of mechanical properties in biology [Arfsten et al., 2010]. As long as not otherwise stated, the behavior of one hypha was calculated from 50 force distance curves.

The force spectroscopic measurements were performed on hyphae, which were cultivated at different environmental conditions, more precisely at different pH value and salt concentrations. For each pH value the cellular spring constants of at least 38 hyphae (with each 50 measurements) were determined and summarized to the median value. The results are depicted in **Fig. 9**. An increase of the pH value in the cultivation medium results in a decrease of the cellular spring constant. Similar results are reported by Gaboriaud et al. (*2005*), who investigated the nanomechanical properties of *Shewanella putrefaciens*. They suggested a higher turgor pressure at low pH values and a softening of the cell wall. However, we also suppose that differences in the cell wall compositions exist. These differences in the composition of the cell walls are conceivable, since the germination process took more time at higher pH values.

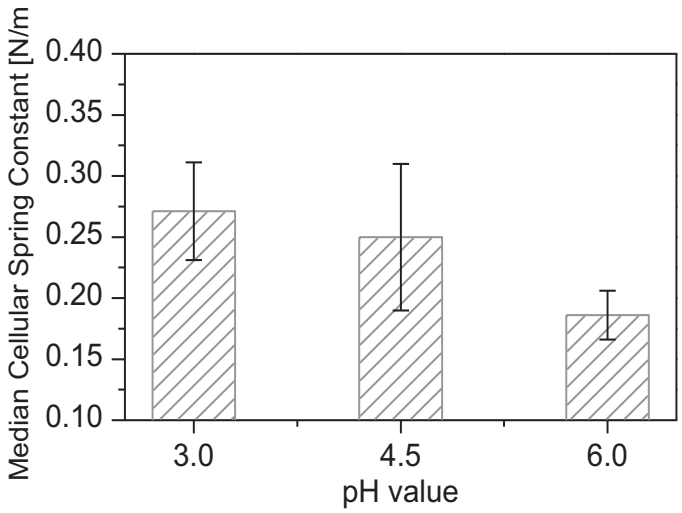

Fig. 9: Effect of the pH value on the cellular spring constant: The mechanical behavior was determined after cultivation of A. niger *at different pH values. The bars represent the confidence interval (confidence level 95%).*

According to Wucherpfennig et al. (*2011*) (B3, Krull/Hempel) the fungal morphology and productivity is also noticeably affected by the osmolality. Beyond that the influence of different osmolalities in the cultivation medium on the mechanical behavior and the size of the hyphae were investigated. The osmolality of the growth medium (Vogel Medium) was determined to be 0.184 osmol/kg. The investigations were carried out at higher osmolalities: 0.5, 1, 2 and 3 osmol/kg. In **Fig. 10** (left) the results of the height measurements are shown. A significant decrease of the height with increasing osmolality can be observed. Two effects can be suggested to explain these results: on the one hand the formation of thinner hyphae in presence of high solute concentrations on the other hand a reduction of the hyphae volume derived from the outflow of intracellular water to balance the osmotic gradient.

The right chart in Fig. 10 depicts the influence of the osmolality on the cellular spring constants by means of a box plot. It shows a minimum of the cell rigidity at an osmolality of 1 osmol/kg. It is suggested, that this minimum is derived by a decreasing turgor pressure on the one hand and an increasing rigidity of the cell wall due to the increasing cell wall curvature of thinner hyphae on the other hand.

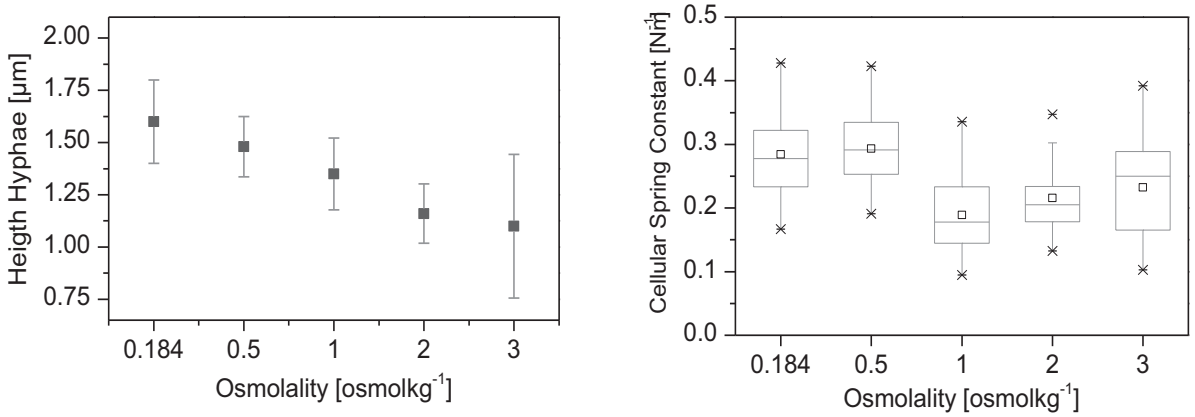

Fig. 10: Left: Influence of the extracellular salt concentration on the height of the hyphae. The height (median) was determined by measuring the z-piezo displacement in the AFM images. Right: Box plot of the cellular spring constants to the osmolality.

Another approach for the measurement of mechanical properties are tensile tests at single hyphae. For this a new experimental set up will be established based on a micro gripper. In cooperation with subproject D2 (Büttgenbach/Dübel) a micro gripper was designed and manufactured to perform tensile tests at single hypha. The hypha is glued at both sides of the gripper and stretched, when the gripper opens. The measurements will be done in a nanoindenter which is capable of measuring force distance curves. By the means of the stress strain curve it is possible to determine the Young modulus. A schematic arrangement of the gripper and a manufactured micro gripper is shown in **Fig. 11**. The experimental realization of the setup is still in progress. It is intended to establish this method till the end of the project.

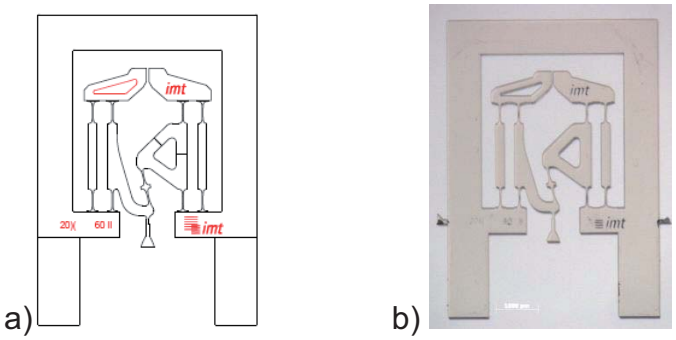

Fig. 11: a) Schematic arrangement of the micro gripper, b) Realized micro gripper.

Macromechanical characterization of *A. niger* hyphae

The macromechanical behavior, more precisely the hydrodynamic induced fragmentation of the *A. niger* pellets, was studied in a double gap rheometer geometry (Searl Type). An automated image analysis for the quantitative characterization of changes in the pellet shape was used. For this different parameters from literature and own research, like the area, perimeter, circularity, aspect ratio, solidity, mean and modal grey value, are chosen to describe the changes in the pellet shape due to hydrodynamic stress [*Reichl et al., 1992; Cox et al., 1998; Paul and Thomas, 1998*]. Based on the results of the image analysis clear changes of the morphology can be noticed at the outer zone of fluffy and hairy pellets during a shear time of 180 min. Thereby a shear rate of 1000 s^{-1} and a applied shear stress of 6.4 down to 4.6 Pa was achieved. Exemplary, this fragmentation characteristic is depicting in **Fig. 12**. The visual changes from a roundish pellet to a star-shaped pellet are verified by parameters like perimeter, aspect ratio, solidity and modal gray value. With the respect to the different mechanisms of the hydrodynamic fragmentation, the shaving off and breaking up of the outer pellet zone according to Cui et al. (*1997*) could be confirmed. In addition another mechanism, the plucking off, was observed. This is a process in which small fragments of mycelia from the outer zone of the pellet are separated from the core which leads to a star-shaped outer appearance opposed to the former round form. This behavior can be explained by Taylor eddies which occurrence is characteristic for double gap rheometers.

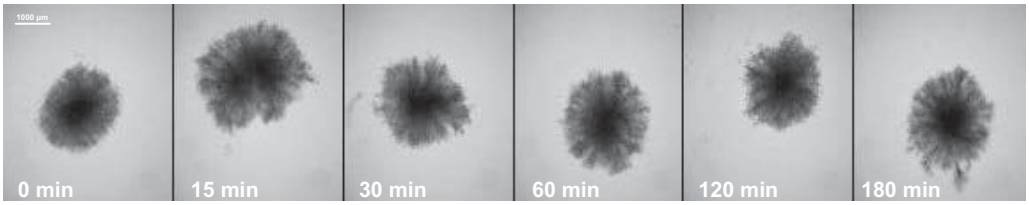

Fig. 12: Images of (different) stressed pellets at several time intervals. The pellets were stressed at a shear rate of 1000 s^{-1}.

Summary

This subproject developed several methods for the measurement of characteristics which are connected to the morphology of *A. niger* cultures. The main part concerned the spore/spore interaction. Direct measurements of adhesion forces were carried out at different environmental conditions. These results were complemented by Zeta potential measurements, aggregation experiments and detailed investigations of the melanin containing surface layer. For the explanation of the experimental results a Poisson-Boltzmann model was developed which is capable of calculating the electrostatic potential profiles of the spores.

Moreover, the adhesion between spores and hyphae was measured in different environmental conditions. These adhesion forces show bigger values than between spores, but the measurements in culture broth disagree with experimental results from subproject B3 (Krull/Hempel). A possible explanation for this fact is a change in the surface structure of the spores during germination.

Another aim of this subproject was the investigation of hyphae breakage. This was done macroscopic in a double gap rheometer followed by picture analysis. Additionally, AFM force spectroscopic measurements were performed on single hypha at different environmental conditions. In the end of the project an experimental setup for tensile tests on single hyphae is developed.

The investigations of this subproject gave a deep insight into the micromechanical properties of *A. niger* spores and hyphae. The developed methods and models can be applied at numerous microscopic investigations of biological material. The main obstacle of the experimental investigations to reach reliable data was the complex behavior of the melanin containing surface coating of *A. niger*. The experiments were very time consuming. Therefore the investigations of the single hyphae breakage are still in progress.

3.2.1.3 References to other works and collaborations in the SFB

Subproject B3 (Krull/Hempel) provided the *A. niger* strain AB 1.13 as well as methods for cultivation in shake flasks and petri dish scale to receive the desired morphology. Furthermore fragmentation of pellets in a double gap rheometer was conducted. For this

purpose existing knowledge regarding the pellet size analysis by laser diffraction was combined with image analysis techniques to characterize changes in the pellet morphology induced by shear stress.

Subproject B4 (Jahn/Nörtemann/Jänsch) supported this subproject by analyzing the protein fraction of the alkali soluble wall material to get a deeper inside to the spore surface composition.

Subproject D2 (Büttgenbach/Dübel) designed and manufactured micro gripper to perform tensile test of single hypha.

3.2.1.4 Comparison with research outside the SFB

The characterization of the adhesion behavior especially the investigation of the surface properties was part of several studies. In this subproject the overall interaction between two spores under different conditions was measured. For example, Dague et al. (2008) found by real time AFM imaging and force mapping a significant change in the spore surface of *A. fumigatus* during the first three hours after inoculation. The hydrophobic crystalline rodlet layer changes into an amorphous more hydrophilic material. It should be noted that the focus of most approaches is set on local force measurements, in contrast to the conducted measurements in this subproject in which the overall interaction between two spores was considered.

The influence to the aggregation behavior of the soluble melanin layer of *A. niger* was the object of inquiry of Priegnitz et al. (*2012*). They compared the aggregation and adhesion of a mutant without melanin with the wild type and found, different to the models suggested in this SFB, that the initial spore interactions only have a small influence to the pellet formation. This is supported by the study of Fontaine et al. (*2010*) where they revealed that the aggregation is induced by α1-3 glucans attached to the cell wall. Moreover a closer look to the chemical composition of the spore surface is possible by chemical force spectroscopy together with immobilization of living cells in porous polymer membranes [*Dufrene, 2008*]. However no comparable publication describing the aggregation behavior in dependence of a variable melanin layer and so a changing surface potential is known.

Unfortunately, there is little literature dealing with the micromechanical properties of *A. niger* hyphae. For example Lee et al. (*2010*) tried to predict the chemical composition and structure of *Aspergillus nidulans* hyphal wall by comparing force spectroscopy values of commercially available β-glucan, chitin and protein with measurements on the hyphal tip surface. Another study found an increase of cell wall elasticity of *Aspergillus versicolor* with corresponding increase of metal ion adsorption [*Das et al., 2008*]. However, more literature dealing with bacteria and yeasts can be found. Arfsten et al. (*2010*) have shown for *Saccharomyces cerevisiae* that the relationship between the turgor pressure and the cellular spring constant is proportional up to a critical turgor pressure corresponding to an extracellular osmotic pressure of 0.75 MPa. In this work not only the measurement parameters were varied but also the salt concentration during the cultivation of *A. niger* was changed. In particular, the determination of cellular spring constants was carried out

under higher ionic strength, that mean higher extracellular osmotic pressure than in the work of Arfsten et al. (*2010*).

Finally, an adoption of the work of Guo et al. (*2011*) regarding a push-to-pull device was conducted]. This enables the possibility of tensile tests of single hypha using a Nanoindenter to gain values for the elasticity especially the Young´s modulus.

In this subproject several shear stress experiments with pellets in a double gap rheometer were carried out. They showed not only shaving or breaking of hypha but also plucking off. A comparable work of Patel et al. (*2010*) deals with the effect of shear stress during the cultivation of *Trichoderma reesei* in a Couette flow bioreactor. They found a higher rate of fragmentation with increasing shear rate. In contrast to this work the pellets were sheared with generally higher rates than Patel et al. (*2010*) reported because no significant change of the rate of fragmentation with increasing shear rate could be observed.

3.2.1.5 Literature

Amanullah, A.; Leonildi, E.; Nienow, A. W.; Thomas, C. R. (2001) Dynamics of mycelial aggregation in cultures of *Aspergillus oryzae*. *Bioproc. Biosyst. Eng*. 24, 101-107

Arfsten, J.; Leupold, S.; Bradtmöller, C.; Kampen, I.; Kwade, A. (2010) Atomic force microscopy studies on the nanomechanical properties of *Saccharomyces cerevisiae*. *Colloids and Surfaces B: Biointerfaces* 79, 284-290

Cox, P.W.; Paul, G.C.; Thomas, C.R. (1998) Image analysis of the morphology of filamentous micro-organism. *Microbiol.* 144; 817-827

Cui, Y. Q.; van der Lans, R. G. J. M. und Luyben, K. C. A. M. (1997) Effect of Agitation Intensities on Fungal Morphology of Submerged Fermentation. *Biotechnol. Bioeng.* 55(5): 715-726

Dague, E.; Alsteens, D.; Latgé, J.-P.; Dufrêne, Y. F. (2008) High-Resolution Cell Surface Dynamics of Germinating *Aspergillus fumigatus* Conidia. *Biophysical Journal* 94, 656-660

Das, S. K.; Das, A. R.; Guha, A. K. (2008) Adsorption Behavior of Mercury on Functionalized *Aspergillus versicolor* Mycelia: Atomic Force Microscopic Study. *Langmuir* 25, 360-366

Dufrene, Y. F. (2008) Atomic force microscopy and chemical force microscopy of microbial cells. Nat. Protoc. 3, 1132-1138

Dynesen, J.; Nielsen, J. (2003) Surface hydrophobicity of *Aspergillus nidulans* conidiospores and its role in pellet formation. *Biotechnol. Prog.* 19, 1049-1052

El-Enshasy, H.; Hellmuth, K.; Rinas, U. (1999) Fungal morphology in submerged cultures and its relation to glucose oxidase excretion by recombinant *Aspergillus niger*. *Appl. Biochem. Biotech.* 81, 1-11

Elmayergi, H.; Scharer, J. M.; Moo-Young, M. (1973) Effects of polymer additives on fermentation parameters in a culture of *A. niger*. *Biotechnol. Bioeng.* 15, 845-859

Fontaine, T.; Beauvais, A.; Loussert, C.; Thevenard, B.; Fulgsang, C. C.; Ohno, N.; Clavaud, C.; Prevost, M. C.; Latge, J. P. (2010) Cell wall alpha1-3glucans induce the aggregation of germinating conidia of *Aspergillus fumigatus*. *Fungal Genet. Biol.* 47, 707-712

Fujita, M.; Iwahori, K.; Tatsuta, S.; Yamakawa, K. (1994) Analysis of pellet formation of *Aspergillus niger* based on shear stress. *J. Ferment. Bioeng.* 78, 368-373

Gaboriaud, F.; Bailet, S.; Dague, E.; Jorand, F. (2005) Surface Structure and Nanomechanical Properties of *Shewanella putrefaciens* Bacteria at two pH values (4 and 10) determined by Atomic Force Microscopy. *J. Bacteriol.* 187, 3864-3868

Galbraith, J. C.; Smith, J. E. (1968) Filamentous growth of *Aspergillus niger* in submerged shake culture. *Trans. Br. Mycol. Soc.* 52, 237-246

Gerin, P. A.; Dufrene, Y.; Bellon-Fontaine, M.-N.; Asther, M.; Rouxhet, P. G. (1993) Surface Properties of the Conidiospores of Phanerochaete chrysosporium and Their Relevance to Pellet Formation. *J. Bacteriol.* 175, 5135-5144

Grimm, L. H.; Kelly, S.; Krull, R.; Hempel, D. C. (2005a) Morphology and productivity of filamentous fungi. *Appl. Microbiol. Biotechnol.* 69, 375-384

Grimm, L. H.; Kelly, S.; Völkerding, I. I.; Krull, R.; Hempel, D. C. (2005b) Influence of mechanical stress and surface interaction on the aggregation of *Aspergillus niger* conidia. *Biotechnol. Bioeng.* 92, 879-888

Guo, Hua; Chen, K.; Oh, Y.; Wang, K.; Dejoie, C.; Syed Asif, S. A.; Warren, O. L.; Shan, Z. W.; Wu, J.; Minor, A. M. (2011) Mechanics and Dynamics of the Strain-Induced M1–M2 Structural Phase Transition in Individual VO2 Nanowires. *Nano. Letters* 11, 3207-3213

Hannan, P.J. (1961) Electrophoretic Properties of Spores of *Aspergillus niger*. *Appl. Environ. Microbiol.* 9, 113-117

Jones, G. E. B. (1994) Fungal adhesion. *Mycol. Res.* 98, 961-981

Koroleva, O.; Kulikova, N.; Alekseeva, T.; Stepanova, E.; Davidchik, V.; Belyaeva, E.; Tsvetkova, E. (2007) A comparative characterization of fungal melanin and the humin-like substances synthesized by <i>Cerrena maxima 0275. *Appl. Biochem. Microbiol.* 43, 61-67

Lee, H. U.; Park, J. B.; Lee, H.; Chae, K. S.; Han, D. M.; Jahng, K. Y. (2010) Predicting the chemical composition and structure of *Aspergillus nidulans* hyphal wall surface by atomic force microscopy. *J. Microbiol.* 48, 243-248

Lyklema, J. (2003) Electrokinetics after Smoluchowski. *Colloids and Surfaces A: Physicochemical and Engineering Aspects* 222, 5-14

Papagianni, M.; Mattey, M.; Kristiansen, B. (1998) Citric acid production and morphology of *Aspergillus niger* as functions of the mixing intensity in a stirred tank and a tubular loop bioreactor. *Biochem. Eng. J.* 2, 197-205

Patel, N.; Choy, V.; White, T.; Munkvold, G.; Thibault, J. (2010) Design of a novel Couette flow bioreactor to study the growth of fungal microorganism. *J. Biotechnol.*145, 264-272

Paul, G.C.; Thomas, C.R. (1998) Characterisation of mycelial morphology using image analysis, Springer Berlin / Heidelberg

Reichl, U.; King, R.; Gilles, E. D. (1992) Characterization of pellet morphology during submerged growth of Streptomyces tendae by image analysis. Biotechnol. Bioeng. 39, 164-170

Ryoo, D.; Choi, C.-S. (1999) Surface thermodynamics of pellet formation in *Aspergillus niger*. *Biotechnol. Lett.* 21, 97-100

Stocks, S.M.; Thomas, C.R. (2001) Viability, Strength, and Fragmentation of *Saccharopolyspora erythraea* in Submerged Fermentation. *Biotechnol. Bioeng.* 75, 702-709

Suijdam, J. C.; Metz, B. (1981a) Fungal pellet breakup as a function of shear in a fermentor. *J. Fermentation Technol.* 59, 329-333

Suijdam, J. C.; Metz, B. (1981b) Influence of engineering variables upon the morphology of filamentous molds. Biotechnol. Bioeng. 23, 111-148

Swan, G. A. (1974) Structure, chemistry, and biosynthesis of the melanins. Fortschritte der Chemie organischer Naturstoffe. Progress in the chemistry of organic natural products. *Progres dans la chimie des substances organiques naturelles* 31, 521-582

Touhami, A.; Nysten, B.; Dufrêne, Y.F. (2003) Nanoscale Mapping of the Elasticity of Microbial Cells by Atomic Force Microscopy. *Langmuir* 19, 4539-4543

Tronchin, G.; Bouchara, J. P.; Ferron, M.; Larcher, G.; Chabasse, D. (1995) Cell surface properties of *Aspergillus fumigatus* conidia: correlation between adherence, agglutination, and rearrangements of the cell wall. *Can. J. Microbiol.* 41, 714-721

Tucker, K. G.; Thomas, C. R. (1992) Mycelial morphology: the effect of spore inoculum level. *Biotechnol. Lett.* 14, 1071-1074

Wheeler, M. H.; Bell, A. A. (1988) Melanins and their importance in pathogenic fungi. *Current topics in Medical Mycology* 2, 338-387

Wucherpfennig, T.; Hestler, T.; Krull, R. (2011) Morphology engineering - Osmolality and its effect on Aspergillus niger morphology and productivity. *Microb. Cell Fact.* 10, 58

Zavgorodnyaya, Yu A.; Demin, V. V.; Kurakov, A. V. (2002) Biochemical degradation of soil humic acids and fungal melanins. *Organic Geochemistry* 33, 347-355

Zhao, L.; Schaefer, D.; Marten, M.R. (2005) Assessment of Elasticity and Topography of *Aspergillus nidulans* Spores via Atomic Force Microscopy. *Appl. Environ. Microbiol.* 71, 955-960

3.2.2 Project Relevant own publications

a) Works that have appeared in publications of a scientific quality assurance at the time of application or final adoption, and book publications

Kampen, Ingo; Kwade, Arno; Flickinger, M. C. (2009) Cell Disruption, Microbial, Micromechanical Properties. Encyclopedia of Industrial Biotechnology, John Wiley & Sons, Inc.

Wargenau, A.; Kwade, A. (2010) Determination of adhesion between single *Aspergillus niger* spores in aqueous solutions using an atomic force microscope. *Langmuir* 26, 11071-11076

Wargenau, A.; Bolten, C.J.; Rohde, M.; Kampen, I.; Fleissner, A.; Kwade, A. (2011) On the origin of the electrostatic surface potential of *Aspergillus niger* spores in acidic environments. Research in Microbiology 162, 1011-1017

Priegnitz, B.-E.; Wargenau, A.; Brandt, U.; Rohde, M.; Dietrich, S.; Krull, R.; Fleißner, A. (2012) The role of initial spore adhesion in pellet and biofilm formation in Aspergillus niger. *Fungal Genet. Biol.* 49, 30-38

b) Other publications

Krull, R.; Cordes, C.; Horn, H.; Kampen, I.; Kwade, A.; Neu, T.R.; Nörtemann, B. (2010) Morphology of filamentous fungi - Linking cellular biology to process engineering using *Aspergillus niger*. In: Biosystems Engineering II – Linking Cellular Networks and Bioprocesses, Series: *Adv. Biochem. Eng./ Biotechnol.,* Vol. 121, Scheper, T. (Series Ed.), Wittmann, C.; Krull, R. (Vol. Eds.), ISBN 978-3-642-13865-2,1-21, Springer Verlag, Heidelberg

3.3 Looking back on the promotion

The project has been funded since July 2008 in the SFB 578. It was completed on June 2012 with the end of the program.

3.3.1 Personnel in the project

	Name, akad. degree, service position	narrower subject of the employee	Institute of University or non-university facility	Participation in the project in hours per week	Category
Basic staff					
Research associate (incl. auxiliary power)	1. A. Kwade Prof. Ing.-Dr. 2. I. Kampen Dr.-Ing.	Process Engineering Mechanical Biotechnology	Institute for Particle Technology Institute for Particle Technology	6 15	Professorship Post-doctoral
Non academic staff	3. S. Michel BTA		Institute for Particle Technology	10	Technical staff
Supportive staff					
Research associate (incl. auxiliary power)	4. A. Wargenau M. Sc. 5. S. Günther 6. K. Lippe	Chemistry Process Engineering Bioengineering Biotechnology	Institute for Particle Technology Institute for Particle Technology Institute for Particle Technology	40 40 40	PhD student PhD student PhD student
	7. N. N., Stud. assistant	Biochemical Engineering, Biotechnology	Institute for Particle Technology	10	Students

Responsibilities of employees (basic staff)

Position 1: Prof. Dr.-Ing. A. Kwade

As project leader Prof. Kwade supported the employees of the subproject B7 on issues concerning the process engineering and the modeling of the complex spore-spore interactions as well as the electrostatic properties caused by the pH dependend melanin coting.

Position 2: Dr.-Ing. I. Kampen

As leader of the working group Biological/Pharmaceutical Particle Technology Dr. Kampen directly supported the responsible coworkers in particular, for issues concerning biological and biotechnological question.

Position 3: S. Michel

The technical assistant Ms. S. Michel conducted several measurement series and supported the preparation of the samples.

Responsibilities of employees (supportive staff)

Position 4: M.Sc. A. Wargenau

Mr. Wargenau established a method for single-cell force measurements of *A.niger* spores. Therefore he found an appropriate possibility to immobilize a single spore to a tipless cantilever and to a silicon carrier via hydrophobic interactions. By using solvent free, light activated epoxy resin for the immobilization to the cantilever tip he could avoid changes on the spore surface and damage to the spore by UV light. To investigate the main interactions between two spores several single cell adhesion force measurements were conducted. The focus first lay upon the verification of the used method. Later he investigated the influence of different pH value and salt concentrations to the adhesion force. Additionally he introduced a statistical evaluation so that the primary force data can be described by a log-normal density function which in turn enables the possibility to identify significant differences. Accordingly to this Mr. Wargenau found a dependency between the pH value as well as the salt concentration and the adhesion force. In order to elucidate these findings he specified the outer surface by chemical analysis, zeta potential measurements, conductometric titrations and microscopy methods. In particular he examined the electrostatic potential and its origin also under different pH values and salt concentrations. In doing so the melanin coating and its partial release, by deprotonation of melanin associated carboxyl-groups, could be ascribed to be crucial. Furthermore, under the same conditons aggregation experiments were carried out to characterize the aggregation behavior right after inoculation. Ultimately, Mr. Wargenau linked the experimental aggregation data to the electrostatic surface potential and developed a numerical model to describe these particular observations.

Position 5: Dipl.-Ing. S. Günther

A method for the investigation of mechanical properties of *A. niger* hyphae in defined aqueous solutions using an atomic force microscope (AFM) was established by Mrs. Günther. This application enables the study of the fungus in the native form. Mrs. Günther showed that the mechanical properties are influenced by different measurement parameters, like the indentation position and speed. Local multiple stress did not result in weakening of the cell wall. Beyond that she investigated the influence of changes in environmental conditions to the cellular spring constant, like the pH and the extracellular salt concentrations. Mrs. Günther completed these results by a statistical consideration. The elastic properties should be determined using a tensile test. Therefore a new technique on the basis of a push-to-pull device is in progress.

The focus of work of Mrs. Günther was also on the macromechanical studies of *A. niger* using a shear system. The changes of the morphology of pellets were determined using an image analysis. Mrs. Günther found, that not only a shaving off and breaking up of the outer pellet zone occurred, but furthermore a plucking off. The reason given for this behavior occurs with the flow profile in the shear system.

Position 6: M.Sc. Biotechnol. K. Lippe

Mr. Lippe used the single-cell force measurement method introduced by position 4 for further investigation of the spore-spore adhesion behavior. Thereby he found a time dependency of contact time to the adhesion force. In addition the increase of multiple de-adhesion events which were already found by Mr. Wargenau (position 4.) suggests that besides electrostatic forces, discrete molecular interactions might play a role. So he measured the adhesion forces in cultivation media with the aim to find changes during the germination of the spores.

Furthermore, the adhesion force between single spores and hyphae were investigated. Here the immobilization method of position 5 and the position 4 as well as the data processing could be combined to get a general overview about the scale of forces appearing here. The finding of higher adhesion forces suggests a greater importance of the second aggregation phase to the morphological development of *A. niger*.

Position 7: Stud. Assistant

The student assistant supported the extensive experimental work in the implementation and evaluation of fungal cultivations as well as in the routine of biotechnological and molecular biological studies.

3.1 General information on the completed project B8

3.1.1 Topic

***Holistic Bioprocess Engineering of Antibody Fragment Secreting* Bacillus megaterium**

3.1.2 Disciplines and field of work

Bioprocess Engineering, Single Cell Analysis, Transcriptomics

3.1.3 Project manager

Jun.- Prof. Dr. Ezequiel Franco-Lara
(b.: 04.10.1969)
Institute of Biochemical Engineering
TU Braunschweig
Gaußstraße 17
38106 Braunschweig
Current address
Evonik Industries AG
Kantstraße 2
33790 Halle

3.2 Development of the subproject

3.2.1 Report

3.2.1.1 Current knowledge at the last application and initial question

From the start of the last application period of the SFB 578, *Bacillus megaterium* was already engineered to produce a couple of products like Penicillin-G-Amidase (90 kDa) [*Yang et al.; 1999*], dextrane sucrase (180 kDa) [*Malten et al., 2005*], levansucrase (110 kDa) [*Biedendieck et al., 2007*] and a hydrolase from *Thermobifida fusca* (27 kDa, TFH) [*Yang et al., 2007*]. The particular *B. megaterium* strains YYBm1 and WH323 were further optimized at the genetic level by subproject A1 (Jahn/Dersch) and for cultivation purposes by the former subproject B5 (Deckwer). For TFH production, the effect of different carbon sources on the central metabolic fluxes and multi-substrate strategies of changing pyruvate/glucose ratios were investigated in detail [*Fürch et al., 2007*]. In general the importance of finding Pareto-optimal points with both maximizing biomass and, at the same time, product concentration was highlighted. Under conditions of recombinant protein production the particular metabolic fluxes of the pentose phosphate pathway were found to be increased [*Fürch et al., 2007*]. Regarding the production and secretion of antibody fragments (ABFs), the process was basically established in shaking flasks relying on complex media compositions [*Jordan et al., 2007*] using the *B. megaterium* strain YYBm1 with a *xylA* deficiency. This strain is based on the sequenced and annotated strain DSM319 and has the big advantage of not metabolizing xylose which is used as external inductor for heterologous protein synthesis. The detailed knowledge

about its genome sequence was one of the main preconditions for extensive transcriptomic analysis.

In this study the lysozyme specific antibody fragment ABF D1.3 scFv was chosen as a model ABF for production in *B. megaterium*. Initial screening experiments for cultivation conditions like temperature and amino acid supplements were done, giving a first hints on beneficial production conditions at higher temperatures of 42°C [*Jordan et al., 2007*]. Besides it was shown for GFP production in *B. megaterium* that certain populations of producing and non-producing cells (up to 25%) occurred at high cell density cultivations (subproject A1 (Jahn/Dersch), [*Biedendieck et al., 2007*]). This fact is the basic motivation to further investigate the behavior of cells on a single cell level where different cell states concerning viability, activity and the specific production status were in the particular focus of the research. In previous studies of secreted products like dextransucrase and TFH, certain bottlenecks in folding and final release steps were pointed out.

The main aims of the last application period of the SFB 578 were firstly the establishment of a defined minimal medium composition, secondly the study of process of antibody production and secretion in depth under controlled bioreactor conditions and thirdly to find potential bottlenecks in production/secretion based on transcriptomic analysis. Traditional methods improving the process performance like optimization of culture medium and bioprocess development towards high cell densities were thereby combined with cutting-edge technologies of flow cytometry and transcriptome analysis. This holistic approach of binding both engineering on genetic level and bioprocess optimization in monitoring and control was in the main focus of particular investigations.

3.2.1.2 Results and applied methods

Medium optimization

The cultivation medium has a great influence on cell productivity. Here, the aim was to develop new defined media compositions with increased ABF D1.3 scFv production and biomass formation qualities. Based on a screening for a suitable carbon source, fructose was found out as an ideal substrate for growth associated production of ABF D1.3 scFv. An inducer concentration of 0.5% xylose was found to be optimal and less influencing the maximal growth rate whilst guaranteeing a high ABF D1.3 scFv production.

While designing a cultivation medium considering a high number of different medium components, an optimization strategy by changing one parameter at one time is simply not practical due to the huge number of necessary experiments. It also has to be considered that certain interactions between these components with a direct effect

on growth and production may take place. Therefore, experimental approaches using a genetic algorithm and statistical design of experiments like Central Composite Design (CCD) were applied. By screening different $(NH_4)_2SO_4$ concentrations in a CCD experiment it was found that high concentrations of 25 g/L directly favored an increased ABF D.1.3 scFv production.

Nine different components of particular metal ions were tested by using a genetic algorithm approach for investigating a large parameter space. Thereby, several media compositions for high functional secretion of ABF D1.3 scFv and slightly increased biomass formation were found (**Fig. 1**) [David *et al., 2010*]. It could be concluded that an increased Mg-fraction and lower Co- and Ca-fractions directly favored higher product formation and secretion. These results were interpreted by annotated genome data (subproject B9 (Münch/Schomburg)) associated to metal dependent enzyme classes where Mg was one of the most important metal ions for biomass generation and the ABF production and secretion process.

Based on an originally complex medium for ABF D1.3 scFv production [*Jordan et al., 2007*] a defined minimal medium with an increased productivity was successfully developed being most important for an appropriate process design, control and investigations at the transcriptome level.

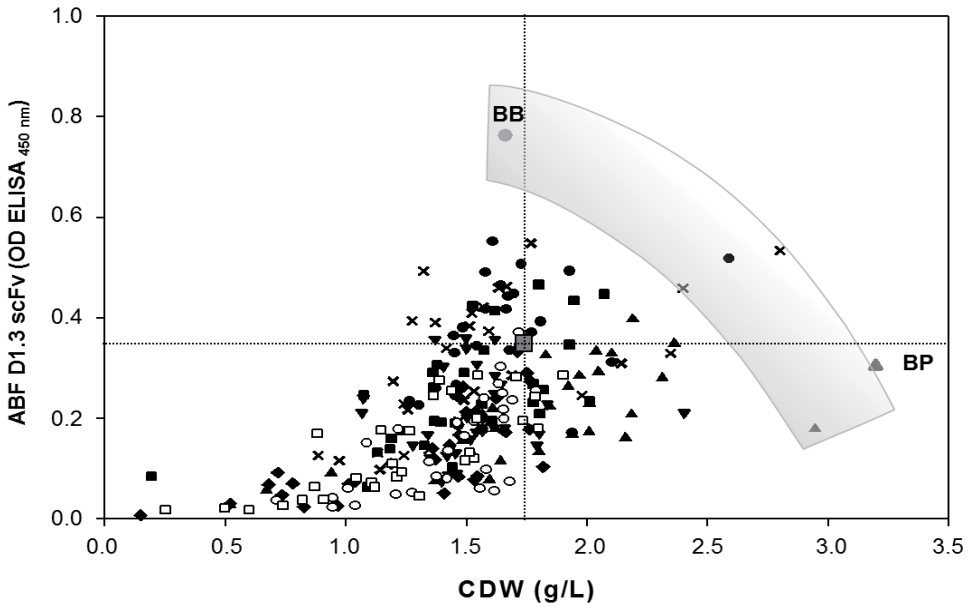

Fig. 1: Medium screening by a genetic algorithm approach for growth and ABF D1.3 scFv production of B. megaterium *YYBm1. 30 media compositions were tested in triplicates in a 96 deep-well plate cultivation platform. Pareto plot for the multi-objective optimization of biomass formation and ABF D1.3 scFv (240 tested media compositions): 0 generation (gen.) (▲), 1 gen. (▼), 2 gen. (■), 3 gen. (♦), 4 gen. (●), 5 gen. (x), 6 gen. (○), 7 gen. (□), previously used medium as control (■) (averaged by values of all generations), ● BP = medium with best ABF D1.3 scFv production, ▲ BB = medium with best biomass formation, shadowed area (Pareto-optimal solution space, (PP)).*

Advanced process monitoring – Single cell analysis

Microorganisms in industrial processes are conventionally considered to behave as uniform populations and therefore are thought to be sufficiently described by average values. These methods are not suitable to provide in depth information about an ongoing bioprocess, e.g. which fraction of cells is active and/or productive.

In this project, the technique of flow cytometry was successfully used to acquire deeper insights on single cell level of *B. megaterium* secreting ABFs. It became possible to distinguish between viable, metabolic active, depolarized, dormant, and dead cells and to discriminate between high and low productive cells. This was realized by establishing specific staining protocols with membrane potential (MP) sensitive dyes like $DiOC_2$ (**Fig. 2**), $DiBAC_4(3)$ and propidium iodide for measuring cell integrity. Besides a production intensity assay for determining single cell productivities was developed by using specific fluorophor coupled detection antibodies. The dynamics in ABF production intensities of single cells were analyzed in detail. It was shown that the secretion through the membrane coupled Sec-pathway and subsequent delayed release from the cell wall structures predominantly increased in the stationary phase of the investigated batch process [*David, et al. 2011*]. Besides the descriptive function of measuring and characterizing heterogeneities concerning the productivity the method also opens up the possibility to selectively screen for high producers.

These newly developed techniques were successfully used to monitor various batch and fed batch processes for ABF production. Whole cell culture based process parameters like dissolved oxygen (DO), carbon dioxide evolution rate and oxygen uptake rate characteristics could directly be correlated to single cell based MP measurements [*David et al., 2011*]. As both parameters of cell viability and integrity are important, they should be monitored simultaneously during bioreactor cultivations and were shown to be most helpful in describing population dynamics and changes in cell physiology. Especially in deciding whether a process is operating in a stable condition or not, the MP estimation is an optimal and very sensitive parameter to adapt process conditions or even to abort the cultivation at early stage when heterogeneities appear or critical physiological values are reached. Therefore a tool for online single cell characterization is most desirable. Measurements based on an impedance microfluidic chip technique (Leister Process Technologies, Axetris Division) were recently shown to be feasible for single cell MP characterization directly comparable to fluorescence based techniques used in this approach [*David et al., 2011*].

The methods were shown to be high resolving tools for at-line monitoring of processes allowing a better process understanding, increasing robustness and forming a firm basis for physiology-based bioprocess development and optimization.

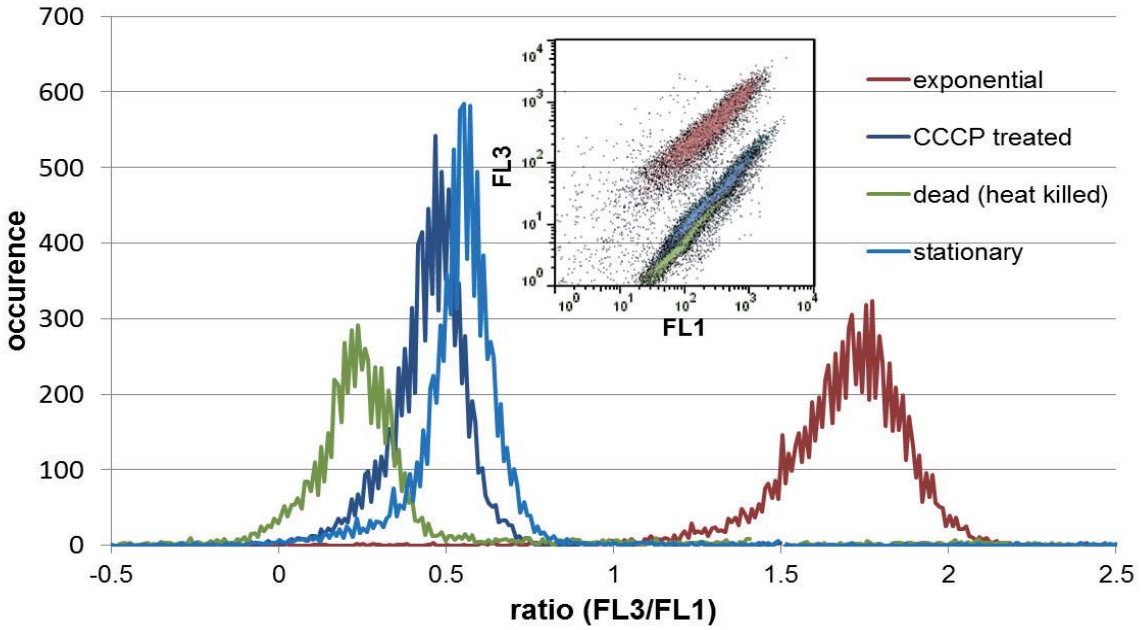

Fig. 2: Single cell analysis of B. megaterium *YYBm1 recombinantly producing ABF D1.3 scFv in a batch process. Membrane potential measurements with $DiOC_2(3)$ staining, subsequent FL3/FL1 ratio analysis regarding different growth stages (exponential and stationary) and treatment with heat and CCCP as negative controls.*

Bioprocess development

The investigated bioprocess is both a production process and simultaneously a secretion process of ABF D1.3 scFv. In this case, it could be demonstrated that the secretion of ABF D1.3 scFv increased when cells entered into the stationary phase. Based on these investigations an adequate process strategy was newly developed. By an adapted online feeding profile controlled growth and starving phases with increased ABF D1.3 scFv secretion were successfully established. The control algorithm used guaranteed comparable growth and starvation phases as the feeding profile was based on online estimated parameters of the particular biomass concentration and the cultivation volume (**Fig. 3**) [*David et al., 2011*]. Other strategies like exponential, linear or DO controlled feedings were not found to promote production or secretion. This may be related to the fact that cells have to undergo during a certain period of time starvation stress in order to develop improved secretion properties. By this approach up to 7-times higher product yields were achieved.

The described strategy of an oscillating fed-batch could successfully be transferred to the 100 L scale in cooperation with the Fraunhofer Institute for Toxicology and Experimental Medicine (ITEM, Braunschweig, Germany). The project won the second place on the BlueCompetition 2011 of the Bluesens © company, which is a worldwide challenge for optimizing the gas analysis application in Bioprocessing.

Besides, the temperature and the hydromechanical stress were investigated as two key parameters with respect to ABF production using a complex medium composition. Maximal production was found at a low volumetric power input of about 60 W/m^3 and high cultivation temperature of 41°C [*Lüders et al., 2011*].

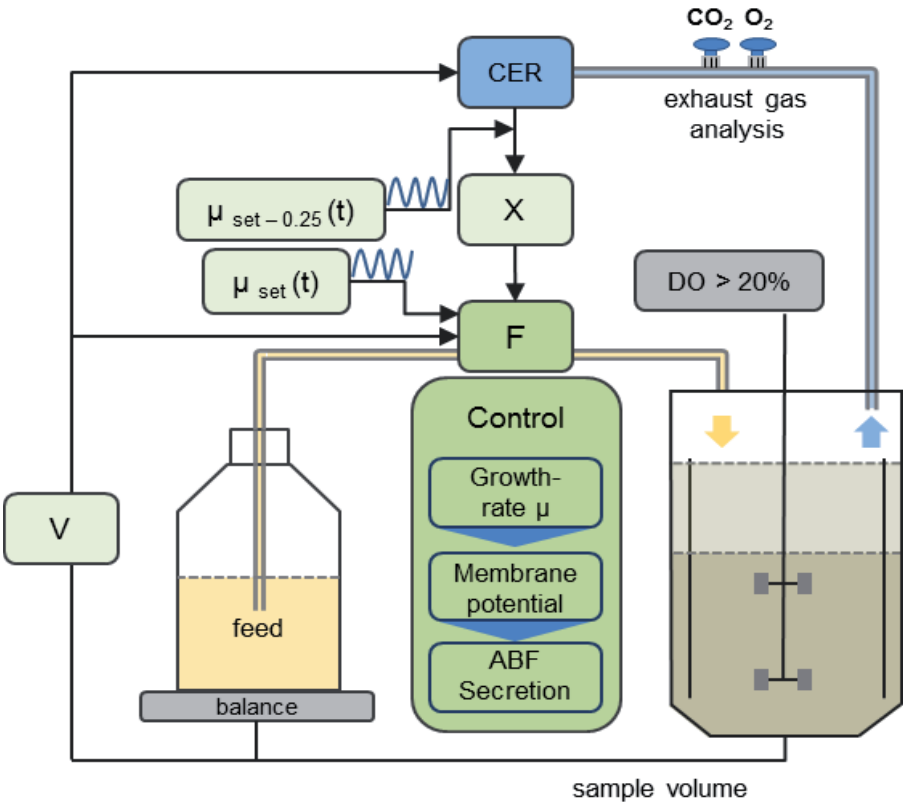

Fig. 3: Bioprocess engineering of recombinant ABF D1.3 scFv producing B. megaterium *YYBm1. Overview of the control mechanism to create a μ-oscillating feeding (F) strategy adapted to the particular biomass concentration (X) present. The biomass is estimated via the exhaust gas analysis related to CO_2 evolution rate (CER) and to the current growth rate $\mu_{set-0.25}$. μ_{set} is time dependent and based on two cosine functions with a defined maximal growth rate μ_{max}. The underlying cultivation volume (V) in the bioreactor is corrected by sample and feed volume.*

Transcriptomic analysis

The aim of increasing the overall process performance was also followed by optimizations based on genetic modifications of the production host. Therefore transcriptome analyses were done to unravel bottlenecks and potential candidates

for optimizing ABF production and secretion. Concluded from the transcriptome experiments it became obvious that the effects of stationary phase coupled increased secretion were not due to a changed expression pattern of ABF D1.3 scFv mRNA. In fact this effect may be related to certain genes which are upregulated during the stationary phase under ABF producing conditions. These include for instance proteins exhibiting folding aiding functions like the foldase PrsA which are important factors for promoting ABF secretion. For this purpose a second plasmid was constructed in close collaboration with the subproject A1 (Jahn/Dersch). The coexpression of the genes encoding for the foldase PrsA and a protein with a putitative PrsA function boosted ABF secretion up to 6-times. Further candidates for coexpression as cold shock proteins, translation initiation factors, components of the Sec-pathway and chaperones derived from transcriptome as well as from proteome analysis are in the current process of investigation in collaboration with subproject A1 (Jahn/Dersch).

3.2.1.3 References to other works and collaborations in the SFB

This project is one of the key projects in the SFB for ABF production with *B. megaterium*. Close collaborations were carried out with the subprojects A1 (Jahn/Dersch) and B10 (Franco-Lara), conducting transcriptome assay experiments, strain designs for coexpression and omics data analysis. Regarding analysis tools and expression of different antibody formats the sub project A6 (Dübel/Hust) is a close collaborator. Bioreactor cultivations up to 5L, carried out in this project, provided the raw material for subproject C2 (Seidel-Morgenstern) for purification purposes. An intense transfer of knowledge and methods took place. Collaborations with the subproject C7 (Garnweitner/Schilling) were related to the selective purification of ABFs with magnetic nanoparticles. Here different particles in the nanometer range were tested with various functionalization patterns. With subproject C6 (Schilling/Ludwig) a first prototype for online product removal by magnetic nanoparticle was constructed. Close collaborations were done with the Fraunhofer Institute for Toxicology and Experimental Medicine (ITEM) regarding the scale-up of the ABF production process to the 100 L scale [*David et al., 2011*]. The company Axetris (Leister Process Technologies) was a close collaboration partner concerning investigations on the single cell level. These were carried out in a microfluidic chip device for impedance measurements. Here both parameters of cell integrity and membrane polarization were investigated and directly compared to the particular flow cytometry analysis [*David et al., 2011*].

3.2.1.4 Comparison with research outside the SFB

The production of monoclonal antibodies is realized in several prokaryotic and eukaryotic production systems. The current systems of choice in pharmaceutical industry especially for therapeutic antibody production are mammalian cells. The

predominant use of mammalian cell cultures has been driven by the need to obtain proteins with complex biochemical structures and resulting superior activity with native structures and function. High extracellular product titers and an advanced secretion and folding apparatus for human glycosylation pattern make them an ideal production platform for monoclonal antibodies. However, the overall costs for development and production are quite high compared to the other systems. Alternative expression platforms are microbial systems. The Gram negative production host *Escherichia coli* displays high production and was engineered for periplasmatic secretion of ABFs. Besides, “leaky” *E. coli* cells were developed by specific gene knockout mutants [*Daßler and Wich, 2006*]. However those leaky strains do not provide so far enough robustness for high cell density cultivations [*Yoon et al., 2010*]. Gram positive expression systems like *Bacillus subtilis* and *B. megaterium* still exhibit relatively low ABF production titers but display a good secretion capable alternative to *E. coli*. Microorganisms like yeast cells and fungi were found to efficiently secrete and at the same time glycosylate whole antibodies and ABFs. As a main drawback these systems sometimes show insufficient glycosylation or even hyper-glycosylation patterns. They also display increased proteolytic activity thus making production processes less reproducible and more difficult to handle. The same is true for insect cells which are based on the baculo-virus-infection system. In some cases they display a high diversity of post-translational modified products and a strong intracellular protein aggregation [*Glover and Hamphreys, 2004*].

The use of a genetic algorithm for media optimization was also proven to be useful in other cases for the production of L-lysin, L-isoleucin, ILE/L-valin by *Corynebacterium glutanicum* [*Weuster-Botz et al., 1996 and 1997*], esterase production in *E. coli* [*Böhling and Voss, 1997*], Δ1-dehydrogenase production by *Arthrobacter simplex* cells [*Weuster-Botz et al., 1995*] and cyanobacteria growth [*Havel et al., 2006*].

Concerning the single cell analysis of bacteria the group around Prof. Susann Müller from the Helmholtz Centre for Environmental Research (UFZ) is known to work on this field. Several current publications concerning bacterial population dynamics in waste-water treatment [*Günther, et al., 2011*], functional single cell analysis [*Müller and Nebe von Caron, 2010*], viability states of bacteria [*Sträuber et al., 2010*] and population heterogeneities in bioprocesses [*Müller et al., 2011*] relate to the methodology.

B. subtilis is the most studied Gram positive model organism. It was intensively investigated on transcriptome and proteome level by the group of Michael Hecker (Greifswald) under glucose starved conditions [*Koburger et al., 2005*], in response to salicylic acid [*Van Duy et al., 2007*] and general stress responses under starvation [*Eymann et al., 2002*]. Also investigations related to the Sec-pathway in *B. subtilis* regarding an overflow secretion through the tat-pathway were done.

3.2.1.5 Literature

Biedendieck, R.; Beine, R.; Gamer, M.; Jordan, E.; Buchholz, K.; Seibel, J.; Dijkhuizen, L.; Malten, M.; Jahn, D. (2007) Export, purification and activities of affinity tagged *Lactobacillus reuteri* levansucrase produced by *Bacillus megaterium*. *Appl. Microbiol. Biotechnol.* 74, 1062-1073

Biedendieck, R.; Yang, Y.; Deckwer, W.-D., Malten, M., Jahn, D. (2007) Plasmid system for the intracellular production and purification of affinity-tagged proteins in *Bacillus megaterium. Biotechnol. Bioeng.* 96, 525-537

Böhling, H.; Voss, H. (1997) Optimization of Protein-Synthesis in Recombinant *E.coli* BL21. *BIOforum Int.* 2, 86-91

Daßler, T.; Wich, G. (2006) EP 1 903 115 B1: Process for the fermentative production of antibodies. European patent

Eymann, C., Homuth, G.; et al. (2002) *Bacillus subtilis* functional genomics: global characterization of the stringent response by proteome and transcriptome analysis. *J. Bacteriol*. 184, 2500

Fürch, T.; Hollmann, R.; Wittmann, C.; Wang, W.; Deckwer, W.D. (2007) Comparative study on central metabolic fluxes of *Bacillus megaterium* strains in continuous culture using 13 C labelled substrates. *Bioprocess Biosyst. Eng.* 30, 47-59

Fürch, T.; Wittmann, C.; Wang, W.; Franco-Lara, E.; Jahn, D.; Deckwer, W.-D. (2007) Effect of different carbon sources on central metabolic fluxes and recombinant protein production in *Bacillus megaterium*. *J. Biotechnol.* 132, 385-394

Glover, D.; Hamphreys, D. (2004) Antibody Fragments. Production, purification and formatting for therapeutic applications. Antibodies, Volume 1, Production and Purification, Subramanian, G. (Ed.), Kluwer Academic New York

Günther, S.; Koch, C.; et al. (2011). "Correlation of community dynamics and process parameters as a tool for the prediction of the stability of wastewater treatment." Environmental Science & Technology.

Havel, J.; Link, H.; et al. (2006) Comparison of genetic algorithms for experimental multi-objective optimization on the example of medium design for cyanobacteria. Biotechnol. J. 1, 549-555

Jordan, E.; Hust, M.; Roth, A.; Biedendieck, R.; Schirrmann, T.; Jahn, D.; Dübel, S. (2007) Production of recombinant antibody fragments in *Bacillus megaterium*. *Microb. Cell Fact.* 6, 2

Koburger, T., Weibezahn, J.; et al. (2005) Genome-wide mRNA profiling in glucose starved *Bacillus subtilis* cells. *Molecular Genetics and Genomics* 274, 1-12

Malten, M.; Hollmann, R.; Deckwer, W.D.; Jahn, D. (2005) Production and secretion of recombinant Leuconostoc mesenteroides dextransucrase DsrS in *Bacillus megaterium*. *Biotechnol. Bioeng*. 89, 206-218

Müller, S., H. Harms, et al. (2011). "Origin and analysis of microbial population heterogeneity in bioprocesses." Current opinion in biotechnology 21(1): 100-113.

Müller, S.; Nebe von Caron, G. (2010) Functional single cell analyses: flow cytometry and cell sorting of microbial populations and communities. *FEMS Microbiol. Rev.* 34, 554-587

Sträuber, H.; Müller, S. (2010) Viability states of bacteria-Specific mechanisms of selected probes. *Cytometry Part A* 77, 623À634

Van Duy, N.; Mäder, U.; Tran, N. P.; Cavin, J.-F.; Tam, L. T.; Albrecht, D.; Hecker, M.; Antelmann, H. (2007) The proteome and transcriptome analysis of *Bacillus subtilis* in response to salicylic acid. Proteomics 7, 698-710

Weuster-Botz, D.; Joksch, K.M.; Schärtges, D.; Wandrey C. (1996) Integrated Developement of Fermentation and Downstream Proessing of L-Isoleucin Production with *Corynebacterium glutanicum*. *Appl. Microbiol. Biotechnol.* 46, 209-219

Weuster-Botz, D.; Kelle, R.; Frantzen, M.; Wandrey C. (1997) Substrate Controlled Fed-Batch Production of L-Lysine with *Corynebacterium glutanicum*. *Biotechnol. Prog.* 13, 387-393

Weuster-Botz, D.; Pramatarova, V.; Spassov, G.; Wandrey, C. (1995) Use of a genetic algorithm in the development of a synthetic growth medium for Arthrobacter simplex with high hydrocortisone dehydrogenase activity. *J. Chem. Tech. Biotechnol.* 64, 386-392

Yang, S.; Huang, Y.H.; Huang, X.D.; Li, S.Y.; Yuan, Z.Y. (1999) High Expression of Penicillin G Acylase Gene from *Bacillus megaterium* in *Bacillus subtilis*. *Acta Biochim. Biophys. Sin.* 31, 601-603

Yang, Y.; Malten, M.; Grote, A.; Jahn, D.; Deckwer, W.-D. (2007) Codon optimized *Thermobifida fusca* hydrolase secreted by *Bacillus megaterium*. Biotechnol. Bioeng. 96, 780-794

Yoon, S. H.; Kim, S. K.; et al. (2010) Secretory production of recombinant proteins in *Escherichia coli*. *Recent Patents on Biotechnology* 4, 23-29

3.2.2 Project relevant own publications

a) Works that have appeared in publications of a scientific quality assurance at the time of application or final acceptance, and book publications

David, F.; Korneli, C.; Schön, M.; Westphal, R.; Franco-Lara, E. (2009) Process optimization of antibody fragment-secreting *Bacillus megaterium* cultivations and its effect on the cell heterogeneity. *New Biotechnol.* 25(1)

David, F.; Westphal, R.; Bunk, B.; Jahn, D.; Franco-Lara, E. (2010) Optimization of antibody fragment production in *Bacillus megaterium*: the role of metal ions on protein secretion. *J. Biotechnol.* 150,115-124

David, F.; Berger, A.; Hänsch, R.; Rohde, M.; Franco-Lara, E. (2011) Single cell analysis applied to antibody fragment production with *Bacillus megaterium*: development of advanced physiology and bioprocess state estimation tools. *Microb. Cell Fact.* 10, 23

David, F.; Steinwand, M.; Hust, M.; Bohle, K.; Ross, A.; Dübel, S.; Franco-Lara, E. (2011) Antibody production in *Bacillus megaterium*: strategies and physiological implications of scaling from microtiter plates to industrial bioreactors. *Biotechno. J.* 6,1516-1531

David, F.; Hebeisen, M.; Schade, G.; Franco-Lara, E.; Di Berardino, M. (2011) Viability and metabolic activity analysis of *Bacillus megaterium* cells by impedance flow cytometry. *Biotechnol. Bioeng.* 109, 483-492

Korneli, C.; David, F.; Godard, T.; Franco-Lara, E. (2011) Influence of fructose and oxygen gradients on fed-batch recombinant protein production using *Bacillus megaterium*. *Eng. Life Sci.* 11, 338-349

Lueders, S.; David, F.; Steinwand, M.; Jordan, E.; Hust, M.; Dübel, S.; Franco-Lara, E. (2011) Influence of the hydromechanical stress and temperature on growth and antibody fragment production with *Bacillus megaterium*. *Appl. Microbiol. Biotechnol.* 91, 81-90

Schädel, F.; David, F.; Franco-Lara, E. (2011) Evaluation of cell damage caused by cold sampling and quenching for metabolome analysis. *Appl. Microbiol. Biotechnol.* 92, 1261-1274

3.3 Looking back on the promotion

The project has been funded since July 2008 in the SFB 578. It was completed on June 2012 with the end of the program.

3.3.1 Personnel in the project

	Name, akad. degree, service position	narrower subject of the employee	Institute of University or non-university facility	Participation in the project in hours per week	Category
Basic staff					
Research associate (incl. auxiliary power)	1. E. Franco-Lara, Jun.-Prof. Dr.-Ing	Biochemical Engineering	Institute of Biochemical Engineering	20	Professorship
Non academic staff	2 Y. Göcke BTA	Biochemical Engineering	Institute of Biochemical Engineering	8	Technical staff
Supportive staff					
Research associate (incl. auxiliary power)	3. F. David Dipl.-Biotechnol	Biochemical Engineering	Institute of Biochemical Engineering	40	PhD student
	4. S. Lüders Dipl.-Biologin	Biochemical Engineering	Institute of Biochemical Engineering	20	PhD student
Non academic staff	5. N. N., Stud. assistant	Biochemical Engineering, Biotechnology		10	Students

Responsibilities of employees (basic staff)

Position 1:

The involved employee in this subproject has supported the PhD-students in their work considering bioprocess engineering, statistical data evaluation, model based optimization, implementation of cultivation and experimental design.

Position 2:

Technical assistance was given by Yvonne Göcke related to experimental support and analytical methods as HPLC, sample preparation and assay development.

Responsibilities of employees (supportive staff)

Position 3: Dipl.-Biotechnol. Florian David

Dipl. Biotechnol. Florian David worked in the area of bioprocess optimization and rational strain design. *Bacillus megaterium* was used to study the production and secretion of the antibody fragment D1.3 scFv. First the aim was to establish a high productive defined cultivation medium. Different media components were screened throughout various cultivation platforms. Statistical design of experiments and a genetic algorithm approach were used to establish an appropriate defined high production medium. As a second step the process was transferred to the L-scale. An optimal bioprocess strategy based on alternating growth and starvation phases was established to gain high product titers of D1.3 scFv. As a final step a 100 L cultivation was done accounting for an advanced process control and considering GMP-guidelines. Flow cytometry was used to gain deeper insights on microbial physiology at single cell level regarding cell viability and integrity and production intensity. Culture heterogeneities were measured and characterized under controlled bioreactor conditions. To obtain additional information about the regulatory processes occurring inside the cell on gene expression level a transcriptome analysis was performed comparing cells with an increased production and secretion status to less producing and non-producing cells.

Position 4: Dipl.-Biol. Svenja Lüders

Dipl.-Biol. Svenja Lüders investigated the bioprocess variables of stirring rate related to shear stress and cultivation temperature regarding the ABF production performance. Here a complex medium was used and the process parameters were optimized by methods of statistical design. The method of 2D gelelectrophoresis was used to study the specific protein patterns under ABF producing conditions.

Position 5: Stud. assistant

The student assistant supported the extensive experimental work in the implementation and evaluation of bacterial cultivations as well as in the routine of biotechnological and molecular biological studies.

3.1 General information on the completed project B9

3.1.1 Topic

***Integrative databases, bioinformatics tools, analysis and modeling for systems biology with* B. megaterium *and* A. niger**

3.1.2 Disciplines and field of work

Bioinformatics, Systems biology

3.1.3 Project manager

Dr. Richard Münch
(b.: 06.05.1974)
Institute of Microbiology
AG Theoretical Microbiology
TU Braunschweig
Spielmannstr. 7
Phone: 0531/391-5847
Fax: 0531/391-5854
E-Mail: r.muench@tu-bs.de

Prof. Dr. Dietmar Schomburg
(b.: 21.04.1950)
Institute of Biochemistry and Biotechnology
TU Braunschweig
Langer Kamp 19B
Phone: 0531/391-8301
Fax: 0531/391-8302
E-Mail: d.schomburg@tu-bs.de

3.2 Development of the subproject

3.2.1 Report

3.2.1.1 Current knowledge at the last application and initial question

Biological Databases

In the last decades the finishing of several hundreds of bacterial genome projects and the introduction of new high-throughput techniques lead to a drastically increase of biological data. A number of bioinformatics platforms regarding prokaryotic genome annotation are available (e.g. [*Fumoto et. al, 2002; Alm et al., 2005; Uchiyama, 2007*]). These large databases are specialized on comparative genomics and are updated with every new sequenced genome. In parallel a great variety of specialized biological databases was developed by different groups. This process resulted in a high diversity of different database systems and data structures which makes it complicated to integrate these data sources on one platform [*Stein, 2003*].

However, new techniques for data integration via webservices and SOAP (Simple Object Access Protocol) allow a platform independent integration of data and services [*Crass et al., 2004*]. Furthermore, it is possible to perform combined data queries and to concatenate services in form of workflows or pipelines [*Hull et al., 2006*]. Besides the structured organization of data and software, the data export and transfer in standardized formats is an essential feature. In this context SBML (Systems Biology Markup Language), MAGE-ML (Microarray Gene Expression Markup Language) or NetCDF (Network Common Data Format) amongst others are commen formats [*Hucka et al., 2003; Spellman et al., 2002*].

Prediction and modeling of gene regulatory and metabolic networks

To develop models of cellular processes in systems biology approaches reliable predictions of metabolic and gene regulatory networks are basis for many detailed analyses and the development of comprehensive models. In case of metabolic networks first enzymes and reactions have to be predicted that are linked to pathways in the next step [*Pinney et al., 2005; Rahman et al., 2005*]. Using a metabolic reaction system the stoichiometric matrix can be derived which is used e.g. for metabolic flux balance analyses, elementary mode and “Extreme Pathway” analyses [*Papin et al., 2004*]. If kinetic parameters and concentrations of enzymes and metabolites are available, kinetic models can be constructed [*Saavedra et al., 2007*].

A gene regulatory network is defined by the interconnected interactions of transcription factors (TFs) with its target genes. In most cases the prediction of gene regulatory networks is realized by pattern matching algorithms of the transcription factor binding site (TFBS) in a genome sequence. Since TFBSs are short and degenerated, these predictions commonly involve high false prediction rates due to the accumulation of false-positive matches [*Benítez-Bellón et al., 2002*]. Topological analysis of global gene regulatory networks revealed a high order of organization into functional modules called network motives [*Shen-Orr et al., 2002; Blais and Dynlacht, 2005*]. Hereby, mathematical modeling and experimental evidence revealed, that regulatory network motives can act as autoinducers, filters, oscillators, amongst others [*Alon, 2007*].

The development of integrative models is currently the biggest challenge. For that purpose, all components involved in a cellular process, including its kinetics, concentration, regulation and interaction have to be described mathematically. This includes essentially all involved biochemical reactions including the half-lives of the components, gene regulation, receptor-ligand interactions, signal transduction and other regulatory mechanisms at the RNA and protein level, where appropriate, spatial parameters such as cell volume, diffusion or compartmentalization have to be considered. Lack of model parameters can be partially complemented by results of quantitative high-throughput experiments or fitted via non-linear regression analyzes. Commonly, deterministic models using coupled ordinary differential equations are applied for this approach [*Cliff et al, 2005; Peercy et al, 2006*]. On single-cell level, when some cellular components are present in low copy number, stochastic effects might occur. In this case, cellular processes can be modeled using stochastic models [*McAdams and Arkin, 1997*].

3.2.1.2 Results and applied methods

Development of an automatic method for the creation of metabolic networks

The development of a metabolic model based on an annotated genome is a highly complex and – up to now – time-consuming process. This has led to the fact that only 20-30 genome-sized metabolic models can be found in the literature so far.

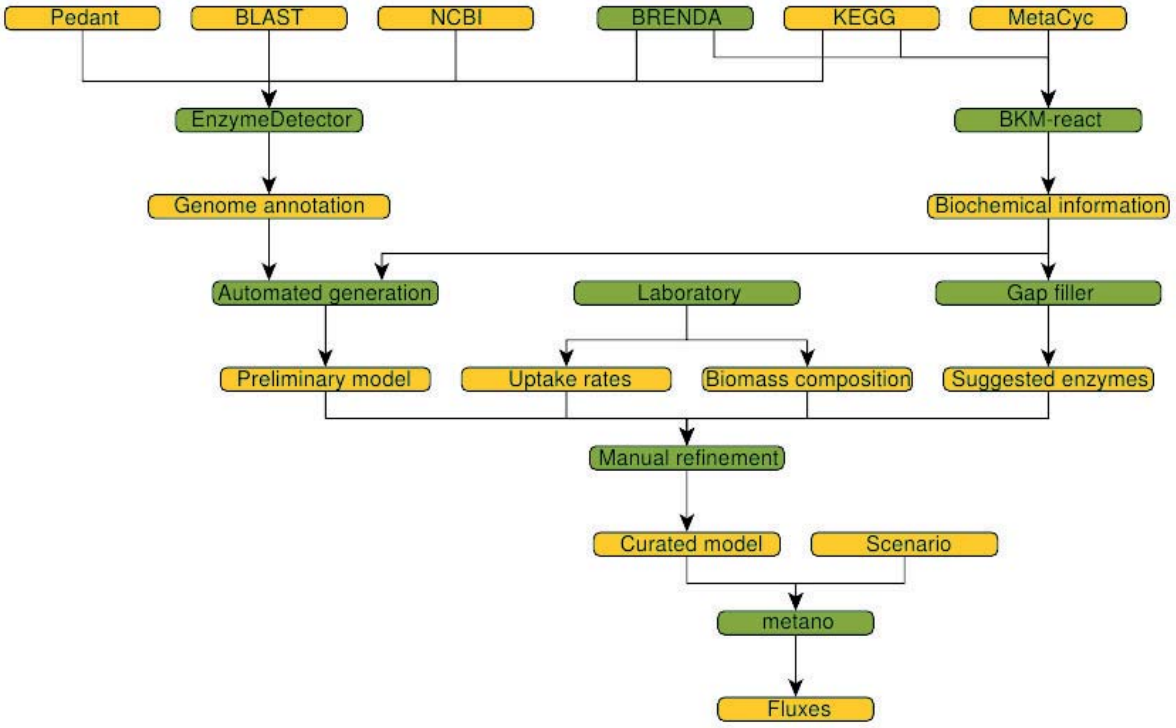

Fig. 1: Flow chart of modeling in genome-wide metabolic networks. Green color indicates the applied method development in this subproject.

The process is described in **Fig. 1**. In the top row there are the highly relevant international databases that provide information either on genome annotation or on enzyme properties and/or pathways. Within this project the BRENDA database was specifically complemented with enzyme-information of the project organisms (see below in “Databases and bioinformatics tools”), for the steps related to enzyme prediction reaction prediction new tools were developed. The creation of a metabolic model involves the following steps:

1) Perform a highly reliable enzyme prediction based on the genome.

2) Include experimental information on pathways and enzymes

3) Based on the enzymes found and predicted for the organism compute a list of biochemical reactions that can occur in the organism.

4) Based on step 3) create a first metabolic network and complement it by filling gaps so that all components of the cell can be synthesized and known carbon and nitrogen sources can be catabolized.

5) Include experimental information from e.g. transcriptome, proteome and metabolome analysis

After step 5 a model exists which can describe and predict metabolic potential and states of the organism and can predict optimal production of a product as well as predict the influence of mutations. In the scope of this project step 1, 2 and 3 of the process were investigated.

1) Enzyme prediction/genome annotation. A first analysis showed that the genome annotations by the major hosts are very different with only about 30% agreement.

An analysis showed that the different websites are far from complete and only between 30 and 90% correct in their predictions (**Fig. 2**). We developed a method that integrates the different predictions (NCBI, KEGG, PEDANT), adds two own methods (one of which, a pattern-based prediction, being between 80 and 90% correct) and experimental information from BRENDA and provides reliability scores for enzyme predictions [*Bannert et al., 2010; Quester and Schomburg, 2011*]. The results are made available to the user on a website (http://enzyme-detector.tu-bs.de).

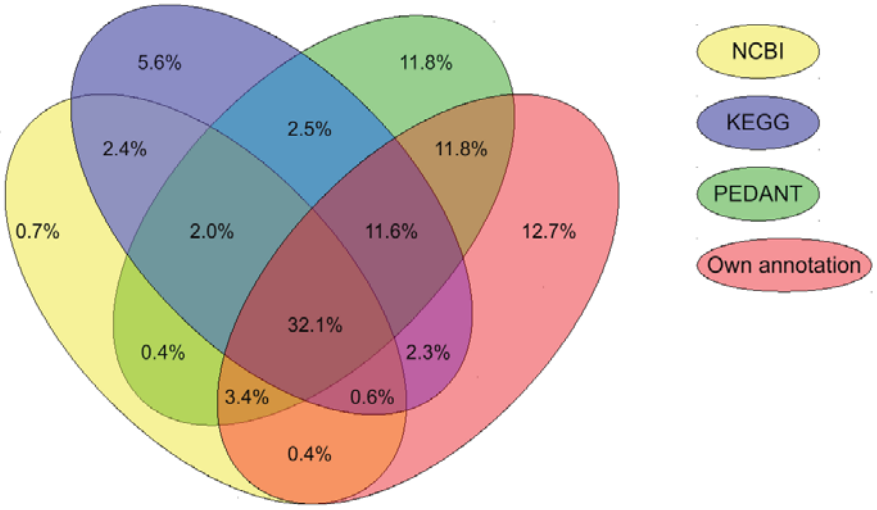

Fig. 2: Conformity of enzyme function predictions of different sites and its own annotation.

2) We complemented BRENDA (http://www.brenda-enzymes.org) [*Scheer et al., 2010*]

3) Reactions for enzymes are available either by the enzyme-centred database BRENDA or by the pathway-centred databases KEGG or METACYC. As the names for metabolites are not at all standardized and often up to 30 different names for a compound are found it is highly complicated to compare and integrate the contents of the databases. We

developed a method to integrate the contents and made the results available to the scientific community on a website (http://bkm-react.tu-bs.de) [*Lang et al., 2011*].

Databases and bioinformatics tools

The PRODORIC database was supplemented with gene regulatory data from *B. megaterium* [*Grote et al., 2009*]. For the prediction of gene regulatory networks the pattern matching tool Virtual Footprint was extended to enable the analysis the *B. megaterium* genome. To provide computer assisted support for the annotation of the *B. megaterium* and *A. niger* genomes a tool called GeneReporter was developed [*Bartsch et al., 2011*]. GeneReporter is a web based tool that reports functional information and relevant literature on a gene or protein sequence of interest. This includes data on protein families, domains, potential cofactors, structure, function, cellular localization, metabolic contribution and corresponding DNA binding sites complement the information on a given gene product of interest. The web site integrates databases and analysis tools as SOAP-based web services from the EBI (European Bioinformatics Institute) and NCBI (National Center for Biotechnology Information). Furtheron, a bioinformatics pipeline for the standardized analysis of microarray data was established for the whole consortium. This was realized using Bioconductor packages [*Reimers and Carey, 2006*] with adaptations to the applied model organisms.

Similarly, the BRENDA database (www.brenda-enzymes.org) was extended by the inclusion of information specific for the two organisms in the project. The database now contains information on 829 different enzymes from *Aspergillus*, 489 of which are from *Aspergillus niger*, and on 1656 different EC-numbers from *Bacillus*, 314 of which are from *Bacillus megaterium*.

In addition two new databases were created for the development and evaluation of metabolic models, i.e. the Enzyme detector database (enzymedetector.tu-bs.de) which delivers an integrated and reliable prediction of enzyme activities in sequenced prokaryotes, and bkm-react (bkm-react.tu-bs.de) which integrates the reaction information given in the three databases BRENDA, KEGG, and METACYC, and allows a compilation of all chemical reactions that can occur in an organism, based on a genome annotation (details for both databases described above).

Development of a software for the analysis of protein production in *B. megaterium* at single cell level

Although high yields of GFP were produced with the applied vector system developed in the subproject A1 (**Fig. 4**) it turned out that the culture showed a significant level of protein production heterogeneity. Fluorescent activated cell sorting (FACS) analyses of bioreactor grown GFP producing *B. megaterium* revealed a stable subpopulation of about 30% non-producers [*Biedendieck et al., 2007, Bunk et al., 2011*]. The non-producing cells were still alive which means that a subpopulation within a culture of clonal cells has arisen.

Moreover, these cells were still proliferating which excludes persistance. The observed phenomenon is called culture heterogeneity where genetically identical cells acquire distinct phenotypes. This effect was further investigated using life cell imaging and time-lapse fluorescence microscopy. For that purpose the image analysis software called TLM-Tracker (Time-Lapse-Movie-Tracker) was developed [*Klein et al., 2012*] (http://www.tlmtracker.tu-bs.de). The program is based on the MatLab platform. Using TLM-Tracker it is possible to track spatial and temporal cell division events and measure the GFP level in each single cell (**Fig. 3**).

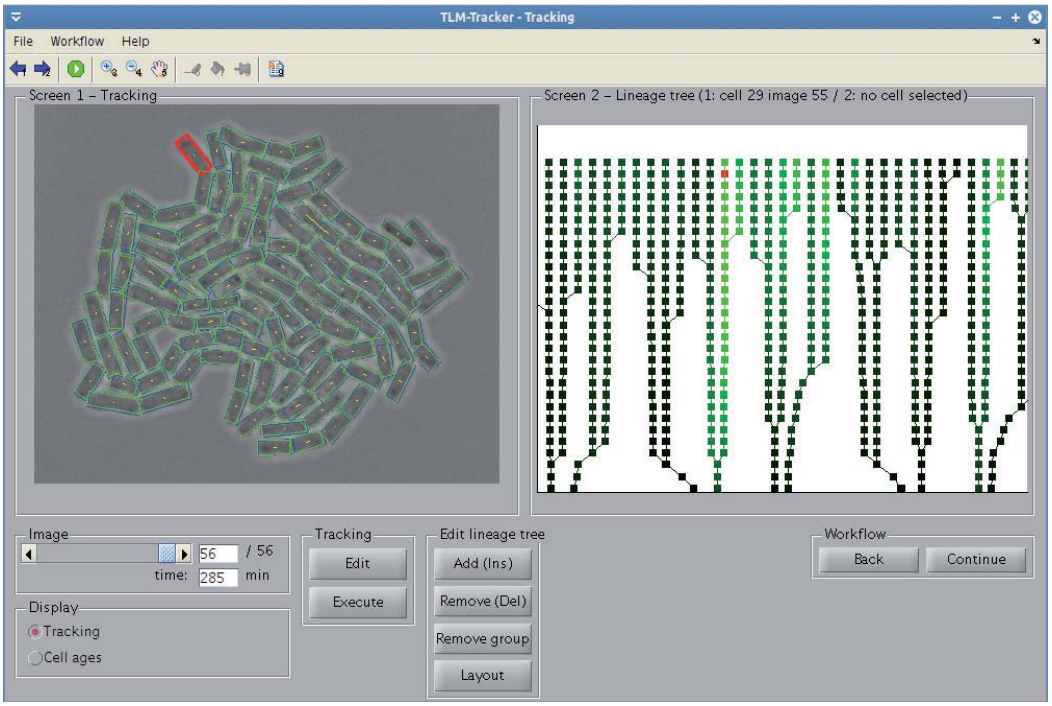

Fig. 3: Screenshot of TLM-Tracker after the segmentation and tracking process of a growing GFP producing B. megaterium microcolony. The left screen shows the recognized cells of one specific frame of the time-lapse movie. In the right screen the derived cell lineage tree including GFP levels is shown (http://www.tlmtracker.tu-bs.de).

TLM-Tracker provides multiple alternative algorithms for segmentation, namely threshold based algorithms, watershed transformation and level-set methods which can be applied for each frame individually. After the segmentation process, several quantitative properties of each cell are determined, such as dimension, position, orientation, cell pole age and area of the cell. Moreover, the mean, maximum and standard deviation of the fluorescence intensity of the cell is calculated. The derived data can be used to generate and analyze cell lineage trees. Derived results gave first insights, that the production of GFP on single cell level revealed a high level of stochasticity and bistable behavior in the cell lineage tree.

Mathematical modeling of the bistable GFP production behaviour

The stable formation of two subpopulations is also called bistability. Bistability can arise from „responsive switching“ mediated by environmental perturbations and from

„spontaneous stochastic switching“ caused by noise in gene expression followed by random transitions between different phenotypes [*Kussell and Leibler, 2005, Acar et al., 2008*]. Based on our experimental results we started mathematical modeling of the gene regulatory circuit.

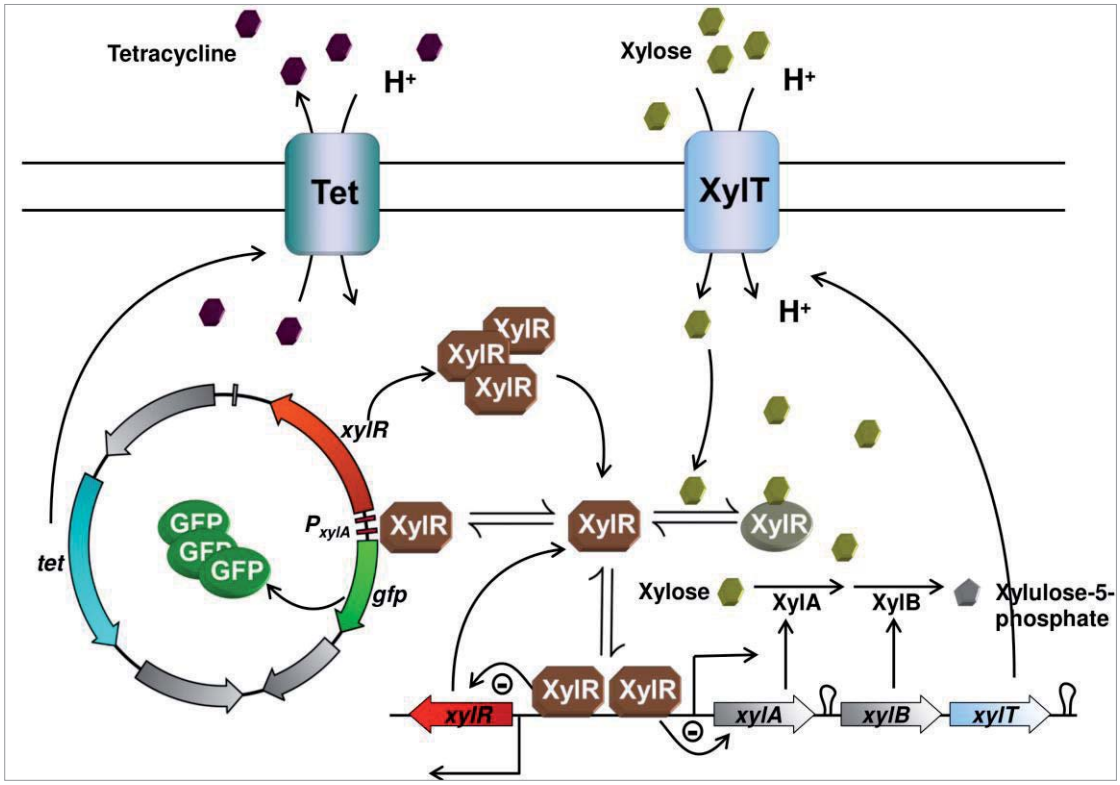

Fig. 4: Schematic overview of the main components involved in the xylose-inducible expression system and their interactions. The xylA *and* xylB *genes encode enzymes involved in xylose degradation, while* xylT *encodes a xylose transporter. In the absence of xylose the expression of the operon is repressed by the xylose repressor XylR while in the presence of xylose the expression of the operon is derepressed. The* xylR *gene is located upstream transcribed in divergent direction to the* xylABT *operon and is autoregulated. For the construction of a xylose-inducible expression system the* xylR *gene and the* P_{xylA} *promoter were cloned into a free replicating broad host range plasmid. For testing and analyzing the expression system the gene for the easily detectable green fluorescent protein (GFP) as a model was fused to the promoter* P_{xylA}.

Importantly, a repressor controlled recombinant protein production process using a high copy vector system differs significantly from the usual repressor mediated gene expression control. The observed bistability of protein production in *B. megaterium* could be explained in parts by the autoregulatory feedback loop of XylR. In addition, a high variability of GFP amounts in individual *B. megaterium* cells was observed. Since the occurance of noise and stochasticity is commonly the result of the behaviour of involved components with low intracellular copy number, our key assumption to explain the observed phenomenon is based on limitations of the regulatory system. The introduction of a freely replicatory plasmid carrying a second *xylR* gene in addition to the chromosomal copy, as done in our production strain, might significantly perturb the steady-state between free diffusing,

inducer bound and inducer free, promoter bound repressor. Hereby, the copy number of plasmids per cell is critical since plasmids are usually distributed randomly during cell division. Variations in the plasmid copy number both influence the levels of XylR and as a consequence of GFP. Additionally, the intracellular xylose level is of special interest. In the described system the amount of free intracellular xylose might get very low for two reasons. First, in qRT-PCR experiments the expression of the xylose transporter gene *xylT* was found identical in both subcultures of producing and low-producing cells. In fact, there should be only basal levels because the genome encoded *xylABT* operon is commonly not affected by XylR due to catabolite repression [*Rygus and Hillen, 1992*]. As a result, the import capacity of xylose might be limited. Second, the availability of high amounts of plasmid encoded XylR might result in an increased binding and therefore a strong reduction of the existing intracellular xylose levels via titration. Low amounts of unbound xylose might shift the equilibrium towards a higher level of active repressor which also affects the fraction of bound repressor to the P_{xylA} promoter. Indeed, our mathematical model explains, that the titration effect can lead to bistable behavior. The described relationships and the proposed model are shown in **Fig. 5**.

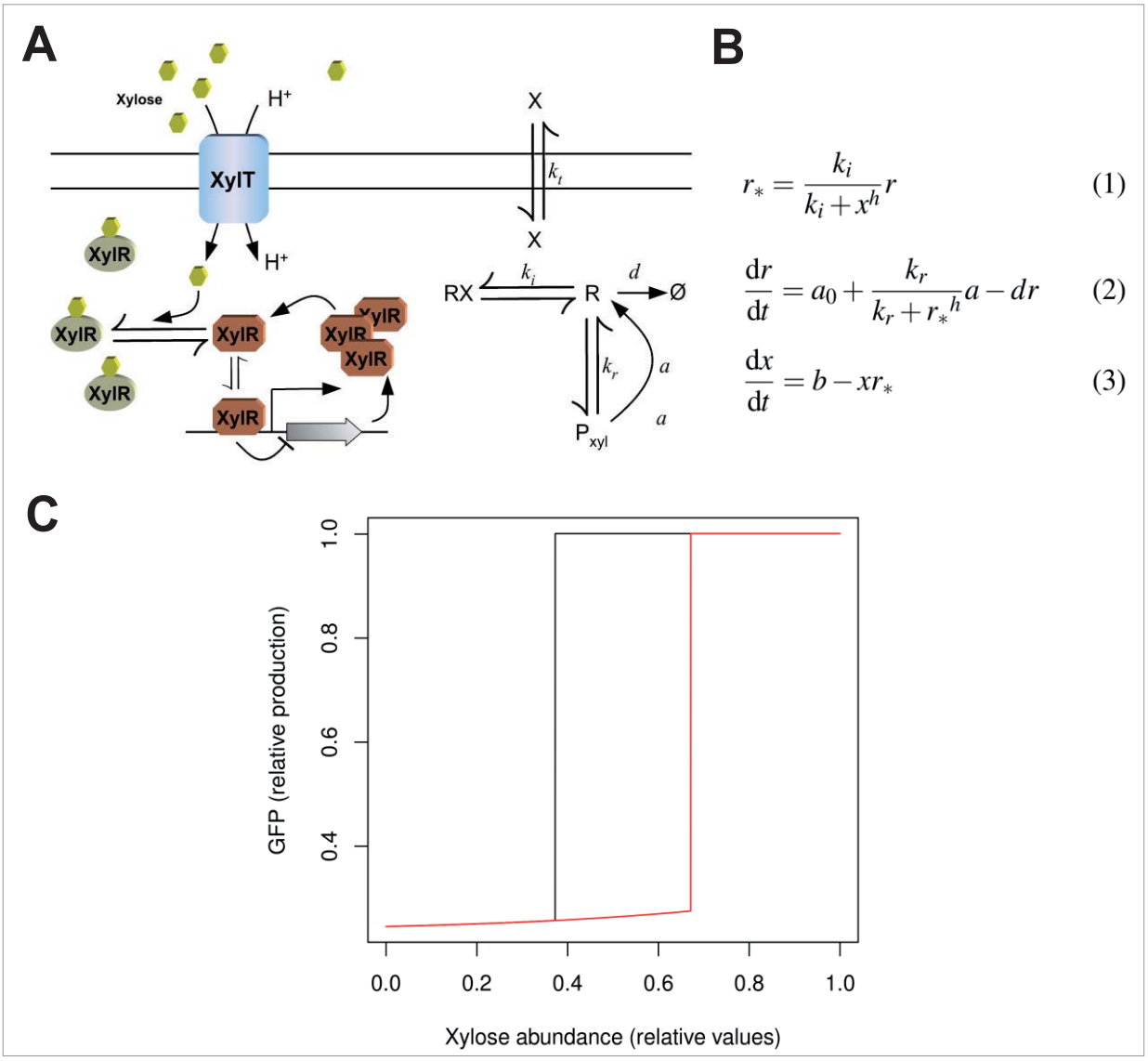

Fig. 5: A) Proposed schematic and conceptional model of XylR and xylose imbalance in the analyzed gene expression system. Highly expressed xylR *and low xylose transport influence the P_{xylA} promoter activity by shifting the equilibrium between active and inactive repressor. B) Mathematical model based on ordinary differential equations. Equation 1 describes the fraction of active repressor r_* as function of xylose x with the half-saturation constant k_i. In equation 2 the autorepression of XylR is modeled with the basal and induced transcription rates a_0 and a, the binding constant k_r and the degradation/dilution rate d. Equation 3 describes the xylose uptake with the rate b and the potential titration effect by the active repressor including the degradation/dilution of xylose. C) Inducer response diagram generated by numerical simulation of the model in Fig. 5 B. Within a certain parameter space the shown system exhibits bistability and hysteresis.*

3.2.1.3 References to other works and collaborations in the SFB

Subproject A1 (Jahn/Dersch): The optimization of the protein production efficiency was supported by bioinformatics analyses and predictions in an iterative process. On the level of transcription, optimal promoter structures were predicted. A software pipeline for the analysis of microarray data was estsablished. On the level of translation, tools for the optimization of the codon usage were developed and successfully applied. Finally, signal peptides for the protein secretion were predicted. Resulting *B. megaterium* strains harboring optimized plasmids for heterologous protein production were analyzed on single cell level in this subproject.

Subproject A6 (Dübel/Hust): Genome analyses and prediction of regulatory networks in *B. megaterium* based on the PRODORIC database were performed in order to improve the production process of antibodies.

Subproject B4 (Jahn/Nörtemann/Jänsch): This collaboration supported the mathematical modeling of protein production in *A. niger* and the life cell analyses under various environmental conditions. Using comparative genomics approaches the genome of A. niger was analyzed for conserved gene regulatory networks. Finally, support in the statistics of microarray analyses was provided.

3.2.1.4 Comparison with research outside the SFB

The developed databases and tools for the automatic creation of metabolic models are unique. There are no databases comparable to BRENDA, Enzyme-Detector or BKM-react.

Many prominent examples for bistability in bacteria are described including lysis/lysogeny in bacteriophage λ, competence development in *Bacillus subtilis*, persister subpopulations in *Escherichia coli*, stringent response in mycobacteria, amongst others (reviewed in [*Dubnau and Losick, 2006*]). However, bistabilitiy in the context of an artificial vector based expression system, was not described, yet.

One interesting case of stochastic switching between phenotypic states is also called ”bet hedging“ which is an example for evolutionary adaptation to fluctuating environmental conditions. Bet hedging means that individuals or subpopulations express a phenotype with reduced fitness that will be adaptive in a future environment [*Philippi and Seger, 1989; Beaumont et al., 2009*]. In extreme case this can lead to self-destructive cooperation where individuals die to provide nutrients for the remaining population [*Ackermann et al, 2008*]. Experimental studies and mathematical modeling approaches revealed that the requirements for a bistable system are regulatory circuits with positive autoregulation and time delay feedback loops [*Xiong and Ferrell, 2003; Ozbudak et al., 2004*]. Bistable systems are able to produce hysteresis which means that cells show a switch like behaviour and are able to self-sustain their current state over several generations within a cell lineage tree. Thus, cells tend to preserve their epigenetic state and transition from one state to the other requires an induction greater than that for the reverse transition. From

this point of view, hysteresis in biological systems can produce memory-like characteristics [*Chang et al., 2010*].

3.2.1.5 Literature

Acar, M.; Mettetal, J.T.; van Oudenaarden, A. (2008) Stochastic switching as a survival strategy in fluctuating environments. *Nat. Genet.* 40, 471-475

Ackermann, M.; Stecher, B.; Freed, N.E.; Songhet, P.; Hardt, W.-D.; Doebeli, M. (2008) Self-destructive cooperation mediated by phenotypic noise. *Nature* 454, 987-990

Alm, E.J; Huang, K.H.; Price, M.N.; Koche, R.P.; Keller, K.; Dubchak, I.L., Arkin, A.P. (2005) The MicrobesOnline Web site for comparative genomics. *Genome Res.* 15, 1015-1022

Alon, U. (2007) Network motifs: theory and experimental approaches. *Nat. Rev. Genet.*, 8, 450-461

Beaumont, H.J.E.; Gallie, J.; Kost, C.; Ferguson, G.C.; Rainey, P.B. (2009) Experimental evolution of bet hedging. Nature 462, 90-93

Benítez-Bellón, E.; Moreno-Hagelsieb, G.; Collado-Vides, J. (2002) Evaluation of thresholds for the detection of binding sites for regulatory proteins in *Escherichia coli* K12 DNA. *Genome Biol.*, 3, 13

Biedendieck, R.; Yang, Y.; Deckwer, W.-D.; Malten, M.; Jahn, D. (2007) Plasmid system for the intracellular production and purification of affinity-tagged proteins in *Bacillus megaterium*. *Biotechnol. Bioeng.* 96, 525-537

Blais, A.; Dynlacht, B.D. (2005) Constructing transcriptional regulatory networks. *Genes Dev.*, 19, 1499-1511

Brazma, A.; Hingamp, P.; Quackenbush, J.; Sherlock, G.; Spellman, P.; Stoeckert, C.; Aach, J.; Ansorge, W.; Ball, C.A.; Causton, H.C.; Gaasterland, T.; Glenisson, P.; Holstege, F.C.; Kim, I.F.; Markowitz, V.; Matese, J.C.; Parkinson, H.; Robinson, A.; Sarkans, U.; Schulze-Kremer, S.; Stewart, J.; Taylor, R.; Vilo, J.; Vingron, M. (2001) Minimum information about a microarray experiment (MIAME)-toward standards for microarray data. *Nat. Genet.* 29, 365-371

Chang, D.-E.; Leung, S.; Atkinson, M.R.; Reifler, A.; Forger, D.; Ninfa, A.J. (2010) Building biological memory by linking positive feedback loops. *Proc. Natl. Acad. Sci. USA* 107, 175-180

Crass, T.; Antes, I.; Basekow, R.; Bork, P.; Buning, C.; Christensen, M.; Claussen, H.; Eberling, C.; Ernst, P.; Gailus-Durner, V.; Glatting, K.; Gohla, R.; Gössling, F.; Grote, K.; Heidtke, K.; Herrmann, A.; O'Keeffe, S.; Kiesslich, O.; Kolibal, S.; Korbel, J.O.; Lengauer, T.; Liebich, I.; van der Linden, M.; Luz, H.; Meissner, K.; von Mering, C.; Mevissen, H.; Mewes, H.; Michael, H.; Mokrejs, M.; Müller, T.; Pospisil, H.; Rarey, M.; Reich, J.G.; Schneider, R.; Schomburg, D.; Schulze-Kremer, S.; Schwarzer, K.; Sommer, I.; Springstubbe, S.; Suhai, S.; Thoppae, G.; Vingron, M.; Warfsmann, J.; Werner, T.; Wetzler, D.; Wingender, E.; Zimmer, R. (2004) The Helmholtz Network for Bioinformatics: an integrative web portal for bioinformatics resources. *Bioinformatics* 20, 268-270

Dubnau, D.; Losick, R. (2006) Bistability in bacteria. *Mol. Microbiol.* 61, 564-572

Durinck, S. (2008) Preprocessing of microarray data and analysis of differential expression. *Methods Mol. Biol.* 452, 89-110

Fumoto, M.; Miyazaki, S.; Sugawara H. (2002) Genome Information Broker (GIB): data retrieval and comparative analysis system for completed microbial genomes and more. *Nucleic Acids Res.* 30, 66-68

Güldener, U.; Münsterkötter, M.; Kastenmüller, G.; Strack, N.; van Helden, J.; Lemer, C.; Richelles, J.; Wodak, S. J.; García-Martínez, J.; Pérez-Ortín, J. E.; Michael, H.; Kaps, A.; Talla, E.; Dujon, B.; André, B.; Souciet, J. L.; Montigny, J. D.; Bon, E.; Gaillardin, C.; Mewes, H. W. (2005) CYGD: the Comprehensive Yeast Genome Database. *Nucleic Acids Res.*, 33, 364-368

Hucka, M.; Finney, A.; et al. & SBML Forum (2003) The systems biology markup language (SBML): a medium for representation and exchange of biochemical network models. *Bioinformatics* 19, 524-531

Hull, D.; Wolstencroft, K.; Stevens, R.; Goble, C.; Pocock, M.R.; Li, P.; Oinn, T. (2006) Taverna: a tool for building and running workflows of services. *Nucleic Acids Res.* 34: 729-732

Ioannidis, J.P.A.; Allison, D.B.; Ball, C.A.; Coulibaly, I.; Cui, X.; Culhane, A.C.; Falchi, M.; Furlanello, C.; Game, L.; Jurman, G.; Mangion, J.; Mehta, T.; Nitzberg, M.; Page, G.P.; Petretto, E.; van Noort, V. (2009) Repeatability of published microarray gene expression analyses. *Nat. Genet.* 41, 149-155

Klipp, E.; Nordlander, B.; Krüger, R.; Gennemark, P.; Hohmann, S. (2005). Integrative model of the response of yeast to osmotic shock. *Nat. Biotechnol.*, 23, 975-982

Kussell, E.; Leibler, S. (2005) Phenotypic diversity, population growth, and information in fluctuating environments. *Science* 309, 2075-2078

McAdams, H.H.; Arkin, A. (1997) Stochastic mechanisms in gene expression. *Proc. Natl. Acad. Sci. U S A* 94, 814-819

Ozbudak, E.M.; Thattai, M.; Lim, H.N.; Shraiman, B.I.; Oudenaarden, A.V. (2004) Multistability in the lactose utilization network of *Escherichia coli*. *Nature*, 427, 737-740

Papin, J.A.; Stelling, J.; Price, N.D.; Klamt, S.; Schuster, S.; Palsson, B.O. (2004) Comparison of network-based pathway analysis methods. *Trends Biotechnol.* 22, 400-405

Peercy, B.E.; Cox, S.J.; Shalel-Levanon, S.; San, K.; Bennett, G. (2006) A kinetic model of oxygen regulation of cytochrome production in *Escherichia coli*. *J. Theor. Biol.* 242, 547-563

Philippi, T.; Seger, J. (1989) Hedging one's evolutionary bets, revisited. *Trends. Ecol. Evol*. 4, 41-44

Pinney, J. W.; Shirley, M. W.; McConkey, G.A.; Westhead, D. R. (2005). metaSHARK: software for automated metabolic network prediction from DNA sequence and its application to the genomes of *Plasmodium falciparum* and *Eimeria tenella*. *Nucleic Acids Res.* 33, 1399-1409

Reimers, M.; Carey, V.J. (2006) Bioconductor: an open source framework for bioinformatics and computational biology. *Methods Enzymol.* 411:119-134

Rygus, T.; Hillen, W. (1992) Catabolite repression of the *xyl* operon in *Bacillus megaterium*. J. Bacteriol. 174, 3049-3055

Saavedra, E.; Marín-Hernández, A.; Encalada, R.; Olivos, A.; Mendoza-Hernández, G.; Moreno-Sánchez, R. (2007) Kinetic modeling can describe in vivo glycolysis in *Entamoeba histolytica*. FEBS J., 274, 4922-4940

Shen-Orr, S.S.; Milo, R.; Mangan, S.; Alon, U. (2002) Network motifs in the transcriptional regulation network of *Escherichia coli*. *Nat. Genet.*, 31, 64-68

Spellman, P.T.; Miller, M.; Stewart, J.; Troup, C.; Sarkans, U.; Chervitz, S.; Bernhart, D.; Sherlock, G.; Ball, C.; Lepage, M.; Swiatek, M.; Marks, W.L.; Goncalves, J.; Markel, S.; Iordan, D.; Shojatalab, M.; Pizarro, A.; White, J.; Hubley, R.; Deutsch, E.; Senger, M.; Aronow, B.J.; Robinson, A.; Bassett, D.; Stoeckert, C. J.; Brazma, A. (2002) Design and implementation of microarray gene expression markup language (MAGE-ML). *Genome Biol.* 3, 0046

Stein, L. D. (2003) Integrating biological databases. *Nat. Rev. Genet.* 4, 337-345

Uchiyama, I. (2007) MBGD: a platform for microbial comparative genomics based on the automated construction of orthologous groups. *Nucleic Acids Res.* 35, 343-346

Xiong, W.; Ferrell, J.E. (2003) A positive-feedback-based bistable 'memory module' that governs a cell fate decision. *Nature*, 426, 460-465

3.2.2 Project Relevant own publications

a) Works that have appeared in publications of a scientific quality assurance at the time of application or final adoption, and book publications

Bannert, C.; Welfle, A.; Aus dem Spring, C.; Schomburg, D. (2010) BrEPS: a flexible and automatic protocol to compute enzyme-specific sequence profiles for functional annotation. *BMC Bioinformatics* 1, 589

Bartsch, A.; Bunk, B.; Haddad, I.; Klein, J.; Münch, R.; Johl, T.; Kärst, U.; Jänsch, L.; Jahn, D.; Retter, I. (2011) GeneReporter-sequence-based document retrieval and annotation. *Bioinformatics* 27, 1034-1035

Bunk, B.; Schulz, A.; Stammen, S.; Münch, R.; Warren, M.J.; Rohde, M.; Jahn, D.; Biedendieck R. (2010) A short story about a big magic bug. *Bioeng. Bugs*. 1, 85-91

Grote, A.; Klein, J,; Retter, I.; Haddad, I.; Behling, S.; Bunk, B; Biegler, I.; Yarmolinetz, S.; Jahn, D.; Münch R. (2009) PRODORIC (release 2009): a database and tool platform for the analysis of gene regulation in prokaryotes. *Nucleic Acids Res.* 37, D61-65

Lang, M.; Stelzer, M.; Schomburg, D. (2011) BKM-react, an integrated biochemical reaction database, *BMC Biochem.* 12, 42

Quester, S.; Schomburg, D. (2011) EnzymeDetector: an integrated enzyme function prediction tool and database, *BMC Bioinformatics* 12, 376

b) Other publications

Egelhofer, V.; Schomburg, I.; Schomburg, D. (2010) Automatic assignment of EC numbers. *PLoS Comput. Biol.* 6, e1000661

Hiller, K.; Hangebrauk, J.; Jäger, C.; Spura, J.; Schreiber, K.; Schomburg, D. (2009) MetaboliteDetector: comprehensive analysis tool for targeted and nontargeted GC/MS based metabolome analysis. *Anal. Chem*. 81, 3429-3439

Münch, R.; Klein, J.; Jahn, D. (2011) Prediction and Analysis of Gene Regulatory Networks in Prokaryotic Genomes. *Systems and Computational Biology - Molecular and Cellular Experimental Systems*. 149-162

Shevchuk, O.; Roselius, L.; Günther, G.; Klein, J.; Jahn, D.; Steinert, M.; Münch R. (2012) InFiRe - a novel computational method for the identification of insertion sites in transposon mutagenized bacterial genomes. *Bioinformatics* 28, 306-310

Scheer, M.; Grote, A.; Chang, A.; Schomburg, I.; Munaretto, C.; Rother, M.; Söhngen, C.; Stelzer, M.; Thiele, J.; Schomburg, D. (2010) BRENDA, the enzyme information system in 2011. *Nucleic Acids Res.* 39, D670-6

Trunk, K.; Benkert, B.; Quäck, N.; Münch, R.; Scheer, M.; Garbe, J.; Jänsch, L.; Trost, M.; Wehland, J.; Buer, J.; Jahn, M.; Schobert, M.; Jahn, D. (2010) Anaerobic adaptation in *Pseudomonas aeruginosa*: definition of the Anr and Dnr regulons. *Environ. Microbiol*. 12, 1719-1733

3.3 Looking back on the promotion

The project has been funded since July 2008 in the SFB 578. It was completed on June 2012 with the end of the program.

3.3.1 Personnel in the project

	Name, akad. degree, service position	narrower subject of the employee	Institute of University or non-university facility	Participation in the project in hours per week	Category
Basic staff					
Research associate (incl. auxiliary power)	1. D. Schomburg, Prof. Dr. rer. nat.	Bioinformatics	Institute of Biochemistry and Biotechnology Department of Bioinformatics	10	Professorship
	2. R. Münch Dr. rer.nat.	Bioinformatics, Microbiology	Institute of Microbiology	10	Post-doctoral
Supportive staff					
Research associate (incl. auxiliary power)	3. I. Biegler Dipl. Ernährungswiss.	Bioinformatics, Microbiology	Institute of Microbiology	40	PhD student
	4. K. Münch Dipl.-Biol.	Bioinformatics, Microbiology	Institute of Microbiology	40	PhD student
	5. n.n., PhD student	Bioinformatics	Institute of Biochemistry and Biotechnology, Department of Bioinformatics	40	PhD student
Non academic staff	6. N.N. Stud. assistant	Bioinformatics, Microbiology	Institute of Microbiology	10	Student

Responsibilities of employees (basic equipment)

Position 1 - 2:

The involved employees in the subproject B9 (Münch / Schomburg) supported the PhD-students in computer programing, mathematical modeling and molecular biological problems.

Responsibilities of employees (auxiliary equipment)

Position 3: Dipl.-Ernährungswiss. I. Biegler

Mrs. Biegler was mainly involved in programing the TLM-Tracker software. This included the application of the MatLab image processing library for segmentation and tracking of cells in time-lapse microscopy movies. Moreover, this work led to a new software with complete user interface for interactive analysis of microscopic images (http://www.tlmtracker.tu-bs.de). In parallel, life cell microscopy techniques for the usage of *Aspergillus niger* in time-lapse experiments were established. In addition this work was associated with the establishment of a bioinformatics analysis pipeline for microarray data generated for *Bacillus megaterium* and *Aspergillus niger*. Finally, Mrs. Biegler was involved in the curation of the PRODORIC database with organism specific data.

.

Position 4: Dipl.-Biol. Karin Münch

Mrs. Münch was involved in the establishment of life cell microscopy and time-lapse microscopy of *Bacillus megaterium*. This work was necessary for the analysis of the observed cell heterogeneity during GFP production on single cell level. In combination with FACS cell sorting results a bistable production behavior was detected leading to cell lineages of either high or low production states. Moreover, key components of the involved regulatory network were measured using quantitative RT-PCR. Finally, this work led to a mathematical model of the involved regulatory circuit that explains the bistability of this system.

Position 5: PhD students

Different PhD students of the group of Prof. Schomburg worked on the bioinformatical analysis of experimental data achieved in B9 and other subprojects.

Position 6: Stud. assistant

The student assistant supported the administration of the server infrastructure, the database annotation as well as the lime-lapse microscopy experiments.

3.1 General information on the completed project B10

3.1.1 Topic

***Systems biotechnology of glycosyltransferase production with* Bacillus megaterium**

3.1.2 Disciplines and field of work

Biochemical engineering, Systems biotechnology

3.1.3 Project manager

Prof. Dr. Dieter Jahn
(b.: 01.08.1959)
Institute of Microbiology
TU Braunschweig
Spielmannstraße 7
38106 Braunschweig
Phone: 0531/391-5801
Fax: 0531/391-5854
E-Mail: d.jahn@tu-bs.de

Jun.- Prof. Dr. Ezequiel Franco Lara
(b.: 04.10.1969)
Institute of Biochemical Engineering
TU Braunschweig
Gaußstraße 17
38106 Braunschweig
Current address
Evonik Industries AG
Kantstraße 2
33790 Halle

3.2 Development of the subproject

3.2.1 Report

3.2.1.1 Current knowledge at the last application and initial question

The base of this new integrated subproject B10 was provided during the first two application periods of this SFB 578 in the subprojects A1 (Jahn/Dersch), A5 (Deckwer) and B8 (Franco-Lara) [*Hollmann and Deckwer, 2004; Malten et al., 2005; Malten et al., 2006; Biedendieck et al., 2007a, b*]. A broad variety of genetic tools for the production and purification of intra- as well as extracellular proteins was available [*Malten et al., 2006; Biedendieck et al., 2007b*]. For the qualification and quantification of the recombinant production processes the green fluorescent protein GFP [*Biedendieck et al., 2007b*] as well as the extracellular levansucrase SacB [*Biedendieck et al., 2007c; Homann et al., 2007*] have been successfully proven as model proteins. Up to 300 mg/l of GFP were produced in high cell density cultivations [*Biedendieck et al., 2007b*] while around 50 mg/l of recombinant levansucrase were found secreted to the growth medium of *B. megaterium* in shaking flask cultivations. Anyway, an upscale to produce and secrete high amounts of recombinant proteins as the levansucrase in higher scales (1 to 5 liter) has not been reached so far [*Hollmann et al., 2006*].

3.2.1.2 Results and applied methods

Cultivation techniques

For *Bacillus megaterium* strains recombinantly producing intracellular and extracellular proteins different cultivation techniques were successfully applied and specialized during

the SFB 578. Besides the high cell density cultivations with a dextransucrase producing strain [*Malten et al., 2005*] further techniques for increasing productivity of different strains were applied like various fed-batch strategies. After testing several standard feeding strategies like exponential or constant feeding, a dissolved oxygen dependent feeding strategy appeared to be most productive. This was successfully shown for the strain YYBm1 carrying a high performance plasmid for the intracellular production of GFP. As GFP is accumulating inside the cell the highest productivity can be obtained when the cells are growing rapidly (growth associated product formation) probably as intracellular space for the product is increasing after every division event. This is the case in the exponential growth phase when cells are proliferating with the maximal growth rate. Therefore, it is most desirable to obtain this stage in a following fed-batch phase as shown in the literature for *Escherichia coli* [*Cutayar and Poillon, 1989*]. The principle of a dissolved oxygen (DO) dependent fed-batch is based on a DO triggered nutrient supply which is activated on rapid increase of oxygen signal due to substrate depletion and instantly deactivated after the nutrient supply. With exactly adjusted control parameters an almost on-demand substrate supply can be realized enabling the cells to grow with maximal growth rate. The highest product yield achieved with this strategy was shown in cooperative experiments with subproject A1 (Jahn/Dersch). The high performance expression plasmid pSSBm85 (developed in subproject A1 (Jahn/Dersch) which was transcriptional and translational optimized for GFP-production was introduced into the mutant strain YYBm1. The recombinant strain was cultivated in a batch cultivation followed by a DO-based fed-batch phase. Hereby, a product titer of 1.25 g/l GFP (38 mg/g_{CDW}) was reproducibly reached [*Stammen et al., 2010*].

Optimization of basic cultivation parameter with a GFP producing model strain

The high performance GFP producing strain was further used in this project for the investigation and optimization of basic cultivation parameters as the intracellular formed GFP is easily detectable and its production is therefore simply followed and evaluated.

- *pH-value*

In bioreactor cultivations the pH can be set and controlled to a constant value. Therefore, bioreactor cultivations where used for screening for the optimal pH-value for growth and production. In 800 mL bioreactors the influence of pH for induced and non-induced stage was investigated for the GFP producing strain within the range of pH 5 to 8. This range turned out to be reasonably chosen as for pH 5 and 8 growth rate was strongly decreased. Also product formation was lowered. Interestingly at pH 6 the amount of the usual by-product acetate was strongly decreased and in contrary the GFP yield slightly increased compared to pH 7. These results could be obtained in batch as well as fed-batch experiments. Also for an extracellular levansucrase producing strain a pH of 6 was optimal for the reasons of missing by-products and increased product formation.

The almost complete absence of by-product formation at pH 6 displays an interesting topic for further analysis with methods of systems biotechnology. For example with transcriptome analysis regulative genes could be detected which are solely responsible for by product formation as main cell processes like biomass formation and product formation are obviously not diminished. They might be targets for genetic strain optimization.

- *Temperature*

Shake flask cultures have been performed to screen for the optimal cultivation temperature in the range from 20 to 41°C (20°C, 30°C, 37°C, 41°C). With 37°C the highest growth rate was obtained, as well as the highest amount of recombinant protein (GFP). The product yield per biomass was about five times higher for 20°C than for 37°C which indicates that mainly cell growth is restricted at lower temperatures and GFP formation rate stays constant. This leads to higher yields at lower temperatures. Regarding the process time criterion 37°C is the most advantageous temperature. Although biomass and product formation is tolerable, higher temperatures (e.g. 41°C) are not recommended for the reason of enhanced by-product formation.

- *Time point of induction*

In induced bioreactor cultivations the influence of different induction time points on growth and production was analyzed. Due to the growth associated product formation an early induction time point should be more advantageous. In appropriate experiments with various time points (induction at different values for optical density) this was confirmed. The highest product yields were obtained for induction at OD 1 at the beginning of the batch phase. For extracellular products different results are likely to be obtained provided that the secreted product remains stable in the culture broth.

- *Concentration of dissolved oxygen (DO)*

In batch cultivations in 3 L bioreactors the influence of the minimum DO concentration which is at least to be constantly held after the normal decrease from 100 % DO was analyzed. Lower values than 20 % DO resulted in a decreased growth rate. The cells are producing more acetate as by-product indicating oxygen limitation. Due to lower growth rates higher GFP yields were obtained as also observed for lower cultivation temperatures. With 20 % or even higher concentrations no enhanced acetate formation could be detected. For cultivating without oxygen limitation at least 20 % DO should be present.

- *Carbon source*

As in subproject B8 (Franco-Lara) for an antibody fragment (ABF) producing strain [*David et al., 2011*] in this project a screening for the optimal carbon source for the GFP high producer was achieved. It has been carried out in 24-deep well plates. Growth and production performance for the six different sources glycerol, fructose, glucose, arabinose, galactose and mannose have been studied. Reasonable growth rates were obtained for glycerol, fructose and glucose. Similar high product yields were obtained for fructose and

glycerol and also on arabinose high GFP amount could be reached. On glycerol very low amounts of the by-product acetate were obtained. Considering growth rate, product and by-product formation fructose or glycerol turned out to be most useful for a production process with *B. megaterium*. To cheapen the process the usability to metabolize industrial raw glycerol which is a waste product in biofuel production was investigated in shake flask experiments. *B. megaterium* is perfectly able to metabolize either pure glycerol or raw glycerol (after sterile filtration) as the obtained product yields are similar.

Tab. 1 summarized the optimal process parameters parameters for recombinant protein production with *B. megaterium.*

Tab. 1: Optimal values of basic cultivation parameters for recombinant protein production with B. megaterium.

Parameter	Best Value Growth	Best Value Product Yield	Best Value Low by-products
pH	6/7	6	6
Temperature	37°C	20°C	20°C
Dissolved oxygen	≥ 20%	10%	≥ 20%
Induction time point	Late phase	Early phase	
Carbon source	Fructose, glucose	Fructose, glycerol, arabinose	Glycerol

Characterization of different production stages and comparison to non-producing stage

The growth stages of recombinant *B. megaterium* (exponential, end of exponential phase, stationary phase) were analyzed by methods of systems biotechnology and compared to a strain containing a plasmid with the same expression system but without a product gene on the plasmid. The aim was to investigate differences in cell metabolism caused by the formation of high amounts of protein product. Four biological replicates of batch experiments were performed with the GFP producer and the non-producer strain. Three sampling time points for polyomic analysis were chosen - mid-exponential phase, end of batch phase (visible by DO-peak) and 2 h after entry into stationary phase. Samples were taken during the whole cultivation for product, by-product and biomass estimation. Rapid sampling techniques were applied for polyomic analysis.

- *Transcriptome analysis*

Transcriptome analyses were performed by DNA microarray techniques. The microarray platform used in this study was provided by Agilent (Agilent technologies, Böblingen, Germany). The 8 x 15k microarray slides were custom-made using the software earray (Agilent technologies) with the help of the just published genome data of *B. megaterium* DSM319 [*Eppinger et al., 2011*]. Treatment of RNA used for microarray analysis was

performed as described for *B. megaterium* in the literature [*Biedendieck et al., 2011]* and according to the instructions of the manufacturers of the used experimental kits in cooperation with subprojects A1 (Jahn/Dersch) and B8 (Franco-Lara).

Results were matched regarding differences between cultivation stages or between the GFP producing and non-producing strain. The genes that were found to be up or down regulated between the stages belong to different cell processes. A lot of ribosomal proteins were found as well as transcriptional or translational regulators. Also some genes involved in amino acid biosynthesis pathways were found.

- *Quantitative metabolome analysis*

Methods of quantitative metabolome analysis are established for many microbial systems (*Corynebacterium glutamicum, Pseudomonas aeruginosa, E. coli, Pseudomonas putida, Sulfolobus solfaricus, Saccharomyces cerevisiae*). Using GC-MS and LC-MS methods it is possible to analyze different types of metabolites. After sampling, extraction and derivatization procedures samples were analyzed via GC/TOF-MS. A typical setup for metabolic profiling via GC coupled to a LECO® Pegasus IV TOF (Leco Corp Inc., St. Joseph, USA) mass analyzer according to Morgenthal and colleagues was used [*Morgenthal et al., 2005*]. Chromatograms were processed using Leco ChromaTOF® software (v4.24) supporting automated baseline correction, peak finding, area calculation, library search and deconvolution of all chromatogram mass spectra and mass-spectral correction for co-eluting metabolites. Further, the retention indices (RI`s) are calculated and suitable fragment mass-to-charge ratios for selective quantification were identified. Compounds were annotated by RI and mass spectra comparison to a user defined spectra library (combination of the Golm Metabolome Database (GMD) and an in house library). Selected fragment ions specific for each individual metabolite were used for peak area quantification. Each compound was normalized by the peak area from the internal standard and by the initial bacterial biomass. These relative response ratios can be directly compared between different samples without knowledge of absolute compound concentrations. Using specific software criteria, it is possible to receive 174 metabolites (features) characterizing *B. megaterium* primary metabolism, however, derivatives and adducts were summed to 84 identified biological compounds. By screening for metabolites with significant changes between two stages (cultivation stage or producing stage) mainly amino acids were found to be more or less present. This is not surprising as they are required in high amounts for recombinant protein synthesis.

- *Quantitative proteome analysis*

Traditional approaches as 2D-PAGE have been successfully used, e.g. in this SFB to analyze the proteome of *B. megaterium* under protein production stage [*Wang et al., 2005*]. For example 150 proteins were identified in project B5 including two extracellular proteases with product degrading effects. A deletion of NprM - the main extracellular protease - resulted in an enormous increase in product amounts [*Wittchen and Meinhardt, 1995*]. Although being a useful tool 2D-PAGE based approaches are limited for analysis of

the entire proteome or time resolved experiments. Gel-free methods like LC-MS analysis enable an investigation of the whole proteome. Because of this gel-free proteome analysis was performed for the described production/non-production experiment. As equipment capacities are limited in Braunschweig, proteome samples of these experiments were analyzed in cooperation with the proteome center in Greifswald (Prof. Hecker). A wide variety of proteins and protein groups were detected. Especially folding assisting proteins as chaperones and stress proteins as cold shock proteins were highly present. Proteins involved in amino acid biosynthesis as well as vitamin biosynthesis were also up-regulated in agreement with the results of metabolome and transcriptome analysis.

- *Cloning targets for supporting recombinant protein production*

In the last part of these experiment series promising candidates for strain optimization or optimization of the protein production system were evaluated by combining results of transcriptome, metabolome and proteome analysis. Recombinant coproduction of these candidates with the recombinant product may lead to enhanced product yields. For the GFP producing strain the chosen candidates are listed in **Tab. 2**.

Tab. 2: Cloning targets for coproduction during recombinant protein production in B. megaterium *to improve production performance.*

BMD number	Protein name	Cell Function
BMD_0537	Biotin biosynthesis protein BioY	Biotin biosynthesis
BMD_2464	Acetyl CoA carboxylase biotin carboxyl carrier protein	Biotin biosynthesis
BMD_2695	Cold shock protein	Stress response
BMD_1780	Hypothetical protein BMD 1780	
BMD_4738	Translation initiation factor IF 3	Translation
BMD_1895	Copper chaperone CopZ copper ion binding protein	Hydrolase
BMD_2208	General stress protein 17M	Stress response
BMD_4732	M42 glutamyl aminopeptidase	Aminopeptidase activity
BMD_0260	10 kDa chaperonin	Protein folding
BMD_1682	Cold shock protein	Stress response
BMD_1404	Cold shock protein	Stress response
BMD_2791	Cold shock protein	Stress response
BMD_0006	DNA gyrase A subunit	DNA-dependent DNA replication

Influence of large scale conditions and large scale adaptation

In large scale processes fluctuations and gradients in substrate and oxygen concentration are likely to occur due to mixing deficiencies. They can contribute to a loss in biomass or product formation [*Enfors et al., 2001; Bylund et al., 1998*]. To avoid expensive changes in reactor configuration after building up a large scale plant it is sensible to investigate the

influence of oxygen and substrate gradients on production performance of a desired bacterial host at lab scale. In the literature many possible scenarios for such experiments are described [*Bylund et al., 1999; Lejeune et al., 2009*]. In this project a scale down reactor was developed and characterized. Scale down bioreactors are described in the literature as a useful tool for investigate the influence of heterogeneous areas on bacterial populations. In general they consist of two compartments which are running in different configurations e.g. regarding the oxygen supply, pH or substrate concentration. The culture broth circulates between both systems overall emulating the heterogeneous environment of a large scale bioreactor.

In this project the scale down reactor consisted of a 3.7 L bioreactor and a 700 mL glass vessel (**Fig. 1**). In the smaller compartment no stirrer was installed and no aeration occurred. The bigger compartment was a standard lab scale bioreactor with stirrer and aeration control. Both compartments where tube-connected and a circulation was realized by a mechanical pump. In fed-batch experiments feeding was performed with a DO-based feeding but feeding was done into the smaller vessel thereby simulating a large scale feeding zone. The scale down reactor was intensively characterized (temperature, residence time estimation by conductivity and density measurements). Afterwards several batch and fed-batch experiments have been carried out with regard to production and growth performance under oxygen and substrate gradients.

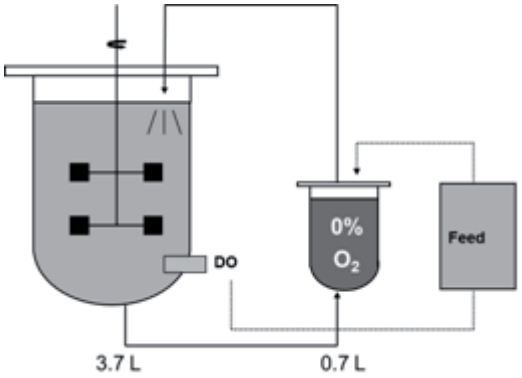

Fig. 1: Two compartment scale down bioreactor cascade with DO-based nutrient supply.used for investigation of the influence of substrate and oxygen gradients on product yield and growth performance of B. megaterium.

The cascade and the feed supply caused substrate and oxygen gradients and led to a decreased yield in recombinant GFP per cell dry weight compared to a standard lab scale cultivation. GFP producing cells are simply detectable via flow cytometry. So the decreased production performance was confirmed [*Korneli et al., 2011*].

- *Fedbatch strategy for metabolic investigation of the influence of large scale gradients on recombinant production*

The principle of a two compartment scale down set-up was simplified in further experiments by using just one lab scale bioreactor with a special feeding strategy mimicking large scale conditions. The feeding principle was a DO-based feeding where the medium dosage can be controlled online in dependence of the actual DO-value in the cultivation. With a P-controlled oxygen dependent feeding profile characteristic oscillations

in dissolved oxygen between 10 and 40 % were reached. By application of a PI-controlled profile a rather constant value of DO could be obtained. Regarding their different intensities of DO fluctuation the profiles were considered as large (high fluctuations) and small scale (low fluctuations).

In large scale cultivations a strong decrease in GFP yield was observed. To investigate the metabolic origin of the loss in product yield at large scale, the concentrations of free intracellular amino acids were analyzed during short time intervals (2 minutes) in the feeding phases. This was done by using the method of fast filtration [*Bolten et al., 2007*].

The concentration of amino acids was estimated via HPLC analysis. For diverse amino acids different fluctuations in their concentrations were observed in both experiments whereas the total pool of amino acids was constant. Except of some outliers the error ratios were rather small (mostly < 15 %) which verifies the applicability of this analytical method for recombinant *B. megaterium*.

At large scale conditions oscillating pattern of amino acid concentration where observed for some amino acids. Also some basic culture variables as carbon dioxide production rate (CPR), substrate concentration where oscillating and could be correlated to the course of amino acid concentration. Also fluctuations in GFP concentration where detected. The stable maintenance of GFP in the cell plasma would overlie a conceivable oscillatory course. The results of amino acid estimation clearly illuminate a strong effect of oxygen and substrate gradients on the central metabolism resulting in decreased product yields. By calculating and heat map imagination of a relative availability of intracellular amino acids (quotient of large scale conditions and small scale concentrations) it can be seen that the supply of certain amino acids is limited, indicated by the red color (**Fig. 2**).

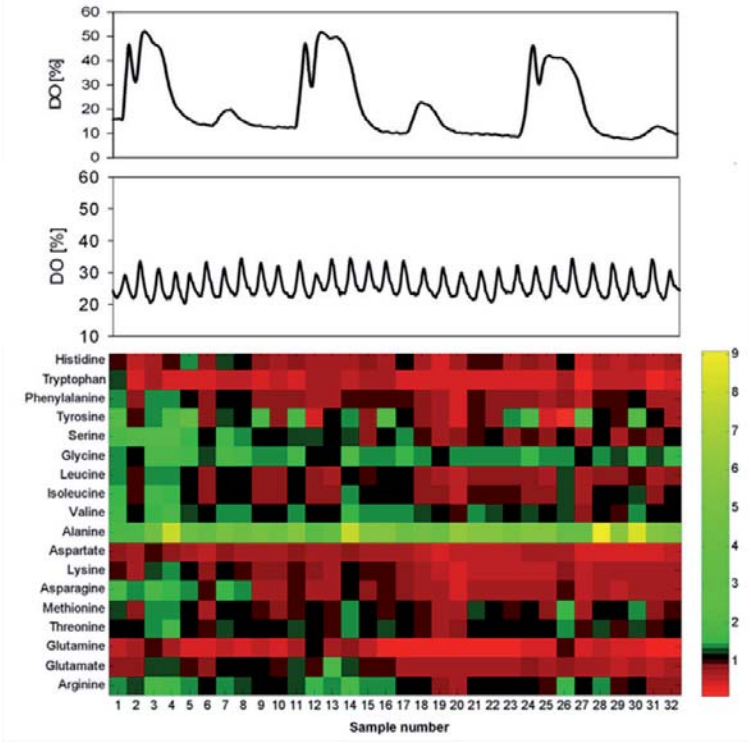

Fig. 2: Heat map visualizing the availability of free intracellular amino acids during the feeding phase of recombinant protein production by B. megaterium *YYBm1 under conditions of large and small scale. The colour code indicates an increased (green) or decreased (red) availability under the large scale conditions as compared to the reference process as indicated by the colour legend aside the graph (Figure was taken from [*Korneli et al., 2012*]).*

An evaluation of this kind is useful for identification of limited amino acids in a production process.

Besides a direct investigation of limiting building blocks a highly resolved data analysis delivers specific characteristics of dynamics and structures of the basic metabolic network of *B. megaterium.* For interpretation from network perspective phase plane plots of particular amino acids were created and compared with the central carbon core metabolism (**Fig. 3**). A stable metabolic performance was observed for small scale conditions. The ratio between different amino acid pools such as glycine/serine, alanine/valine or glutamate/glutamine remained rather constant. Quite the opposite behavior was obtained for the large scale process, obviously being a main consequence of the intermittent feeding and probably the reduced production. Furthermore, the dynamics of various amino acid pools could be correlated and exposed a coordinated picture of the whole network. This includes e.g. DO dependent regular changes of the ratio between glutamate/glutamine as well as phase shifted oscillation of glycine/serine. Coordination could be found between amino acids belonging to the same family sharing the carbon precursor block (green segments). The strongly coordinated dynamic course of e. g. alanine, leucine or valine for large and small scale appear possible to be originated from dynamic changes in the availability of their metabolic precursors from glycolysis, pentose phosphate pathway or TCA cycle. Blue modules indicate coordination in between the nitrogen metabolism where amino acids as glutamate, glutamine, alanine or aspartate act as central transamination donors. All these interactions express that the limitation of a single metabolite result from the connections in a system wide reaction network. Therefore, process optimization regarding metabolic targets should always be done with a holistic point of view on the metabolic network. To optimize the large scale production process the feed solution was extended for a large scale experiment. Regarding the results of the metabolic finger printing it was enriched with tryptophan, aspartate, histidine, glutamine and lysine which were the five most limiting amino acids identified. By this feed supply the yield of recombinant GFP was increased about 100% during the feed phase compared to the small scale reference process. As the intracellular concentrations of the added amino acids were enhanced up to six fold the cells took them up and used them among other cellular process efficiently for recombinant protein production. Next to the amino acid pools of these five amino acids also other amino acid pools were changed underlining the strongly interconnected character of the central carbon metabolism network of *B. megaterium [Korneli et al., 2012].*

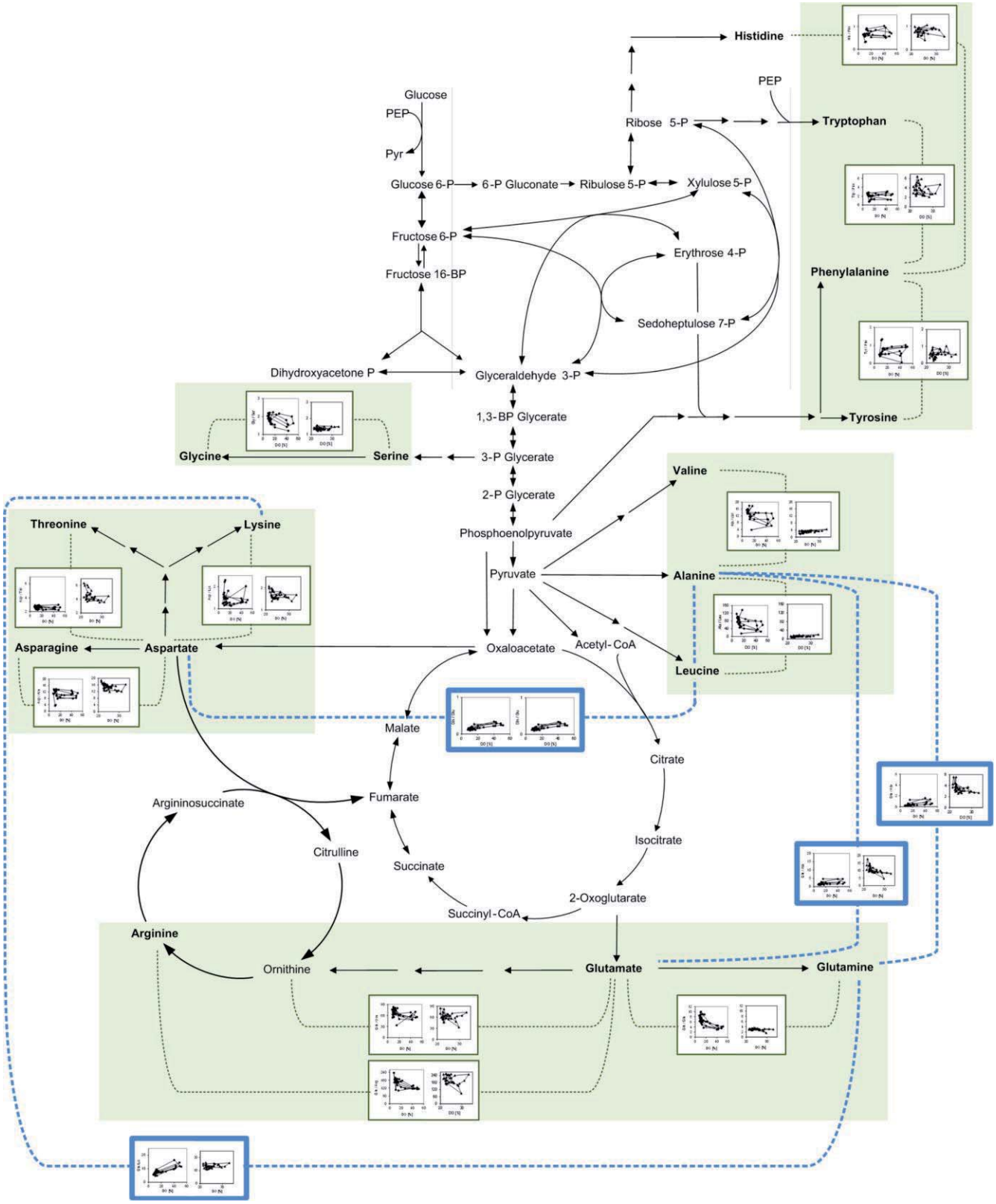

Fig. 3: Characteristics of the metabolic network B. megaterium *YYBm1 during recombinant GFP production under large and small scale conditions. The data show the oscillatory behavior of selected amino acids or amino acid pairs during fed-batch production via phase plane plots from conditions of large (left boxes) and small scale (right boxes). Time correlated behavior between directly (dashed lines) and indirectly linked metabolites (dotted lines) is indicated. Figure was taken from Korneli et al. (*2012*).*

Cloning of a glycosyltransferase producing strain

In cooperation with subproject A1 (Jahn/Dersch) a new strain was constructed which recombinantly produces and secrets the homologous levansucrase SacB from *B. megaterium*. The corresponding gene was vector encoded on the control of the optimized xylose inducible promoter resulting in the plasmid pRBBm112. For general characterization the recombinant strain carrying pRBBm112 was cultivated on complex and minimal medium in shake flasks, respectively. Product formation after induction occurred in parallel to growth. The enzyme stably remained in the culture broth and was not degraded even in the stationary phase. In SDS-PAGE analysis it could be shown the levansucrase is the by far most prominent protein (95 %) in the raw culture supernatant. Therefore, quantification can simply be done with standard BSA-protein tests. An enzyme assay for estimating enzyme activity was developed. Here, a defined amount of culture supernatant is incubated in reaction buffer and with surplus of the enzyme substrate sucrose for 30 minutes. One mole of sucrose is converted to 1 mole of glucose and 1 mole of fructose. The concentration of glucose is measured in a glucose analyzer and then allows an estimation of enzyme activity in units per liter. In these first experiments enzyme activities of 20,000 U/L (12,000 U/g_{CDW}) corresponding 250 mg/L protein could be achieved.

High cell density production process with a producer strain

Finally, a high cell density fed-batch process for the secretion of recombinant proteins was developed. First, the usability of raw glycerol as substrate has been proven by doing shake flaks experiments compared with pure lab glycerol. No significant differences in productivity were achieved. Considering the optimized cultivation parameter a HCDC fed-batch with raw glycerol as sole carbon source has been used for the production of high amounts of recombinant extracellular levansucrase (up to 1 g/l).

Hence, the importance and usability of *B. megaterium* for industrial production was shown as two completely different recombinant products - intra- and extracellular - could be produced in g/l scale.

3.2.1.3 References to other works and collaborations in the SFB

In collaboration with subproject A1 (Jahn/Dersch) high cell density fed-batch cultivations were done to obtain high product titer of intracellular GFP and prove the high production capacities using the high performance plasmid pSSBm85. The high producer strain of these experiments were created in subproject A1 (Jahn/Dersch) and afterwards exchanged with this subproject. By application of a DO-based fed-batch strategy, which has been proven to be useful within the studies of this subproject high amounts of the recombinant product GFP was obtained [*Stammen et al., 2010*].

The systems biotechnology experiment regarding non-producing and producing cultivation stages was done in collaboration with subprojects A1 (Jahn/Dersch), B8 (Franco-Lara) and B9 (Münch/Schomburg). Cultivations and basic process parameters as well as polyomic sampling procedures were done in collaboration with B8 (Franco-Lara). Transcriptome analysis was done by A1 (Jahn/Dersch). Metabolome analysis and statistical evaluation was done together with A1 (Jahn/Dersch) and B9 (Münch/Schomburg). Within these collaboration methods, strains and analytic procedures were exchanged considering also possible cloning targets for further genetic strain optimization.

As was shown that some glycosyltransferases might be too large to be properly secreted by *B. megaterium* information about other possible glycoslytransferases were exchanged between the subprojects A1 (Jahn/Dersch), A7 (Heinz/Seibel) B3 (Krull/Hempel) and B8 (Franco-Lara). Furthermore an appropriate strain was constructed by subproject A1 (Jahn/Dersch) and methods as enzyme assays and protein analysis techniques were exchanged between A7 (Heinz/Seibel), B3 (Krull/Hempel) and B8 (Franco-Lara). Information and data were exchanged with project B11 with regard to metabolic network analysis by means of ^{13}C-based flux analysis.

3.2.1.4 Comparison with research outside the SFB

Fed-batch experiments are applied in many research groups to achieve high product amounts. Also DO-based fed-batch strategies are widely applied, e.g. for HCDC processes with *E. coli* [*Cutayar and Poillon, 1989*]. Using a model protein (here GFP) for highlighting the influence of heterogeneous environmental conditions is established as well but so far not for *B. megaterium*. DO-based fed-batch and scale down experiments have been used to investigate the expression of a GFP coupled stress reporter protein [*Delvigne et al., 2009*]. The difference to the research of this subproject is the general focus of the experiments. The research here is straightly focused on the metabolic and physiologic performance of only *B. megaterium* under various environmental conditions and is less interested in the technical scaling up procedure itself. The application of the specialized debottlenecking feeding strategy was developed for the first time as the observed special oxygen oscillations have been only described for autonomously appearing in yeasts [*Henson et al., 2004*].

Further research groups discovered a disadvantageous effect of mixing deficiencies especially for the biomass formation in baker's yeast production [*George et al., 1998*]. But their research also focused on bioreactor configuration and how this can be improved to enhance production. No investigation of metabolic bottlenecks particularly for recombinant protein production with *B. megaterium* has been done so far.

Holistic systems biotechnology experiments are new for *B. megaterium* as the technological platform was established in Braunschweig in the last years within this SFB and is now available [*Biedendieck et al., 2011*]. In general bacteria of the genus Bacilli are widely used with regard to systems biotechnological tasks. Especially the closely related

Bacillus subtilis has been intensively studied by using polyomics technologies [*Buescher et al., 2012*].

The experiments revealed the great potential of *B. megaterium* for industrial production. Therefore, it is most useful to be familiar with the specific requirements of *B. megaterium* which can be estimated by holistic approaches of systems biotechnology which should be used even more extensive in the future.

3.2.1.5 Literature

Biedendieck, R.; Beine, R.; Gamer, M.; Jordan, E.; Buchholz, K.; Seibel, J.; Dijkhuizen, L.; Malten, M.; Jahn, D. (2007a) Export, purification and activities of affinity tagged *Lactobacillus reuteri* levansucrase produced by *Bacillus megaterium*. *Appl. Microbiol. Biotechnol* 74, 1062-1073

Biedendieck, R.; Yang, Y.; Deckwer, W.D.; Malten, M.; Jahn, D. (2007b) Plasmid system for the intracellular production and purification of affinity-tagged proteins in *Bacillus megaterium*. *Biotechnol. Bioeng.* 96, 525-537

Biedendieck, R.; Gamer, M.; Jaensch, L.; Meyer, S.; Rohde, M.; Deckwer, W.D.; Jahn, D. (2007c) A sucrose-inducible promoter system for the intra- and extracellular protein production in *Bacillus megaterium*. *J. Biotechnol.* 132, 426-430.

Biedendieck, R.; Borgmeier, C.,Bunk, B.; Stammen, S.; Scherling, C.; Meinhardt, F.; Wittmann, C.; Jahn, D. (2011) Systems biology of recombinant protein production using *Bacillus megaterium*. *Methods Enzymol,* 500, 165-195

Bolten, C. J.; Kiefer, P.,Letisse, F.; Portais, J. C.; Wittmann, C. (2007) Sampling for metabolome analysis of microorganisms. *Anal. Chem.* 79, 3843-3849

Buescher, J. M.; Liebermeister, W.; Jules, M.; Uhr, M.; Muntel, J.; Botella, E.; Hessling, B.; Kleijn, R. J.; Le Chat, L.; Lecointe, F.; Mäder, U.; Nicolas, P.; Piersma, S.; Rügheimer, F.; Becher, D.; Bessieres, P.; Bidnenko, E.; Denham, E. L.; Dervyn, E.; Devine, K. M.; Doherty, G.; Drulhe, S.; Felicori, L.; Fogg, M. J.; Goelzer, A.; Hansen, A.; Harwood, C. R.; Hecker, M.; Hubner, S.; Hultschig, C.; Jarmer, H.; Klipp, E.; Leduc, A.; Lewis, P.; Molina, F.; Noirot, P.; Peres, S.; Pigeonneau, N.; Pohl, S.; Rasmussen, S.; Rinn, B.; Schaffer, M.; Schnidder, J.; Schwikowski, B.; van Dijl, J. M.; Veiga, P.; Walsh, S.; Wilkinson, A. J.; Stelling, J.; Aymerich, S.; Sauer, U. (2012) Global network reorganization during dynamic adaptations of *Bacillus subtilis* metabolism. *Science* 335, 1099-1103

Bylund, F.; Collet, E.,Enfors, S. O.; Larsson, G. (1998) Substrate gradient formation in the large-scale bioreactor lowers cell yield and increases by-product formation. *Bioprocess Biosyst. Eng.* 18, 171-180

Bylund, F.; Guillard, F.; Enfors, S. O.; Trägårdh, C.; Larsson, G. (1999) Scale down of recombinant protein production: a comparative study of scaling performance. *Bioprocess Biosyst. Eng.* 20, 377-389

Cutayar, J. M.; Poillon, D. (1989) High cell density culture of *Escherichia coli* in a fed-batch system with dissolved oxygen as substrate feed indicator. *Biotechnol. Lett.* 3, 155-160

David, F.; Steinwand, M.; Hust, M.; Bohle, K.; Ross, A.; Dübel, S.; Franco-Lara, E. (2011) Antibody production in *Bacillus megaterium*: Strategies and physiological implications of scaling from microtiter plates to industrial bioreactors. *Biotechnol. J.* 12, 1516-1531

Delvigne, F.; Boxus, M.; Ingels, S.; Thonart, P. (2009) Bioreactor mixing efficiency modulates the activity of a prpoS::GFP reporter gene in *E. coli*. *Microb. Cell. Fact* 8

Enfors, S. O.; Jahic, M.; Rozkov, A.; Xu, B.; Hecker, M.; Jürgen, B.; Krüger, E.; Schweder, T.; Hamer, G.; O'Beirne, D.; Noisommit-Rizzi, N.; Reuss, M.; Boone, L.; Hewitt, C.; McFarlane, C.; Nienow, A.; Kovacs, T.; Tragardh, C.; Fuchs, L.; Revstedt, J.; Friberg, P. C.; Hjertager, B.; Blomsten, G.; Skogman, H.; Hjort, S.; Hoeks, F.; Lin, H. Y.; Neubauer, P.; van der Lans, R.; Luyben, K.; Vrabel, P.; Manelius, A. (2001) Physiological responses to mixing in large scale bioreactors. *J. Biotechnol.* 8, 175-185

Eppinger, M.; Bunk, B.; Johns, M. A.; Edirisinghe, J. N.; Kutumbaka, K. K.; Koenig, S. S. K.; Creasy, H. H.; Rosovitz, M. J.; Riley, D. R.; Daugherty, S.; Martin, M.; Elbourne, L. D. H.; Paulsen, I.; Biedendieck, R.;

Braun, C.; Grayburn, S.; Dhingra, S.; Lukyanchuk, V.; Ball, B.; Ul-Qamar, R.; Seibel, J.; Bremer, E.; Jahn, D.; Ravel, J.; Vary, P. S. (2011) Genome sequences of the biotechnologically important *Bacillus megaterium* strains QM B1551 and DSM319. *J. Bacteriol.* 193, 4199-4213

George, S.; Larsson, G.; Olsson, K.; Enfors, S. O. (1998) Comparison of the Baker's yeast process performance in laboratory and production scale. *Bioprocess Eng.* 18, 135-142

Henson, M. A. (2004) Modeling the synchronization of yeast respiratory oscillations. *J. Theor. Biol.* 231, 443-458

Hollmann, R.; Deckwer, W. D. (2004) Pyruvate formation and suppression in recombinant *Bacillus megaterium* cultivation. *J. Biotechnol.* 111, 89-96

Hollmann, R.; Malten, M.; Biedendieck, R.; Yang, Y.; Wang, W.; Jahn, D.; Deckwer, W.-D. (2006) *Bacillus megaterium* as a host for recombinant protein production. Eng. Life Sci. 6, 470-474

Homann, A.; Biedendieck, R.; Götze, S.; Jahn, D.; Seibel, J. (2007) Switching from polymers to oligosaccharides - Functional modification of a novel levansucrase from *Bacillus megaterium* by site-directed mutagenesis. *Biochem. J.* 407, 189-198

Lejeune, A.; Delvigne, F.; Thonart, P. (2009) Influence of bioreactor hydraulic characteristics on a *Saccharomyces cerevisiae* fed-batch culture: hydrodynamic modelling and scale-down investigations. *J. Ind. Microbiol. Biotechnol.* 37, 225-236

Malten, M.; Hollmann, R.; Deckwer, W.-D.; Jahn, D. (2005) Production and Secretion of Recombinant *Leuconostoc mesenteroides* Dextransucrase DsrS in *Bacillus megaterium*. *Biotechnol. Bioeng.* 89, 206-218

Malten, M.; Biedendieck, R.; Gamer, M.; Drews, A. C.; Stammen, S.; Buchholz, K.; Dijkhuizen, L.; Jahn, D. (2006) A *Bacillus megaterium* plasmid system for the production, export, and one-step purification of affinity-tagged heterologous levansucrase from growth medium. *Appl. Environ. Microbiol.* 72, 1677-1679

Morgenthal, K.; Wienkoop, S.; Scholz, M.; Selbig, J.; Weckwerth, W. (2005) Correlative GC-TOF-MS-based metabolite profiling and LC-MS-based protein profiling reveal time-related systemic regulation of metabolite-protein networks and improve pattern recognition for multiple biomarker selection. *Metabolomics* 1, 109-121

Stammen, S.; Müller, B. K.; Korneli, C.; Biedendieck, R.; Gamer, M.; Franco-Lara, E.; Jahn, D. (2010) High-yield intra- and extracellular protein production using *Bacillus megaterium*. *Appl. Environ. Microbiol.* 76, 4037-4046

Wang, W.; Hollmann, R.; Fürch, T.; Nimtz, M.; Malten, M.; Jahn, D.; Deckwer, W. D. (2005) Proteome analysis of a recombinant *Bacillus megaterium* strain during heterologous production of a glucosyltransferase. *Proteome Sci.* 3

Wittchen, K. D.; Meinhardt, F. (1995) Inactivation of the major extracellular protease from *Bacillus megaterium* DSM319 by gene replacement. *Appl. Microbiol. Biotechnol.* 42, 871-877.

3.2.2 Project Relevant own publications

a) Works that have appeared in publications of a scientific quality assurance at the time of application or final adoption, and book publications

Stammen, S.; Müller, B.K.; Korneli, C.; Biedendieck, R.; Gamer, M.; Franco-Lara, E.; Jahn, D. (2010) High yield intra- and extracellular protein production using *Bacillus megaterium*. *Appl. Environ. Microbiol.* 76, 4037-4046

Biedendieck, R.; Bunk, B.; Fürch, T.; Franco-Lara, E.; Jahn, M.; Jahn, D. (2010) Systems Biology of Recombinant Protein Production in *Bacillus megaterium*. In: “Biosystems Engineering I: Creating Superior Biocatalysts”, Springer-Verlag Series “Advances in Biochemical Engineering/ Biotechnology, Vol. 120, 133-162

Korneli, C.; David, F.; Godard, T.; Franco-Lara, E. (2011) Influence of fructose and oxygen gradients on fed-batch recombinant protein production using *Bacillus megaterium*. *Eng. Life Sci.* 11, 338-349

Korneli, C.; Bolten, C. J.; Godard, T.; Franco-Lara, E.; Wittmann, C. (2012) Debottlenecking recombinant protein production in *Bacillus megaterium* under large-scale conditions-targeted precursor feeding designed from metabolomics. *Biotechnol. Bioeng.* 109, 1538-1550

3.3 Looking back on the promotion

The project has been funded since July 2008 in the SFB 578. It was completed on June 2012 with the end of the program.

3.3.1 Personnel in the project

	Name, akad. degree, service position	narrower subject of the employee	Institute of University or non-university facility	Participation in the project in hours per week	Category
Basic staff					
Research associate (incl. auxiliary power)	1. E. Franco-Lara, Jun.-Prof. Dr.-Ing	Biochemical Engineering	Institute of Biochemical Engineering	10	Professorship
	2. D. Jahn, Prof. Dr.	Microbiology	Institute of Microbiology	4	Professorship
Non-academic staff	3. Namuth, T., BTA	Biochemical Engineering	Institute of Biochemical Engineering	5	
Supportive staff					
Research associate (incl. auxiliary power)	4. C. Korneli, Dipl.-Biotechnol.	Biochemical Engineering	Institute of Biochemical Engineering	40	PhD student
	5. J. Melzer, Dr.	Microbiology	Institute of Microbiology	20	Postdoc
Non academic staff	6. N. N., Stud. assistant	Biochemical Engineering, Biotechnology, Microbiology	Institute of Biochemical Engineering, Institute of Microbiology	10	Students

Responsibilities of employees (basic staff)

Position 1 - 3:

The involved employees in the subproject B10 (Jahn / Franco-Lara) of the Institute of Microbiology and the Institute of Biochemical Engineering have supported the involved staff (PhD-student, technical staff member, postdoc) in bioprocess and molecular biological experiments as well as in the development of reaction models, the implementation of cultivation and analysis and the construction of experimental facilities.

Responsibilities of employees (supportive staff)

Position 4: Dipl.-Biotechnol. Claudia Korneli

To evaluate the usability *of B. megaterium* for industrial production Ms. Korneli has analyzed the production process of recombinant proteins with *B. megaterium* from different point of views. At first she used a GFP producing model strain for investigation of basic process parameter as pH, temperature, DO concentration or carbon source. With regard to industrial large scale application she analyzed typical large scale drawbacks at lab scale by application of different scale down strategies. Thus, metabolic bottle necks were elucidated by application of systems biotechnology methods.

Position 5: Dr. Jana Melzer

During the whole application period Dr. Melzer was involved in the area of transcriptome analysis, especially in custom-made DNA-micro arrays as well as in the use of special molecular biological and microbiological methods. Beside the organization of the realization of the practical work she worked closely together with position 3 (T. Namuth) and position 4 (C. Korneli). Especially the transcriptome data demanded very difficult analyses and interpretations of the results until they could be used within this SFB also in other subprojects (A1, B8).

Position 6: Stud. assistant

The student assistant supported the extensive experimental work in the implementation and evaluation of bacterial cultivations as well as in the routine of biotechnological and molecular biological studies.

3.1 General information on the completed project B11

3.1.1 Topic

Metabolic network dynamics for production of recombinant glycosyltransferases

3.1.2 Disciplines and field of work

Biochemical engineering, Systems biotechnology

3.1.3 Project manager

Prof. Dr. Christoph Wittmann
(b.: 03.03.1967)
Institute of Biochemical Engineering
Technische Universität Braunschweig
Gaußstrasse 17, 38106 Braunschweig
Phone: 0531/391-7651
Fax: 0531/391-7652
E-Mail: c.wittmann@tu-bs.de

3.2 Development of the subproject

3.2.1 Report

3.2.1.1 Current knowledge at the last application and initial question

The production of glycosyltransferases by *Aspergillus niger* and *Bacillus megaterium* is linked to a network of metabolic and regulatory interactions within the underlying metabolism – a complex and only partly understood interplay. Towards knowledge-based improvement of strains and processes, the project aims at quantitative characterization at the level of metabolic networks – fluxes and metabolites. These have proven valuable towards a deeper understanding of cellular processes and their optimization [*Stephanopoulos et al., 1998; Deckwer et al., 2006*]. Within the concept of systems biology, fluxes and metabolites appear central, as they directly reflect the phenotype, whereas the other "omics" data often do not provide direct conclusions. Thus, metabolic network analysis provides an important contribution to systems wide models and their testing and improvement to describe, predict and optimize the complex behavior of biological networks [*Sauer, 2006*].

In this regard, the project focusses on the central carbon metabolism, performing key tasks in the synthesis of target proteins. In an initial project phase, corresponding experimental and computational methods to approach fluxes and metabolites in *A. niger* and *B. megaterium* should be developed, to be applied for the investigations of strains and processes within the framework of the SFB, including close interaction with other sub-projects from parts A and B for the identification of metabolic limitations and rational optimization of production.

3.2.1.2 Results and applied methods

In silico metabolic network analysis of *Aspergillus niger* [*Melzer et al., 2009*]

First, the metabolic network of the complex eukaryotic fungus *A. niger* was approached on the modeling level. For this purpose a large-scale stoichiometric model of the carbon core metabolism with about 100 reactions and pathways and the relevant cellular compartments was established on basis of genome information, data bases and primary literature, as shown in **Fig. 1**. Using elementary flux mode analysis, it was then possible to compute the entire theoretical solution space for the underlying fluxes as previously shown [*Krömer et al., 2006*].

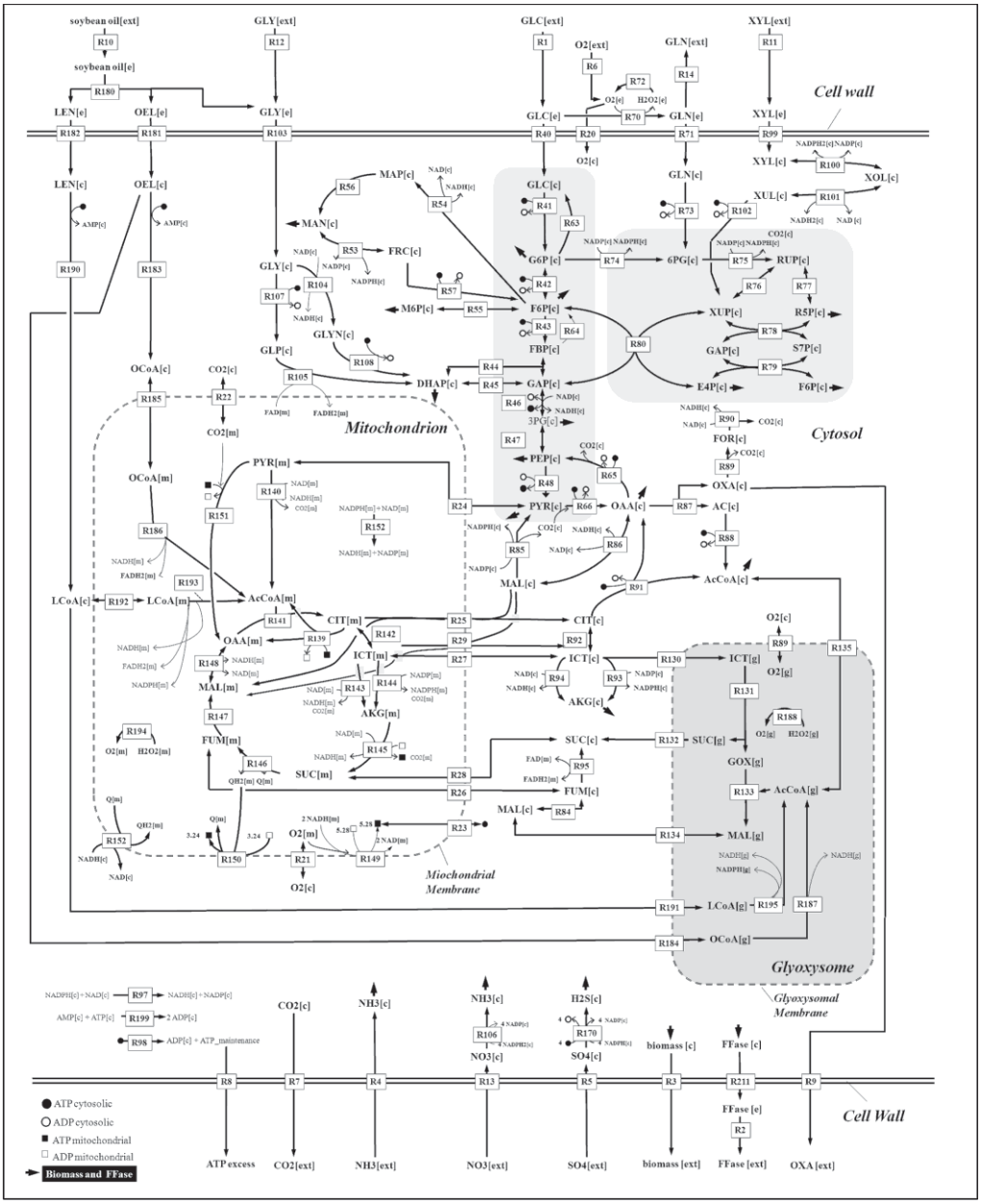

Fig. 1: Metabolic model for Aspergillus niger*. Reactions and metabolites are compartmentalized between extracellular [e], cytosol [c], mitochondrion [m] and glyoxysome [g] compartments. Numbers next to the arrows refer to the detailed model description in the supplement.*

In cooperation with sub-project B4 (Jahn/Nörtemann/Jänsch), optimum yields and pathways could be predicted for *A. niger* in a variety of different scenarios on basis of the calculated modes, including *in silico* mutants, different substrates as well as different target products. This provided important insights into the basic properties of the metabolic network of this microorganism. Subsequently, a novel computational strategy was developed, named Flux Design, which allows the identification of genetic targets via flux correlation to a chosen objective flux towards improved biotechnological production strains with optimally designed fluxes. This novel approach, Flux Design, meanwhile used by other groups as well, computes elementary modes and, by search through the modes, identifies targets to be amplified (positive correlation) or down-regulated (negative correlation). Supported by statistical evaluation, a target potential could be attributed to the identified reactions in a quantitative manner. Up to more than 20,000 modes were obtained for each case, differing strongly in production performance and intracellular fluxes. For enzyme production in *A. niger* flux correlation analysis suggested a number of targets, including non-obvious ones (**Fig. 2**).

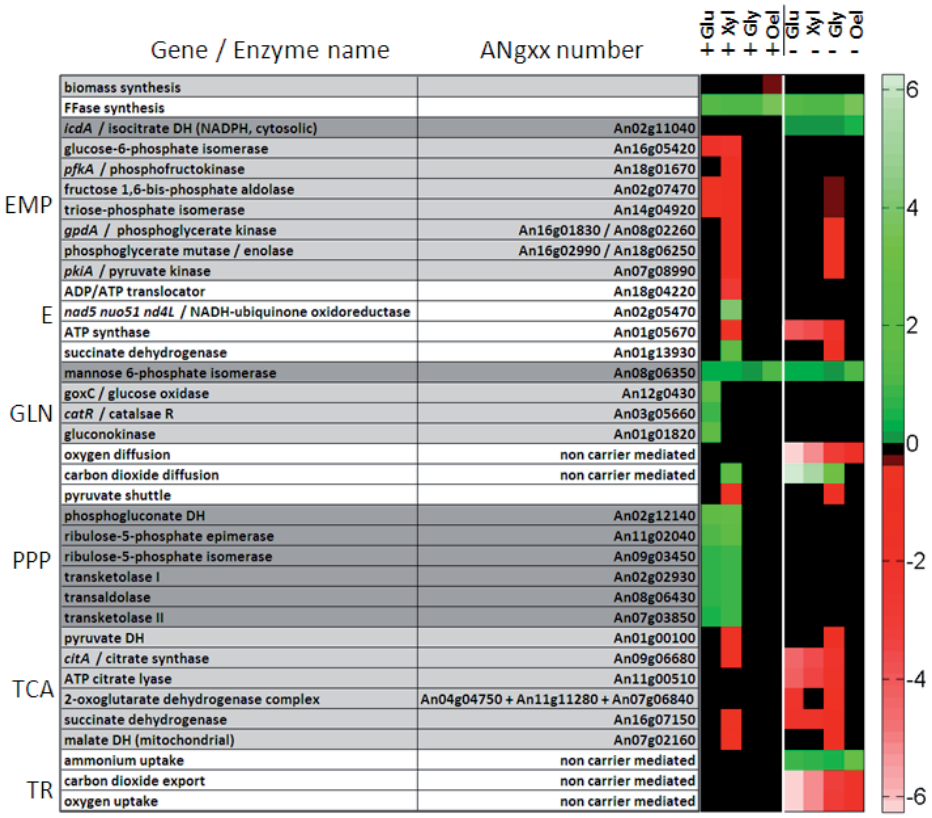

Fig. 2: Prediction of genetic targets for improved fructofuranosidase production in A. niger *based on the target validity coefficient. This coefficient was obtained from correlation of flux through metabolic reactions with fructofuranosidase production flux within the calculated elementary modes. A positive value (green colour) relates to a reaction, which positively correlates with the production, whereas negative correlation is indicated by a negative value (red colour). Black colour indicates statistically insignificant values. The investigated biological scenarios comprise growth- (+) and non-growth-associated production (-) on glucose (Glu), glycerol (Gly), xylose (Xyl) and oleate (Ole) as carbon source.*

Hereby, the relevance of most targets depended on the metabolic state of the cell and also on the carbon source. Objective flux correlation analysis provided a detailed insight into the metabolic networks of industrially relevant prokaryotic and eukaryotic microorganisms. It was shown that capacity, pathway usage and relevant genetic targets for optimal production partly depend on the network structure and the metabolic state of the cell which should be considered in future metabolic engineering strategies. The presented strategy can be generally used to identify priority sorted amplification and deletion targets for metabolic engineering purposes under various conditions and thus displays a useful strategy to be incorporated into efficient strain and bioprocess optimization. Currently, the novel *in silico* strategy is evaluated and validated by constructing and evaluation a first set of designer mutants predicted together with external partners from fungal genetics.

^{13}C metabolic flux analysis of *Aspergillus niger* [*Driouch et al., 2012a*]

The method of choice to quantify pathway fluxes today is ^{13}C fluxomics, integrating isotope studies with mass spectrometric labelling analysis and isotopomer modelling for flux estimation and statistics [*Wittmann, 2007*]. This appeared central for the given project to unravel the underlying properties of the metabolism of *A. niger*. The concept of metabolic flux ratio analysis, previously applied to yeasts and other fungal strains [*Sauer et al., 2006*] was successfully applied and adapted to study the compartmented network of *A. niger*, including careful revision of the network topology and cellular composition. Subsequently, it was applied to analyze different production strains for the recombinant production of the glycosylated enzyme fructofuranosidase (**Fig. 3**).

Linking *in-silico* and *in-vivo* fluxes [*Driouch et al., 2012a*]

A. niger was analyzed by ^{13}C metabolic flux analysis of different production strains for the recombinant production of the glycosylated enzyme fructofuranosidase, a biocatalyst of commercial interest for the synthesis of pre-biotic sugars. In batch culture on a minimal glucose medium, the recombinant strain *A. niger* SKAn1015, expressing the fructofuranosidase encoding *suc1* gene secreted 45 U/mL of the target enzyme, whereas the parent wild type SKANip8 did not exhibit production. It could be shown that the production of the recombinant enzyme induced a significant change of *in vivo* fluxes in central carbon metabolism, as assessed by ^{13}C metabolic flux ratio analysis (**Fig. 3**). For the first time, this provided a flux insight into fructofuranosidase producing *A. niger*. Most notably, the flux redistribution enabled an elevated supply of NADPH via activation of the cytosolic pentose phosphate pathway (PPP) and mitochondrial malic enzyme, whereas the flux through energy generating TCA cycle was reduced. In addition, the overall possible flux space of fructofuranosidase producing *A. niger* was investigated *in silico* by elementary flux mode analysis. This provided theoretical flux distributions for multiple scenarios with differing production capacities. Subsequently, the measured flux changes linked to improved production performance were projected into the *in silico* flux space in close interaction with sub-project B4. This provided a quantitative evaluation of the achieved optimization and a priority ranked target list for further strain engineering. Interestingly, the metabolism was shifted largely towards the optimum flux pattern by sole expression of the

recombinant enzyme which seems an inherent attractive property of *A. niger.* Selected fluxes, however, changed contrary to the predicted optimum and thus revealed novel targets – including reactions linked to NADPH metabolism and gluconate formation. This work displays one of the pioneering studies to integrate *in-silico* pathway simulation with the *in-vivo* state of real producers, an approach which appears very useful and straightforward in future strain engineering.

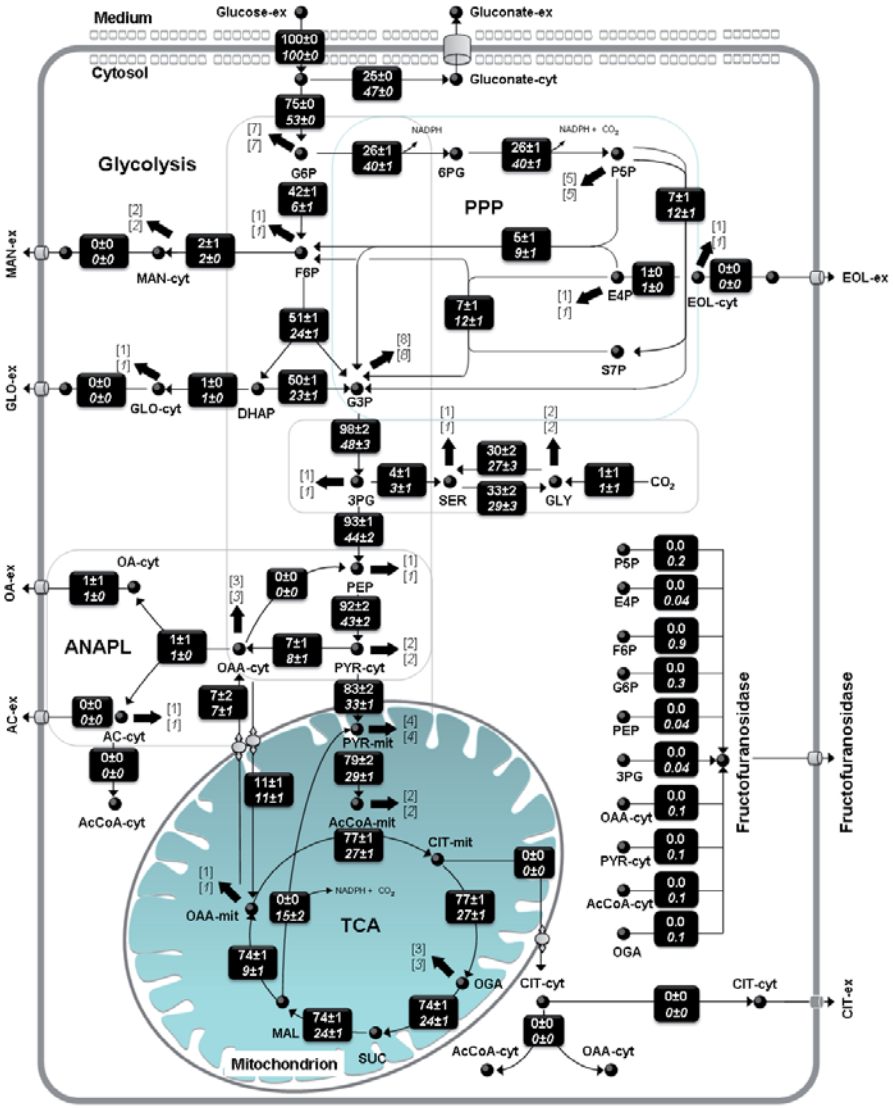

Fig. 3: Metabolic flux distribution of A. niger *SKANip8 (wild-type, top) and SKAn1015 (recombinant fructofuranosidase producer, bottom) on glucose minimal medium. All fluxes are normalized to the specific glucose uptake rate, which was 1.13 mmol/g/h for the wild type and 1.17 mmol/g/h for the producer, respectively.*

Morphology Engineering of *Aspergillus niger* [*Driouch et al., 2010a*]

One of the outstanding and, unfortunately often problematic, characteristics of the filamentous fungus *A. niger* is its complex morphology in submerged culture. Hereby, the productivity in biotechnological processes is often correlated with the morphological form [*Kaup et al., 2007*]. The high importance of the correct morphology for good performance

has stimulated attempts to manipulate the growth characteristics of filamentous fungi, which, however, require conditions incompatible with effective production such as extreme pH value causing enzyme instability or high stirring rate resulting in increased energy costs. To overcome these limitations, supplementation with microparticles was used – in collaboration with B3 – as novel approach to control the morphological development of *A. niger*. With careful variation of size and concentration of talc micro particles added, a number of distinct morphological forms including pellets of different size, free dispersed mycelium and short hyphae fragments could be reproducibly created (**Fig. 4**).

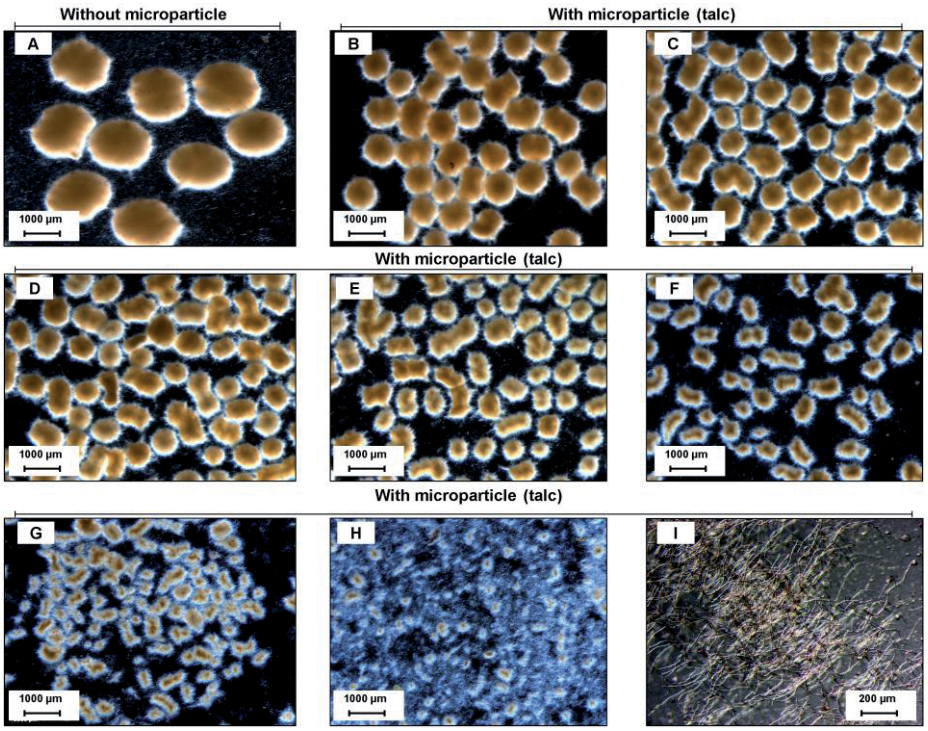

Fig. 4: Morphology engineering of A. niger *SKAn1015 by microparticle supplementation in submerged culture. Hydrous magnesium silicate (6 µm particle size) was added at varied concentration: control without talc (A), 0.01 g/L (B), 0.1 g/L (C), 0.4 g/L (D), 0.6 g/L (E), 1.0 g/L (F), 2.0 g/L (G), 3.0 g/L (H), 5.0 g/L (I), Image analysis was performed by light microscopy after 72 h of cultivation.*

Aluminum oxide particles similarly affected morphology, showing that this effect is largely independent of the chemical particle composition. Exemplified for different recombinant *A. niger* strains enzyme production could be strongly enhanced by the addition of microparticles. Linked to the formation of freely dispersed mycelium, titers for glucoamylase expressed as intracellular enzyme (88 U/mL) and fructofuranosidase secreted into the supernatant (77 U/mL), were up to four fold higher in shake flasks. Moreover, accumulation of the undesired by-product oxalate was suppressed by up to 90 %. Using co-production of glucoamylase with green fluorescent protein in specifically designed reporter strains, provided by sub-project A1, enzyme production was localized

within cellular aggregates of *A. niger*. For pelleted growth, protein production was maximal only within a thin layer at the pellet surface and markedly decreased in the pellet interior, whereas the interaction with the microparticles created a highly active biocatalyst with the dominant fraction of cells contributing to production. Overall, the use of microparticles allows a targeted and rather precise engineering of cellular morphology which creates novel possibilities for future design and optimization of bioprocesses with *A. niger* and also other fungi.

Creation of fungal core-shell pellets by titanate micro particle [*Driouch et al., 2012b*]

In addition, microparticles allowed the design of superior bio-pellet morphologies. The novel approach recruited the intended addition of titanate micro particles ($TiSiO_4$, 8 µm) to the growth medium. As tested for two recombinant strains producing fructofuranosidase and glucoamylase, the enzyme titer by the titanate-enhanced cultures in shake flasks was increased 3.7 fold to 150 U/mL (for fructofuranosidase) and 9.5 fold to 190 U/mL (for glucoamylase) as compared to the control. This could be successfully utilized for improved enzyme production in stirred tank reactors. Stimulated by the particles, the achieved final glucoamylase activity of 1,080 U/mL (fed-batch) and 320 U/mL (batch) was sevenfold higher as compared to the conventional processes. The major reason for the enhanced production was the close association between the titanate particles and the fungal cells. Already below 2.5 g/L the micro-material was found inside the pellets, including single particles embedded as 50 to 150 µm particle aggregates in the center resulting in core shell pellets. With increasing titanate levels the pellet size decreased from 1700 µm (control) to 300 µm. Fluorescence based resolution of GFP production revealed that the large pellets of the control were only active in a 200 µm surface layer. This matches with the critical penetration depth for nutrients and oxygen typically observed for fungal pellets. The biomass within the titanate derived fungal pellets, however, was completely active. This was due a reduced thickness of the biomass layer via smaller pellets as well as the core shell structure. Moreover, also the created loose inner pellet structure enabled a higher mass transfer and penetration depths for up to 500 µm. The creation of core-shell pellets has not been achieved previously by the addition of micro particles, e.g. made of talc or alumina. Due to this, the present work opens further possibilities to use micro particles for tailor-made morphology design of filamentous fungi, especially for pellet based processes which have a long and strong industrial relevance for industrial production.

Microparticle-enhanced production of fructofuranosidase [*Driouch et al., 2010b, Wucherpfennig et al., 2012*]

A comprehensive approach of bioprocess design at various levels was next used to optimize microbial production of extracellular fructofuranosidase, important as biocatalyst to derive fructo-oligosaccharides with broad application in food or pharmaceutical industry.

In a first screening towards an optimized medium, glucose, nitrate, Fe^{2+} and Mn^{2+} were identified as beneficial for production. A minimal medium with optimized concentration of these key nutrients, obtained by central composite design experiments and quadratic modeling, provided a threefold increased fructofuranosidase activity in the culture supernatant (400 U/mL) as compared to the original medium. Utilizing the optimized medium, the process was then transferred into a fed-batch operated bioreactor. Hereby, the intended addition of talc microparticles allowed engineering the morphology of *A. niger* into a highly active mycelial form, which strongly boosted production. Fructofuranosidase production was highly specific as confirmed by SDS-PAGE analysis. The secreted enzyme activity of 2,800 U/mL, corresponding to about 3 g/L of fructofuranosidase, achieved by the microparticle enhanced fed-batch process, is ten-fold higher than that of any other process reported so far, so that the presented bioprocess strategy appears as a milestone towards future industrial fructofuranosidase production (**Fig. 5**).

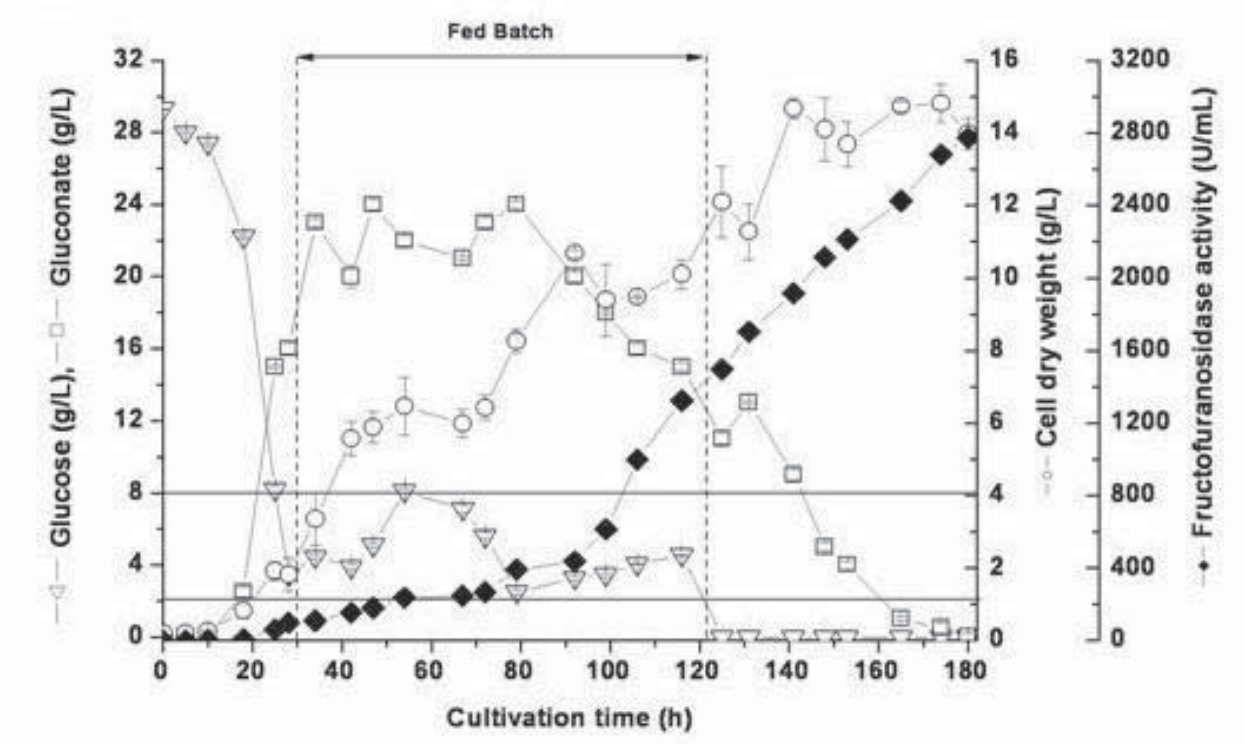

Fig. 5: Fructofuranosidase production by A. niger *SKAn1015 in fed-batch culture on the optimized medium with addition of talc microparticles (6 µm, 5 g/L) using 3 L stirred tank bioreactors.*

Across the value-chain – application of the enzyme for high-efficiency biosynthesis of pre-biotic neo-sugars [*Driouch et al., 2010c*]

It was now relevant to evaluate the full value of the developed process by application of the produced enzyme to a biotransformation of substantial commercial interest. For this purpose we now carried out additional experiments coupling the steps of (i) production of fructofuranosidase by *A. niger* using the described microparticle based process, (ii) enzyme preparation from the culture broth and (iii) its application to the biosynthesis of

high-value short-chain fructo-oligosaccharides of the inulin type, pre-biotics with substantial commercial interest. Fructofuranosidase was produced in submerged culture by a micro particles enhanced batch-process using the recombinant strain *A. niger* SKAn1015 as described above. Operated in normal batch mode, an enzyme level of 900 U/mL was obtained after 100 h. Culture supernatant, clarified from cells and microparticles by filtration, was mixed with sucrose solution (pH 5.4, 50 mM phosphate buffer) to an initial concentration of 500 g/L sucrose and subsequently incubated under slight rotation at 50 °C. Within only 10 minutes, sucrose was almost completely converted into the desired products, indicated by the high level of about 450 g/L fructo-oligosaccharides. As assessed together with sub-project A7, the formed products comprised the high value compounds 1-kestose (55%), 1-nystose (38%), and 1F β-fructofuranosyl-nystose (7%), respectively. By extension of the incubation time, the product spectrum could be successfully shifted towards the higher weight fructo-oligosaccharides, i. e. 1F β-fructofuranosyl-nystose. Overall, the results demonstrate that the novel approach is an effective strategy for biotechnological enzyme production by filamentous fungi. We did not observe any negative interference with subsequent application of the enzyme produced for bio-catalysis. In fact, with minimal pre-treatment the enzyme obtained allowed highly efficient bioconversion towards pre-biotics of commercial interest.

Metabolic network analysis of *Bacillus megaterium* for different bioprocess environments

In addition, also the metabolic network of *B. megaterium*, the second important microbial host used for recombinant production within the SFB, was investigated. *B. megaterium* was analyzed on the fluxome level. For this purpose, a metabolic model (in cooperation with sub-project B4 (Jahn/Nörtemann/Jänsch)) was created that reflected all relevant pathways in carbon core metabolism. This model was then implemented into the flux software OpenFlux [*Queek et al., 2009*]. In addition, the cellular composition of the bacterium was analyzed. This approach was then applied to characterize the metabolism of *B. megaterium* with regard to the influence of process parameters such as carbon source, salinity and temperature, providing interesting insights into growth and production performance. Beyond previous approaches, the work - carried out in cooperation with sub-project B8 - focused particularly on process relevant conditions of large-scale bioprocesses, reflecting the typical scenario used today in industrial protein production. These are inherently linked to incomplete mixing and gradients for oxygen and other nutrients across the reactor. Shortly, the impact of such gradients, expected for large production scale, was investigated for producing green fluorescent protein (GFP). Specifically designed scale-down studies, mimicking the intermittent and continuous nutrient supply of large and small scale processes, were carried out for this purpose. The recombinant strain revealed a 40 % reduced GFP yield for the large scale conditions. In line with extended carbon loss via formation of acetate and carbon dioxide, this indicated obvious limitations in the underlying metabolism of *B. megaterium* under the large scale

conditions. Quantitative analysis of intracellular amino acids via validated fast filtration protocols revealed that their level strongly differed between the two scenarios. During cultivation in large-scale set-up, the availability of most amino acids, serving as key building blocks of the recombinant protein, was substantially reduced. This was most pronounced for tryptophan, aspartate, histidine, glutamine and lysine. In contrast alanine was increased, probably related to a bottleneck at the level of pyruvate which also triggered acetate overflow metabolism. The precursor quantifications could then be exploited to verify the presumed bottlenecks and improve recombinant protein production under large scale conditions. Addition of only 5 mM tryptophan, aspartate, histidine, glutamine and lysine to the feed solution increased the GFP yield by 100 %, as shown in cooperation with B8. This rational concept of driving the lab scale productivity of recombinant microorganisms under suboptimal feeding conditions emulating large scale can easily be extended to other processes and production hosts.

3.2.1.3 References to other works and collaborations in the SFB

The research in this sub-project strongly interacted with other sub-projects of the SFB, as visualized by a number of joint publications (see 3.2.3).

Intense cooperation was carried out with sub-projects A1 (Jahn/Dersch) on the construction and analysis of GFP reporter strains and enzyme over-producing strains of *Aspergillus niger* [*Driouch et al., 2010b, c*], with A7 (Heinz/Seibel) on the application of fructofuranosidase as biocatalyst for the biosynthesis of neo-sugars from sucrose [*Driouch et al., 2010c*], with B3 (Krull/Hempel) on analysis and engineering of fungal morphology [*Driouch et al., 2012b; Wucherpfennig et al., 2012*], with B4 (Jahn/Nörtemann/Jänsch) on metabolic network simulation of *A. niger* and model-based medium design [*Melzer et al., 2009; Driouch et al., 2012a*] and with B8 (Franco-Lara) on metabolomics based optimization of large scale protein production in *B. megaterium* [*Korneli et al., 2012*].

The interdisciplinary expertise generated in the different sub-projects appeared highly complementary and crucial to integrate e.g. different omics technologies for systems-level strain and process design, linking experiments and modeling in an iterative way towards improved understanding and finally achieve a substantial, knowledge-based improvement of production performance by *A. niger* and *B. megaterium.*

3.2.1.4 Comparison with research outside the SFB

The results obtained here, display important contributions to our understanding of the metabolism of *A. niger* and *B. megaterium*. To date, most studies towards optimized production of recombinant proteins focus on the terminal steps of protein translation, folding and secretion – all quite essential steps in the entire production chain, but at the same time relying on efficient supply of building blocks, energy and cofactors driving metabolism and protein synthesis (**Fig. 7**). In this light the results from this sub-project,

focusing on the upstream carbon core metabolism, highlighted in green and orange in the Figure, address so far disregarded targets. Thus, they nicely complement with previously reported approaches, and more important, provide a new concept of value, also for other recombinant production hosts and target proteins. The same holds for the developed approach for morphology engineering by micro particles, a novel concept of relevance also for a range of other filamentous microorganisms, broadly used in industrial biotechnology.

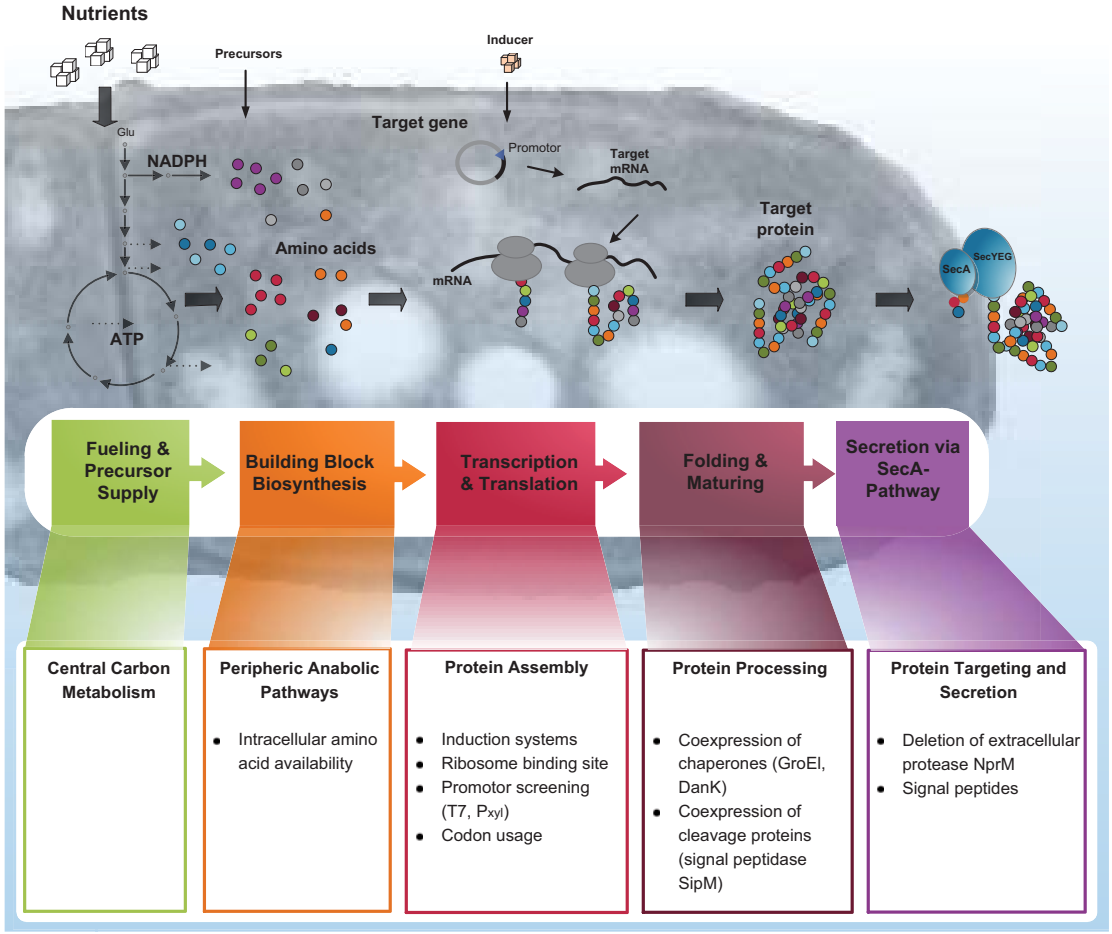

Fig. 7: Systems metabolic engineering of B. megaterium *for recombinant protein production. The systems wide concept combines and integrates cellular engineering along the entire metabolic pipeline, far beyond transcription and translation of the target protein.*

3.2.1.5 Literature

Deckwer, W.D.; Jahn, D.; Zeng, A.P.; Hempel, D.C. (2006) Systembiologische Ansätze zur Prozessentwicklung. *Chem. Ing. Techn.* 78, 193-208

Krömer, J.O.; Wittmann, C.; Schröder, H.; Heinzle, E. (2006) Metabolic pathway analysis for rational design of L-methionine production by *Escherichia coli* and *Corynebacterium glutamicum*. *Metabol. Eng.* 8, 353-363

Quek, L.E.; Wittmann, C.; Nielsen, L.K.; Krömer, J.O. (2009) OpenFLUX: Efficient modeling software for ^{13}C-based metabolic flux analysis. *Microb. Cell Fact.* 8, 25

Sauer, U. (2006) Metabolic networks in motion: ^{13}C-based flux analysis. Mol. Syst. Biol. 2, 62

Stephanopoulos, G.; Aristidou, A.A.; Nielsen, J. (1998) Metabolic Engineering - Principles and Methodologies. San Diego, Academic Press.

3.2.2 Project relevant own publications

a) Works that have appeared in publications of a scientific quality assurance at the time of application or final adoption, and book publications

Driouch, H.; Sommer, B.; Wittmann, C. (2010a) Morphology engineering of *Aspergillus niger* for improved enzyme production. *Biotechnol. Bioeng.* 105, 1058-1068, awarded as spot light paper

Driouch, H.; Roth, A.; Dersch, P.; Wittmann, C. (2010b) Optimized bioprocess for production of fructofuranosidase by recombinant *Aspergillus niger*. *Appl. Microbiol. Biotechnol.* 87, 2011-2024

Driouch, H.; Roth, A.; Dersch, P.; Wittmann, C. (2010c) Filamentous fungi in good shape: Microparticles for tailor-made fungal morphology and enhanced enzyme production. *Bioeng. Bugs* 2, 1-5

Driouch, H.; Melzer, G.; Wittmann, C. (2012a) Integration of in vivo and in silico metabolic fluxes for improvement of recombinant protein production. *Metab. Eng.*, in press

Driouch, H.; Hänsch, R.; Wucherpfennig, T.; Krull, R.; Wittmann, C. (2012b) Improved enzyme production by superior bio-pellets of *Aspergillus niger* - Targeted morphology engineering using titanate micro particles. *Biotechnol. Bioeng.* 109, 462-471

Korneli, C.; Bolten, C.J.; Godard, T.; Franco-Lara, E.; Wittmann, C. (2012) Debottlenecking recombinant protein production in *Bacillus megaterium* under large scale conditions - targeted precursor feeding designed from metabolomics. *Biotechnol. Bioeng.*, 109, 1538-1550, awarded as spot light paper

Melzer, G.; Eslahpazir, M.; Franco-Lara, E.; Wittmann, C. (2009) Flux Design: In silico design of cell factories based on correlation of pathway fluxes to desired properties. *BMC Syst. Biol*. 3, 120, awarded as highly accessed article

Wucherpfennig, T.; Lakowitz, A.; Driouch, H.; Krull, R.; Wittmann, C. (2012) Customization of *Aspergillus niger* morphology through addition of talc micro particles. *J. Vis. Exp.*, in press

3.3 Looking back on the promotion

The project has been funded since January 2009 in the SFB 578. It was completed on June 2012 with the end of the program.

3.3.1 Personnel in the project

	Name, academic degree, position	narrower subject of the employee	Institute of University	Participation in hours per week	Category
Basic staff					
Academic staff	1. C. Wittmann Prof. Dr.	Biochemical Engineering	Institute of Biochemical Engineering	10	Professor
Non academic staff	2. Y. Göcke, BTA	Biotechnology	Institute of Biochemical Engineering	4	Technical staff
	3. D. Rasch, CTA	Biochemical Engineering	Institute of Biochemical Engineering	2	Technical staff
	4. R. Jonas Dipl.-Ing. (FH)	Biotechnology	Institute of Biochemical Engineering	2	Technical staff
Supportive staff					
Research associate (incl. auxiliary power)	5. H. Driouch Dipl.-Biotechnol.	Biotechnology	Institute of Biochemical Engineering	40	PhD student
	6. Dr.-Ing. T. Fürch Dipl.-Biotechnol.	Biotechnology	Institute of Biochemical Engineering	40	Postdoc
	7. T. Godard Dipl.-Ing.	Biochemical Engineering	Institute of Biochemical Engineering	40	PhD student
Non academic staff	8. N. N., Student assistant	Biochemical Engineering, Biotechnology		10	Student

Responsibilities of employees (basic staff)

Position 1 - 4:

The principal investigator guided, designed and supervised the project. The technicians, given in positions 2-4 supported the academic staff in bioprocess development, cultivation and bio-analytics, construction of experimental set-up and microscopy.

Responsibilities of employees (supportive staff)

Position 5: Dipl.-Biotechnol. Habib Driouch

Mr. Dipl.-Biotechnol. Driouch was responsible for the metabolic network analysis of *A. niger.* The included a broad range of experimental and computational methods such as model-based medium design, bio-process-development in batch and fed-batch mode. In addition he developed the novel concept of fine-tuned morphology engineering using micro-particles and its application to superior enzyme production as well as detailed evaluation of the strategy by GFP-reporter strains and confocal laser scanning microscopy. In addition he performed metabolic flux analysis by ^{13}C isotope studies and isotopomer modeling and integrated the obtained data with *in silico* fluxes for strain prediction. He also supervised student assistants.

Position 6: Dr.-Ing. Tobias Fürch

Dr. Fürch supported the project by expertise on metabolic modeling and simulation which provided an important starting point to establish metabolic network analysis.

Position 7: Dipl.-Ing. Tibault Godard

Mr. Godard established ^{13}C metabolic flux analysis for *B. megaterium*. This included the creation of a metabolic model of the carbon core metabolism, its implementation into the flux software OpenFlux and experimental validation and refinement of tracer cultivations and labeling analysis. Moreover, he contributed significantly to analysis of the cellular composition, a requirement to access anabolic fluxes in this bacterium. Using this set-up, he studied the impact of important process parameters such as temperature and osmotic stress on the flux level. In addition, he contributed to metabolomics analysis of *B. megaterium*, producing GFP as model protein.

Position 8: Stud. assistant

Student assistants supported the extensive experimental work in the implementation and evaluation of fungal cultivations as well as in the routine of biotechnological and systems biology studies. Through the close interaction an intensive training of the students in up-front research could be obtained.

3.0 Project area C: Process technique

Project-No.	Topic	Disciplines and field of work	Project manager, institution
C2	Continuous chromatographic separation of ternary and pseudo-ternary mixtures	Chemical and thermal process engineering, Biochemical engineering	A. Seidel-Morgenstern, Institute for Process Engineering, Chair for Chemical Process Engineering, Otto-von-Guericke-University Magdeburg
C6	Nanoanalytics for protein production processes	Biochemical analysis, Transport processes, Morphology	M. Schilling and F. Ludwig, Institut für Elektrische Messtechnik und Grundlagen der Elektrotechnik, TU BS
C7	Protein purification with functionalized magnetic nanoparticles	Nanoparticle technology Protein purification, Nanoanalytics	G. Garnweitner, Institute for Particle Technology, TU BS / M. Schilling, Institut für Elektrische Messtechnik und Grundlagen der Elektrotechnik, TU BS

3.1 General information on the completed project C2

3.1.1 Topic

Continuous chromatographic separation of ternary and pseudo-ternary mixtures

3.1.2 Disciplines and field of work

Chemical and Thermal Process Engineering, Biochemical Engineering

3.1.3 Project manager

Prof. Dr.-Ing. Andreas Seidel-Morgenstern
(b.: 9.8.1956)
Institute for Process Engineering
Chair for Chemical Process Engineering, Otto-von-Guericke-University Magdeburg
Postfach 4120, 39016 Magdeburg
Tel: 0391 / 67-18643, Fax: 0391 / 67-12028
E-Mail: anseidel@vst.uni-magdeburg.de

3.2 Development of the subproject

3.2.1 Report

3.2.1.1 Current knowledge at the last application and initial question

The subproject C2 was focused on the development of novel processes that combine the attractive features of gradient elution chromatography and the continuous simulated moving bed process. These innovative and more efficient processes can isolate continuously a target component of an N-component mixture with high purity and yield. Several model systems and complex biological mixtures produced in the frame of the SFB578 were included in our investigations during the whole funding period.

After a short summary of the main results achieved in the first funding periods, results will be described related to the development of a process suitable for continuous chromatographic separation of ternary and pseudo-ternary mixtures. To achieve such challenging separations, modifications of the classical simulated moving bed technology were theoretically investigated and experimentally validated.

The knowledge regarding preparative chromatography available prior to our investigations was summarized in the three proposals submitted. Important references are summarized under 3.2.1.5. Before starting the third period (2008 - 2012) several new multi-column configurations were suggested to tackle the complexity of complex mixtures originating from fermentation processes. Preliminary work on continuous separation of ternary mixtures has been explored using simplified models for a variety of connection options. Concepts investigated are based on coupling of two SMB units [*Chiang, 1998; Hritzko et al., 2002*], on introducing side streams [*Best and Arlt, 2000*], on using gradients [*Strohlein et al., 2006, Krättli et al. 2011*], on increasing the numbers of zones [*Nicolaos et al., 2001a and 2001b; Abel et al., 2004; Wankat, 2001*] or on exploiting intermittent regimes [*Jermann*

et al. 2012]. However, not much systematic work was available. More recently, *Carta and Jungbauer* (*2010*) gave an overview about the status of this field.

3.2.1.2 Results and applied methods

Below will be summarized essential results achieve in the C2-project. At first a short summary will be given about essential findings of the first two periods, which served as the basis for the currently ending third phase.

In the first two funding periods (2/2001 to 1/2004 and 2/2004 to 1/2008) fundamental studies on the chromatographic separation of model compounds and real systems were performed (Bone growth factor (BMP-2), oligosaccharides and monosaccharides). In this particular case, the use of gradients in batch (single column) and continuous (SMB) separations were quantitatively described and evaluated [*Antos and Seidel-Morgenstern, 2002*]. The essential basis for this is the knowledge of the corresponding equilibrium compositions of the considered analytes in the mobile and stationary phases. The influence of gradients on the equilibrium model for two component systems was determined (cyclic ketones and lysozyme). The separation processes could be described with a simple pseudo-homogeneous dispersion model which could be used for the optimization of operating conditions. The prediction capabilities of the model findings were applied for the design of the production of high purity dimers of the bone growth factor BMP-2. In cooperation with the former subproject B1 (Rinas) the influence of the salt content on the distribution equilibrium for the monomer and the dimer of the BMP-2 was examined and quantified. In this case, Heparin acts as an affinity ligand for BMP-2. The samples provided by subproject B1 were in a concentration range in which the adsorption isotherm could be considered to be linear. In **Fig. 1**, the relationship between the adsorption constant $K_{H,i}$, and the salt concentration c_{Salz} is depicted. As it can be seen, the binding strength of the dimer increases much faster than that of the monomer when the salt content is decreasing [*Gueorguieva et al., 2006*].

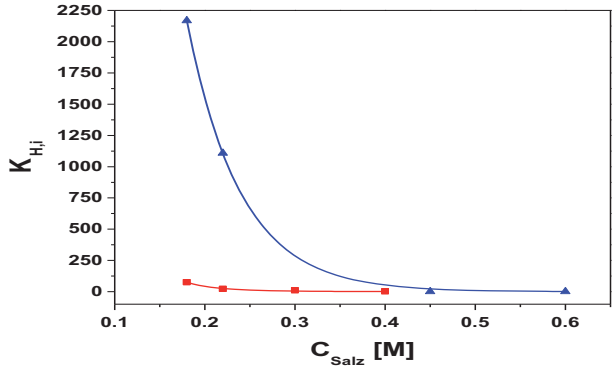

Fig. 1: Adsorption constants $K_{H,i}$ for the monomer (red squares) and dimer (blue triangles) of the BMP-2 as a function of salt concentration [Gueorguieva et al., 2006]. Stationary phase: Heparin Sepharose HiTrap.

With these adsorption isotherms and the parameters of the separation columns and apparatus, a suitable SMB process was designed. The selection of suitable operating parameters and the potential success of the purification were evaluated before the execution of the experimental work with the help of simulation tools. To ensure high purity

even with changing batches, the open-loop method was chosen to avoid cross contamination. At these conditions the regeneration zone was not necessary for the liquid phase and the number of zones was reduced to three. An additional and novel pre-equilibration zone was required for this separation task. This kind of solution is particularly suitable to avoid and reduce operational problems when using salt gradients. In **Fig. 2a** the SMB unit is shown schematically. The focus of systematic experiments was on the experimental implementation of a continuous separation of monomers and dimers of the bone growth factor BMP-2 using salt gradients.

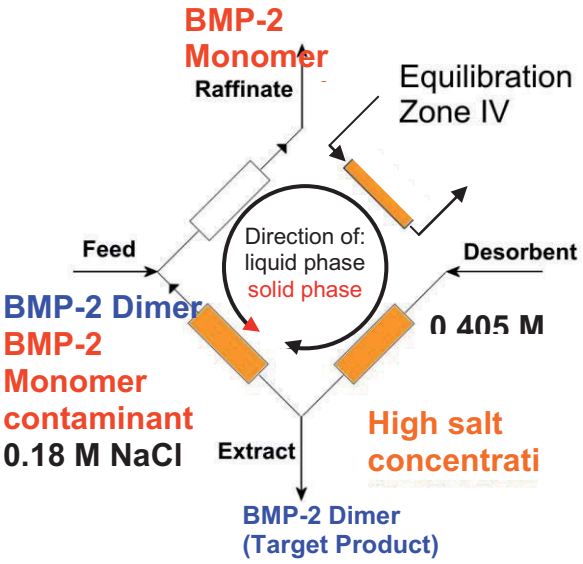

Fig. 2a: Schematic representation of a 3-zone open-loop SMB gradient for the purification of BMP-2 dimer. Stationary phase: Heparin Sepharose HiTrap [*Gueorguieva et al., 2007*].

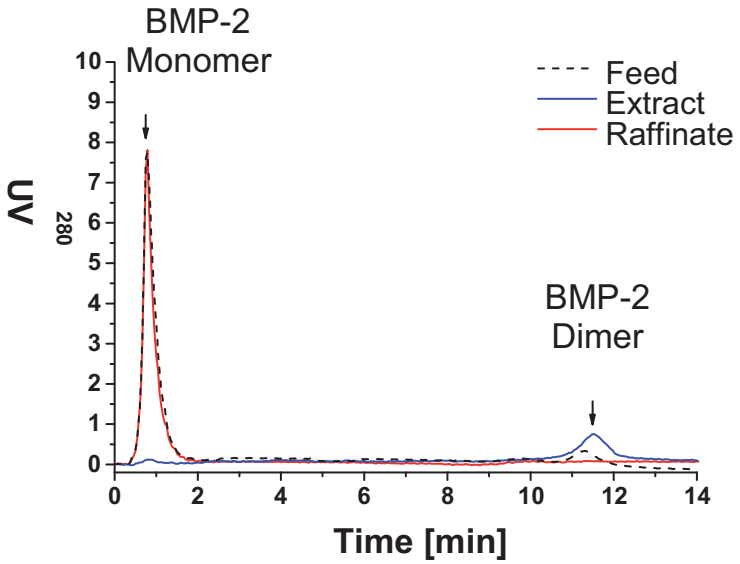

Fig. 2b: Chromatographic analysis of the extract and raffinate of the gradient SMB chromatography of BMP-2 in a single column. Stationary phase: Heparin-Sepharose HiTrap.

Subsequently the focus of activities was transferred to the purification of monoclonal antibodies produced by subproject A6 (Dübel/Hust). The thermodynamics of selected separation media (adsorption isotherm parameters) and the model-based selection and implementation of appropriate operational modes (batch, continuous, isocratic, gradient) were investigated. Some alternatives were found to the established standard procedures (affinity chromatography with protein A or protein G). As a model protein the bovine immunoglobulin G (IgG) antibody was selected. The model protein was purified in the presence of lysozyme and bovine serum albumin (BSA). Additionally, dextran coated polystyrene beads were used, because these beads represent a suitable model substance for high molecular weight impurities. These components were combined in three different model systems:

Model system 1: IgG and dextran coated polystyrene beads (200 nm)

Model system 2: IgG and lysozyme

Model system 3: IgG, lysozyme and BSA

Heparin Sepharose, which is known to be a weak cation exchanger, was identified as a very suitable ion exchange material. This stationary phase was used e.g. in model system 2. The adsorption behavior of both substances was described by a linear isotherm with sufficient accuracy in a concentration range up to 1 g / L. In these experiments bovine serum albumin (BSA) was investigated as the third component in model system 3 (**Fig. 3**).

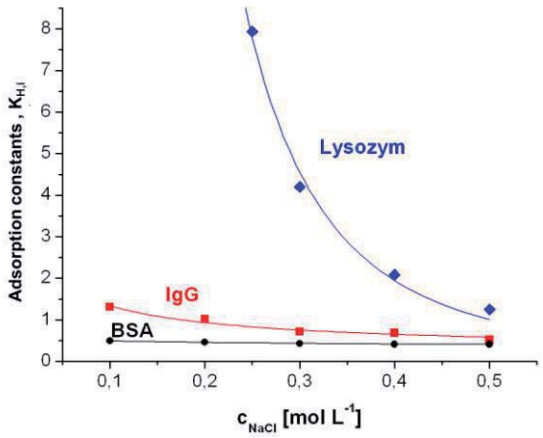

Fig. 3: Adsorption constants $K_{H,i}$ for IgG (black squares), lysozyme (blue diamonds) and BSA (red circle) from pulse experiments as a function of salt concentration. Stationary phase: Heparin-Sepharose HiTrap.

It was found that lysozyme exhibited the highest binding strength and was most affected by the salt concentration. On the other hand, IgG was adsorbed significantly less and was much less affected by the salt concentration. BSA does not bind to the heparin phase in the considered range of salt concentrations. Since this model system can be separated using isocratic or gradient conditions, both operating modes were investigated experimentally.

Successful isocratic separation was performed with 4 zones, and in an open-loop mode. Complete separation between IgG and lysozyme was achieved [*Keßler et al., 2007*]. Analytical chromatograms corresponding to collected samples of the two outlet streams (extract and raffinate) and of the mixture to be separated (feed) in the cyclic-steady-state as well as the operating parameters are shown in **Fig. 4** and **Tab. 1**.

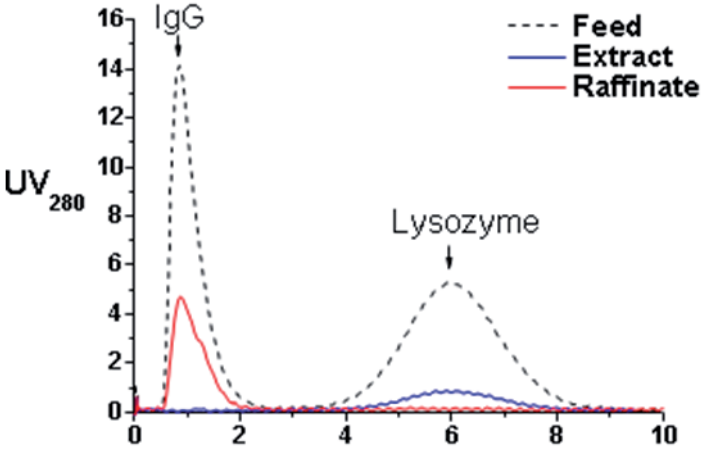

Fig. 4: Chromatographic analysis of the extract and raffinate of the isocratic SMB chromatography of the model system 2.

Tab.1: Summary of the operating parameters for the isocratic SMB separation of model system 2.

Feed concentration	0.25 gL^{-1}
Salt concentration	0.25 M NaCl
Buffer	20 mM NaH_2PO_4 pH 7.0
K_{IgG}	0.25
$K_{Lysozym}$	5.2
Switching time	8.09 min
Feed	0.15 mL min^{-1}
Raffinate	0.31 mL min^{-1}
Extract	0.98 mL min^{-1}
Column volume	2/2/2/2 = 8 mL

Since the antibody exhibited in this system the highest affinity for the stationary phase, it was possible to purify and concentrate the antibody with the aid of a suitable specifically designed gradient SMB process in a single step (**Fig. 5**).

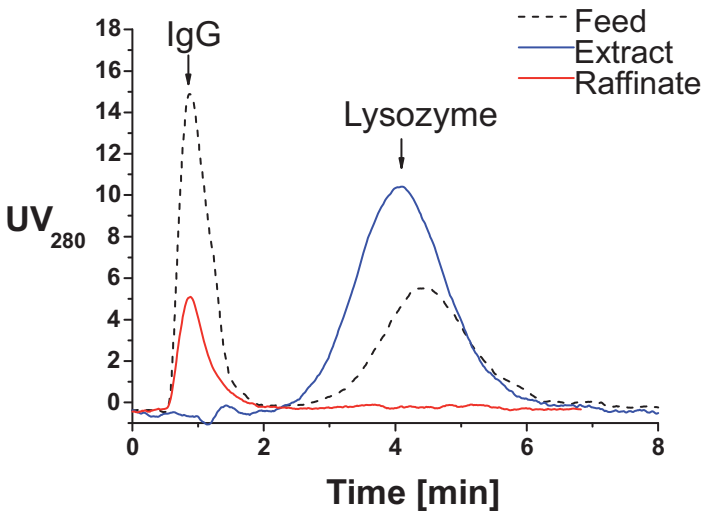

Fig. 5: Chromatographic analysis of the extract and raffinate of the gradient SMB chromatography of the model system 2 Stationary phase: Heparin-Sepharose HiTrap.

Tab.2: Summary of operating parameters for the gradient SMB separation of model system 2.

Feed concentration	0.5 g L^{-1}
Gradient	Zone I & II: 0.40 M NaCl Zone III: 0.25 M NaCl
Buffer	20 mM NaH_2PO_4 pH 7.0
K_{IgG}	Zone I & II : 1.5 Zone III : 2.37
$K_{Lysozym}$	Zone I & II : 2.71 Zone III : 6.19
Switching time	2.2 min
Feed	1 mL min^{-1}
Raffinate	1.7 mL min^{-1}
Extract	0.56 mL min^{-1}
Column volume	2/2/2 = 6 mL

Since the antibody eluted last on any of the observed ion exchange phases, hydrophobic interaction chromatography (HIC) was also investigated systematically and found to be applicable. This is an interesting alternative to ion exchange chromatography, as the strength of the interaction can be modulated in both techniques by addition of a salt.
In addition to the experiamental work devoted to apply continuous gradient chromatography, also theoretical and conceptual studies were performed for the optimization of existing and developing new chromatographic modes. Here in particular options for the the continuous separation of ternary mixtures using advanced multi-column concepts were studied [*Keßler and Seidel-Morgenstern, 2006*]. Exploiting partly results achieved in the first two project periods two patents could be filed successfully [*Kessler and Seidel-Morgenstern, 2008 and 2010; Schramm et al., 2006 and 2009*].

In the third currently ending funding period (2/2008 to 1/2012) initially conceptual work was carried out devoted to identify the best option to perform improved separation of ternary or quasi-ternary mixtures. In a quite general case, the target substance can be seen as the intermediately eluting component (target component T=B). It is possible to combine all substances eluting before and after the target component into two groups A and C. Fraction A comprises the components 1 to T-1 and fraction C the components T +1 to N in a N-component mixture. In this way any complex multi-component system can be reduced to a ternary separation problem (**Fig. 6**). In the course of the project a concept was

developed to describe the migration behavior of the relevant components 1, T-1, T, T+1 and N based on apparent adsorption constants.

The formulation proposed in Fig. 6 allows handling a variety of real separation tasks with the tools developed for ternary systems. New SMB operating modes were studied such as SMB under isocratic conditions using Size Exclusion Chromatography (SEC) and the fractionation and feedback SMB (FF-SMB) [*Keßler and Seidel-Morgenstern, 2008*; *Li et al. 2010a and 2010b*] . In addition, two classical closed-loop SMBs were interconnected and tested for the experimental validation of the separation of a ternary mixture. Finally, the start-up and shut-down periods of the processes were optimized [*Li et al. 2011*].

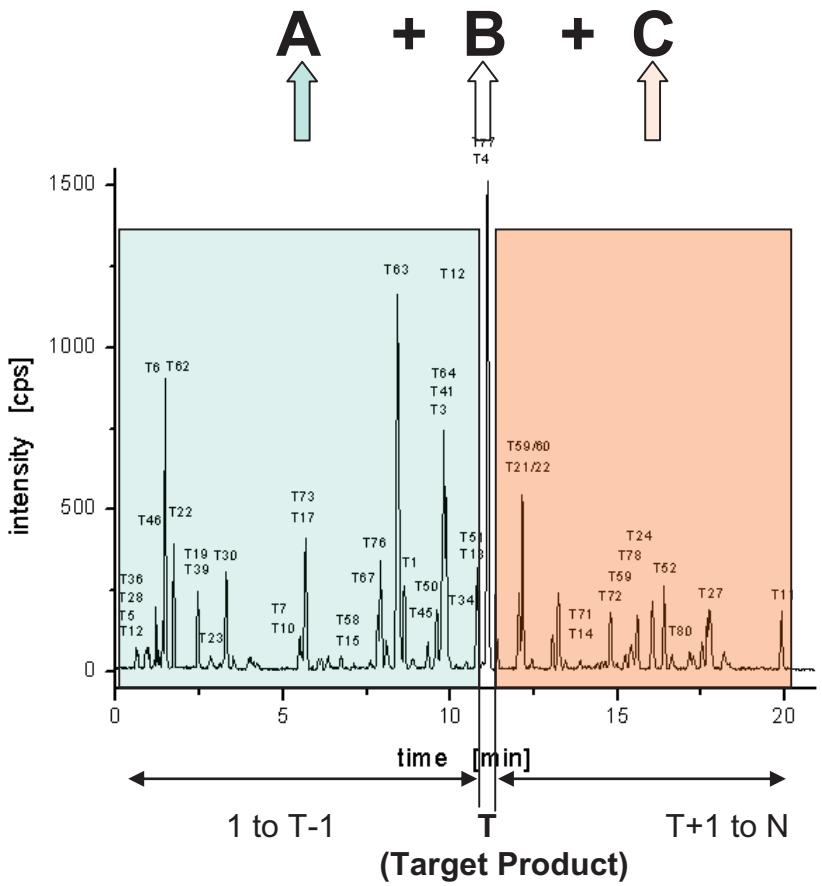

Fig 6: Specific composition of a real multicomponent mixture considered as a pseudo-ternary mixture.

Based on work by *Nicolaos et al.* (*2001a and 2001b*) focus was set on studying the feasibility of an isocratic 8-zone SMB for both linear and nonlinear isotherms. Such an 8-zone arrangement is due to the structural similarity to the conventional 4-zone processes of increasing interest. Such a process may not be able to separate the three components from each other when the required internal feedback is performed without any modifications. This finding was confirmed already in earlier work [*Kessler and Seidel-Morgenstern, 2006*]. This publication has suggested some process modifications to enable the separation of a ternary separation in an appropriate apparatus. A particular interesting possibility to perform such a separation is the extension of the classical 4-zone SMB

principle to eight zones, including the continuous internal recirculation of one of the streams as depicted in **Fig. 7**. In this figure A and C might represent either individual substances or groups of substances. The theoretical analysis performed showed that a simple and direct feedback from the raffinate or extract stream could cause problems in a 8-zone SMB unit operated under isocratic conditions. For this reason, various implementation options were proposed and their potential was evaluated by simulation studies. Particularly promising seems to be the implementation shown in Fig. 7, which uses an additional continuous concentrating step that renders the separation possible. Using these findings suitable isocratic separations were designed for model systems that have both linear and non-linear adsorption isotherms.

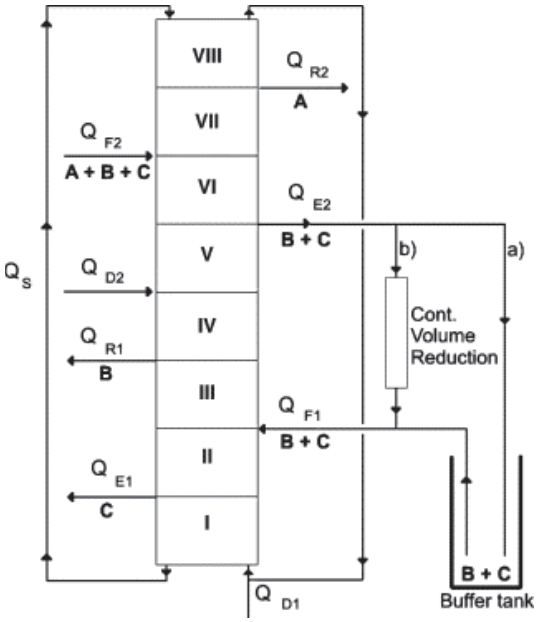

*Fig. 7: Schematic representation of a proposed device for continuous chromatographic separation of a ternary mixture into an 8-zone SMB unit [*Keßler and Seidel-Morgenstern, 2006*].*

Extending the results of the isocratic case, we further evaluated theoretically, whether the use of gradient in such an 8-zone process with internal feedback is feasible. Such a gradient process can be realized if in all three inlet streams (eluent inlet between zones VIII and I, eluent inlet between zones IV and V, feed inlet between zones VI and VII, **Fig. 8**) there is a different solvent strength, e.g. by varying the concentrations of a salt.

In addition to this conceptual work contributions were made to improve the precision of numerically simulating convection dominated chromatographic processes under nonlinear condition developing high resolution finite volume schemes *[Javeed et al, 2001].*

Experimental work was focused in the third funding period on validating the practical feasibility of the ternary SMB process and on further exploiting the potential of gradient SMB-chromatography.

Regarding the 8-zone ternary SMB process, after building up a corresponding unit, just recently a very successful continuous separation of a model mixture of three cycloketones could be achieved. Currently we write a corresponding publication describing these results.

A gradient-assisted open-loop SMB process was developed successfully capable to isolate the protein streptokinase from a lysate using hydrophobic interaction chromatography [*Palani et al., 2011, Gueorguieva et al., 2011*].

Main focus of the still ongoing work is to study the purification and isolation of the adsorption-desorption behavior of a histidine-tagged single-chain Fragment variable antibody (ABF D1.3 scFv) on a commercial immobilized metal ion affinity chromatography (IMAC) column was intensively investigated. A clarified cell culture supernatant originating from *Bacillus megaterium* (subproject B8: Franco-Lara) was characterized using single column experiments in a pH-gradient elution mode (**Fig.** 8a and **8b**). The antibody fragment (ABF) is the most retained component in the cell culture supernatant due to the presence of a histidine affinity tail. Therefore, a simplification can be done by lumping the undesirable proteins eluting before the target biomolecule as impurities (IMP) and considering the clarified cell culture supernatant as a pseudo-binary mixture. It is rather clear that the mobile phase pH dominates the elution of the antibody fragment and the closest eluting protein impurity (IMP). The influence of the mobile phase pH on the adsorption equilibrium constants was determined for both components (ABF and IMP) from pulse experiments by single batch column experiments under isocratic pH elution conditions. Our results revealed that the adsorption-desorption behavior is in the investigated range linearly correlated with the pH of the mobile phase.

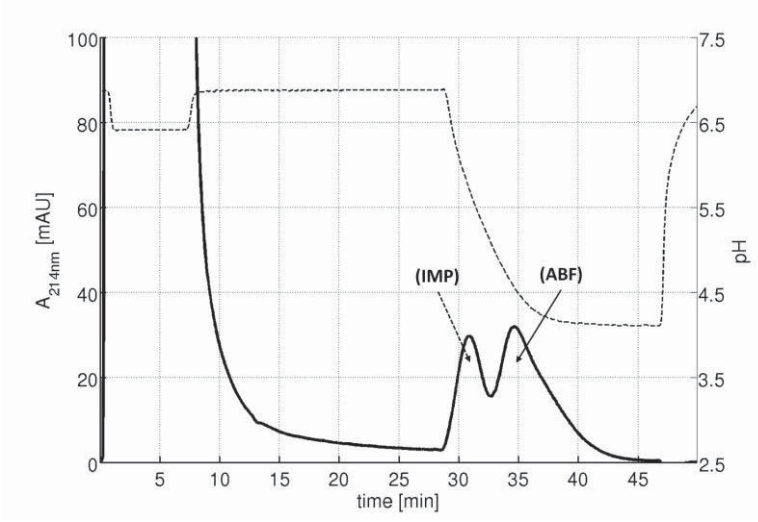

Fig. 8a: Chromatographic elution profile of diluted clarified cell culture supernatant containing the single-chain antibody fragment using a stepwise pH gradient. The recorded pH at the column outlet is depicted as a dashed line.

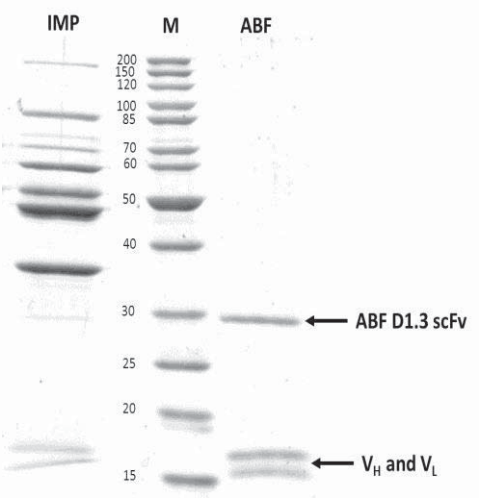

Fig. 8b: SDS-PAGE analysis showing fractions as indicated: Lane (IMP) protein impurity; lane (M) protein marker with molecular masses given in kilodaltons (kDa); lane (ABF) antibody fragment.

Based on the dependence of the adsorption isotherm parameters on the mobile phase pH, an open-loop three-zone two-step pH gradient Simulated Moving Bed (SMB) process is

suggested for the continuous chromatographic purification of antibody fragments. The process is theoretically investigated through the simulation of an equivalent True Moving Bed (TMB) process using an equilibrium stage model. The simulation of the countercurrent process delivers for certain operating points inside the complete separation region internal concentration profiles, where the target protein (ABF) can be continuously obtained at the extract port at high purity [*Martínez Cristancho et al., 2012*].

A 3-zone open-loop 2-step pH-gradient SMB unit was designed using two different fluid phases with distinct monohydrogen phosphate ion concentrations (or pH values) at the two inlet ports. This establishes two different pH-conditions in zones I and II, and in zone III. The purification of the ABF D1.3 scFv by tuning the adsorption-desorption behavior within the SMB unit basically imposes non-adsorbing conditions in zones I and II, and adsorbing conditions in zone III. A model capable to describe the hypothetical True Moving Bed (TMB) chromatography concept was used to analyze this process and to identify a region of operating parameters allowing for complete separation. An equilibrium cell model developed earlier [*Beltscheva et al., 2003]* was used to estimate the internal concentration profiles of the antibody fragment, the critical impurity and the protein impurity.

In **Fig. 9** can be seen that the internal concentration profiles of ABF, CRI and IMP differ strongly between two possible operating points I and II depicted in the separation diagram (**Fig. 10**). The most valuable result emerging from an inspection of the internal concentration profiles is the fact, that the antibody fragment at the extract is contaminated by the critical impurity when the operating point is outside the complete separation region for ABF and CRI (i.e operating point I). There are also differences between the two operating points regarding the enrichment of the antibody fragment, which is defined as the ABF concentration in the extract port over the ABF concentration in the feed. The productivities of operating points I and II were predicted to be 3.4 and 2.9 mg/day/ml$_{stat\ phase}$, respectively. The productivity of the discontinuous chromatographic process is 0.96 mg/day/ml$_{stat\ phase}$ and, thus, significantly lower than the productivities reached in the continuous mode.

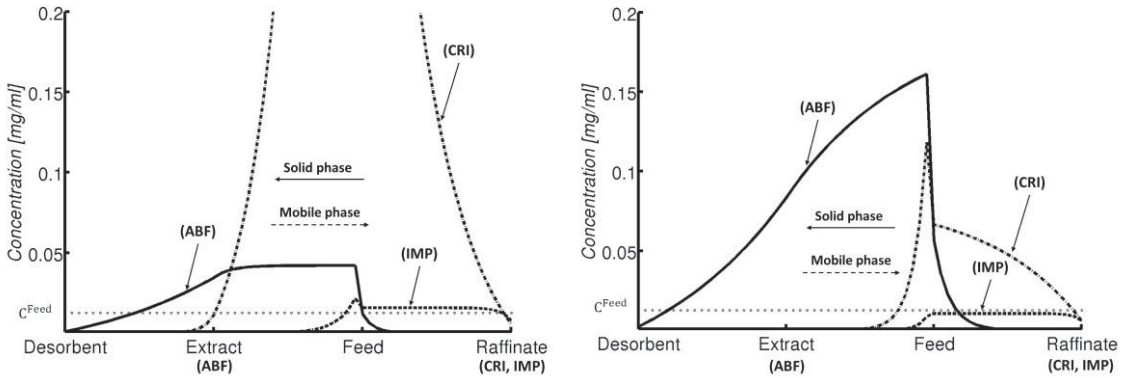

Fig. 9: Predicted internal concentration profile for ABF, IMP and CRI according to operating point I (left) and II (right).

The experimental validation of the promising separation process decribed is currently underway.

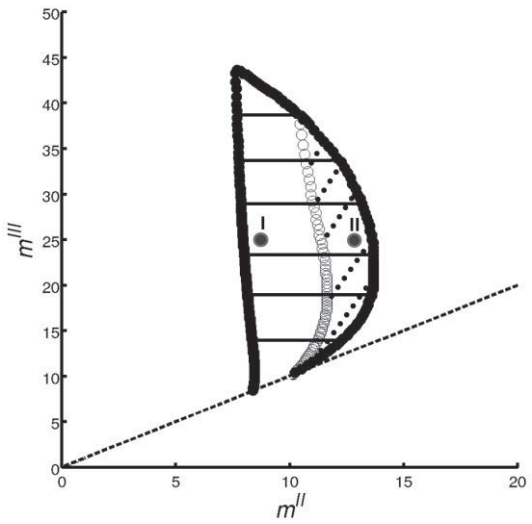

*Fig. 10: Simulation results for the three-zone open-loop two-step gradient TMB process. Two different separation regions in the m^{II},m^{III}-plane for the separation ABF-IMP (horizontal lines) and ABF-CRI (dotted diagonals) and operating points I and II [*Martínez Cristancho et al., 2012*].*

3.2.1.3 References to other works and collaborations in the SFB

In the third funding period, due the focus of the experimental work on the purification of single-chain Fragment variable antibody (ABF D1.3 scFv), there was an intensive collaboration and communication in particular with subprojects B8 (Franco-Lara) and A6 (Dübel).

3.2.1.4 Comparison with research outside the SFB

Two groups at the ETH in Zurich led by Prof. Morbidelli and Prof. Mazzotti worked in parallel to our activities on developing chromatographic processes capable to treat continuously multi-component mixtures. The so-called MCSGP process (multi-column solvent gradient purification) exploits a periodic switch between continuous operation and batchwise elution [*Krättli et al., 2011*]. The intermittent SMB-process [*Jermann et al, 2012*] is based in interrupting the feed supply in certain subintervals of the process. Both variants are interesting and could be validated experimentally. A final comparison with our variants developed during this project has not been done yet. A fair comparison is not trivial. It requires evaluating optimized systems and is planned for the future.

3.2.1.5 Literature

Abel, S.; Bäbler, M. U.; Arpagaus, C.; Mazzotti, M.; Stadler, J. (2004), Two-fraction and three-fraction continuous simulated moving bed separation of nucleosides. *J. Chromatogr. A* 1043, 201

Antos, D.; Seidel-Morgenstern, A. (2002) Continuous step gradient elution for preparative separations. *Sep. Sci.Technol.* 37, 1469

Beltscheva, D.; Hugo, P.; Seidel-Morgenstern, A. (2003) Linear two-step gradient counter-current chromatography: Analysis based on a recursive solution of an equilibrium stage model. *J. Chromatogr. A*, 989, 31-45

Beste, Y. A.; Arlt, W. (2000) Trennung von ternären Mischungen mit einer simulierten Gegenstromchromatographie mit Seitenstromentnahme. *Chem. Ing. Tech.* 72, 1105

Carta, G.; Jungbauer, A.; Protein Chromatography, Wiley, Weinheim, 2010

Chiang, A. S. T. (1998) Continuous Chromatographic Process Based on SMB Technology. *AIChE J*. 44, No.8, 1930

Gueorguieva, L.; Vallejo, L.F.; Rinas, U.; Seidel-Morgenstern A. (2006), Discontinuous and continuous separation of the monomeric and dimeric forms of human bone morphogenetic protein-2 from renaturation batches. J. Chromatogr. A 1135, 142

Hritzko, B. J.; Xie, Y.; Wooley, R. J.; Wang, N.-H. L. (2002), Standing-Wave Design of Tandem SMB for Linear Multicomponent Systems. *AIChE J*. 48, No.12, 2769

Keßler, L.C.; Seidel-Morgenstern, A. (2006) Theoretical study of multicomponent continuous countercurrent chromatography based on connected 4-zone units. *J. Chromatogr. A* 1126, 323

Keßler, L.C.; Gueorguieva, L.; Rinas, U.; Seidel-Morgenstern, A. (2007) Step Gradients in 3-zone simulated moving bed chromatography: Application to the purification of antibodies and bone morphogenetic protein-2. J. Chromatogr. A. 1176, 69

Jermann S., Katsuo S., Mazzotti M. (2012) Intermittent simulated moving bed process for chromatographic three fraction separation. *Organic Process Research &Design*, 16, 311

Nicolaos, A.; Muhr, L.; Gotteland, P.; Nicoud, R.-M.; Bailly, M. (2001b) Application of equilibrium theory to ternary moving bed configurations (four+four, five+four, eight and nine zones): I. Linear case. *J. Chromatogr.* A 908, 71

Nicolaos, A.; Muhr, L.; Gotteland, P.; Nicoud, R.-M.; Bailly, M. (2001a) Application of the equilibrium theory to ternary moving bed configurations (4+4, 5+4, 8 and 9 zones): II. Langmuir case. *J. Chromatogr. A* 908, 87

Strohlein, G.; Aumann, L.; Mazzotti, M.; Morbidelli, M. (2006) A continuous, counter-current multi-column chromatographic process incorporating modifier gradients for ternary separations. J. Chromatogr. A 1126, 338

Krättli M., Ströhlein G., Aumann L., Müller-Späth T., Morbidelli M. (2011) Closed loop control of the multi-column solvent gradient purification process. *J. Chromatogr. A*, 1218, 9028

Wankat, P. C. (2001) Simulated Moving Bed Cascades for Ternary Separations. *Ind. Eng. Chem. Res*. 40, 6185

3.2.2 Project relevant own publications

a) Works that have appeared in publications of a scientific quality assurance at the time of application or final adoption, and book publications

Gueorguieva, L.; Palani, S.; Rinas, U.; Jayaraman, G.; Seidel-Morgenstern, A. (2011) Recombinant protein purification using gradient-assisted simulated moving bed hydrophobic interaction chromatography. Part II: Process design and experimental validation. *J. Chromatogr. A*, 1218, 6402-6411

Javeed, S.; Qamar, S.; Seidel-Morgenstern, A.; Warnecke, G. (2011) Efficient and accurate numerical simulation of nonlinear chromatographic processes. *Computers and Chemical Engineering* 35, 2294-2305

Keßler L.C. Seidel-Morgenstern A. (2008) Improving performance of simulated moving bed chromatography by fractionation and feed-back of outlet streams. J. Chromatogr.A, 1207, 55

Li S., Kawajiri Y., Raisch J., Seidel-Morgenstern A. (2010a) Optimization of simulated moving bed chromatography with fractionation and feedback: Part I. Fractionation of one outlet. J. Chromatogr. A, 1217, 5337

Li S., Kawajiri Y., Raisch J., Seidel-Morgenstern A. (2010b) Optimization of simulated moving bed chromatography with fractionation and feedback: Part II. Fractionation of both outlets. J. Chromatogr. A, 1217, 5349

Li S., Kawajiri Y., Raisch J., Seidel-Morgenstern A. (2011) Optimization of startup and shutdown operation of simulated moving bed chromatographic processes. J. Chromatogr. 1218, 3876

Martínez Cristancho, C.A.; David, F.; Franco-Lara, E.; Seidel-Morgenstern, A. (2012), Discontinuous and continuous purification of single-chain antibody fragments using immobilized metal ion affinity chromatography. submitted to *J. Biotechnol.*

Palani, S.; Gueorguieva, L.; Rinas, U.; Seidel-Morgenstern, A.; Jayaraman, G. (2011) Recombinant protein purification using gradient-assisted simulated moving bed hydrophobic interaction chromatography. Part I: Selection of chromatographic system and estimation of adsorption isotherms. *J. Chromatogr. A*, 1218, 6396-6401

c) Patents

Keßler, L. C.; Seidel-Morgenstern A. "Verfahren und Vorrichtung zur chromatographischen Trennung von Komponenten mit teilweiser Rückführung von Gemischfraktionen", „Method and device for chromatographic separation of components with partial recovery of mixed fractions“, “Procédé et dispositif destinés à la séparation chromatographique de composants avec retour partiel de fractions de mélange”. EP 1 982 752 B1 (25.08.2010), WO 2008/125679 A1 (23.10.2008), US 2010/0186587 A1 (29.07.2010)

Schramm, H.; Kienle, A.; Kaspereit, M., Seidel-Morgenstern, A. „Verfahren und Vorrichtung zur chromatographischen Trennung von Komponenten“, “Method and Device for Chromatographic Component Separation”, “Procédé et Dispositif de Séparation de Composants par Chromatographie”, DE 102 35 385 B4 (05.10.2006), US 7,479,228 B2 (20.01.2009), EP 1 526 907 B1 (11.03.2009)

3.3 Looking back on the promotion

The project has been funded since 2001 in the SFB 578. It was completed in June 2012 with the end of the program.

3.3.1 Personnel in the project

	Name, acad. degree, service position	narrower subject of the employee	Institute of University or non-university facility	Participation in the project in hours per week	Category
Basic staff					
Research associate (incl. auxiliary power)	1. A. Seidel-Morgenstern, Prof. Dr.-Ing.	Process Engineering	Institute of Chemical Process Engineering	4	Professorship
Non academic staff	2. M. Chrobog, CTA	Process Engineering	Institute of Chemical Process Engineering	6	Technical staff
Supportive staff					
Research associate (incl. auxiliary power)	3. C. A. Martínez Cristancho, M.Sc.	Process Engineering	Institute of Chemical Process Engineering	40	PhD student
Non academic staff	4. various Stud. assistants	Process Engineering	Institute of Chemical Process Engineering	10	Students

Responsibilities of employees (basic staff)

Position 1 - 2: Andreas Seidel-Morgenstern, Marlies Chrobog

The employees involved in this subproject C2 of the Institute of Chemical Process Engineering at the Otto-von-Guericke University Magdeburg supported the PhD-students in their conceptual (Seidel-Morgenstern) and experimental work in the laboratory (Chrobog).

Responsibilities of employees (supportive staff)

Position 3: Carlos Andrés Martínez Cristancho

The scientific staff deals with the theoretical design and implementation of the SMB experiments. For this, good theoretical understanding of the thermodynamic processes and especially experimental skills are required. In parallel, theoretical studies are carried out using intensive model mathematical formulation and their implementation using the appropriate and available software.

Existing SMB units were used to carry out continuous chromatographic separations. After the experiments, the results were evaluated systematically.

Position 4: Student assistants

Various student assistants supported the extensive experimental work (discontinuous and continuous purifications studies, HPLC-analysis of samples).

3.1 General information on the completed project C6

3.1.1 Topic

Nanoanalytics for protein production processes

3.1.2 Disciplines and field of work

Biochemical analysis, transport processes, morphology

3.1.3 Project manager

Prof. Dr. Schilling, Meinhard (b. 30.08.1961)
Dr. Ludwig, Frank (b. 03.08.1958)
TU Braunschweig, Institut für Elektrische Messtechnik und Grundlagen der Elektrotechnik, Hans-Sommer-Str. 66, 38106 Braunschweig
Phone: 0531-391-3866 / 0531-391-3863
Fax: 0531-391-5768 / 0531-391-5768
E-Mail: m.schilling@tu-bs.de / f.ludwig@tu-bs.de

3.2 Development of the subproject

3.2.1 Report

3.2.1.1 Current knowledge at the last application and initial question

Based on the results achieved in the previous reporting period (2004-2008), the activities were focused on the following fields: optimization of the fluxgate magnetorelaxometry technique for an online analysis, the investigation and optimization of binding assays based on magnetic markers (especially the time-resolved study of specific and unspecific bindings), the investigation of the release behavior of hydrogels as promising drug delivery systems.

In the previous reporting period, fluxgate magnetorelaxometry (MRX) as a novel technique for the realization of homogeneous, magnetic nanoparticle (MNP) based binding assays was developed and established. In contrast to SQUID (superconducting quantum interference device) MRX, which has been developed and utilized by other groups [*Eberbeck et al., 2006; Chemla et al., 2000; Enpuku et al., 2001*], fluxgate MRX possesses a number of advantages, e.g., allowing one to realize a compact and portable analytical tool.

With the developed MRX system and in collaboration with subprojects B2 (Hempel/Horn) and B4 (Jahn/Nörtemann /Jänsch), binding assays based on the streptavidin-biotin binding were realized. In one binding system, commercial streptavidin-functionalized iron oxide nanoparticles were bound to biotinylated agarose beads having diameter of a few µm. It was demonstrated that unbound MNPs relax via the Brownian mechanism with a time constant in the µs to ms range whereas the relaxation of MNPs bound to the large agarose beads takes place via the internal Néel mechanism with a time constant in the ms to s range. First experiments on the detection of cDNA were carried out.

In close collaboration with subproject D1 (Menzel/Bunjes), the formation and entrapment capacity of hydrogels was studied. Hydrogels represent promising candidates for drug-delivery systems with long release rates. The polymerization kinetics and the physical entrapment capacity of photo-cross-linked hydroxyethyl methacrylate hydroxyethylstarch hydrogels were investigated by using MNPs as probes. By analyzing their magnetic relaxation behavior, the amounts of physically entrapped and mobile nanoparticles could be determined. This investigation allowed us to optimize the UV light irradiation time and to determine the amount of physically entrapped nanoparticles in the hydrogel network. It was found that the polymerization kinetics is faster for decreasing nanoparticle concentration but not all nanoparticles could be physically entrapped in the network.

It turned out that the realization of MRX based homogeneous binding assays strongly depends on the availability of proper magnetic markers. Therefore, the fluxgate MRX technique - in combination with refined physical models - was also applied for the comprehensive characterization of magnetic nanoparticles. The analysis of experimental MRX curves recorded on suspended as well as on immobilized MNPs allowed us to determine the particle's structure parameters such as core and hydrodynamic size distributions as well as to study their stability in various media.

3.2.1.2 Results and applied methods

Optimization of the fluxgate magnetorelaxometry technique for an online analysis

In the previous period of the project, the fluxgate magnetorelaxometry (MRX) was developed and established. In MRX, the MNPs – acting as markers – are aligned by a magnetization pulse (magnitude of a few mT, duration of a few seconds), and after switching off the field, the temporal decay of the particle's magnetic moment is measured. The decay of the magnetic moment of a MNP can take place via two mechanisms: the Brownian and the Néel relaxation. In the former mechanism the whole particle can rotate, including its shell and attached biomolecules, whereas in the latter case only the magnetic moment changes by thermal fluctuations. For a binding assay which is based on a change of the relaxation behavior, the MNPs must have a sufficiently large magnetic core so that relaxation takes place via the Brownian mechanism if the MNPs are suspended (**Fig. 1**). As can be seen, proper MNPs allow the realization of both solid- and liquid-phase bioassays. For an online analysis, the latter approach is of interest.

In addition to the realization of homogeneous binding assays, fluxgate MRX was routinely utilized for the characterization of magnetic core-shell nanoparticles applying the algorithms developed in the previous reporting period [*Ludwig et al., 2008; Ludwig et al., 2009; Ludwig et al., 2012*].

The MRX analyzer was applied for the optimization of magnetic core-shell nanoparticles in the framework of two diploma theses in a laboratory environment at the company Merck KGaA, and the practical experiences were used for further improvements.

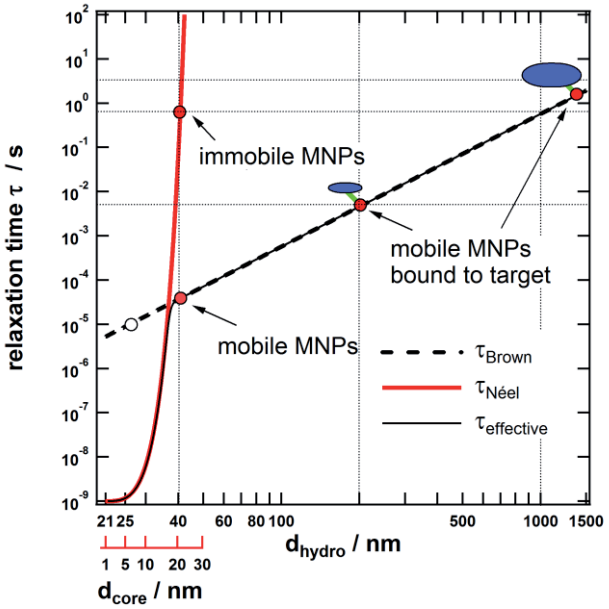

Fig. 1: Dependence of the relaxation time on core and hydrodynamic diameter, respectively. Red circles represent the different relaxation times of a solid-phase assay for MNP with a core diameter of 20 nm. The blue ovals illustrate the case of a liquid-phase assay where the specific binding of a biological target yields to an enlargement of the hydrodynamic diameter.

In the last year of the previous reporting period, a compact MRX measurement system, housed in an 19‘‘ case was built representing an important step from the bulky laboratory test setup towards an online analytical tool. Despite its compactness, the first version of the so-called MRX analyzer suffered from a number of deficiencies which were eliminated in the second and third version of the device. A photo of the latest version is depicted in **Fig. 2**. As can be seen, one important improvement was to replace the original drawer, containing the complete measurement head including sample, sensors and magnetization coil, by a much smaller one which simply serves to load the sample. The fact that the sensor/coil assembly is stationary provided a significant improvement in stability and thus reproducibility of measurement results.

Fig. 2: Photo of third generation of MRX analyzer.

Although fluxgate MRX is a powerful technique for the characterization of MNPs and for the realization of homogeneous bioassays, it is restricted to a relaxation time window between about 1 ms and a few seconds. To extend the time/frequency window, a setup for the measurement of the complex (ac) susceptibility was built, allowing one to study relaxation times down to a few µs [*Ludwig et al., 2010*]. The ac susceptometer is an important tool for the characterization of smaller MNPs (cf. Fig. 1) having shorter relaxation

times but for the realization of an online analytical technique it has the disadvantage of comparably long measurement times [*Ludwig, 2010*]. Thus, it cannot be utilized for investigations, e.g., of binding kinetics.

A third magnetic technique which is potentially suited for the MNP characterization as well as for the realization of binding assays is Magnetic Particle Spectroscopy (MPS). Similarly to the ac susceptibility, the MNP are excited by a sinusoidal magnetic field and the MNP's signal is recorded using a gradiometric detection coil. In contrast to ac susceptibility, the excitation field amplitude in MPS is large so that the nonlinear range of the particle's magnetization curve is explored, yielding to the excitation of higher harmonics in the detection signal. A fast Fourier transform of the detection signal provides a rich spectrum of harmonics being characteristic for the given MNPs. The MPS system built at the institute allows the measurements of the harmonic spectrum in dependence of excitation field amplitude and frequency as well as on static background field [*Wawrzik et al., 2010; Wawrzik et al., 2012; Schilling et al., pending patent*]. Since MPS combines both static and dynamic magnetization properties, the harmonic amplitudes of bound and unbound differ and can thus be used to analyze the binding status of the MNP [*Rauwerdink and Weaver, 2010; Wawrzik et al., 2012*]. Like MRX, MPS is a very fast measurement technique so that it is well suited for studying binding kinetics. In addition, first experiments towards the realization of an online analytical tool showed that MPS can even be applied if the sample under test is not stationary (e.g., if the medium is continuously pumped through the sensor head).

To extend the MNP-based nanoanalytic techniques with respect to a spatial information, a Magnetic Particle Imaging (MPI) system was developed [*Wawrzik et al., 2009; Wawrzik et a., 2010; Wawrzik et al., 2012*]. Like MPS, this system relies on the harmonic response of MNPs. By moving a so-called field-free point (FFP) through the volume of interest and combining it with sophisticated reconstruction algorithms, an image of the spatial distribution of MNPs can be obtained with real-time temporal resolution. MPI was proposed by Philips Research [*Gleich and Weizenecker, 2005*]. The built MPI system which was designed for measurements on mice is shown in **Fig. 3**. Extending the system by the use of two sets of excitation frequencies, the system has the potential for the discrimination of the spatial distributions of bound and unbound MNPs [*Wawrzik et al., 2012*].

Fig. 3: Photo of the complete MPI system at the EMG. The rack on the left side contains the excitation and detection electronics. The shield the MPI system from external interferences, the system is housed inside a copper shielding box.

Time-resolved quantification of specific and unspecific binding

Continuing the investigations on the streptavidin-biotin binding assay, time-resolved studies were performed. To distinguish between unbound and bound MNPs, the MRX curves were fitted with the following phenomenological equation:

$$B(t) = B_{off} + B_{unbound} \cdot \exp\left(-\left(\frac{t}{\tau_{ub}}\right)^{\beta}\right) + B_{bound} \cdot \ln\left(1+\frac{\tau_b}{t}\right)$$

Here, $B_{unbound}$ and B_{bound} are relative numbers for the amount of unbound and bound MNPs, τ_{ub} and τ_b are phenomenological time constants, β is an exponent accounting for the multidispersity of unbound particles and B_{off} is an offset signal. To minimize the number of free fitting parameters, τ_{ub}, τ_b and β were determined on mobile and immobilized reference samples, respectively. **Fig. 4** (left) shows the amount of bound, i.e., immobilized MNPs in dependence of agarose content. The sample volume amounted to 150 µL containing 10 µL of StAv-MNP (10 mg/mL). At a biotin agarose content of 32.5 µL, about 92% of the MNP are immobilized, the specificity of the binding was proven by blocking of the streptavidin binding sites with free biotin (open symbols). Details can be found in [*Heim et al., 2009*].

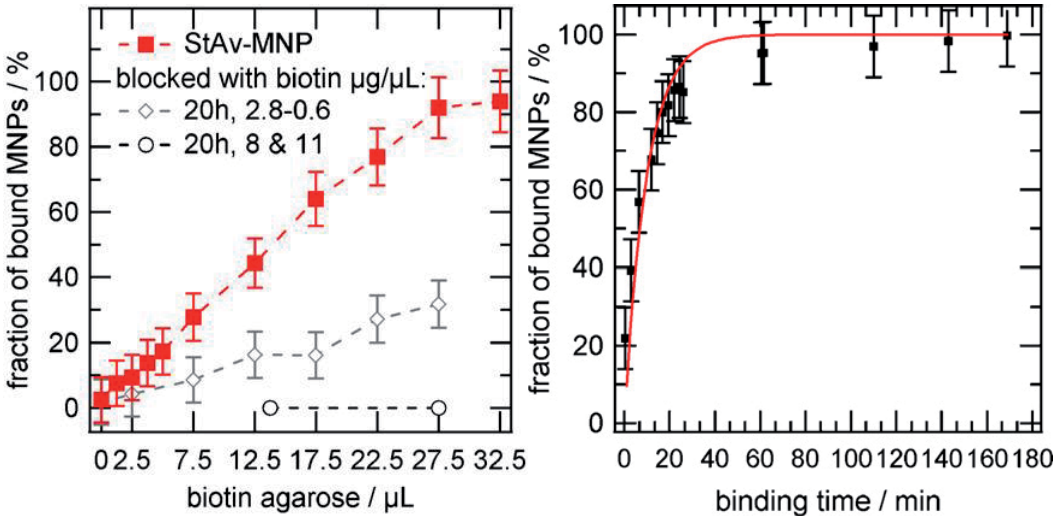

Fig. 4: Fraction of bound StAv–MNPs in dependence of amount of biotin agarose (left). Open data points are blocked StAv–MNPs with various content of free biotin. Reaction kinetics of StAv–MNPs binding to biotin agarose (right). The sample was shaken before each measurement. The line shows the first order kinetics fit with a time constant of about 10 min.

Fig. 4 (right) depicts the temporal evolution of the amount of bound MNPs for 22.5 µL biotin agarose and the fit with a first-order binding kinetics model.

Another binding assay based on the streptavidin-biotin binding and which is closer related to the SFB is schematically depicted in **Fig. 5**. As analyte, biotinylated BSA (albumin from bovine serum) proteins were used. Here, because of the small size of the BSA protein compared to the StAv–MNPs, the BSA protein acts as a linker that crosslinks the StAv–MNPs. In **Fig. 6**, the relative amount of cross-linked MNPs is depicted versus biotin labeled BSA content. A maximum crosslinking is found at 28.33 µmol/L of biotinylated BSA. A further increase in BSA content yields to a decrease of crosslinked MNPs since all streptavidin binding sites at the MNPs are occupied by BSA proteins.

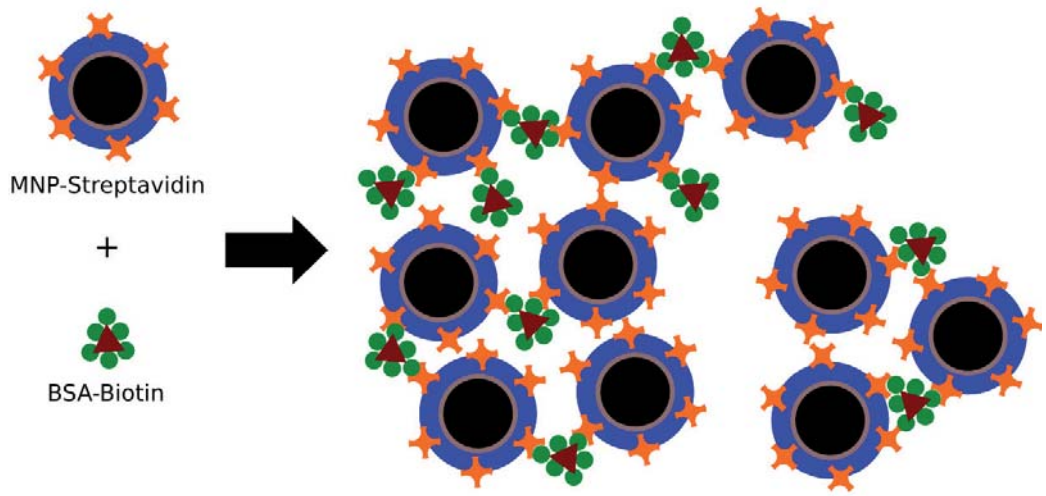

Fig. 5: Schematic illustration of the StAv-MNPs – BSA-biotin binding assay.

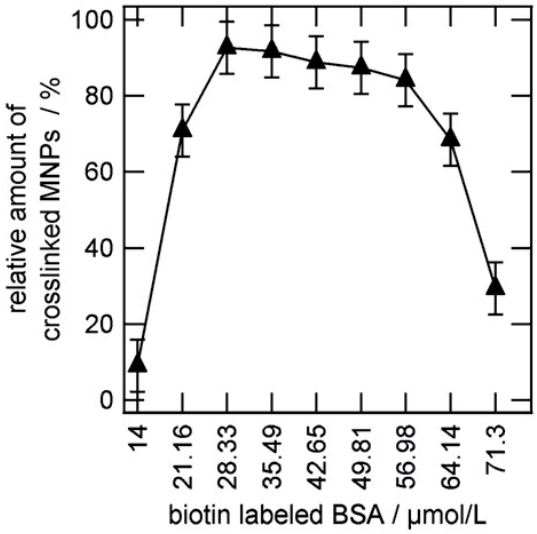

Fig. 6: Relative amount of crosslinked StAv-MNPs versus concentration of biotin-BSA.

Investigation of release properties of hydrogels

Whereas in the previous reporting period, the polymerization kinetics and the physical entrapment capacity of photo-cross-linked hydroxyethyl methacrylate hydroxyethylstarch hydrogels was studied in collaboration with subproject D1 (Menzel/Bunjes) [*Heim et al., 2008*], here the release profiles of MNP embedded in hydrogel cylinders and microspheres was investigated in dependence of degree of substitution and UV irradiation time. The procedure to distinguish between mobile and immobilized MNPs was the same as used for the binding assays described before.

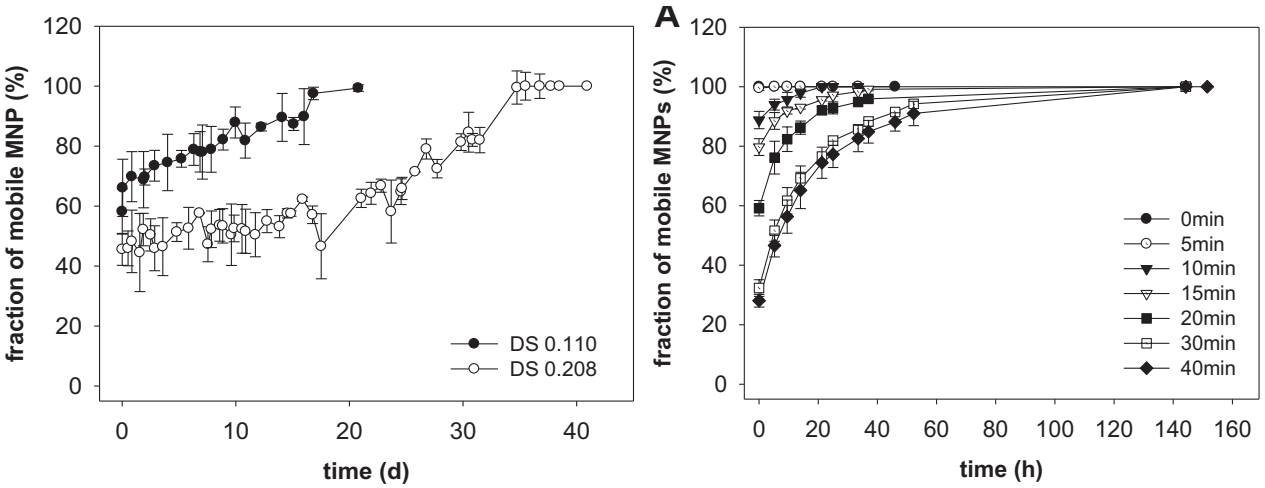

Fig. 6: Fraction of mobile MNP versus time for different degrees of substitution (left) and for different UV irradiation times.

Fig. 7 (left) shows the fraction of mobile MNPs versus time for two different degrees of substitution. As can be seen, a smaller degree of substitution corresponding to a lower network density results in a faster release of MNPs by diffusion and degradation. In Fig. 6 (right), the effect of the irradiation time is depicted. The irradiation time determines the crosslinking during the hydrogel production process and thus the macroscopic structure. Longer irradiation times yield to a higher fraction of immobilized MNPs [*Heim et al., 2008*] with negligible differences between the cylinders crosslinked for 30 min or 40 min. Hence, the fraction of mobile MNPs before the release process is minimum for long irradiation times. As can be seen in Fig. 6 (right), smooth release profiles were obtained from MRX measurements. For comparison, release profiles of incorporated fluorescently labeled substances from hydrogel cylinders or microspheres were recorded using the half-change method. Importantly, MRX provides the amount of mobile markers whereas in the half-change method using fluorescent labels only the released ones are detected. Thus, the combination of both techniques may provide more information on the internal hydrogel structure. Advantages of the MRX techniques are that measurements can be performed on closed systems and that magnetic markers possess a better long-term stability than fluorescent ones. It must be mentioned, however, that the size of the used MNPs ($d_h \cong 100$ nm) is considerably larger than that of the used fluorescent labels and proteins.

3.2.1.3 References to other works and collaborations in the SFB

The activities in this subproject C6 were carried out in collaboration with the following other subprojects in the SFB:

Binding assays: B3 (Krull/Hempel), B4 (Jahn/Nörtemann/Jänsch), B8 (Franco-Lara) and A6 (Dübel(Hust)

Hydrogels: D1 (Menzel/Bunjes)

MNP characterization, magnetic property simulation and magnetic coil design: C7 (Schilling/Garnweitner)

Images with the field-emission scanning electron microscope at the institute were recorded on various biological samples for different other SFB projects (e. g., A1 (Jahn/Dersch), B3 (Krull/Hempel), B7 (Kwade/Kampen) und D2 (Büttgenbach/Dübel)).

The development of the fluxgate MRX system was performed in collaboration with the Physikalisch-Technische Bundesanstalt (PTB), Institut Berlin. The SQUID MRX system at the PTB was taken as a reference system and used to calibrate our fluxgate systems [*Ludwig et al., 2009*].

3.2.1.4 Comparison with research outside the SFB

There has been increasing interest over the last years in the application of magnetic nanoparticles in various fields of medicine and bioanalysis. For many years, Fe_3O_4 nanoparticles have been used as contrast agent in Magnetic Resonance Imaging (MRI) and in magnetic separation. Among the novel and promising applications are the magnetic drug targeting [*Alexiou et al., 2000*], magnetic hyperthermia [*Jordan et al., 1999*], magnetic biochips based on GMR sensors [*Megens and Prins, 2005; Schotter et al., 2002; Rife et al., 2003*], magnetic particle imaging [*Gleich and Weizenecker, 2005; Weizenecker et al., 2009; Goodwill et al., 2012]*] and the so-called magnetic relaxation immunoassays (MARIA) [*Kötitz et al., 1995; Weitschies et al., 1997*]. Advantages of using magnetic nanoparticles as markers for biological targets are their long-term stability and non-toxicity (at least iron oxide), that they can be applied in opaque media such as blood and that they can be manipulated by means of magnetic gradient fields. Examples are magnetic stirring to decrease the incubation time, magnetic washing of unbound markers and concentrating of markers at the sensor's site.

Magnetic relaxation assays possess – compared to conventional magnetic biochips – the advantages that no washing steps are required and that relatively easily liquid-phase assays can be realized. Such liquid-phase assays are especially for the realization of an online analytical technique desirable.

After the pioneering work at the Institut für Diagnostikforschung, Berlin, in cooperation with the Friedrich-Schiller Universität Jena and the Physikalisch-Technischen Bundesanstalt, Institut Berlin [*Kötitz et al., 1995; Weitschies et al., 1997*], a number of groups worked on various approaches to realize bioassays based on the change of the relaxation behavior of MNP when bound to biological targets (e.g., [*Chemla et al., 2000; Lee et al., 2002; Grossman et al., 2003; Enpuku et al., 2001; Romanus et al., 2002; Flynn and Bryant, 2005; Horng et al., 2006; Hong et al., 2006; Yang et al., 2006; Hong et al., 2007; Carvalho et al., 2007; DiIorio et al., 2007; Krause et al., 2007; Meyer et al., 2007; Eberbeck et al., 2011*]). Interestingly, the activities over the last few years focused on the realization of liquid-phase assays. Besides the relaxation based assays, alternative approaches are pursued in which antibodies immobilized on chips are used to specifically detect complexes consisting of magnetic markers, antibody and antigen. The readout of the

magnetic signal provided by the bound magnetic particles can be realized using a GMR or TMR sensor integrated into the chip or via external magnetic sensor arrays [*Schotter, 2002; Rife et al., 2003; Megens and Prins, 2005*]. Using such methods, sensitivities comparable to those achieved with optically detected fluorescence markers can be achieved [*Enpuku et al., 2001*].

A rather new alternative to the relaxation-based bioassays was recently proposed by Schotter et al. [*Schotter et al., 2007; Schrittwieser et al., 2012*]. Here the advantage of the magnetic relaxation assay, namely the realization of homogeneous assays with the need to wash out unbound markers, with the extremely high sensitivity when optically detecting markers are combined. Their bioassay is based on magnetic nanorods coated with a gold layer. The magnetic nanorods can easily be manipulated by a magnetic field pulse, an ac or rotating magnetic field but their relaxation behavior is analyzed by measuring the anisotropic surface plasmon resonance. This novel bioassay is realized in tight collaboration between the Institut für Elektrische Messtechnik und Grundlagen der Elektrotechnik of the TU Braunschweig and the Austrian Institute of Technology in Wien in the framework of the European Commission Framework Programme 7 under the NAMDIATREAM project (NMP-2010-246479). This approach is, however, not suited for an online analysis as it was the goal of the given project.

3.2.1.5 Literature

Alexiou, C.; Arnold, W.; Klein, R. J.; Parak, F. G.; Hulin, P.; Bergemann, C.; Erhardt, W.; Wagenpfeil, S.; Lübbe, A. S. (2000) Locoregional cancer treatment with magnetic drug targeting. *Cancer Res.* 60, 6641-6648

Carvalho, H. R.; Bruno, A. C.; Louro, S. R. W.; Costa Ribeiro, P. (2007) Application of an RF-SQUID to detect magnetic nanoparticles used in immunoassays. *IEEE Trans. Appl. Supercond.* 17, 820-822

Chemla, Y. R.; Grossman, H. L.; Poon, Y.; McDermott, R.; Stevens, R.; Alpers, M. D.; Clarke, J. (2000) *Proc. Natl. Acad. Sci. USA* 97, 14268

Dilorio, M.; Yang, K.; Pisanic, T. (2006) New applications of magnetic assays using high temperature SQUIDs. *Applied Superconductivity Conference (ASC'06),* Seattle, Washington (unpublished)

Eberbeck, D.; Wiekhorst, F.; Steinhoff, U.; Trahms, L. (2006) Aggregation behaviour of magnetic nanoparticle suspensions investigated by magnetorelaxometry. *J. Phys. Condens. Matter* 18, S2829-S2846.

Eberbeck, D.; Wiekhorst, F.; Steinhoff, U.; Trahms, L. (2009) Quantification of biomolecule agglutination by magnetorelaxometry. *Appl. Phys. Lett.* 95, 213710-1 – 3

Enpuku, K.; Minotani, T. (2001) Biological immunoassay with high-T_c supercodncuting quantum interference device (SQUID) magnetometer. *IEICE Trans. Electron.* E84-C(1), 43-48

Flynn, E. R.; Bryant, H. C. (2005) A biomagnetic system for in vivo cancer imaging. *Phys. Med. Biol.* 50, 1273-1293

Gleich, B.; Weizenecker, J. (2005) Tomographic imaging using the nonlinear response of magnetic particles, *Nature* 435, 1214-1217

Goodwill, P. W.; Saritas, E. U.; Croft, L. R.; Kim, T. N.; Krishnan, K. M.; Schaffer, D. V.; Conolly, S. M. (2012) X-Space MPI: Magnetic Nanoparticles for Safe Medical Imaging. *Adv Mater.* (online)

Grossman, H. L.; Myers, W. R.; Vreeland, V. J.; Bruehl, R.; Bertozzi, C. R.; Clarke, J. (2003) *Proc. Natl. Acad. Sci. USA* 101, 129

Hong, C.-Y.; Wu, C. C.; Chiu, Y. C.; Yang, S. Y.; Horng, H. E.; Yang, H. C. (2006) Magnetic susceptibility reduction method for magnetically labeled immunoassay. *Appl. Phys. Lett*. 88, 212512-1 - 3

Hong, C.-Y.; Chen, W. S.; Jian, Z. F.; Yang, S. Y.; Horng, H. E.; Yang, L. C.; Yang, H. C. (2007) Wash-free immunomagnetic detection for serum through magnetic susceptibility reduction. *Appl. Phys. Lett.* 90, 074105-1 – 3

Horng, H. E.; Yang, S. Y.; Hong, C.-Y.; Liu, C. M.; Tsai, P. S.; Yang, H. C.; Wu, C. C. (2006) Biofunctionalized magnetic nanoparticles for high-sensitivity immunoassay detection of human C-reactive protein. *Appl. Phys. Lett.* 88, 252506-1 - 3.

Jordan, A.; Scholz, R.; Wust, P.; Fahling, H.; Felix, R. (1999) Magnetic fluid hyperthermia (MFH): cancer treatment with ac magnetic field induced excitation of biocompatible superparamagnetic nanoparticles. *J. Magn. Magn. Mater.* 201, 413-419

Kötitz, R.; Trahms, L.; Koch, H.; Weitschies, W. (1995) Ferrofluid relaxation for biomagnetic imaging, in: Biomagnetism: Fundamental Research and Clinical Applications. Baumgartner C.; Deecke, L.; Williamson, S. J. (editors), Elsevier Science, Amsterdam (pp. 785)

Krause, H.-J.; Wolters, N.; Zhang, Y.; Offenhäuser, A.; Miethe, P.; Meyer, M. H. F.; Hartmann, M.; Keusgen, M. (2007) Magnetic particle detection by frequency mixing for immunoassay applications. *J. Magn. Magn. Mater.* 311, 436-444

Lee, S.-K.; Myers, W. R.; Grossman, H. L.; Cho, H.-M.; Chemla, Y. R.; Clarke, J. (2002) Magnetic gradiometer based on a high-transition temperature superconducting quantum interference device for improved sensitivity in biosensors. *Appl. Phys. Lett.* 81, 3094-3096

Ludwig, F.; Mäuselein, S.; Heim, E.; Schilling, M. (2005) Magnetorelaxometry of magnetic nanoparticles in magnetically unshielded environment utilizing a differential fluxgate arrangement. *Rev. Sci. Instrum.* 76, 106102-1 - -3

Megens, M. and Prins, M. (2005) Magnetic biochips: a new option for sensitive diagnostics, *J. Magn. Magn. Mater.* 293, 702-708.

Meyer, M. H. F.; Krause, H.-J.; Hartmann, M.; Miethe, P.; Oster, J.; Keusgen, M. (2007) *Francisella tularensis* detection using magnetic labels and a magnetic sensor based on frequency mixing. *J. Magn. Magn. Mater.* 311, 259-263

Meyer, M. H. F.; Hartmann, M.; Krause, H.-J.; Blankenstein, G.; Mueller-Chorus, B.; Oster, J.; Miethe, P.; Keusgen, M. (2007) CRP determination based on a novel magnetic biosensor. *Biosens. Bioelectron.* 22, 973-979

Rife, J.C.; Miller, M.M.; Sheehan, P.E.; Tamanaha, C.R.; Tondra, M.; Whitman, L.J. (2003), Design and performance of GMR sensors for the detection of magnetic microbeads in biosensors. *Sensors and Actuators A* 107, 209–218

Rauwerdink, A. M.; Weaver, J. B. (20120, Viscous effects on nanoparticle magnetization harmonics. *J. Magn. Magn. Mater.* 322, 609-613

Romanus, E.; Hückel, M.; Groß, C.; Prass, S.; Weitschies, W.; Bräuer, R.; Weber, P. (2002) Magnetic nanoparticle relaxation measurement as a novel tool for in vivo diagnostics. *J. Magn. Magn. Mater.* 252, 387-389

Schotter, J.; Kamp, P.B.; Becker, A.; Pühler, A.; Brinkmann, D.; Schepper, W.; Brückl, H.; Reiss, G. (2002) A biochip based on magnetoresistive sensors. *IEEE Trans. Magn.* 38, 3365-3367

Schotter, J.; Bethge, O.; Maier, T.; Brueckl H. (2007) Optische Messverfahren zur molekularen Detektion anhand von Relaxationsmessungen in optisch anisotropen Nanopartikeln. Austrian patent number 503.845, 2007, PCT application number WO/2008/124853

Schrittwieser, S.; Ludwig, F.; Dieckhoff, J.; Soulantica, K.; Viau, G.; Lacroix, L.-M.; Lentijo Mozo, S.; Boubekri, R.; Maynadié, J.; Huetten, A.; Brueckl, H.; Schotter, J. (2012), Modeling and Development of a Biosensor Based on Optical Relaxation Measurements of Hybrid Nanoparticles. *ACS Nano* 6, 791-801

Weitschies, W.; Kötitz, R.; Bunte, T.; Trahms, L. (1997) Determination of relaxing or remanent nanoparticle magnetization provides a novel binding-specific technique for the evaluation of immunoassays. *Pharm. Pharmacol. Lett.* 7, 5-8

Weizenecker, J.; Gleich, B.; Rahmer, J.; Dahnke, H.; Borgert, J. (2009) Three-dimensional real-time *in vivo* magnetic particle imaging, Phys. Med. Biol. 54, L1-L10

Yang, H. C.; Yang, S. Y.; Fang, G. L.; Huang, W. H.; Liu, C. H.; Liao, S. H.; Horng, H. E.; Hong, C.-Y. (2006) Magnetic relaxation measurement in immunoassay using high-transition-temperature superconducting quantum interference device system. *J. Appl. Phys.* 99, 124701-1 – 5

3.2.2 Project relevant own publications

a) Works that have appeared in publications of a scientific quality assurance at the time of application or final adoption, and book publications

Heim, E.; Harling, S.; Ludwig, F.; Menzel, H.; Schilling, M. (2008). Fluxgate magnetorelaxometry for characterization of hydrogel polymerization kinetics and physical entrapment capacity. *J. Phys.: Condens. Matter* 20, 204106-1 - 5

Heim, E.; Ludwig, F.; Schilling, M. (2009) Binding assays with streptavidin-functionalized superparamagnetic nanoparticles and biotinylated analytes using fluxgate magnetorelaxometry. *J. Magn. Magn. Mater.* 321, 1628-1631

Ludwig, F.; Heim, E.; Schilling, M.; Enpuku, K. (2008) Characterization of superparamagnetic Fe_3O_4 nanoparticles by fluxgate magnetorelaxometry for use in biomedical applications. *J. Appl. Phys.,* Volume 103, Number 7, 07A314-1 - 3

Ludwig, F.; Heim, E.; Schilling, M. (2009) Characterization of magnetic core-shell nanoparticles by fluxgate magnetorelaxometry, ac susceptibility, transmission electron microscopy and photon correlation spectroscopy – a comparative study. *J. Magn. Magn. Mater.* 321, 1644-1647

Ludwig, F.; Heim, E.; Eberbeck, D.; Schwarz, K.; Trahms, L.; Schilling, M. (2009) Comparison and calibration of fluxgate and SQUID magnetorelaxometry techniques for the characterization of magnetic core-shell nanoparticles . *IEEE Trans. Magn.* 45, 4857-4860

Ludwig, F.; Guillaume, A.; Schilling, M.; Frickel, N.; Schmidt, A. M. (2010) Determination of core and hydrodynamic size distributions of $CoFe_2O_4$ nanoparticle suspensions using ac susceptibility measurements. *J. Appl. Phys.* 108, 033918

Ludwig, F. (2010) Characterization of Magnetic Core-Shell Nanoparticle Suspensions Using ac Susceptibility for Frequencies up to 1 MHz. AIP Conference Proceedings Vol. 1311, 249-254

Ludwig, F.; Wawrzik, T.; Schilling, M. (2012) Characterization of Magnetic Nanoparticles for Magnetic Particle Imaging by Magnetorelaxometry, AC Susceptibility, Magnetic Particle Spectroscopy and Static Magnetization Measurements. Magnetic Particle Imaging, Buzug; T. M. and Borgert J. (Eds.), Springer Proceedings in Physics, Vol. 140, Springer Berlin Heidelberg, 35-40

Schilling, M.; Ludwig, F. (2008) Proteins and patients – magnetic nanoparticles as analytic markers. *Advances in Solid State Physics* 46, 87-89

Wawrzik, T.; Ludwig, F.; Schilling, M. (2009) Assembly for one-dimensional magnetic particle imaging. IFMBE Proceedings, Volume 25, 898-900 (on CD)

Wawrzik, T.; Ludwig, F.; Schilling, M. (2010) Two-dimensional magnetic particle imaging. Magnetic Nanoparticles – Particle Science, Imaging Technology, and Clinical Applications, Proceedings of First International Workshop on Magnetic Particle Imaging, World Scientific (pp. 100-105)

Wawrzik, T.; Hahn, J., Ludwig, F.; Schilling, M. (2010) Magnetic particle spectroscopy for the evaluation of field-dependent harmonics generation. Magnetic Nanoparticles – Particle Science, Imaging Technology, and Clinical Applications. Proceedings of First International Workshop on Magnetic Particle Imaging, World Scientific (pp. 86-91)

Wawrzik, T.; Ludwig, F.; Schilling, M. (2010) Multivariate Magnetic Particle Spectroscopy for Magnetic Nanoparticle Characterization. AIP Conference Proceedings Vol. 1311, 267-270

Wawrzik, T.; Schilling, M.; Ludwig, F. (2012) Perspectives of magnetic particle spectroscopy for magnetic nanoparticle characterization. Magnetic Particle Imaging, Buzug; T. M. and Borgert J. (Eds.), Springer Proceedings in Physics, Vol. 140, Springer Berlin Heidelberg, 41-45

Wawrzik, T.; Ludwig, F.; Schilling, M. (2012) Magnetic Particle Imaging: Exploring particle mobility. Magnetic Particle Imaging, Buzug; T. M. and Borgert J. (Eds.), Springer Proceedings in Physics, Vol. 140, Springer Berlin Heidelberg, 19-23

b) Other publications

Heim, E. (2009) Fluxgate-Magnetrelaxometrie magnetischer Nanopartikel in der Bioanalytik. In: Berichte aus dem Institut für Elektrische Messtechnik und Grundlagen der Elektrotechnik, Band 31, Schilling, M. (Hrsg.), Mensch und Buch-Verlag Berlin, ISBN 978-3-86664-722-0, zgl. Dissertation TU Braunschweig

c) Patents (pending / granted)

Schilling, M.; Ludwig, F.; Wawrzik, T. (18.03.2010) Vorrichtung und Verfahren, um geometrische und magnetische Eigenschaften von Nanopartikeln zu bestimmen, Deutsches Patent No. DE 10 2010 011 936 A1 (pending)

3.3 Looking back on the promotion

The project has been funded since July 2004 in the SFB 578. It was completed on June 2012 with the end of the program.

3.3.1 Personnel in the project

	Name, acad. degree, service position	narrower subject of the employee	Institute of University or non-university facility	Participation in the project in hours per week	Category
Basic staff					
Research associate (incl. auxiliary power)	1. M. Schilling, Prof. Dr. rer. nat.	Electrical measurement science	Institut für Elektrische Messtechnik und Grundlagen der Elektrotechnik	3	Professorship
	2. F. Ludwig, Dr. rer. nat.	Electrical measurement science	Institut für Elektrische Messtechnik und Grundlagen der Elektrotechnik	5	Senior scientist
Non academic staff	3. B. Kuhn, PLA Technical staff	Electrical measurement	Institut für Elektrische Messtechnik und Grundlagen der Elektrotechnik	6	Technical staff
	4. H. Schmidt, J. Pförtner, H. Müller, technical staff	Machine shop	Institut für Elektrische Messtechnik und Grundlagen der Elektrotechnik	4	Technical staff
Supportive staff					
Research associate (incl. auxiliary power)	5. E. Heim Dr.-Ing..	Electrical measurement science	Institut für Elektrische Messtechnik und Grundlagen der Elektrotechnik	40	PhD student
	6. T. Wawrzik, Dipl.-Ing.	Electrical measurement science	Institut für Elektrische Messtechnik und Grundlagen der Elektrotechnik	40	PhD student
Non academic staff	7. N. N., Stud. assistant	Electrical measurement		10	Students

Responsibilities of employees (basic staff)

Position 1 - 4:

The involved employees in the subproject C6 (Schilling/Ludwig) of the Institut für Elektrische Messtechnik und Grundlagen der Elektrotechnik support the PhD students in all aspects of their work. Besides the project management, Dr. Ludwig assisted the activities by developing theoretical models for the analysis of relaxation curves. The members of the machine shop supported the subproject by building various mechanical setups (MRX, ac susceptibility and magnetic particle spectroscopy).

Responsibilities of employees (supportive staff)

Position 5: Dr.-Ing. Erik Heim

Erik Heim continued in this reporting period his work from the previous one. The focus of his work was the further improvement of the fluxgate magnetorelaxometry technique and its application for the characterization of magnetic nanoparticles, the realization of homogeneous binding assay and the study of the formation, entrapment capacity and release behavior of hydrogels.

Position 6: Dipl.-Ing. Thilo Wawrzik

Thilo Wawrzik continued the work on subproject C6 beginning in 2/2008.In addition to the further establishment of the fluxgate magnetorelaxometry technique and its application for the MNP characterization and realization of homogeneous bioassays, his work focused on the development of magnetic particle imaging (MPI) and magnetic particle spectroscopy (MPS). MPI is a new imaging modality allowing the real-time measurement of the 2D or 3D distribution of magnetic nanoparticles. MPS can be considered as a 0D MPI system which can also be used for the comprehensive characterization of MNP and the realization of relaxation-based bioassays. In comparison with fluxgate MRX, MPI has the advantages that it is susceptible to larger range particle sizes and that – due to the very short measurement time – it has a large potential for an online analysis.

Position 7: Stud. assistant

Various student assistants supported the extensive experimental work, e.g., performing and analyzing magnetorelaxometry measurements and developing electronic components for the various setups.

3.1 General information on the completed project C7

3.1.1 Topic

Protein purification with functionalized magnetic nanoparticles

3.1.2 Disciplines and field of work

Nanoparticle technology, Protein purification, Nanoanalytics

3.1.3 Project manager

Jun.-Prof. Dr. Georg Garnweitner
(b.: 11.04.1978)
Institute for Particle Technology
TU Braunschweig

Volkmaroder Str. 5
Phone: 0531/391-9615
Fax: 0531/391-9633
E-Mail: g.garnweitner@tu-bs.de

Prof. Dr. Meinhard Schilling
(b.: 30.08.1961)
Institut für Elektrische Messtechnik
und Grundlagen der Elektrotechnik (emg)
TU Braunschweig
Hans-Sommer-Str. 66
Phone: 0531/391-3866
Fax: 0531/391-5768
E-Mail: m.schilling@tu-bs.de

3.2 Development of the subproject

3.2.1 Report

3.2.1.1 Current knowledge at the last application and initial question

The downstream processing of biotechnological products such as proteins still presents a big challenge and leaves a wide range for possible optimization. In contrast to chromatography, which requires the prior separation of cell fragments by centrifugation or filtration, the use of functionalized magnetic nanoparticles in principle allows the separation directly from the complex cultivation medium. Iron oxide nanoparticles have shown preferable properties for a specific and highly effective separation. Usually the magnetic nanoparticles are obtained via the coprecipitation method which is long known as a simple strategy to Fe_3O_4 nanoparticles [*Massart, 1981*]; with this method however a control of particle size and shape is hardly possible and often only low crystallinity of the product is obtained. In contrast, particles synthesized by the nonaqueous synthesis show defined size and shape but they are not hydrophilic and have the tendency to agglomerate in aqueous dispersion.

The currently available magnetic particle purification systems cannot be used for large-scale purification processes as they are costly and re-usability is limited. Additionally, their direct use during cultivation for a continuous removal of products is not possible yet and is difficult in principle for these systems, because of the wide size distribution and restricted knowledge about the shape and the state of agglomeration of the particles, which leads to suboptimal control over the separation with a high loss of product.

Therefore, the synthesis of magnetic nanoparticles with defined and optimized size of the magnetic core and a well-known and very reproducible size distribution is of eminent importance for the investigation, optimization and introduction of magnetic purification and separation processes to become an interesting alternative to chromatographic approaches. Due to these facts in the context of this project hydrophilic particles had to be synthesized by nonaqueous synthesis with cores large enough for high magnetic forces for an efficient separation and with very reproducible size distribution.

The goal of this subproject was to obtain well stabilized, water-compatible Fe_3O_4 nanoparticles with a covalently bound functionalization that serve for an efficient separation of specific proteins, the target proteins of the SFB, out of a cell suspension. By the use of functionalized single-core magnetic nanoparticles, a large specific surface area for a high capacity to bind the product should be obtained.

One way to realize the stabilization and functionalization of the particles is the so called “grafting to”-method, where the groups used for functionalization are linked to anchoring groups prior to binding them to the particle surface. Alternatively, in the “grafting from”-method the functional group is grown step-wise starting at specific functional groups on the particle surface. Both approaches can lead to a highly stable system without compromising the magnetic properties of the particles. In this subproject, the realization of a molecular functionalization was targeted, without large macromolecules such as polymers shielding the magnetic cores and reducing the active surface of the system. Also with respect to the functionalization process, the system needs to be reproducible, recyclable and allow a potential scale-up.

Furthermore, the development of magnetic separation methods with homogenous gradient fields and thus homogenous adsorbance force is desirable to achieve highly specific separation and filtration of the protein-carrying magnetic particles.

3.2.1.2 Results and applied methods

Synthesis of superparamagnetic iron oxide nanoparticles

First the iron oxide nanoparticles were produced in a solvothermal synthesis with the non-aqueous solvent benzyl alcohol using iron(III)acetylacetonate as organic precursor. However it was noted that the particles were not stable in water. Hence a new synthesis had to be established, using triethylene glycol as reaction medium and as well iron(III)acetylacetonate. The particles produced with this synthesis were hydrophilic and therefore suitable for the desired application.

To better understand the synthesis mechanism, a detailed study was performed comparing the two solvents benzyl alcohol (BA) and triethylene glycol (TEG) [*Grabs et al., 2012*]. An aim of this study was not only to investigate the influence of the two different media on the particle formation process but also the particle properties, especially their compatibility with different media.

The iron oxide nanoparticles were synthesized varying the process parameters, concentration of precursor, the reaction time and the reaction temperature analyzing the particle size, the magnetic properties and the stability in different solvents. Additionally, also the synthesis was not only preformed in lab scale in an autoclave (45 mL) but also a reactor (1600mL) and the influence of the scale-up was analyzed especially by studying the development of the hydrodynamic particle size as measured by dynamic light scattering (DLS). The particles synthesized in TEG have a size of 8 nm after 12 h of reaction, which increases with the reaction time to about 30 nm after 15 h, which was shown to be due to slight agglomeration even though the solvent acts as a stabilizer. TEM images proved that the particles from the reactor in TEG show a uniform size and shape. The kinetics of crystallization and magnetization during the particle synthesis were additionally studied and compared for the two media.

The structure and the crystallinity were determined by powder X-ray diffractometry (PXRD) whilst the magnetic properties were measured by SQUID magnetometry. The crystallinity of the samples was different for both solvents, particularly its development over the reaction time. For the BA system the crystallinity did not increase significantly from 0.25 h to 1.5 h but after 4 h a sharp increase was noted, whereas for TEG, the first sample was amorphous but afterwards the crystallinity increased continuously. This shows that the reaction medium does not only influence the particle formation, but also the crystallization process following the initial nucleation step. The development of the magnetization of the sample was observed to be analogous to the crystallization kinetics.

The particles were generally well dispersed in solvents with a similar polarity as judged by Rohrschneider's index of polarity [*Grabs et al., 2012*]. The stability was judged by sedimentation time. As expected, the particles synthesized in BA showed higher compatibility with organic solvents, agglomerating in polar solvents such as water. The particles produced in TEG were more stable in polar solvents and did not agglomerate in water. As a high compatibility with aqueous systems is essential for the use in protein purification, for all functionalization and protein purification investigations the particles synthesized in TEG were used.

In the emg, single core magnetic iron-oxide nanoparticles were synthesized [*Lak et al., 2012*] by using an iron-oleate precursor. Initially 80 mmol of sodium oleate was poured into a round bottom flask connected to a Schlenk line and degassed three times using evacuation-filling with argon. Afterwards, 24 mmol of $FeCl_3 \cdot 6H_2O$ dissolved in 36 mL distilled water, 48 mL of ethanol and 84 mL of hexane were loaded into the flask using the Schlenk-line technique. The mixture was heated to reflux under flow of argon for 4 h. The obtained dark reddish top layer was intensively washed three times with 60 mL distilled water in a separatory funnel and next hexane was evaporated off using a rotary evaporator. The resultant reddish waxy product was dried in a vacuum oven at 70ºC for 24 h (**Fig. 1**).

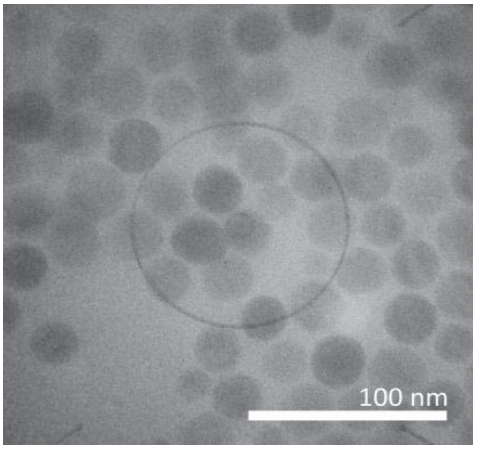

Fig. 1: TEM image of iron oxide nanoparticles from iron oleate.

In a typical MNPs synthesis procedure, 2 mmol iron-oleate, 6 mmol oleic acid and 7.8 g docosane (hydrocarbon $C_{22}H_{46}$, solid at room temperature) were loaded into a three-neck round bottom flask attached to a Schlenk-line and degassed for 30 minutes at 100ºC, ending by filling with argon. After that, the solution was heated to 370 ºC at a rate of 3 ºC/min (using a temperature controller) to reflux under flow of argon for 30 minutes. The resulting black suspension was cooled down to 60ºC. Afterwards, MNPs were washed and separated by adding a 4:1 acetone/hexane mixture and centrifuging the obtained solution. This process was repeated two times. The obtained MNPs are readily dispersible in chloroform due to the presence of oleic acid on their surfaces. This synthesis produces nanoparticles with up to 25 nm core size in narrow size distributions in organic solvents which are ideally suited for magnetic separation. The process was investigated and optimized for highest reproducibility to obtain the required volume samples for further size separation experiments prior to the stabilization and functionalization in aqueous solutions.

All magnetic nanoparticles were analyzed thoroughly by transmission electron microscopy, photon correlation spectroscopy and various magnetic measurement methods (Magnetorelaxometry, AC susceptibility, Magnetic Particle Spectroscopy) in cooperation with SFB subproject C6 (Schilling/Ludwig).

Functionalization of iron oxide nanoparticles

The functionalization of the iron oxide nanoparticles was performed in separate processing steps following the synthesis. The organic species covering the particle surface need to fulfill two purposes: First of all they have to stabilize the particles against agglomeration in aqueous media and second they need to enable the selective adsorption of the product protein from a cultivate supernatant. For this a system has to be found that allows a selective and reversible interaction with the product proteins. The recombinant antibody fragments produced in other subprojects of the SFB (A6 (Dübel/Hust), B8 (Franco-Lara)) featured a *His*-tag that could be utilized for purification. For a selective and reversible binding the well-known Ni-

nitrilotriacetic acid (Ni-NTA) complexation strategy [*Schäfer et al., 2002; Safarik et al., 2004*] was utilized. In contrast to commercial systems and other reports a purely covalent binding of the complexation group to the nanoparticles surface was targeted in order to ensure best stability and recyclability.

To achieve this objective various functionalization approaches were investigated. Initially, a two-step functionalization of the particles involving the binding of the protein-specific ligand via click chemistry was investigated (**Fig. 2**). First, (3-iodopropyl)-trimethoxysilane was bound to the particle surface. In a next step, the silane-modified nanoparticles were reacted with NaN_3 (DMF/H_2O) to obtain (3-azidopropyl)-functionalized particles. These particles could be successfully coupled to propargyl alcohol by means of click chemistry ($CuSO_4$ catalyst, THF/H_2O). However, the determination of the quantity of azide groups on the particle surface as well as their mode of binding turned out to be difficult. This strategy was abandoned also because of experimental difficulties experienced for the synthesis of ethynyl-substituted NTA derivatives.

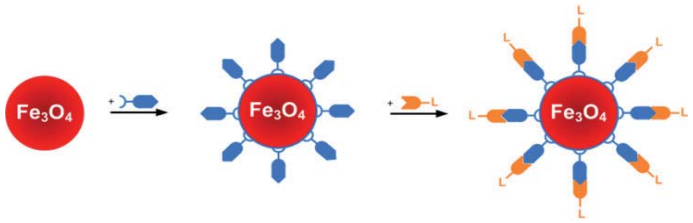

Fig 2: Two-step functionalization of the particles.

Alternatively, an easier experimentally strategy of coupling NTA via the amino- group of N_α,N_α-bis(carboxymethyl)-L-lysine was investigated. Therefore, three different silanes to be used as linkers were compared: (3-mercaptopropyl)-trimethoxysilane (MPTMS), (3-aminopropyl)trimethoxysilane (APTMS) and (3-glycidyloxypropyl)-trimethoxysilane (GLYMO). When modifying the iron oxide particles with MPTMS, strong agglomeration was observed. The stability for the nanoparticles modified with APTMS and GLYMO was comparable, being slightly better when using GLYMO. Hence, the further functionalization was carried out using GLYMO-modified particles (**Fig. 3**). Therefore, the synthesized particles were transferred to a 45 ml steel autoclave and the solvent TEG was added as well as a defined amount of $Fe(acac)_3$ and GLYMO. The addition of $Fe(acac)_3$ triggers a second growth step of the particles, which strongly enhances the binding of the silane. The reaction was left to proceed for variable time periods at 200°C.

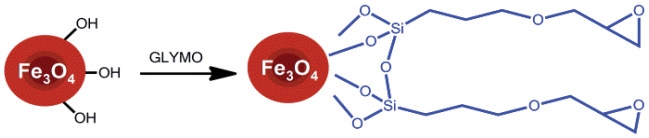

Fig. 3: First step: Functionalization with GLYMO.

In a second step, the ligand N_α,N_α-bis(carboxymethyl)-L-lysine was added to obtain NTA-functionalized nanoparticles (**Fig. 4**). A defined amount was added to the

washed particles and left to react at 55 °C overnight. In a last step an aqueous $NiSO_4$ solution was added to the particles. The Ni^{2+} ions induce the formation of a tridentate Ni-NTA complex that can specifically and reversibly immobilize recombinant proteins engineered with a 6x*His* tag.

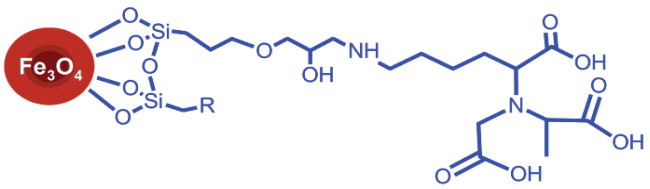

Fig. 4: Second step: Coupling with the ligand NTA.

The composition of the samples was determined by elementary analysis, examining the nitrogen content of the functionalized nanoparticles, which in combination with thermogravimetric analysis made possible a quantitative analysis of the NTA content of the nanoparticles. By the addition of dimethylglyoxime, a gravimetric analysis of the nickel content was carried out [*Tschugaeff, 1905*].

When performing purification experiments with the particles functionalized in this manner, difficulties were observed: The protein was selectively adsorbed but it was not possible to desorb the protein when using standard elution conditions (500 mM Imidazol and 100mM HEPES). Regarding this problem, prior to optimizing the functionalization of the particles the protein binding process and the elution conditions were evaluated. First of all experiments were carried out with pure solutions of recombinant antibodies obtained from subproject A6 (Dübel/Hust). It was confirmed by SDS-PAGE that the protein was bound and could be magnetically separated from the solution. By using suspensions of the culture medium provided by subproject B8 (Franco-Lara), the selective separation of the protein was verified. In both cases a subsequent separation of the protein from the particles was only possible with a highly acidic elution buffer which compromised the quality of the separated protein. Presumably, this was due to an unspecific adsorption of the ligand via free COOH or NH_2 groups directly to the particle surface instead of covalent coupling to GLYMO, possibly also permitting a direct interaction of the protein itself with the incompletely covered particle surface, resulting in unspecific and non-reversible binding.

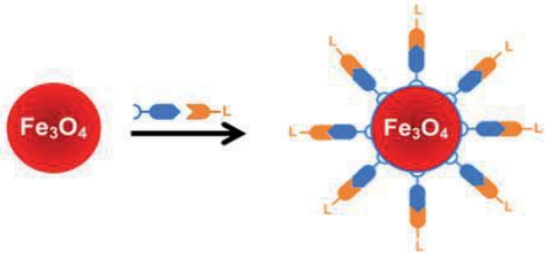

Fig. 5: One-step functionalization of the particles.

For this reason, a second approach was pursued where the functionalization of the particles was targeted with a one-step process (**Fig. 5**). Here, GLYMO is coupled to

the NTA derivate prior to the binding to the particle surface. For the one-step functionalization approach, different methods were investigated for a reliable coupling reaction of GLYMO to NTA that would also be feasible at large scales.

The first strategy was developed in analogy to the coupling of bis(benzimidazol-2-ylalkyl)amines to GLYMO as reported by Hoorn et al. [*Hoorn, 1997*]. The coupling reaction had to be modified due to the limited solubility of the NTA ligand in methanol. Thus, an aqueous solution of the ligand was added to GLYMO in a molar ratio of 1:1, followed by adjusting the pH to 11 and heating the mixture to 65 °C overnight, followed by evaporation of the water *in vacuo*. NMR spectroscopy however showed that no complete covalent linkage was achieved between ligand and silane, however under the used condition the polycondensation of GLYMO to silica started to occur, resulting in siloxy bonds preventing the subsequent binding of the silane to the nanoparticle surface.

Alternatively, the synthesis of GLYMO-NTA was performed in analogy to the procedure developed by Anspach [*Anspach, 1994*] for the reaction of GLYMO with iminodiacetic acid (IDA). Briefly, N_α,N_α-bis(carboxymethyl)-L-lysine was added to a mixture of 10 M NaOH and water at 0 °C. Then GLYMO was added dropwise (molar ratio of 1:1), and the mixture was stirred for 4 h at room temperature, then at 65 °C for 18 h. For the subsequent functionalization of the iron oxide nanoparticles, the pH of the reaction solution was adjusted to 11 and the solution subsequently added to the particles in an aqueous suspension. The reaction was left to proceed for 3 h at 95 °C. Afterwards the particles were magnetically separated and washed twice with H_2O. For the formation of the NTA-Ni complex, a variable amount of $NiSO_4$ aqueous solution was added and after 24 h the supernatant was removed and the particles dispersed in water. In analogy to the two-step approach, a quantitative analysis of the functionalization was carried out by elementary analysis. The quantity of NTA bound to the particle surface was determined based on the detected amount of nitrogen.

Protein purification experiments

The GLYMO-NTA particles obtained by the last-mentioned one-step approach were utilized for extensive investigations of protein purification. When adding the functionalized particles to the cell suspension obtained from subproject B8 (Franco-Lara), and staying in contact with the cell suspension for 20 min, the targeted protein was bound and could be magnetically separated from the impurities. After washing the particles three times with washing buffer consisting of culture medium and HEPES buffer, no non-specifically bound proteins were detected when analyzing the particles by SDS-PAGE, with only the desired protein attached to the particle surface. To improve the purification process, a detailed study was carried out varying the amount of GLYMO and NTA added to the particles. In **Fig. 6** the amount of protein purified with the particles functionalized with variable quantities of GLYMO-NTA (with a molar equivalent of $NiSO_4$ to NTA 1:1 for each system) is displayed, for the

samples directly after separation and after washing three times with the washing buffer. The densitometric analysis of the SDS-PAGE bands was carried out with the software imageJ™ .

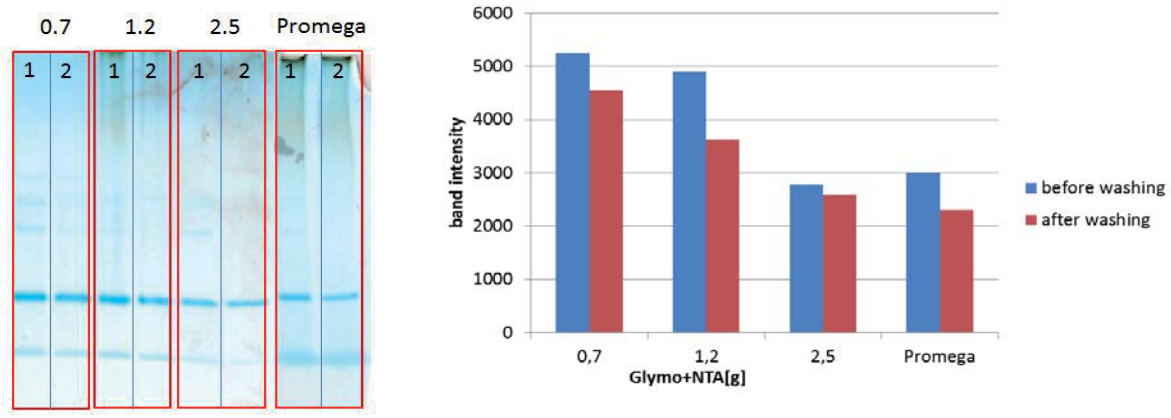

Fig. 6 Left: SDS-PAGE for different amounts of GLYMO-NTA bound to the particle surface in comparison with a commercial system; 1: band before washing, 2: after three washing steps. Right: band intensity indicating the amount of protein bound before and after washing the particles.

Interestingly, the amount of bound protein was found to be highest for a smaller amount of GLYMO-NTA used for the functionalization. Therefore, we conclude that due to the small particle size, steric hindrance prevents the adsorption of higher amounts of protein if the concentration of reactive sites bound to the particle surface is increased. Comparing the amount of protein bound before and after three washing steps, on the other hand, the sample treated with the highest concentration of GLYMO-NTA showed the least loss of bound protein, indicating a more stable binding. In comparison to the commercial Promega MagneHis™ system, it can be stated that the separation of the protein is very efficient, outperforming the commercial system for equal particle concentrations. Further experiments were carried out varying the amount of $NiSO_4$ added to the functionalized particles. Current results indicate that when adding a molar equivalent of 1:1 $NiSO_4$ to NTA, best performance with highest amount of protein bound to the particle surface is observed. When adding a molar ratio of 2:1, less protein was bound and the purification was less efficient.

The long-term stability of the GLYMO-NTA ligand was tested as well, by functionalizing particles with aged GLYMO-NTA that had been synthesized 14 days prior to functionalization. Interestingly, significantly higher amounts of protein were immobilized on the nanoparticles, with however very high losses observed during the washing steps. Therefore, the observed effect is attributed to unspecific binding in these samples. Furthermore, particles that were functionalized and then stored for a period of time prior to purification showed better performance with the concentration of bound protein being even higher before and after washing.

In addition to the NTA-Ni coupling approach, alternative purification strategies of the proteins were tested as well to highlight the flexibility of the system. For example, the single-step functionalization of the particles with N-phosphonomethyl iminodiacetic acid (PMIDA) following the protocol developed by Mohapatra et al. [*Mohapatra et al., 2010*] was carried out (**Fig. 7**). The nanoparticles were washed twice after the synthesis and then dispersed in water, adjusting the pH to 11. Various amounts of PMIDA were added and the mixture was shaken overnight. The particles were separated magnetically and dispersed in water adding variable amounts of $NiSO_4$. After 12 h, the supernatant with excess amounts of $NiSO_4$ was removed and the particles were redispersed in water.

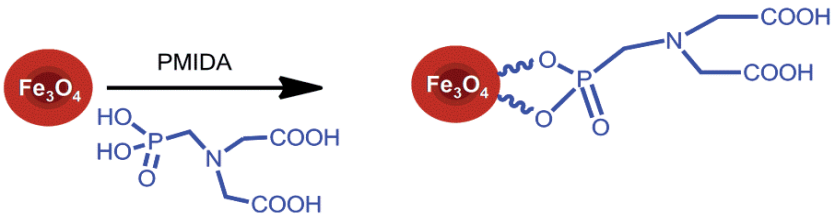

Fig. 7: Functionalization with PMIDA.

Protein purification experiments were carried out also for this system. The amount of protein bound to the PMIDA-functionalized particles was in the same range as for the previous system (**Fig. 8**). However, the stability of the binding was significantly higher, with only minor losses or even a little increase in band intensity (attributed to inhomogeneities in the medium during sample preparation) pointing to high stability during the 3-step washing treatment. When increasing the amount of PMIDA added to the particles, the detected protein concentration was higher; this trend however is verified in ongoing experiments. This system also showed to be more effective for equal particle concentration than the commercial system.

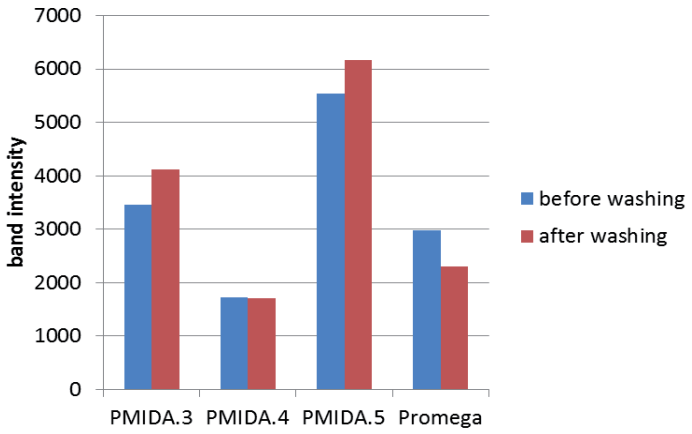

Fig. 8: Amounts of protein immobilized to the PMIDA-functionalized particles compared to the commercial system as detected by SDS-PAGE.

Optimization of the magnetic separation

For the separation experiments with functionalized magnetic nanoparticles a set-up providing the required magnetic gradients is needed. For these experiments commercially available magnetic columns employ permanent magnets. This simple approach works well with functionalized magnetic beads in commercial systems, containing a multitude of magnetic cores. This way the magnetic beads provide high magnetic moments and are enriched in the magnetic column in the magnetic field of a permanent magnet.

Functionalized magnetic single core particles as developed in this subproject possess much larger total surface and many more advantages as described above. On the other hand, due to their small size stronger magnetic fields with more homogenous magnetic field gradients are desirable both to achieve a fractionation of the nanoparticles and to ensure an optimum protein purification.

From all simulation calculations, also for magnetic particle imaging – as described in subproject C6 (Schilling/Ludwig) – we know that air coil magnets will not provide the necessary forces for reliable separation. Therefore, larger electromagnets with high permeable cores were employed, resulting in the set-up depicted in **Fig. 9**. With this set-up experiments for the magnetic separation have been realized.

Fig. 9: Set-up with an electromagnet for magnetic separation of magnetic nanoparticles with a commercial magnetic column from Miltenyi Biotec GmbH.

To investigate the efficient magnetic separation of the particles from the cell suspensions, a series of experiments was carried out with dispersions of the functionalized particles before and after addition of $NiSO_4$, as the addition of $NiSO_4$ triggered an agglomeration of the particles due to higher ionic strength in the medium. The core size of the magnetic particles used for these investigations was about 10 nm, whilst the hydrodynamic diameter as measured by DLS was around 25 nm for the aqueous dispersion, increasing to 900 nm after $NiSO_4$ addition.

As visible in **Fig. 10**, with an increasing magnetic field strength a larger fraction of nanoparticles is withheld in the magnetic column. Whilst a field strength of around 100 mT is required to withhold all particles with a hydrodynamic diameter of 25 nm, after addition of $NiSO_4$ all particles were withhold even at a magnetic field strength of 20 mT, indicating that agglomerated particles behave similarly to multicore magnetic particles and can be efficiently separated with the available set-up.

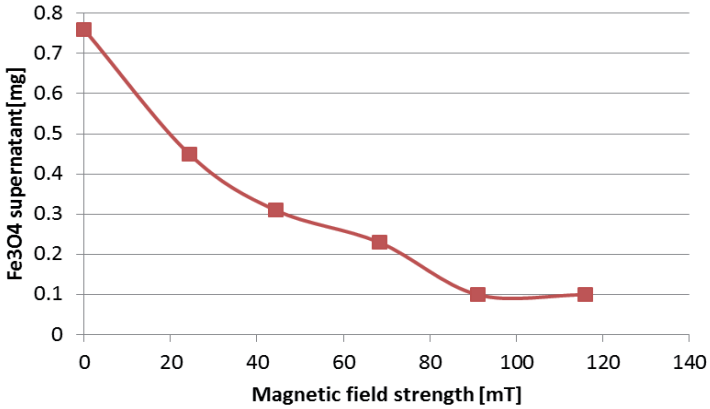

Fig. 10: Separation experiments of the particles from aqueous dispersion when varying the magnetic field strength.

3.2.1.3 References to other works and collaborations in the SFB

Cooperations with the following sub-projects within the SFB were maintained:

Subproject A6 (Dübel/Hust): collaboration on the selective immobilization of antibodies to the functionalized nanoparticles, using samples of recombinant antibodies obtained from this subproject; know-how exchange on selection of ligands for antibody purification.

Subproject B8 (Franco-Lara): extensive collaboration on the purification of antibodies using culture suspensions obtained from this subproject; currently, the use of magnetic nanoparticles for product removal during the cultivation is being investigated; collaboration on protein analytics (SDS-PAGE, ELISA).

Subproject C2 (Seidel-Morgenstern): know-how exchange on selective immobilization strategies of different proteins.

Subproject C6 (Schilling/Ludwig): magnetic particle imaging, analytics of magnetic nanoparticles.

3.2.1.4 Comparison with research outside the SFB

The magnetic separation of biomolecules by use of iron oxide nanoparticles is a widely investigated field. Within Germany, larger research projects on this topic are established especially at Karlsruhe Institute of Technology, where larger EU projects Nanobiomag and MagPro2Life on the establishment of magnetic separation methods also on larger scale have been/are coordinated. Here, also the continuous removal of

biosurfactants from biotechnological production by magnetic separation has been reported [*Heyd, 2011*], as well as the in situ separation of proteases [*Käppler, 2009*]. However, large multicore particles of µm in size were used, with the magnetic nanoparticles being prepared by standard precipitation processes and encapsulated in silica [*Käppler, 2009*] or in alginate beads [*Heyd, 2011*]. In other works, the purification is achieved via magnetic beads [*Hickstein et, 2008; Käppler et al., 2008*].

The use of covalently functionalized individual Fe_3O_4 single-core nanoparticles for magnetic separation obtained from nonaqueous processes, as targeted in this project, has to the authors' knowledge not been investigated elsewhere yet. Although some first works showed that individual metal-core nanoparticles could be functionalized and used for selective protein adsorption using *His*-tagged GFP [*Xu et al., 2004; Lee et al., 2006*], the state of agglomeration of these functionalized nanoparticles was not discussed, and also scale-up and reproducibility issues were not investigated. In another report on the use of Ni-decorated iron oxide nanoparticles, on the other hand no covalent functionalization strategy was realized, but the unspecific adsorption of Ni^{2+} to stabilized iron oxide nanoparticles, which represents a much less defined system [*Lee and Lee, 2007*]. For such systems, no reversibility and recyclability of the nanoparticles can be expected.

3.2.1.5 Literature

Beari, F.; M. Brand; et al. (2001) Organofunctional alkoxysilanes in dilute aqueous solution: new accounts on the dynamic structural mutability. *J. of Organometallic Chemistry* 625(2), 208-216

Ansbach, B. F. (1994) Silica-based metal chelate affinity sorbents I. Preparation and characterization of iminodiacetic acid affinity sorbents prepared via different immobilization techniques. *J. of Chromatography A* 672(1–2), 35-49

Heyd, M.; Franzreb, M.; Berensmeier, S. (2011) Continuous rhamnolipid production with integrated product removal by foam fractionation and magnetic separation of immobilized *Pseudomonas aeruginosa*. *Biotechnol. Prog.* 27(3), 706-716

Hickstein, B.; Peuker, U.A. (2008) Characterization of protein capacity of nanocation exchanger particles as filling material for functional magnetic beads for bioseparation purposes. Biotechnol. Prog. 24(2), 409-416.

Hoorn, H. J.; de Joode, P.; Dijkstra, D. J.; Driessen, W. L.; Kooijman, H.; Veldman, N.; Spek, A. L.; Reedijk, J. (1997) Metal-binding affinity of a series of bis-benzimidazoles immobilized on silica. *J. of Materials Chemistry* 7(9), 1747-1754

Käppler, T.; Hickstein, B.; Peuker, U.A.; Posten, C. (2008) Characterization of magnetic ion-exchange composites for protein separation from biosuspensions. *J. of Bioscience and Bioengineering* 105(6), 579-585

Käppler, T.; Cerff, M.; Ottow, K.; Hobley, T.; Posten, C. (2009) In situ magnetic separation for extracellular protein production. Biotechnol. Bioeng. 102 (2), 535-545

Lee, I.S.; Lee, N.; Park, J.; Kim, B.H.; Yi, Y.-W.; Lee, I.H.; Paik, S.R.; Hyeon, T. (2006) Ni/NiO core/shell nanoparticles for selective binding and magnetic separation of histidine-tagged proteins. *J. of the American Chemical Society* 128(33), 10658-10659

Lee, K.S.; Lee, I.S. (2007) Decoration of superparamagnetic iron oxide nanoparticles with Ni^{2+}: agent to bind and separate histidine-tagged proteins. *Chemical Communications* (6), 709-711

Massart, R. (1981) Preparation of aqueous magnetic liquids in alkaline and acidic media. *IEEE Transactions on Magnetics* 17(2), 1247-1248

Mohapatra, S.; Pramanik P. (2009) Synthesis and stability of functionalized iron oxide nanoparticles using organophosphorus coupling agents. *Colloids and Surfaces A: Physicochemical and Engineering Aspects* 339(1–3), 35-42

Safarik, I.; Safarikova, M. (2004) Magnetic techniques for the isolation and purification of proteins and peptides. *Biomagnetic Research and Technology* 2, 7

Schäfer, F.; Römer, U.; Emmerlich, M.; Blümer, J.; Lubenow, H.; Steinert, K. (2002) Automated high-throughput purification of 6xHis-tagged proteins. *J. of Biomolecular Techniques* 13(3), 131-142

Tschugaeff, L. (1905) Über ein neues, empfindliches Reagens auf Nickel. *Berichte der deutschen chemischen Gesellschaft* 38(3), 2520-2522

Xu, C.; Xu, K.; Gu, H.; Zhong, X.; Guo, Z.; Zheng, R.; Zhang, X.; Xu, B.(2004) Nitrilotriacetic Acid-Modified Magnetic Nanoparticles as a General Agent to Bind Histidine-Tagged Proteins. *Journal of the American Chemical Society* 126, 3392-3393

3.2.2 Project relevant own publications

a) Works that have appeared in publications of a scientific quality assurance at the time of application or final adoption, and book publications

Grabs, I.-M.; Bradtmöller, C.; Menzel, D.; Garnweitner, G. (2012) Formation mechanisms of iron oxide nanoparticles in different nonaqueous media. *Crystal Growth and Design* 12, 1469-1475

Lak, A.; Wawrzik, T.; Ludwig, F.; Schilling, M. (2012) Synthesis of Single-Core Iron Oxide Nanoparticles as a Potential Tracer for Magnetic Particle Imaging. Proceedings of IWMPI, Lübeck 2012, Springer-Verlag (in press)

Lak, A.; Ludwig, F.; Grabs, I.-M.; Garnweitner, G.; Schilling, M. (2010) Influence of Synthesis Parameters on Magnetization and Size of Iron Oxide Nanoparticles. AIP Conference Proceedings 1311, 224-230

Wawrzik, T.; Ludwig, F.; Schilling, M. (2010) Two-dimensional magnetic particle imaging. Magnetic Nanoparticles – Particle Science, Imaging Technology, and Clinical Applications, Proceedings of First International Workshop on Magnetic Particle Imaging, World Scientific, 100-105

Wawrzik, T.; Ludwig, F.; Schilling, M. (2009) Assembly for One-dimensional Magnetic Particle Imaging. IFMBE Proceedings 25/II, 898-900

b) other publications

Grabs, I.-M.; Garnweitner, G. (2011) Formation mechanisms of magnetic nanoparticles in non aqueous media. 8th European Congress of Chemical Engineering, Berlin, 25.-29. 09. 2011

Grabs, I.-M.; Garnweitner, G. (2010) Gezielte Funktionalisierung magnetischer Nanopartikel zur Aufreinigung von Biomolekülen. Chemie Ingenieur Technik 82, 1576-1577

Grabs, I.-M.; Garnweitner, G. (2010) Gezielte Funktionalisierung magnetischer Nanopartikel zur Aufreinigung von Biomolekülen. 28. Dechema-Jahrestagung der Biotechnologen und ProcessNet-Jahrestagung, Aachen, 23. 09. 2010

Grabs, I.-M.; Garnweitner, G. (2010) Functionalisation of magnetic nanoparticles for protein purification. 6th World Congress on Particle Technology, Nürnberg, 26.-29. 04. 2010

Lak, A.; Wawrzik, T.; Remmer, H.; Ludwig, F. and Schilling, M. (2011) In-situ study of iron oxide nanoparticle growth kinetics by means of magnetic particle spectroscopy. Ferrofluid workshop 2011

M. Schilling, invited talk, Okinawa Institute of Science and Technology, Okinawa, Japan, Biomedical imaging of function: Brain-Computer-Interface and magnetic Nanomarkers (10.03.2010)

M. Schilling, invited talk, Colloquium of SFB 855 (Kiel), EKG und EEG mit kapazitiven Elektroden - Prinzip und Anwendungen (27.06.2012)

3.3 Looking back on the promotion

The project has been funded since July 2008 in the SFB 578. It was completed on June 2012 with the end of the program.

3.3.1 Personnel in the project

	Name, acad. degree, service position	narrower subject of the employee	Institute of University or non-university facility	Participation in the project in hours per week	Category
Basic staff					
Research associate (incl. auxiliary power)	1. G. Garnweitner, Prof. Dr. rer. nat.	Nanotechnology, Materials science	Institute for Particle technology (iPAT)	10	Professorship
	2. M. Schilling, Prof. Dr. rer. nat.	Physics, Electrotechnics	emg	4	Professorship
Non academic staff	3. C.-D. Laser	Technical Assistent	iPAT	8	Technical staff
	4. B. Kuhn	Technical Assistent	emg	4	Technical staff
	5. H. Schmidt J. Pförtner H. Müller	Workshop		4	Technical staff
Supportive staff					
Research associate (incl. auxiliary power)	6. D. Laventine, Dr. rer. nat.	Chemistry	iPAT	40	Post Doc
	7. I.-M.Grabs, Dr. rer. nat.	Chemistry	iPAT	40	Post Doc
	8 I. Masthoff, Dipl.-Ing.	Biochemical Engineering	iPAT	40	PhD student
	9. M. Gerloff, Dipl.-Wi-Ing.	Electrical Engineering	emg	8	PhD student
	10. C. Brendel, Dipl.-Ing.	Electrical Engineering	emg	8	PhD student
	11. A. Hirsch, Dipl.-Phys.	Electrical Engineering	emg	8	PhD-student
	12 R. Piel, Dipl.-Ing.	Electrical Engineering	emg	8	PhD student
	13 D. Rühmer, Dipl.-Ing.	Electrical Engineering	emg	8	PhD student
	14 C. Kuhlmann	Electrical Engineering	emg	8	PhD student
	15 Aidin Lak, MSc Mat. Sci.	Electrical Engineering	emg	40	PhD student
Non academic staff	16. A. Becker Stud. assistant	Biochem. Engineering		10	Student

Responsibilities of employees (basic staff)

Position 1 :

Prof. Dr. G. Garnweitner is head of the junior research group “Nanoparticles and Nanocomposites” at iPAT. He supervised this project as project leader for the iPAT.

Position 2 :

Prof. Dr. M. Schilling is head of the EMG. He supervised this project as project leader for the emg.

Position 3:

C.-D. Laser is part of the technical staff working at iPAT He provided help regarding the characterization processes of the synthesized nanoparticles.

Position 4:

B. Kuhn is technical specialist working at the EMG. He is in charge of routine maintenance of all installation.

Position 5:

H. Schmidt, H. Müller and J. Pförtner are working in the mechanical workshop at the EMG and supported the sub-project installing all necessary equipment needed for the magnetic separation column.

Responsibilities of employees (supportive staff)

Positions 6,7,8:

D. Laventine, I.-M. Grabs and I. Masthoff planned, coordinated and performed the main synthetic and analytical works on behalf of the iPAT. Focus of their work was the development, investigation and optimization of the nonaqueous nanoparticle synthesis as well as the functionalization of the nanoparticles, their characterization and performance of purification experiments.

Positions 9-15:

Aidin Lak prepared the magnetic nanoparticles in emg and optimized the preparation for high reproducibility. He also investigated in Monte-Carlo-Simulations the agglomeration behaviour. M. Gerloff, C. Brendel, A. Hirsch, R. Piel, D. Rühmer and C. Kuhlmann contributed to the separation set-up investigations both experimentally and by simulations.

Position 16: Student assistant

The student assistant Andre Becker supported the experimental work regarding the synthesis and functionalization of the iron oxide particles. He helped with routine laboratory work.

3.0 Project area D: Application technique

Project-No.	Topic	Disciplines and field of work	Project manager, institution
D1	Drug delivery systems for the controlled release of proteins	Polymer chemistry, Pharmaceutical technology	H. Menzel, Institut für Technische Chemie, TU BS / H. Bunjes, Department of Pharmaceutical Sciences, TU BS
D2	Microchips for protein analytics and diagnostics	Biochemical analytics, Protein engineering, Lab-on-chip	S. Büttgenbach, Institute for Microtechnology, TU BS / S. Dübel, Department of Biotechnology, TU BS

3.1 General information on the completed project D1

3.1.1 Topic

Drug delivery systems for the controlled release of proteins

3.1.2 Disciplines and field of work

Polymer Chemistry, Pharmaceutical Technology

3.1.3 Project manager

Prof. Dr. Henning Menzel
(b.: 14.02.1961)
Institut für Technische Chemie
TU Braunschweig
Hans-Sommer-Str. 10
38106 Braunschweig
Phone: 0531/391-5361
Fax: 0531/391-5357
E-mail: h.menzel@tu-bs.de

Prof. Dr. Heike Bunjes
(b.: 09.02.1967)
Institut für Pharmazeutische Technologie
TU Braunschweig
Mendelssohnstr. 1
38106 Braunschweig
Phone: 0531/391-5657
Fax: 0531/391-8108
E-mail: heike.bunjes@tu-bs.de

3.2 Development of the subproject D1

3.2.1 Report

3.2.1.1 Current knowledge at the last application and initial question

Drug delivery systems (DDS) based on degradable hydrogels are promising candidates for the controlled delivery of therapeutic proteins [*Peppas et al., 2000*]. Due to the high water content hydrogels show low tissue irritation and provide a good environment for protein incorporation. The crosslinked polymer network can protect the protein from *in vivo* degradation and side effects may be minimized by a local application of the DDS, for example in the form of injectable microspheres [*van de Weert et al., 2005*]. The protein is incorporated during the gelation process and then released by diffusion and network degradation [*van Dijk-Wolthuis et al., 1997*]. Important parameters for the controlled release are therefore the density of the network, its degradation properties and the molecular size of the incorporated active substance [*Kamath and Park, 1993*].

The general aim of this project is the development of novel hydrogel-forming polymers and corresponding hydrogel delivery systems for the controlled release of therapeutic proteins like antibodies (**Fig. 1**).

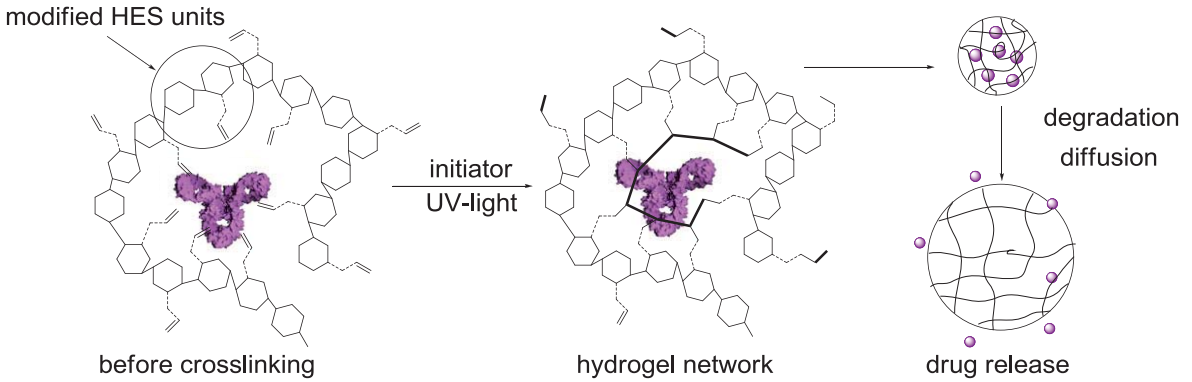

Fig. 1: Incorporation of the protein during hydrogel formation by photo-crosslinking and subsequent release by protein diffusion and degradation of the polymer network.

During the preceding funding period hydroxyethyl starch (HES) with crosslinkable hydroxyethyl methacrylate side groups (HES-HEMA) was synthesized and characterized. Hydrogels were produced by photopolymerization. Variation in the degree of substitution (DS) resulted in adjustable network densities and consequently in variable release kinetics. Because of their limited water solubility, the processability of HES-HEMA polymers was not optimal. Hydrogels displayed some turbidity caused by phase separation processes during crosslinking. In addition, HES-HEMA based hydrogel microspheres had encapsulation efficiencies for FITC-dextran 70 kDa of less than 60 % and a high initial burst release was observed for these systems. For the administration of pharmaceutically relevant proteins higher encapsulation efficiencies are preferable. Moreover, a burst release is usually undesired in controlled release applications.

In the current period the project thus aimed at the development and synthesis of optimized hydroxyethyl starch based derivatives with better water solubility. Scale up of the polymer synthesis was another important issue to supply enough material for a comprehensive characterization of the resulting hydrogels and for the performance of *in vitro* and *in vivo* release studies. To create a rationale for the development of hydrogel delivery systems for the controlled release of protein drugs the correlations between network density of the hydrogels, diffusion processes within the network and the release kinetics for differently sized incorporated substances have to be evaluated. A comparison of the *in vitro* and *in vivo* release behavior is necessary to provide information on the suitability of the *in vitro* methods to predict the release under *in vivo* conditions.

3.2.1.2 Results and applied methods

Optimization of polymer synthesis and bulk hydrogel formation

Hydroxylethyl starch (HES 130 kDa/DS 0.4) has a good water solubility and biocompatibility and was therefore used as starting material for an improved prepolymer. New crosslinkable HES derivatives were synthesized. For the modification of hydroxyethyl starch, methacrylate groups were linked either directly to the HES backbone via an ester bond (HES-MA) or via polyethylene glycol spacers with 6 or 10 ethyleneoxide units and a

carbonate group (HES-P(EG)$_6$MA, HES-P(EG)$_{10}$MA). The HES-P(EG)$_n$MA derivatives were produced in a two step synthesis via carbonyldiimidazole (CDI) activation of polyethylene glycol methacrylate following a general synthetic route first described by van Dijk-Wolthuis et al. (*1997*) (**Fig. 2**).

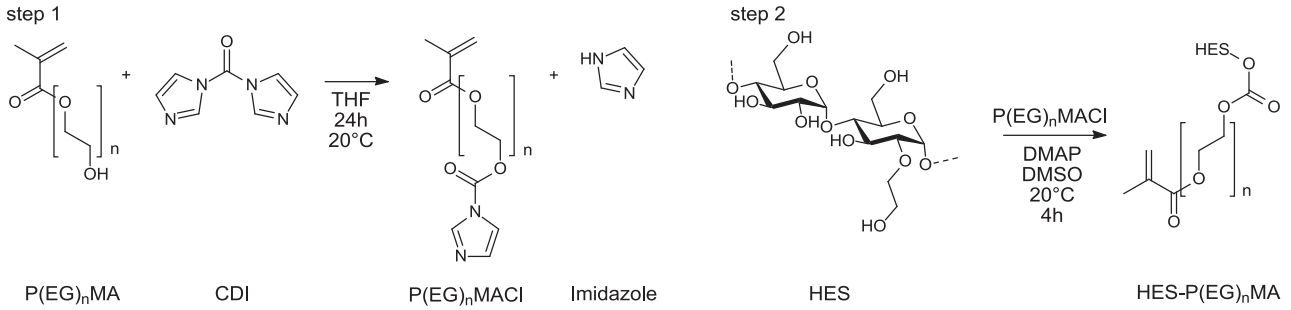

Fig. 2: Synthesis of HES-P(EG)$_n$MA derivatives via initial activation of P(EG)$_n$MA using CDI.

Because of the oligoethylene glycol spacer HES-P(EG)$_n$MA polymers have improved water solubility as compared to HES-HEMA. Carbohydrates with this type of linker are degraded by hydrolysis of the carbonate ester linkage [*van Dijk-Wolthuis et al., 1997*]. In case of HES-MA a methacrylate group was bound to the HES backbone via an ester linkage (**Fig. 3**).

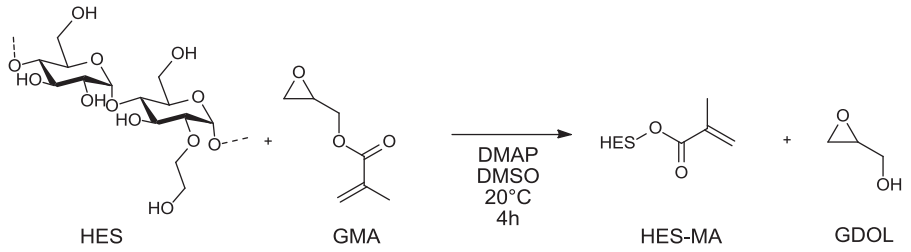

Fig. 3 Synthesis of HES-MA using GMA to directly link a methacrylate group on the starch backbone.

Direct linkage via an ester bond leads to a higher stability against hydrolysis [*van Dijk-Wolthuis et al., 1997*]. For both polymer series (HES-P(EG)$_n$MA and HES-MA) different degrees of substitutions (DS) are accessible allowing adjustable network densities. Each synthesis was optimized regarding the reaction time, reproducibility and addition of inhibitors and scaled up to batches with a polymer yield of up to 50 g. Depending on the DS clear HES-MA and HES-P(EG)$_6$MA solutions in the range of 10 – 30 wt% could be prepared which allowed additional variation of the hydrogel crosslinking density. HES-P(EG)$_{10}$MA solutions with more than 10 wt% were turbid.

The methacrylate groups of both polymer types enabled photo-crosslinking in the presence of an initiator. To optimize the crosslinking parameters swelling measurements and oscillation rheology were performed. In **Fig. 4A** the swelling ratios of HES-MA and HES-P(EG)$_6$MA hydrogels prepared from differently concentrated solutions are plotted as

function of time. The results show a strong influence of the polymer concentration on the network density. However, also the polymer type and the DS (data not shown) influence crosslink density. For HES-MA higher degrees of substitution are necessary to obtain approximately the same network density as for HES-P(EG)$_6$MA. This is probably caused by reduced mobility of the methacrylic group in the course of the crosslinking process.

UV-irradiation time and initiator concentration were optimized to minimize the risk of protein damage by radicals [*Lin et al., 2007*]. Typically the photoinitiator Irgacure®2959 was used, however this initiator has limited water solubility and is effective only with light of a wavelength below 370 nm. Therefore, lithium phenyl-2,4,6-trimethylbenzoyl-phosphinate (LAP) was synthesized according to Fairbanks et al. [2009]. This initiator exhibits a similarly low cytotoxicity, but better water solubility and can be used at wavelengths of 366-405 nm [*Fairbanks et al., 2009*].

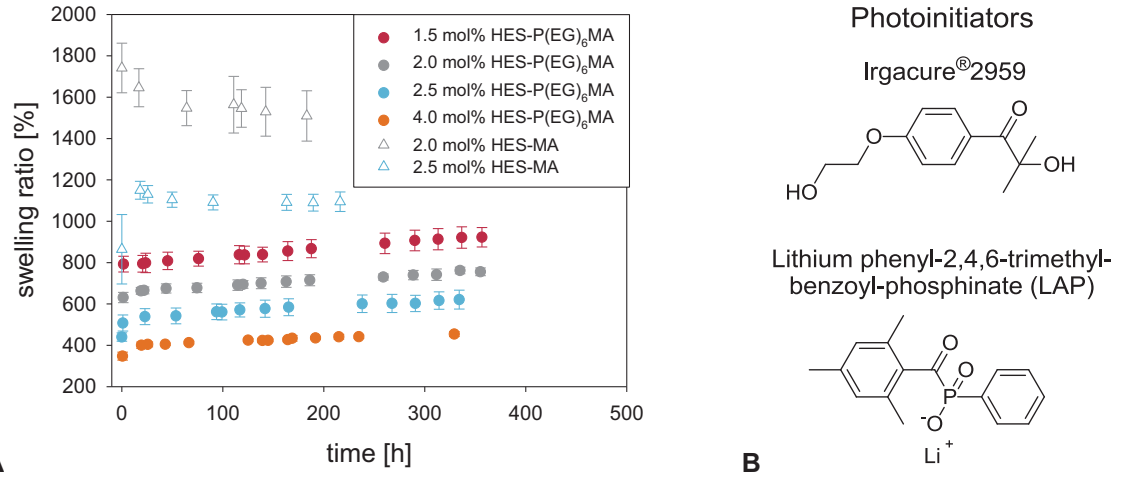

Fig. 4: Influence of polymer type and concentration on the swelling ratio (phosphate buffer pH 7.4) of bulk hydrogels for HES-MA (DS 0.05) and HES-P(EG)$_6$MA (DS 0.05) crosslinked using 0.02 wt% LAP for 20 min at 405 nm (mol fraction calculated using average molar mass of repeating units; M_{HES}(178 g/mol)+$M_{sidegroup}$xDS= 183 g/mol for HES-MA and 197 g/mol for HES-P(EG)$_6$MA) (A); photoinitiators used for hydrogel formation (B).

Production and characterization of hydrogel microspheres

Hydrogel microspheres were prepared by a water-in-water emulsion process (**Fig. 5**) according to a general procedure developed for HES-HEMA in the preceding funding period [*Schwoerer et al., 2010*]. The preparation process was optimized for the new polymers (HES-MA and HES-P(EG)$_n$MA) and the influence of the type and amount of incorporated substances on the particle size distribution and encapsulation efficiency was studied in detail.

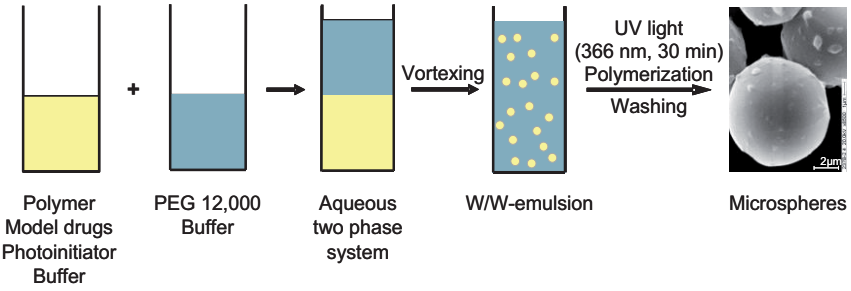

Fig. 5: Production process of hydrogel microspheres by a water-in-water emulsion method.

After optimization all microsphere batches produced showed narrow particle size distribution with a d50 value of around 10 µm (**Fig. 6A**). Investigation of the encapsulation efficiency resulted in higher incorporated amounts of 80 to 98 % for FITC-dextran 70 kDa (FD70) in HES-MA and HES-P(EG)$_6$MA hydrogel microspheres (**Fig. 6B**) compared to the previously studied HES-HEMA as well as HES-P(EG)$_{10}$MA (< 75%). The uniform distribution of FD70 within hydrogel microspheres was confirmed by confocal laser scanning microscopy. Since HES-P(EG)$_{10}$MA and HES-HEMA showed lower water solubility and encapsulation efficiencies, the other two polymers (HES-P(EG)$_6$MA and HES-MA) were used for further studies.

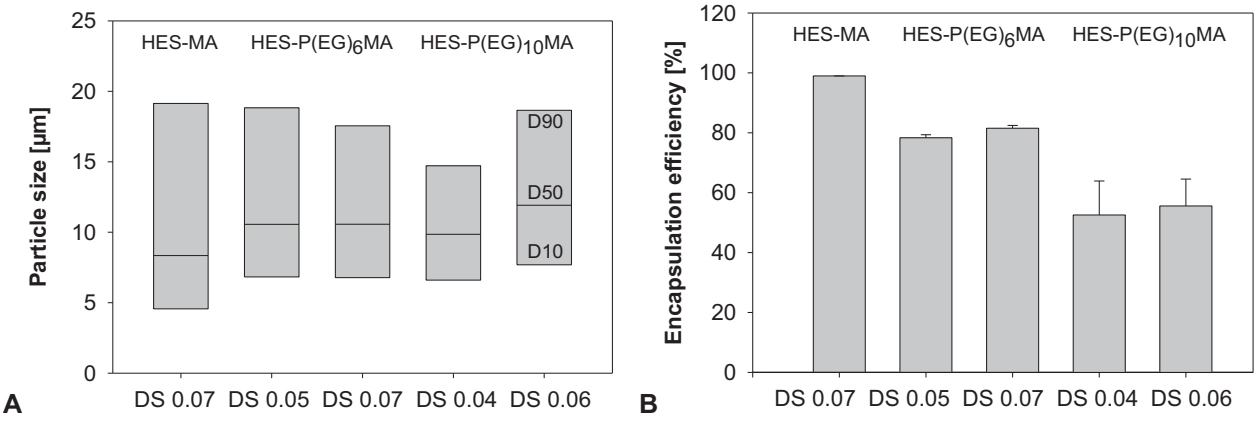

Fig. 6: Particle size distributions (A) and encapsulation efficiencies (B) of FITC-dextran 70 kDa containing hydrogel microspheres produced by the standard procedure from various polymers with different degree of substitution.

Hydrogel structure

Because the hydrogel structure and network density are supposed to determine drug diffusion and release rate [*Franssen et al., 1999*] these parameters were further investigated. A porous structure was observed for hydrogel discs using cryo-SEM (**Fig. 7A**). The pore sizes decreased with increasing polymer concentration, which may be regarded as a consequence of the increased network density. The pore size of microspheres was found to be similar to those of 20-30 wt% gel discs (**Fig. 7B**). Since the mesh sizes calculated from swelling data obtained with hydrogel discs were two orders of

magnitude smaller than the pores observed by SEM, a hydrogel structure having pores and meshes has to be assumed.

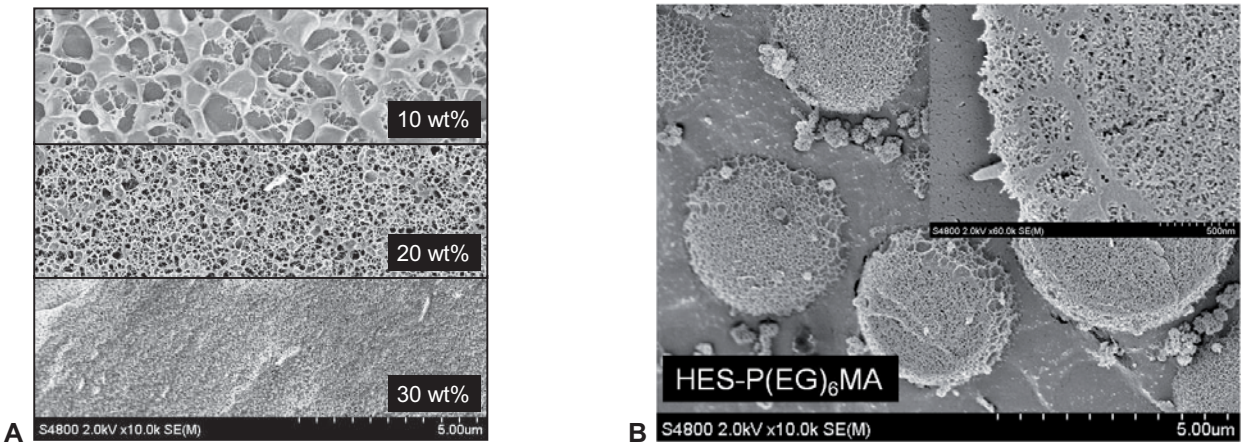

Fig. 7: Cryo-SEM images of bulk hydrogels with different polymer concentrations (A) and of HES-P(EG)$_6$MA microspheres (B).

With this model of the hydrogel structure (**Fig. 8**) the experimental data obtained in release studies (described below) can be explained. Initial burst release is probably caused by diffusion from the pore volume. The fraction of substances entrapped in the much smaller meshes can only be released by diffusion after degradation of the network. Since this process is much slower a constant release over a long period is observed.

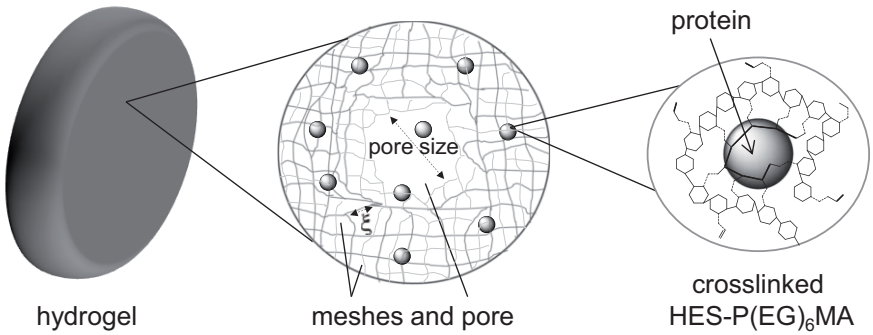

Fig. 8: Scheme of hydrogel structure containing pore and meshes.

Measurements of mobility within the hydrogel

The protein mobility and the influence of network density on diffusion processes within the polymer network are of particular interest to understand the release rates observed. Green fluorescent protein (GFP) loaded bulk hydrogels were nondestructively analyzed by fluorescence anisotropy and fluorescence recovery after photobleaching (FRAP). The data provide information about the rotational and translational diffusion of GFP inside the hydrogel. The results of fluorescence anisotropy decay showed that GFP rotation is mainly retarded by the viscosity of the solution. Since the differences in GFP rotation before and after crosslinking were quite low, a binding of GFP to the polymer matrix to a large extent seems unlikely (**Fig. 9A**). Comparison of the results for macroscopic hydrogel samples

with those obtained with GFP loaded hydrogel microspheres provide information about the polymer concentration of the particles. Although a 2 wt% polymer solution was used for particle preparation, the resulting microspheres showed a GFP rotation similar to bulk gels with 20-30 wt% polymer (**Fig. 9B**). Consequently, it has to be assumed that the gel forming polymers are concentrated in the w/w-emulsion process. This hypothesis is supported by comparison of pore sizes determined by cryo-SEM (Fig. 7).

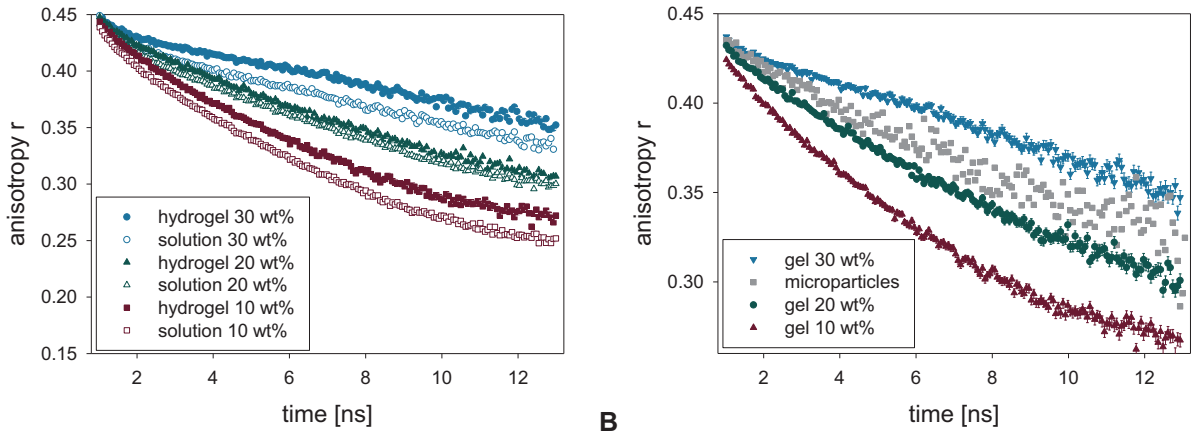

Fig. 9: Anisotropy decay of green fluorescent protein in different HES-P(EG)$_6$MA (DS 0.05) solutions before and after crosslinking (A) and in hydrogel microspheres and hydrogel discs with different polymer concentrations (B).

Fluorescence recovery after photobleaching (FRAP) provided information about the translational diffusion of GFP. A small area of the sample was photobleached and the diffusion of intact GFP from the surroundings was observed for a period of 3 h. The translational diffusion was strongly hindered for crosslinked samples (**Fig. 10**). This result suggested that GFP is trapped within the meshes of the hydrogel. Release can only occur after degradation of the polymer network.

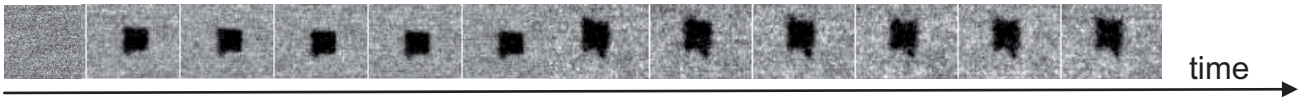

Fig. 10: FRAP images of GFP in a HES-P(EG)$_6$MA (20 wt%, DS 0.05) hydrogel disc. Time increases from left (0=before bleaching) to right (3 h after bleaching).

Another nondestructive characterization method based on the magnetic relaxation behavior of embedded superparamagnetic nanoparticles (MNPs) was used to study the mobility within hydrogel systems (described in detail in the report of C6). With fluxgate magnetorelaxometry (MRX) measurements, hydrogel polymerization kinetics and physical entrapment capacity were analyzed [*Heim et al., 2007, 2008*]. In addition the release of MNPs was studied and correlated with the crosslinking time during the production process. In addition, the influence of the macroscopic structure (bulk cylinders or microspheres) was studied for HES-P(EG)$_6$MA hydrogels. The results were in good agreement with those from conventional release studies performed by the half-change method (see below). The MRX measurements also indicated that a certain amount of entrapped MNPs are still able

to rotate within hydrogel meshes and therefore are able to undergo Brownian relaxation. Hence, the combination of MRX and fluorescence methods led to a better understanding of the mobility of incorporated substances in hydrogel network structures.

Influence of hydrogel structure on the *in vitro* release

The influence of the type of hydrogel-forming polymer, the polymer concentration and the size of incorporated FITC-labeled dextrans, IgG and scFv on the release from hydrogel cylinders and microspheres was investigated. The release profiles depended on the type of polymer: HES-P(EG)$_n$MA and HES-MA resulted in less burst release and more constant release profiles compared to the previously studied HES-HEMA polymers. With increasing polymer concentration (**Fig. 11A**) and therefore higher network density the burst release became less pronounced. Presumably, more of the encapsulated substance is entrapped in the hydrogel meshes and the smaller pores. Despite the difference in size and with that in surface to volume ratio, hydrogel cylinders and microspheres showed similar release rates, when a concentration of ~25 wt% is assumed for the microspheres (see above). The release of differently sized substances (FITC-dextran 20, 70, 150, 250, 500 kDa, FITC-scFv, FITC-IgG) from HES-P(EG)$_6$MA (DS 0.05) hydrogel microspheres was studied under accelerated conditions (human serum as release medium, **Fig. 11B**). The results revealed that the ratio between the hydrodynamic diameter of the incorporated substance on one hand and the pore and mesh size of the hydrogel on the other hand are the essential parameters defining the release kinetics. The comparison of the release profiles of dextrans with an IgG antibody and an antibody fragment (the latter was produced in cooperation with subproject A6) confirmed the good suitability of FITC-dextrans as model substances for the release studies.

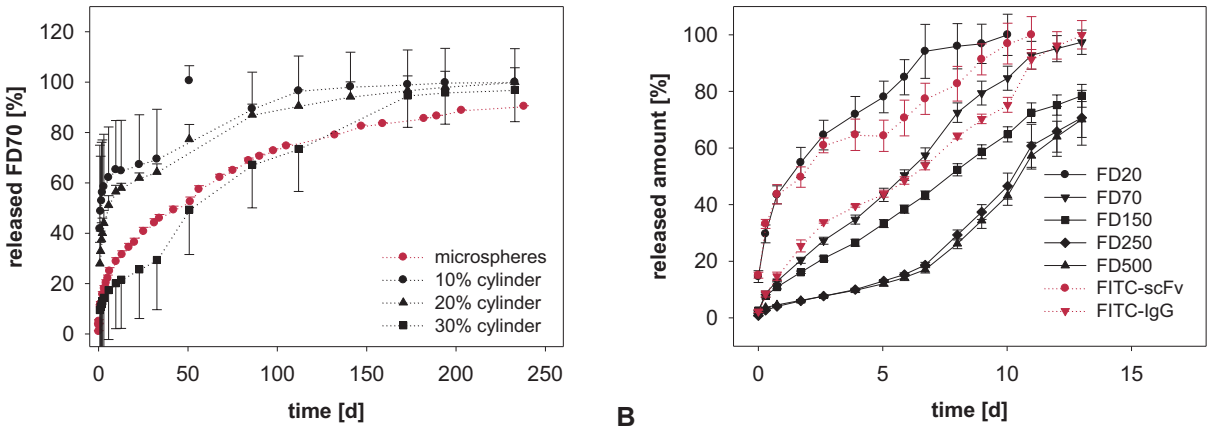

Fig. 11: Comparison of release profiles from hydrogel microspheres and hydrogel cylinders (polymer concentration 10, 20, 30 %) with incorporated FD70 (+ or - standard deviation), (A) and release profiles from HES-P(EG)$_6$MA (DS 0.05) hydrogel microspheres with incorporated FD20, FD70, FD150, FD250, FD500, FITC-scFv, FITC-IgG (± standard deviation) (B).

In vitro - in vivo correlation

Due to a limited comparability with *in vivo* conditions *in vitro* release studies may not be highly predictive for the *in vivo* release behavior. To identify *in vitro* release conditions leading to results that reflect the *in vivo* behavior as closely as possible comparative studies were performed in PBS (pH 7.4), in PBS containing α-amylase, in carbonate buffer (pH 9.6) and in human serum (pH 7.2).

In vitro release studies in PBS showed a sustained release of incorporated FITC-labeled IgG from hydrogel discs (**Fig. 12A**). For HES-P(EG)$_6$MA hydrogel discs the release kinetics changed when human serum was used as release medium (**Fig. 12B**) due to faster hydrolysis of the carbonate ester linkage. The release from HES-MA discs was generally slower than from HES-P(EG)$_6$MA hydrogel discs and just slightly influenced by a change of the release medium. While the release of FITC-IgG from HES-P(EG)$_6$MA hydrogel discs with 20 and 30 wt% polymer concentration is very similar, the release from HES-MA hydrogel discs depends much stronger on the concentration of the prepolymer.

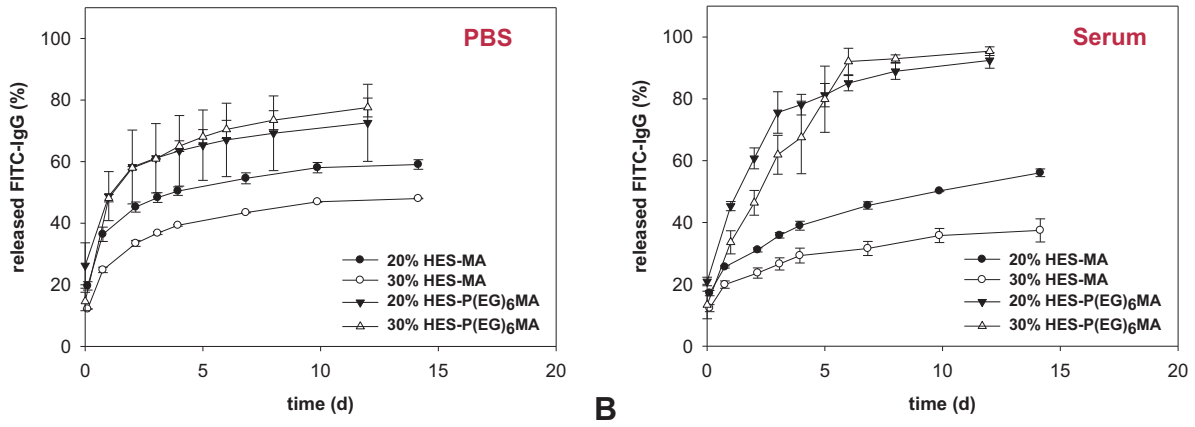

Fig. 12: In vitro *release of FITC-IgG from HES-P(EG)$_6$MA and HES-MA hydrogel discs containing 20 wt% or 30 wt% polymer in PBS (A) and human serum (B).*

To establish an *in vitro - in vivo* correlation *in vivo* release studies from delivery systems administered subcutaneously to mice were performed by the use of a non-invasive *in vivo* imaging system (IVIS), which tracks the loss of fluorescently labeled substances. In comparison to conventional *in vivo* studies, this method enables the observation of individual animals over an extended period of time leading to an improved quality of the data. **Fig. 13** shows the IVIS generated images of a mouse with two implanted HES-MA hydrogel discs scanned at defined points in time. Fluorescence emission of hydrogel discs with higher concentration (30 wt%, right side of the mouse) lasted longer compared to discs with lower concentration (20 wt%, left side of the mouse). In line with the *in vitro* experiments, HES-P(EG)$_6$MA hydrogel discs led to a faster loss of fluorescence intensity than HES-MA discs.

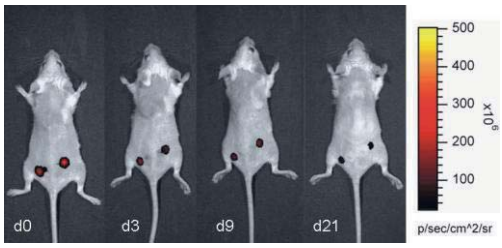

Fig. 13 Time course of reduction in fluorescence intensity after implantation of FITC-IgG loaded HES-MA hydrogel discs (left side of the mouse: 20 %, right side: 30 %; time course from day 0 (d0) to day 21 (d21)). As control the mouse carried unloaded discs implanted into the neck which did not lead to any fluorescence signal.

Quantitative analysis of the fluorescence intensity with time confirmed these results (**Fig. 14**). The fluorescence signals of 20 wt% HES-P(EG)$_6$MA hydrogel discs had disappeared already 5 days after implantation. In contrast 24 % fluorescence was detected for 20 wt% HES-MA hydrogels after the same time. The release from hydrogel microspheres was also investigated *in vitro* and *in vivo*. After 9 days only about 46 % of the incorporated FITC-IgG was released from HES-P(EG)$_6$MA microspheres in PBS but a faster release of 72 % in human serum and a complete loss of fluorescence intensity after 10 days *in vivo* was observed.

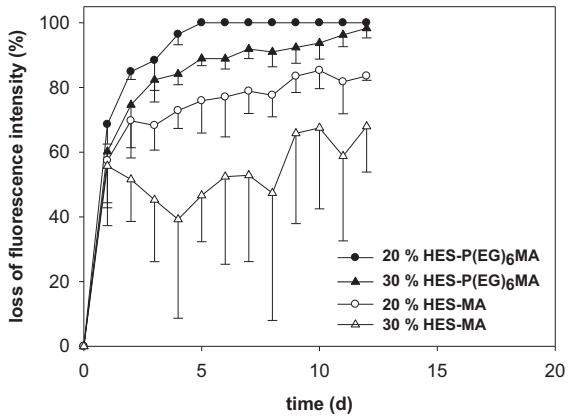

Fig. 14 In vivo release of FITC-IgG from HES-P(EG)$_6$MA and HES-MA hydrogel discs with 20 wt% and 30 wt% polymer content (- standard deviation).

Comparing the *in vitro* and *in vivo* data, a faster release was found *in vivo* than *in vitro*. *In vitro* results obtained with human serum had a much better correlation with the *in vivo* results for both hydrogel systems. Still, conventional *in vitro* release studies performed in PBS provided a correct ranking of the sustained release potential of the different hydrogel systems despite being poorly similar with regard to the absolute release rate. In this respect serum would be preferable but an optimized strategy to avoid contamination of this highly susceptible medium is needed for long-term investigations.

In conclusion, the newly synthesized HES-MA polymer was more promising for a sustained drug release from hydrogel cylinders than HES-P(EG)$_6$MA. The release rates could be triggered by the polymer concentration within hydrogel cylinders. To further adjust the degradation properties, drug delivery systems containing mixtures of the two polymers could be used. In preliminary studies retarded release was observed from mixed HES-P(EG)$_6$MA/HES-MA microspheres compared to pure HES-P(EG)$_6$MA hydrogel microspheres.

3.2.1.3 References to other works and collaborations in the SFB

Hydrogel drug delivery systems as produced in this subproject are an attractive delivery system for the administration of therapeutically relevant biomacromolecules such as antibodies and peptides. In cooperation with subproject A6 (Dübel/Hust) single chain fragment variables (scFv) were produced in *E. coli* and were incorporated in hydrogel systems. The release was detected by fluorescence measurements of labeled antibodies and fragments and by newly developed ELISA for the activity of the protein drugs. The elastic properties of the hydrogel system were studied by nanoindentation (B7, Kwade/Kampen), the distribution of incorporated FITC-labeled proteins and model drugs was determined by confocal laser scanning microscopy (Institute of Plant Biology, TU Braunschweig, Hänsch). The mobility of substances encapsulated in hydrogels was investigated by fluorescence anisotropy measurements and fluorescence recovery after photobleaching (Institute of Physical Chemistry, TU Braunschweig, Gericke) as well as with magnetorelaxometry (C6, Schilling/Ludwig). These data resulted in a structural model of hydrogels containing pores and meshes. The porous structure could be confirmed by cryo-SEM images (Institute of Chemistry, University of Potsdam, Thiersch/Koetz). Feasibility studies to produce hydrogel microspheres by microfluidic devices were accomplished in cooperation with subproject D2 (Büttgenbach/Dübel). To gain information about the correlation of *in vitro / in vivo* release rates, *in vivo* studies were performed in cooperation with the Helmholtz-Center for Infection Research (Müller) using an *in vivo* imaging system. This method allowed monitoring of individual animals over an extended period of time leading to improved quality of data. Additionally, a much smaller number of animals than in conventional animal studies was required.

3.2.1.4 Comparison with research outside the SFB

There are several approaches for the development of hydrogel based drug delivery systems. Most of these can be categorized as follows: (i) degradable, (ii) smart or intelligent and (iii) biomimetic hydrogels [*Lin and Metters, 2006*]. Degradable hydrogels can be cleaved by enzymatic or hydrolytic degradation of the polymer backbone which can be, e.g., dextran or starch [*Van Thienen et al., 2005*]. Due to its good biocomparability HES [*Woo et al., 2001*] was chosen here as basic material for polymer synthesis. The modification of the backbone, especially with polyethylene glycol methacrylate, resulted in a polymer with high water solubility and a good behavior in the water-in-water emulsion (see below). An important aspect of a drug delivery system is the kind of administration. An alternative to bulk hydrogel implants are injectable hydrogel systems [*Nguyen and Lee, 2010*], like microparticles [Ghugare et al., 2012] or nanogels [*Sasaki and Akiyoshi, 2010*]. There are various ways to produce microspheres [*Sinha and Trehan, 2003*] and many possible variations, e.g. addition of polyelectrolyte coatings [*De Geest et al., 2007*] or coating with exploding lipid membranes [*De Geest et al., 2006*]. All these systems have many possible applications like the delivery of growth factors [*Chen et al., 2005*], cells

[*Ballios et al., 2010*] or other proteins [*Shi et al., 2011*]. In the present project the production process of microspheres by a water-in-water emulsion process avoided the use of organic solvents which can exert negative effects on the protein functionality. The microspheres obtained displayed favorable properties like narrow particles size distributions and high encapsulation efficiencies. Under optimized conditions almost the complete amount of the added model substances (differently sized FITC-dextrans, FITC-scFv, FITC-IgG, MNPs) could be incorporated into the microspheres. The encapsulation effiencies were at least as good as for dextran-based particles [*Franssen et al., 1999*]. The release mechanism of degradable hydrogels mostly depends on diffusion and degradation processes [*Hoare and Kohane, 2008*]. The basic methods for characterization of hydrogels are swelling measurements, oscillation rheology and release studies which were also used for the optimization of the systems under investigation here. More advanced techniques for the investigation of hydrogel structures are, for example, NMR-TEM combinations [*Bernin et al., 2011*], characterization of diffusion processes by FRAP and NMR [*Brandl et al., 2009*] or FCS and fluorescence anisotropy [*Lee et al., 2010*] have been reported. In this subproject various methods were combined to investigate the properties of bulk hydrogels and hydrogel microparticles and the behavior of incorporated (model) drug substances. Data obtained by the use of fluorescence methods (anisotropy, FRAP and FCS), magnetorelaxometry, cryo-SEM, conventional release studies as well as in vivo imaging led to novel comprehensive information about the relations between hydrogel structure, size and structure of incorporated substances and diffusion processes. *In vivo* biocompatibility studies on dextran-based hydrogel systems by Cadee et al. (*2000*) revealed their good compatibility and led to conclusions concerning the degradability of such hydrogels. *In vivo* release data were, however, not collected by this group. During the course of this subproject, a better understanding of the degradation and drug release properties of the tested hydrogel systems resulted from *in vitro* - *in vivo* correlations for the HES-based hydrogel drug delivery systems.

3.2.1.5 Literature

Ballios, B.G.; Cooke, M.J.; van der Kooy, D.; Shoichet, M.S. (2010) A hydrogel-based stem cell delivery system to treat retinal degenerative diseases. *Biomaterials* 31, 2555–2564

Bernin, D.; Goudappel, G.-J.; van Ruijven, M.; Altskar, A.; Strom, A.; Rudemo, M.; Hermansson, A.-M.; Nyden, M. (2011) Microstructure of polymer hydrogels studied by pulsed field gradient NMR diffusion and TEM methods. *Soft Matter* 7, 5711–5716

Brandl, F.; Kastner, F.; Gschwind, R.M.; Blunk, T.; Teßmar, J.; Göpferich, A. (2010) Hydrogel-based drug delivery systems: Comparison of drug diffusivity and release kinetics. *J. Control. Release* 142, 221–228

Cadée, J.A. (2000) In vivo biocompatibility of dextran-based hydrogels. *J. Biomed. Mater. Res*. 50, 397-404

Chen, F.; Wu, Z.; Wang, Q.; Wu, H.; Zhang, Y.; Nie, X.; Jin, Y. (2005) Preparation and biological characteristics of recombinant human bone morphogenetic protein-2-loaded dextran-co-gelatin hydrogel microspheres, in vitro and in vivo studies. *Pharmacology* 75, 133–144

Cohen, S.; Yoshioka, T.; Lucarelli, M.; Hwang, L.H.; Langer, R. (1991) Controlled delivery systems for proteins based on poly(lactid/glycolic acid) microspheres. *Pharmaceut. Res.* 08, 713–720

Fairbanks, B. D.; Schwartz, M. P.; Bowman, C. N.; Anseth, K. S. (2009) Photoinitiated polymerization of PEG-diacrylate with lithium phenyl-2,4,6-trimethylbenzoylphosphinate: polymerization rate and cytocompatibility. *Biomaterials* 30, 6702-6707

Franssen, O. (1999) Controlled release of a model protein from enzymatically degrading dextran microspheres. *J. Control. Release 59*, 219-228

Franssen, O. (1999) Degradable dextran hydrogels: Controlled release of a model protein from cylinders and microspheres. *J. Control. Release* 60, 211-221

Geest, B.G. de; Sanders, N.N.; Sukhorukov, G.B.; Demeester, J.; Smedt, S.C. de (2007) Release mechanisms for polyelectrolyte capsules. *Chem. Soc. Rev.* 36, 636–649

Geest, B.G. de; Stubbe, B.G.; Jonas, A.M.; van Thienen, T.; Hinrichs, W.L.J.; Demeester, J.; Smedt, S.C. de (2006) Self-exploding lipid-coated microgels. *Biomacromolecules* 7, 373–379

Ghugare, S.V.; Chiessi, E.; Cerroni, B.; Telling, M.T.F.; Sakai, V.G.; Paradossi, G. (2012) Biodegradable dextran based microgels: a study on network associated water diffusion and enzymatic degradation. *Soft Matter* 8, 2494

Heim, E.; Harling, S.; Pöhling, K.; Ludwig, F.; Menzel, H.; Schilling, M., (2007) Fluxgate magnetorelaxometry of superparamagnetic nanoparticles for hydrogel characterization. *J. Magn. Magn. Mater.* 311, 150–154

Heim, E.; Harling, S.; Ludwig, F.; Menzel, H.; Schilling, M.(2008) Fluxgate magnetorelaxometry for characterization of hydrogel polymerization kinetics and physical entrapment capacity. *J. Phys-Condens. Mat.* 20, 204106

Hoare, T.R.; Kohane, D.S. (2008) Hydrogels in drug delivery: Progress and challenges. *Polymer* 49, 1993-2007

Kamath, K.R.; Park, K. (1993) Biodegradable hydrogels in drug delivery: modern hydrogel delivery systems. *Adv. Drug Deliver. Rev.* 11, 59–84

Lee, J.S.; Zhou, W.; Meng, F.; Zhang, D.; Otto, C.; Feijen, J. (2010) Thermosensitive hydrogel-containing polymersomes for controlled drug delivery. *J. Control. Release* 146, 400–408

Lin, C.-C.; Metters, A.T. (2006) Hydrogels in controlled release formulations: Network design and mathematical modeling: Computational Drug Delivery. *Adv. Drug Deliv. Rev.* 58, 1379-1408

Lin, C.-C.; Sawicki, S. M.; Metters, A. T. (2008) Free-radical-mediated protein inactivation and recovery during protein photoencapsulation. *Biomacromolecules* 9, 75-83

Nguyen, M.K., Lee, D.S., (2010). Injectable biodegradable hydrogels. Macromol. Biosci. 10, 563–579.

Peppas, N.A.; Bures, P.; Leobandung, W.; Ichikawa, H. (2000) Hydrogels in pharmaceutical applications, *Eur. J. Pharm. Biopharm.* 50, 27-46

Sasaki, Y.; Akiyoshi, K. (2010) Nanogel engineering for new nanobiomaterials: from chaperoning engineering to biomedical applications. *Chem. Record.* 10, 366-376

Shi, W.; Ji, Y.; Zhang, X.; Shu, S.; Wu, Z. (2011) Characterization of pH- and thermosensitive hydrogel as a vehicle for controlled protein delivery. *J. Pharm. Sci.* 100, 886–895

Sinha, V.R.; Trehan, A. (2003) Biodegradable microspheres for protein delivery. *J. Control. Release* 90, 261–280

Van de Weert, M.; Jorgensen, L.; Horn Moeller, E.; Frokjaer, S. (2005) Factors of importance for a successful delivery system for proteins. *Expert Opin. Drug Deliv.* 2, 1029–1037

Van Dijk-Wolthuis, W.N.E.; Franssen, O.; Talsma, H.; van Steenbergen, M.J.; Kettenes-van den Bosch, J.J.; Hennink, W.E. (1995) Synthesis, characterization and polymerization of glycidyl methacrylate derivatized dextran. *Macromolecules* 28, 6317–6322

Van Dijk-Wolthuis, W.N.E.; van Steenbergen, M.J.; Underberg, W.J.M.; Hennink, W.E. (1997) Degradation kinetics of methacrylated dextrans in aqueous solution. *J. Pharm. Sci.* 86, 413-417

Van Thienen, T.G.; Lucas, B.; Flesch, F.M.; van Nostrum, C.F.; Demester, J.; De Smedt, S.C. (2005) On the synthesis and characterization of biodegradable dextran nanogels with tunable degradation properties. *Macromolecules* 38, 8503-8511

Van Thienen, T.G.; Raemdonck, K.; Demeester, J.; Smedt, S.C. de (2007) Protein release from biodegradable dextran nanogels. *Langmuir* 23, 9794–9801

Woo., B.H.; Jiang., G.; Jo., Y.W.; DeLuca., P.P. (2001) Preparation and characterization of a composite PLGA and poly(acryloyl hydroxyethyl starch microsphere system for protein delivery. *Pharm. Res.* 18, 1600-1606

3.2.2 Project relevant own publications

a) Works that have appeared in publications of a scientific quality assurance at the time of application or final adoption, and book publications

Harling, S.; Schwoerer, A.; Scheibe, K.; Daniels, R.; Menzel, H. (2010) A new hydrogel drug delivery system based on Hydroxyethylstarch derivatives. *J. Microencapsul.* 27, 400-408

Kamoun, E.A.; Menzel, H. (2010) Crosslinking behavior of dextran modified with hydroxyethyl methacrylate upon irradiation with visible light – Effect of concentration, coinitiator type and solvent. *J. Appl. Polym. Sci.* 117, 3128-3138

Schwoerer, A.D.A.; Harling, S.; Scheibe, K.; Menzel, H.; Daniels R. (2009) Influence of degree of substitution of HES-HEMA on the release of incorporated drug models from corresponding hydrogels. *Eur. J. Pharm. Biopharm.* 73, 351-356

Wöhl-Bruhn, S.; Badar, M.; Bertz, A.; Tiersch, B.; Koetz, J.; Menzel, H.; Müller, P.P.; Bunjes, H.; Comparison of *in vitro* and *in vivo* protein release from hydrogel systems. *J. Controlled Release*, in press

Wöhl-Bruhn, S.; Bertz, A.; Harling, S.; Menzel, H.; Bunjes, H. (2012) Hydroxyethylstarch-based polymers for the controlled release of biomacromolecules from hydrogel microspheres. *Eur. J. Pharm. Biopharm.,* http://dx.doi.org/10.1016/j.ejpb.2012.04.017.

b) Other publications

Bertz, A.; Wöhl-Bruhn, S.; Bunjes, H.; Menzel, H. (2010) Hydroxyethyl starch polyethylene glycol methacrylate hydrogels for drug delivery. 20th Polymer networks group, Goslar, Germany, poster

Bertz, A.; Ehlers, J.-E.; Wöhl-Bruhn, S.; Bunjes, H.; Gericke, K.-H.; Menzel, H. (2011) How to study the mobility of green fluorescent protein in a hydrogel based delivery system. Biofuture 2011, Gent, Belgium, oral presentation

Bertz, A.; Ehlers, J.-E.; Wöhl-Bruhn, S.; Bunjes, H.; Gericke, K.-H.; Menzel, H. (2012) Protein mobility in a hydrogel based drug delivery system analyzed by fluorescence methods. Makromolekulares Kolloquium 2012, Freiburg, Germany, poster

Harling, S. (2010) Hydrogele als Drug Delivery Systeme basierend auf Hydroxyethylstärke. PhD thesis Technische Universität Braunschweig.

Schwoerer, A.D.A. (2010) Hydroxyethylstärke-Hydroxyethylmethacrylat-Hydrogele als Freisetzungssystem für Proteine. PhD thesis Technische Universität Braunschweig

Wöhl-Bruhn S.; Bertz A.; Menzel H.; Bunjes, H. (2010) Influences on the formulation process of hydrogel microparticles for the controlled release of proteins. 7th World Meeting on Pharmaceutics, Biopharmaceutics and Pharmaceutical Technology, Valetta, Malta, poster

Wöhl-Bruhn, S.; Bertz, A.; Menzel, H.; Bunjes, H. (2011) Influences on the release profile from hydrogel microparticles and investigations on the stability of incorporated antibodies. 2011 Colorado Protein Stability Conference, Breckenridge, USA, poster

Wöhl-Bruhn, S.; Badar, M.; Bertz, A.; Menzel, H.; Müller, P.-P.; Bunjes, H. (2012) Hydrogel drug delivery systems for the controlled release of antibodies - release studies *in vitro* and *in vivo*. 8th World Meeting on Pharmaceutics, Biopharmaceutics and Pharmaceutical Technology, Istanbul,Turkey, oral presentation

3.3 Looking back on the promotion

The project has been funded since July 2004 in the SFB 578. It was completed on June 2012 with the end of the program.

3.3.1 Personnel in the project

	Name, acad. degree, service position	narrower subject of the employee	Institute of University or non-university facility	Participation in the project in hours per week	Category
Basic staff					
Research associate (incl. auxiliary power)	1. H. Bunjes, Prof. Dr. rer. nat.	Pharmaceutical Technology	Institute of Pharmaceutical Technology	5	Professorship
	2. H. Menzel, Prof. Dr. rer. nat.	Polymer Chemistry	Institute of Technical Chemistry	5	Professorship
Non academic staff	3. N.N.	Pharmaceutical Technology	Institute of Pharmaceutical Technology	10	Technical Staff
	4. N.N.	Polymer Chemistry	Institute of Technical Chemistry	2	Technical Staff
Supportive staff					
Research associate (incl. auxiliary power)	5. A. Schwoerer Pharmacist	Pharmaceutical Technology	Institute of Pharmaceutical Technology	40	PhD student
	6. S. Wöhl-Bruhn, Pharmacist	Pharmaceutical Technology	Institute of Pharmaceutical Technology	40	PhD student
	7. Steffen Harling, Dipl.Chem.	Polymer Chemistry	Institute of Technical Chemistry	40	PhD student
	8. A. Bertz, Dipl. Chem.	Polymer Chemistry	Institute of Technical Chemistry	40	PhD student
Non academic staff	9. N.N.	Biotechnology	Institute of Pharmaceutical Technology, Institute of Technical Chemistry	10	Students

Responsibilities of employees (basic staff)

Position 1 - 2: Prof. Dr. H. Bunjes, Prof. Dr. H. Menzel

The principle investigators guided and supported the work of the PhD students within the project. This involved discussions on general research strategies, suitable experimental techniques and interpretation of data as well as support with writing reports and publications. Prof. Dr. H. Menzel guided the work concerned with the synthesis and characterization of the precursor polymers as well as the preparation of the hydrogels and made contacts with the corresponding cooperation partners. Prof. Dr. H. Bunjes was concerned with the projects parts dealing with microparticle preparation and characterization as well as release studies.

Position 3 - 4:

The technical staff supported the project work concerning specialized experimental techniques like electron microscopy, spectroscopy and cell culture work.

Responsibilities of employees (supportive staff)

Position 5: Pharmacist Ariane Schwoerer

A. Schwoerer wrote reports and publications and introduced S. Wöhl-Bruhn to the experimental methods.

Position 6: Pharmacist Stefanie Wöhl-Bruhn

S. Wöhl-Bruhn optimized a preparation method for hydrogel microparticles from hydroxyethylstarch-based polymers (HES-MA, HES-P(EG)$_n$MA) for the controlled release of proteins. She investigated the influence of different production parameters and incorporated substances (e.g. size, hydrophilicity, amount) on the particles size, the encapsulation efficiency, the distribution within the microparticles (with Prof. Hänsch, IFP) and the release profile from hydrogel microspheres. Furthermore, she determined the influence of different release media on the release profile and identified *in vitro* conditions reflecting the *in vivo* conditions as closely as possible. In cooperation with the Helmholtz-Centre for Infection Research (HZI, Prof. Müller) Mrs. Wöhl-Bruhn worked on *in vivo* release experiments in living mice leading to *in vitro* - *in vivo* correlations for the release studies. The stability of incorporated antibodies was tested with biochemical methods (cooperation A6 Dübel/Hust). Furthermore, magnetorelaxometry measurements were performed in cooperation with subproject C6 (Schilling/Ludwig) to gain information about the properties of the hydrogel network. The use of microsystems for the production of hydrogel microspheres was tested in cooperation with subproject D2 (Büttgenbach/Dübel).

Position 7: Dipl.-Chem. Steffen Harling

S. Harling wrote reports and introduced A. Bertz to the experimental methods, like polymer synthesis, production and characterization of hydrogels.

Position 8: Dipl.-Chem. Andreas Bertz

A. Bertz performed the optimization of the synthesis and their scale up (50 g) for HES-P(EG)$_6$MA, HES-P(EG)$_{10}$MA and HES-MA polymers. Large amounts of polymers were regularly produced with different degrees of substitution, to provide sufficient material for a wide variety of characterization methods and studies of the project/cooperation partners. Mr. Bertz investigated the influence of various crosslinking parameters (polymer type, concentrations, irradiation time, degree of substitution) on the network density by swelling measurements and oscillation rheology with Irgacure®2959 at 366 nm and LAP at 366 and 405 nm (additionally in combination with the coinitiator NPG) as photoinitiators. In addition, mesh sizes were calculated; for the calculations data from dn/dc, GPC, swelling and density measurements was collected. The pore structure of hydrogels and hydrogel microparticles were imaged by cryo-SEM in cooperation with the University of Potsdam (Prof. Koetz). Furthermore the diffusion processes within the hydrogel network were examined by (a) fluorescence anisotropy, (b) fluorescence correlation spectroscopy and (c) fluorescence recovery after photobleaching in cooperation with the institutes of physical chemistry of the TU Braunschweig and TU Clausthal (Prof. Gericke (a) and (c) and Prof. Oppermann (b) and (c)) and (d) magnetorelaxometry in cooperation with subproject C6.

Position 9: Stud. assistants

The student assistants supported the extensive experimental work in the routine of swelling and rheology measurements as well as release studies.

3.1 General information on the completed project D2

3.1.1 Topic

Microchips for protein analytics and diagnostics

3.1.2 Disciplines and field of work

Biochemical Analytics, Protein Engineering, Lab-on-Chip

3.1.3 Project manager

Prof. Dr. rer. nat. Stephanus Büttgenbach
(b.: 25.01.1945)
Institute for Microtechnology (IMT)
TU Braunschweig
Langer Kamp 8
D-38106 Braunschweig
Phone: +49-531-391-3320
Fax: +49-531-391-8101
E-Mail: s.buettgenbach@tu-bs.de

Prof. Dr. rer. nat. Stefan Dübel
(b.: 13.01.1960)
Department of Biotechnology (DBT)
TU Braunschweig
Spielmannstraße 7
D-38106 Braunschweig
Phone: +49-531-391-5732
Fax: +49-531-391-5763
E-Mail: s.duebel@tu-bs.de

3.2 Development of the subproject

3.2.1 Report

Point-of-care diagnostics is becoming more and more important because of its benefits for the patients, allowing much quicker diagnosis and start of treatment. The most widely used point-of-care test to date is the erythrocyte sedimentation rate indicating an inflammation or infection. However, it does not allow specifying the type of inflammation and increases and decays rather slowly, limiting its value to indicate the exact progress of the disease. Therefore, more specific parameters are preferred as indicators for inflammatory diseases. C-reactive protein (CRP) has been identified as a superior parameter, but it requires a sophisticated and time consuming detection method, not suited for point-of-care applications. Consequently, CRP has been used as a model molecule for the development towards a point-of-care analysis system in this subproject. The essential feature of this system is a rapid analysis without the requirement for sophisticated liquid handling steps. This is best achieved by the online monitoring of a lable free detection in a flow through system. A desirable feature of such a system is the capability to measure different samples by repeatedly using the same detection chip, this both allowing for calibration providing high accuracy, and economic advantages. The developed method has broad application since the detector antibody can be changed, to measure a large variety of clinically relevant parameters. The microfluidic setup further will allow facile parallelisation in future setups to determine a larger number of samples or parameters in parallel.

3.2.1.1 Current knowledge at the last application and initial question

Quartz crystal microbalance

Quartz crystal microbalances (QCMs) are widely-used as biosensors [*Becker and Cooper 2011*]. In 2005, for the first time recombinant antibody fragments isolated from an scFv antibody fragment library have been coupled to a QCM sensor [*Shen et al. 2005*]. Except

for one further publication of these authors [*Shen et al., 2007*] an account of the use of recombinant scFv antibodies in QCMs has not been given until the present application. Aizawa et al. (*2006*) report on QCM based immunosensors for CRP detection. The antibodies have been immobilized on the gold electrode using a self assembled monolayer (SAM). However, these tests have not been performed in a fluidic system, but the QCM had to be dehydrated after each step why this system was not suited for point-of-care diagnostics. Another possibility is the *latex piezoelectric immunoassay* (LPEIA) [*Aizawa et al. 2001; Kurosawa et al., 2003 and 2004*]. This device uses latex beads coated with CRP antibodies which agglomerate with the agent to be detected. A QCM serves as a detector. The advantage of this method is the amplification of the measuring signal via the latex beads.

CRP diagnostics using other sensor principles

Hosokawa et al. (*2006*) realized an enzyme-linked immunosorbent assay (ELISA) at the channel wall of a polydimethylsiloxane (PDMS) fluidic system. The surface had to be prepared immediately before application and could not be regenerated. Furthermore, for analysis a fluorescence camera was needed. Hu et al. (*2006*) reported on an extremely sensitive detection method for CRP using surface plasmon resonance (SPR) and coupling of antibodies via SAM. Meyer et al. (*2006*) utilized in their SPR system a chip coated with strepdavidin, on top of which biotinylated antibodies had been immobilized. Also it is possible to detect CRP using cantilevers [*Lee et al., 2004*]. However, the fabrication of cantilevers is much more complex than that of QCM. Since in the work of Lee et al. the cantilevers had to be dehydrated before usage, it was not possible to perform the measurement within a fluidic system. Meyer et al. (*2007*) described a method for the determination of CRP using magnetic beads. Biotinylated anti-CRP antibodies were immobilized on the magnetic beads via avidin. A different anti-CRP antibody was immobilized on the surface of a sintered filter which is arranged within the reaction volume. Beads bound to filter via CRP were detected by a magnetic reader: the beads were excited at two distinct frequencies and the response signal generated at the beat frequency was detected.

CRP antibodies and Antibody Engineering

The standard assay for the detection of proteins relevant to diagnostics is the ELISA (Enzyme Linked Immuno Sorbent Assay). This test requires sequential pipetting of reaction partners, labeled secondary antibodies and colour chemicals – a tedious and time consuming procedure. Further, after a single sample, an ELISA assay tube cannot be re-used. The use of QCM as a lable free detection system eliminates the complicated fluidic handling steps of the ELISA. The essential reagent for detection on both ELISA and QCM is a good antibody to CRP. The benefits of a flow through / microfluidic system could best be utilized if the antibody coated CRP detection surface could be regenerated for another measurement. This also adds a significant advantage: the system can be calibrated with samples of known concentration, thus allowing a very accurate measurement. Using

current *in vivo* antibody selection and evolution methods [*Dübel et al., 2012; Thie et al., 2011; Colwill et al., 2011; Bradbury et al, 2011*], antibodies can be generated which are pre-selected to perform well on this kind of assay. The in vitro selection allows to control the biochemical conditions of an antibody in the very moment of its selection. Here, the essential parameter to select for (in addition to CRP binding) is stability against denaturation.

Findings and developments from the last application phase

During the last application phase anti-CRP-ScFvs had been developed and coupled to the QCM surface for CRP detection. Furthermore, QCMs were integrated into a microfluidic system. An affinity chromatography unit had been miniaturized, characterized and tested in combination with the QCMs. First developments towards an integrated lab-on-chip system for CRP detection included the design and fabrication of microvalves based on hydrogel actuators [*Ayala et al., 2007*] as well as considerations concerning the microfluidic interface and control of the system. Antibody engineering was initiated to assess and improve the properties of the antibodies used for CRP detection.

Initial question

The present application phase centered on the advancement of the combination of improved detection antibody and microfluidic system towards detection of CRP in whole blood. One objective was the development of antibody fragments adapted to the respective components of the lab-on-chip system, the affinity chromatography unit and the QCM, and their immobilization on the appropriate surfaces.

A second objective was the extraction of blood plasma in order to protect the microfluidic system against perturbation through blood cells. Concurrently, the integration of all components into a computer controlled micro analysis system should be pursued.

3.2.1.2 Results and applied methods

Antibody engineering was initiated to assess and improve the properties of the antibodies selected before. In detail, two strategies were followed to create and improve antibodies suitable for CRP detection on the chip: (1) novel selections were done using an improved antibody phage display library (Hal4/7/8), and (2) the already selected antibodies were mutagenized via error prone PCR to enhance their biochemical properties (e.g. affinity, stability, dimerization) by *in vitro* molecular evolution. Candidates with best characteristics regarding to binding ability of CRP under denaturizing conditions such as high temperatures, salt concentrations and extreme pH values were generated. Using these methods, a panel of stable antibody clones suited for both applications (affinity enrichment and detection) was identified and are now available. The recombinant antibodies were tested for stability as well as their compatibility to novel elution methods (high pH, salt concentrations) during the screening procedure. The immobilization of antibodies on the gold electrodes of the QCMs was optimized by investigation of different coupling mechanisms, including self assembling monolayers. A robust coupling method was

identified. In addition, other antibody formats (Fab, scFab, scAb, scFv-Fc, scIgG, and IgG) were created and assessed for their compatibility to coupling onto the sensor chip. These optimazations were performed in close collaboration with subproject A6 (Dübel/Hust).

Optimizations and modifications of antibody fragments used in the affinity enrichment were comparable to those used for the quartz sensor. In addition to the application of several different antibody formats, the matrix of this module can be varied. An epoxy activated sepharose can be used for coupling of CRP specific scFvs. After binding CRP can be eluted and conducted onto the QCM sensor. Alternatively, scFvs can be immobilized on a nickel chelate affinity matrix via the C-terminal His_6-tag. In this case elution of CRP can be obtained with Ethylenediaminetetraacetic acid (EDTA). EDTA can also be used for elution of CRP after calcium dependant binding to its physiological partner Phosphorylcholine. In presence of EDTA calcium ions were complexed and CRP is released.

The flow characteristics of the lab-on-chip system have been optimized by simulation of the individual microfluidic components. In particular, improvement of the fluidic structures with regard to the prevention of dead volumes and the adjustment of the individual cross sections has been taken into account.

To enable a CRP detection based on samples of whole blood, a separation process for the extraction of blood plasma, which could be integrated into the complete system, has been prospected for. Two alternative methods have been investigated: first the extraction of blood serum using an ultrasonic micro flow-through cell and secondly the utilization of centrifugal forces and flow stresses in microfluidic channels for separation of cellular blood components. For automated CRP determination a measuring program including closed loop control of the valves has been developed.

Optimization of flow characteristics

A first work package centered on the optimization of the microfluidic structures with regard to the prevention of dead volumes and the adjustment of individual cross sections. For this purpose, the total flow system has been divided into individual components in order to match the memory footprint of the simulation tool. As an example, **Fig. 1** illustrates the optimization strategy of the QCM flow cell. In particular, the uniform fluid flow across the active area of the QCM has been addressed in order to enable signals as strong as possible. The entrance angle has been varied between 15°, 30° and 45° and different radii have been adopted for the vertex of the entrance channel. The alternative with best results with regard to required space and to uniformity of flow characteristics exhibits an entrance angle of 30° and radii of $r_1=r_2=5393$ µm.

Another example is the improvement of the grid structure for the containment of the bead suspension in the affinity chromatography unit (**Fig. 2**). The retention of the beads as well as the uniformity of the flow through the unit could be improved.

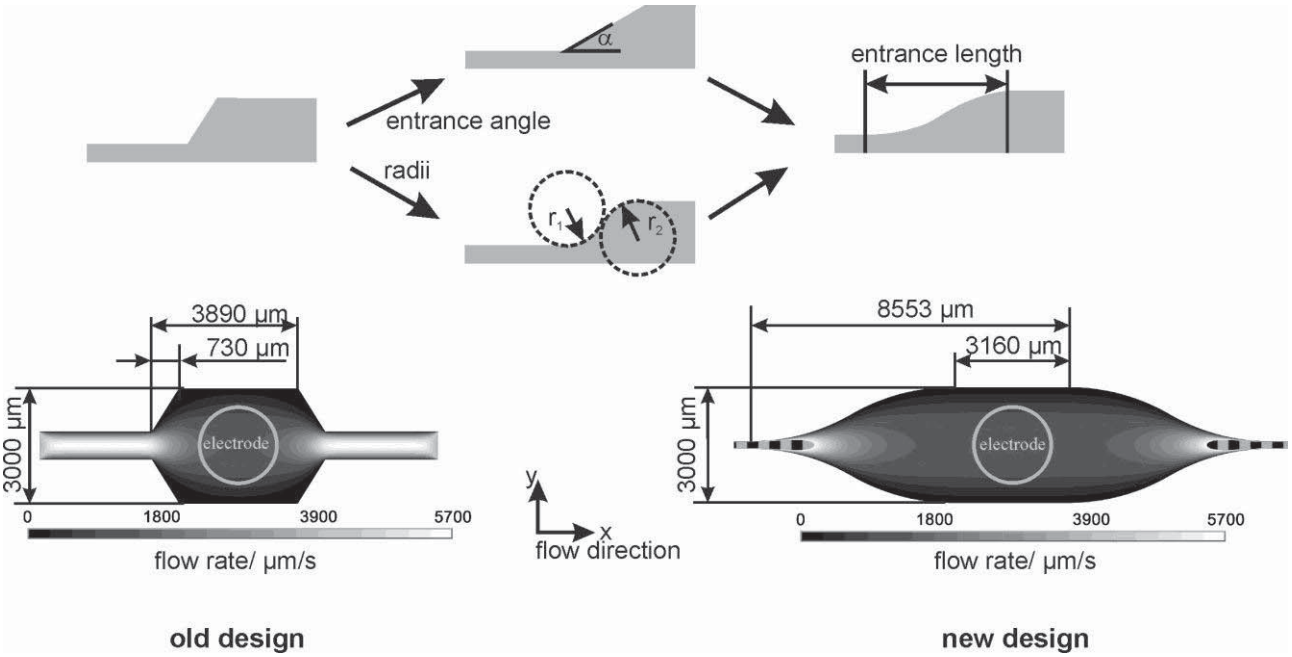

Fig. 1: Optimization of the QCM flow cell design.

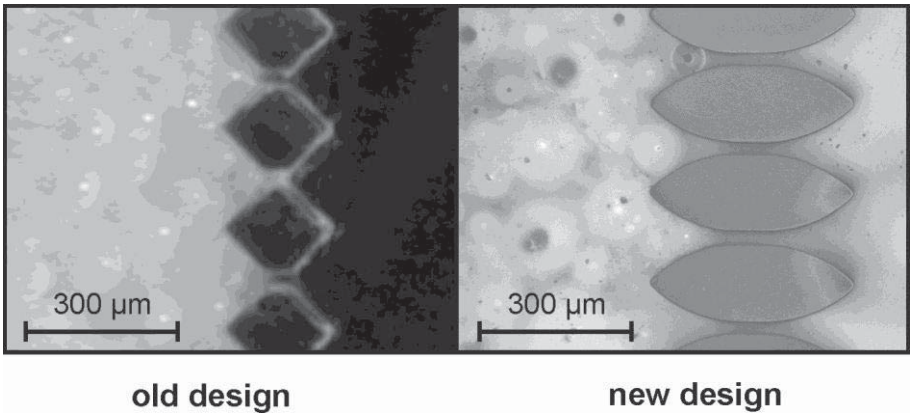

Fig. 2: Optimization of the grid structure of the affinity chromatography unit.

Extraction of blood plasma

Ultrasonic micro flow-through cell: In cooperation with Prof. Laurell, University of Lund, Sweden, a test system for the extraction of blood serum using an ultrasonic flow-through cell has been set up. The separation is based on the effect of a standing wave in the channel. The blood cells concentrate at the wave nodes or anti-nodes. Thereby the blood serum can be separated from the cellular blood components (**Fig. 3**). Separation systems made available to us by Prof. Laurell as well as home-made systems have been investigated. Using diluted blood samples (hematocrit up to 10%) a separation effect could be detected, but blood serum completely free of blood cells could not be obtained. Furthermore, the integration of the ultrasonic cell into the total system turned out to cause technological difficulties due to the material differences (glass-glass or glass-silicon for the ultrasonic cell, PDMS and glass for the lab-on-chip system).

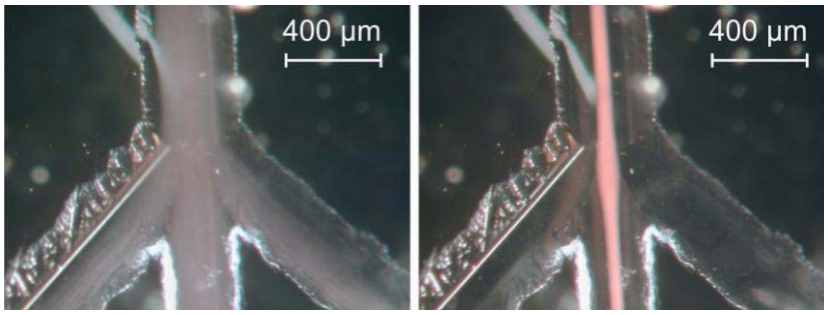

Fig. 3: Extraction of blood plasma using an ultrasonic flow-through cell made of glass; without (left) and with (right) ultrasonic excitation (hematocrit 1%).

Due to the inferior separation characteristics, the problematic integrability and the great number of peripheral devices needed the centrifugal separation mechanism described in the following has been preferred.

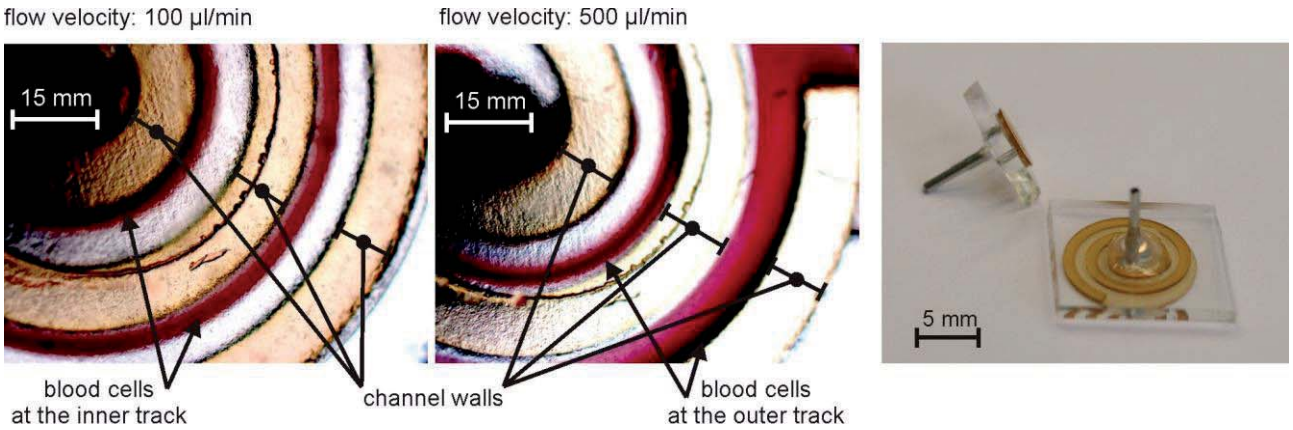

Fig. 4: left: Preliminary tests of blood separation in spiral channels; right: two different spiral structures.

Centrifugal separation system: As a second method the separation of blood cells via centrifugal forces has been investigated. Preliminary experiments have been performed using spiral structures made of the resist SU-8 and a single layer of PDMS (**Fig. 4**, right).

These experiments exhibited the interesting behavior of blood or particle-laden fluids, respectively, in non-linear channels (Fig. 4, left). In curved channels Dean forces, which are generated through a laminar secondary flow, have great influence on the behavior of the particles. Depending on the flow velocity either the centrifugal forces or the Dean forces predominate or they even out, and the cells or particles arrange themselves at definite positions in the channel [*Carlo et al., 2007; Carlo, 2009*]. To further improve the separation effect the Zweifach-Fung effect has been utilized. Thereby the two outlets of the separation unit, one for the blood cells and one for the blood plasma, are designed in such a way that at the branching point (A, **Fig. 5**, left) different flow velocities are obtained for the two channels. Due to the occuring forces the cells start to rotate and move towards the channel with the higher flow velocity. Preliminary experiments showed that at least a ratio of the flow velocities of 8:1 has to be reached to obtain blood serum free of cells. Therefore, different system designs have been developed, simulated and tested (Fig. 5) [*Balck et al., 2009; Demming et al., 2009*].

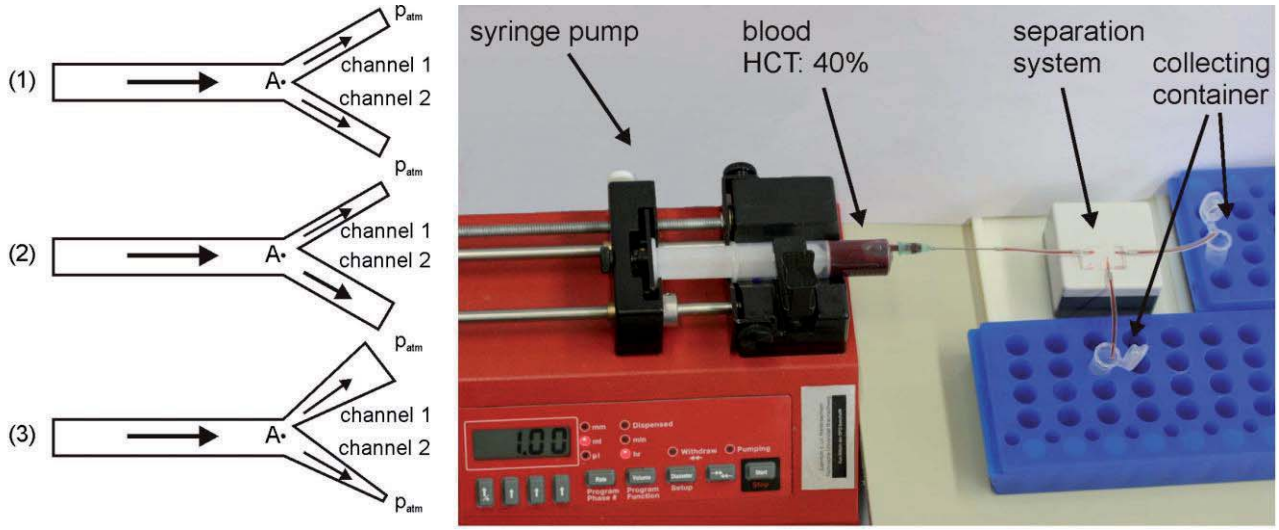

Fig. 5: left: Different designs of the Zweifach-Fung separation system; right: experimental set-up.

The separation method based on the Zweifach-Fung effect has been combined with the spiral channels to form a novel separation system (**Fig. 6**, left). The micrograph in Fig. 6 shows the great influence of the Zweifach-Fung effect. The system has been designed for low flow velocities. Due to the Dean forces the blood cells arrange themselves at the inner channel wall. This is supported by the Zweifach-Fung effect, since the inner channel possesses the smaller channel width and therefore the higher flow velocity at the branching point. If the flow velocity is increased the blood cells move towards the outer channel wall, since the centrifugal forces dominate. As can be seen in Fig. 6, the Zweifach-Fung effect is still effective and deflects part of the blood cells.

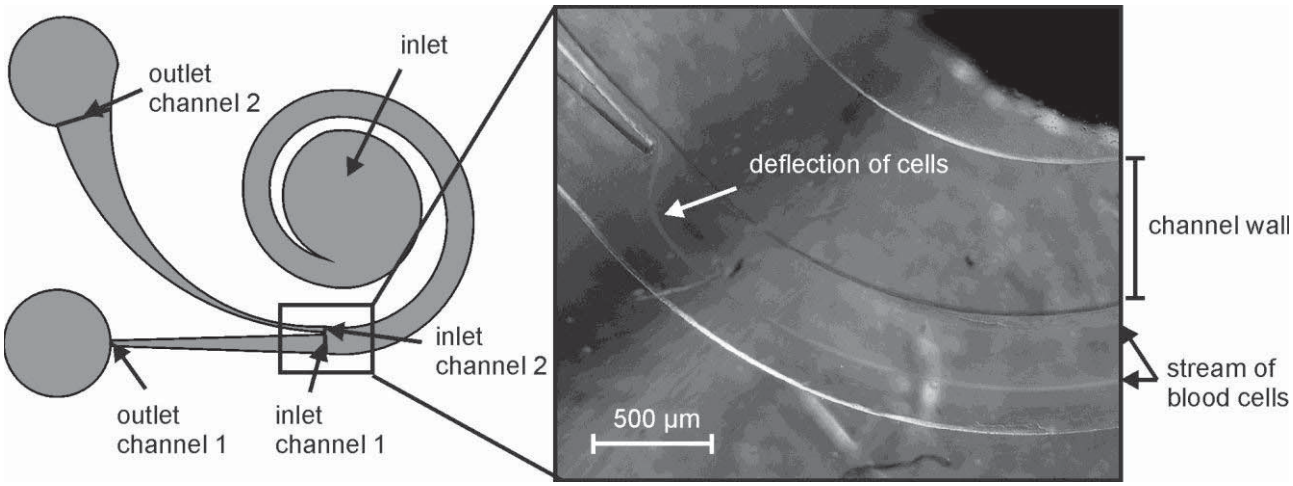

Fig. 6: left: Design of the Zweifach-Fung-spiral-combi separation system; right: separation experiment with 2% hematocrit and flow velocity of 500 µl/h.

For low values of hematocrit excellent separation results have been obtained. The novel Zweifach-Fung-spiral-combi concept has also high potential for the separation of whole blood. For this, however, a still more extensive parametric study is necessary, since many influencing factors have to be considered.

Integration of the complete system

The hydrogel valves, which have been developed during the last application phase and further improved during the present phase [*Ayala et al., 2007; Michalzik et al., 2008*], have been integrated together with the affinity chromatography unit and the QCM flow cell into a lab-on-chip system (**Fig. 7**) [*Balck et al., 2011*]. However, the hydrogel valves turned out to have only limited suitability due to their low response time and to the fact that external valves are needed for their activation. In addition, the complex fabrication technology resulted in a low yield, and the developed fluidic interface tended towards leakage.

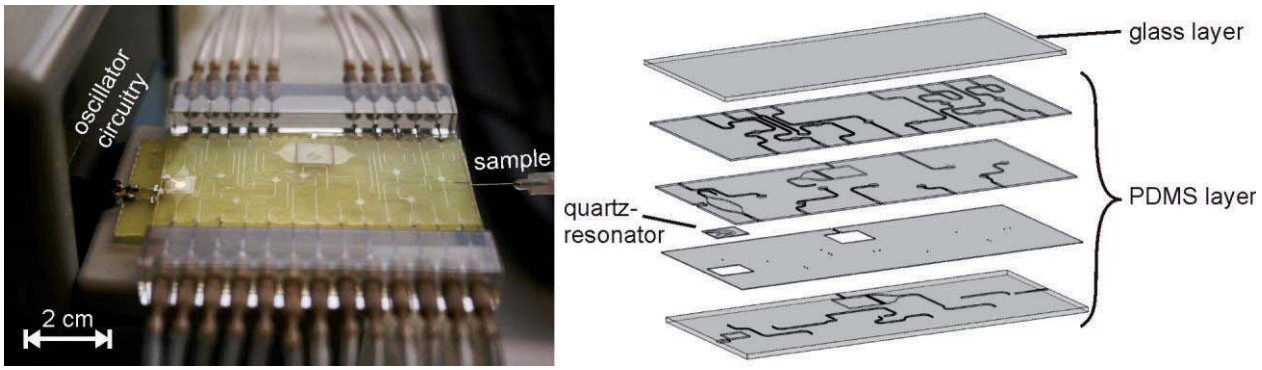

Fig. 7: left: Complete first generation lab-on-chip system; right: scheme of the different layers of the system.

For this reason the lab-on-chip system has been redesigned completely. In this context also the blood separation system has been integrated. In contrast to the first generation system, which consisted of four PDMS and one glass layer in addition to the QCM (Fig. 7, right), the redesigned system consists of only two PDMS and one glass layer in addition to

the QCM cell (**Fig. 8**, right). Furthermore, the dimension of system could be reduced to about one third. These improvements were possible due to the fact that the hydrogel valves and the related eight external valves could be replaced by only seven external valves. In addition, of the intended four peristaltic pumps only two were needed for the redesigned system. The complete system can be easily changed. It only has to be inserted into an adapter, the cover will be fixed using three knurled-head screws.

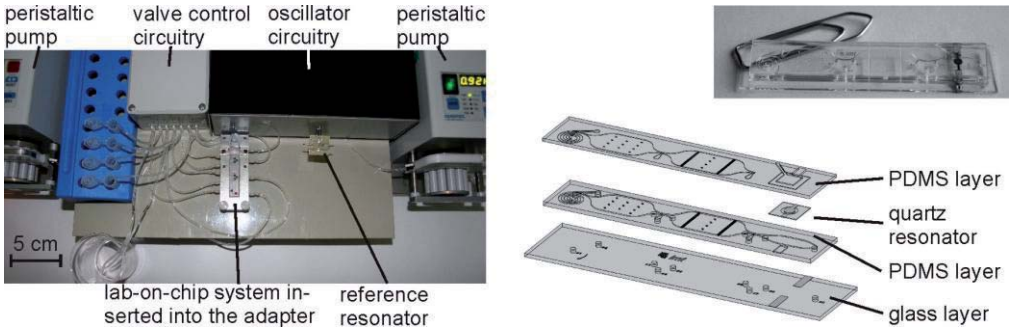

Fig. 8: left: Experimental set-up of the complete second generation lab-on-chip system; right: photograph (top) and scheme (down) of the system.

Generation and optimization of antibody fragments by *in vitro* selection/evolution

After random mutagenesis of genes encoding for two different CRP specific scFvs using error prone PCR, two mini mutation libraries have been created [*Fröde, 2012*]. These libraries have been screened for candidates with improved biochemical properties. Several candidates with increased CRP binding abilities were identified (**Fig. 9**).

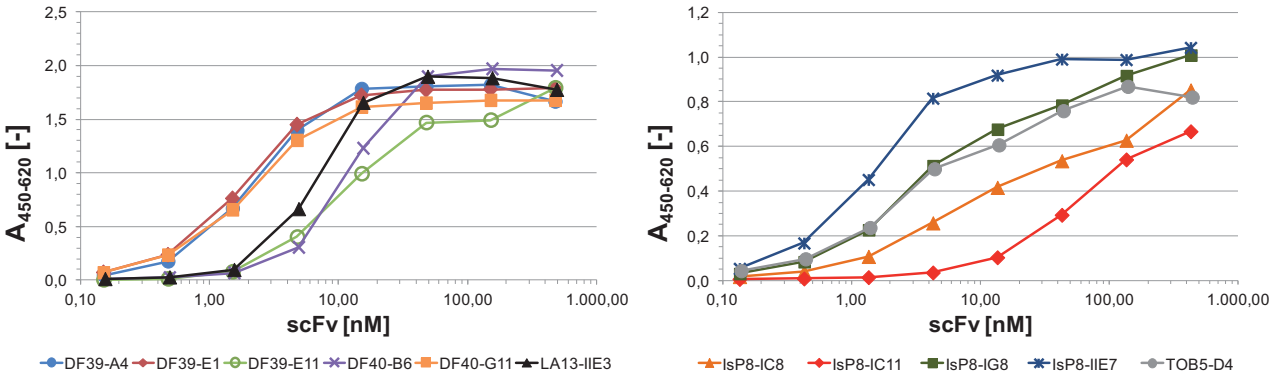

Fig.9: Binding abilities of mutated antibody variants in comparison to their wildtype LA13-IIE3 (left) and TOB5-D4 (right).

These novel scFv variants were further biochemically characterized (e.g. Size Exclusion Chromatography, Surface Plasmon Resonance). In addition two different stability assays have been established for testing the storage halflife and heat stability of all candidates (**Fig. 10**).

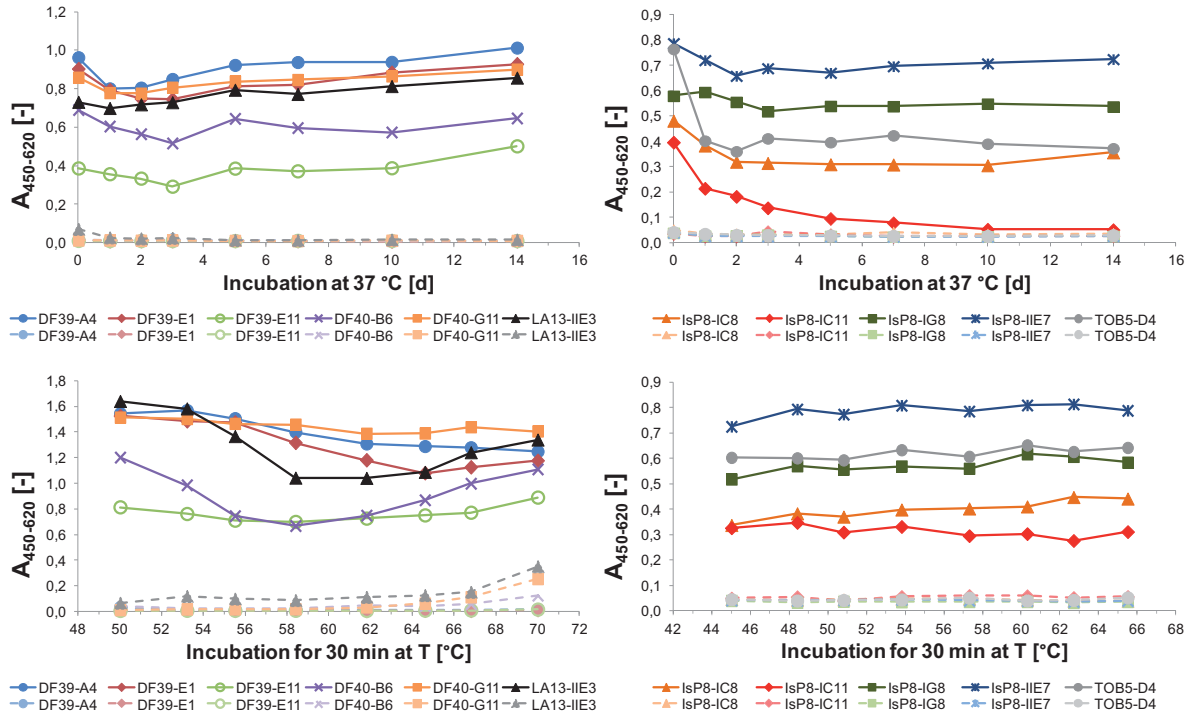

*Fig. 10: Stability assay of mutated LA13-IIE3- (**left**) and TOB5-D4 candidates (**right**). (**Top**) Storage stability assay: Incubation for 0, 1, 2, 3, 5, 7, 10 and 14 days at 37 °C; (**bottom**) Heat stability assay: Incubation in thermocycler for 30 min at 45 - 70 °C.*

Optimization of the coupling of antibodies to the gold surfaces

Following a detailed literature research four different methods of coupling of antibodies to gold surfaces have been investigated. The experiments have been performed in model reactors (gold coated wells of a polypropylene micro titer plate) [*Al-Halabi, 2008*] as well as directly on the QCM gold electrode [*Michalzik, 2009*]. In the model reactor the immobilized antibodies have been detected enzymatically. Conclusions concerning the concentration of the coupled antibodies have been drawn from absorption measurements at a wavelength of 450 nm. **Fig. 11** shows the efficiency of the different coupling methods [*Al-Halabi, 2008; Michalzik, 2009*].

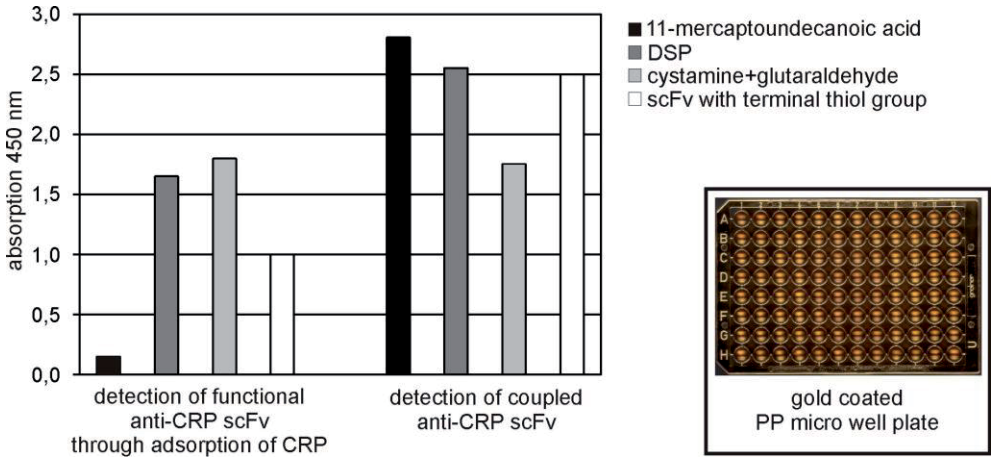

*Fig. 11: left: Efficiency of different coupling methods for the immobilization of antibody fragments on gold surfaces [*Al-Halabi 2008, Michalzik 2009*]; right: gold coated polypropylene micro well plate.*

In **Tab. 1**, the QCM frequency shifts for the different coupling methods are summarized. The largest frequency shift and thus the optimum adsorption of antibody fragments have been measured for the use of cystamine and glutaraldehyde.

However, when using 11-mercaptoundecanoic acid, better results were obtained for the subsequent adsorption of CRP. The frequency shifts in case of application of antibody fragments with an additional terminal thiol group turned out to be smaller compared to the first two methods. No adsorption of scFv fragments and therefore no adsorption of CRP could be detected for DSP layers [*Michalzik, 2009*]. The measurement results exhibit large standard deviations. This is mainly due to different concentrations of the antibody fragment solutions. Furthermore, small air bubbles occurred during the measurements due to the temperature rise of the fluid within the tubes. These bubbles influence the pressure acting on one side of the sensor and can have effects on the resonance frequency and the standard deviation. Repeated measurements of the adsorption of CRP using the same sensor exhibited considerably smaller deviation. From this it can be concluded that each sensor should be calibrated using a CRP solution of known concentration before measurement [*Michalzik, 2009.*]

*Tab. 1: Test of different coupling methods for the immobilization of antibody fragments on the gold electrodes of QCMs through measurement of the frequency shift due to adsorption of scFv fragments and subsequent adsorption of CRP [*Michalzik, 2009*].*

cystamine + glutaraldehyde		DSP		11-mercapto-undecanoic acid		scFv with terminal thiol group	
scFv fragment	CRP	scFv fragment	CRP	scFv fragment	CRP	scFv fragment	CRP
-389 Hz ± 130 Hz	-175 Hz ± 53 Hz	0 Hz	0 Hz	-311 Hz ± 156 Hz	-242 Hz ± 36 Hz	-162 Hz ± 48 Hz	-110 Hz ± 20 Hz

On the contrary, the experiments performed in the model reactor showed a coupling of antibody fragments when using DSP layers. This illustrates that the coupling behavior in the stationary state can be different from that in through flow. In addition, it has to be

recognized that the QCM is an oscillating system which may influence molecules of the order of proteins [*Michalzik, 2009*].

Development of an automated measurement protocol

In order to automatize the measuring procedure a LabView® program has been developed. After entering the relevant parameters, for example the process steps order and the number of repetitions, the measurement procedure runs automatically. After a frequency change has been detected the following step will be delayed until a stable frequency is achieved again. The current step, the current switching status of the valves as well as the developing of the resonance frequency are indicated. Also the frequency shift due to adsorption of CRP is displayed.

QCM based CRP detection using different antibody fragments and formats

After characterizing their basic biochemical properties, several CRP specific antibody fragments and formats were generated, produced and the best candidates were selected to be used for QCM based CRP measurements (**Tab. 2**).

Tab. 2: QCM based detection of CRP using different CRP specific antibody fragments.

Antigen	Antibody fragment	Antibody fragment coupleable	# of possible Measurements	Measurable Antigen Concentration [mg/mL]
CRP	DF39-E1-scFv	+	7 / 10*	0,25 – 1,0
	DF39-E1-scFv-Fc	+	-	-
	DF40-G11-scFv	+	5	0,5 – 1,0
	IsP8-IIE7-scFv	+	13	0,025 – 1,0
	IsP26-F11-scFv	-	-	-
	IsP26-G1-scFv	-	-	-
	IsP29-H1-scFv	-	-	-
	LA13-IIE3-scFv	+	14 / 50*	0,25 – 1,0
	LA13-IIE3-scFv-Fc	+	-	-
	TOB5-D4-scFv	+	20	0,05 – 1,0
	TOB5-D4-scFv	+	>100	0,025 – 1,0
	TOB5-D4-scFv-Fc	+	14*	0,1 – 1,0
	4C28-C6-IgG2a	-	-	-
	4C28-CRP36-IgG2a	+	-	-
Lysozyme	D1.3-scFv	+	>42	0,5 – 10
BSA	HSA-11-IgG2a	+	>11*	5,0 – 50

CRP concentration dependent detection could be demonstrated for several recombinant antibodies, e.g. LA13-IIE3 (**Fig. 12**, A) and its derivatives DF39-E1 (Fig. 12, B) and DF40-G11. The best results (sensitivity and possible number of CRP measurements) could be achieved using TOB5-D4 scFv (Fig. 12, C and D) and the the corresponding scFv-Fc fusion (Tab. 2). Significantly, when using two different commercially available CRP specific IgGs, no CRP detection could be shown. Baseline drift could be compensated by careful data analysis.

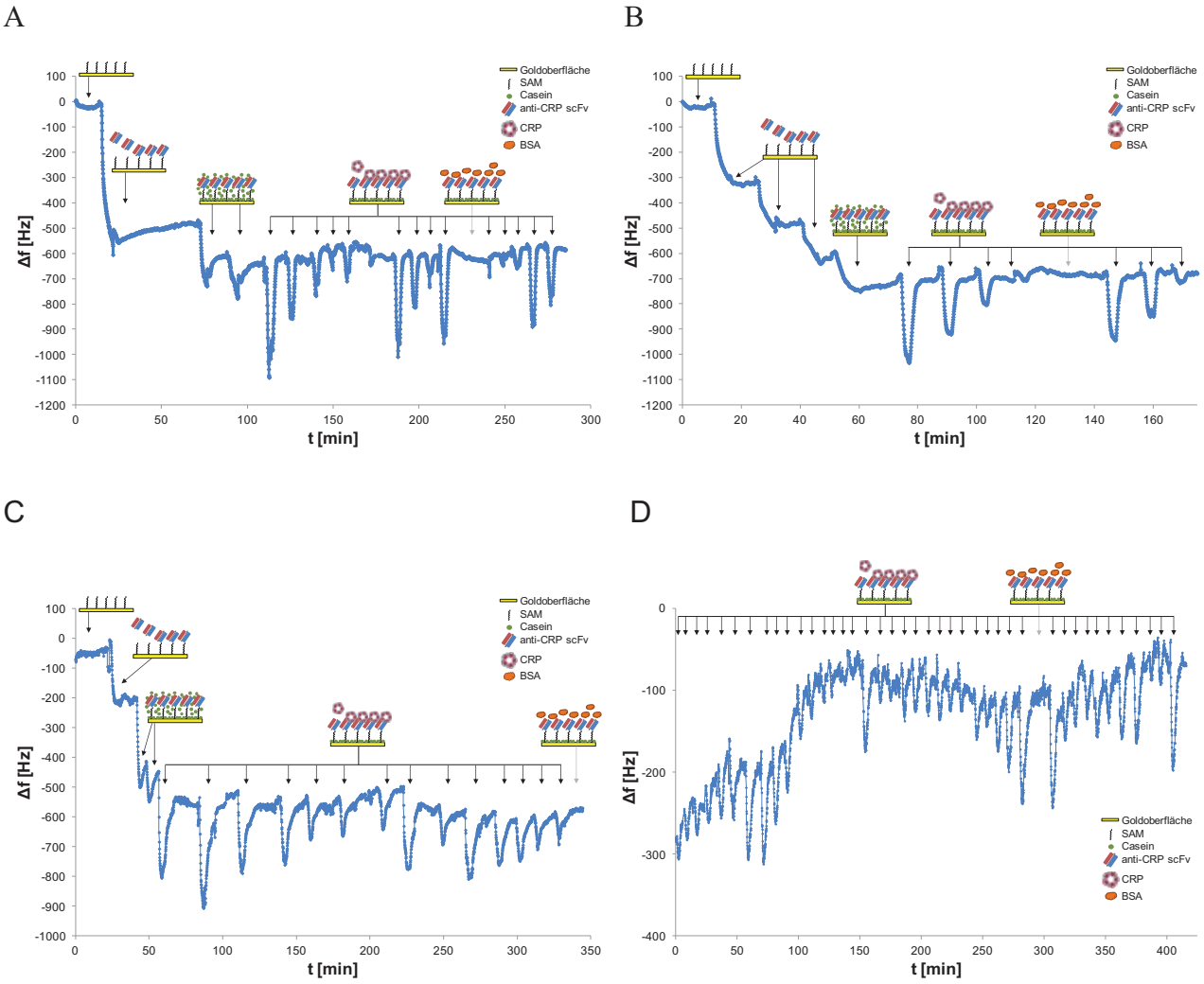

Fig. 12: Multiple concentration dependent CRP specific measurements with QCM using different antibody fragments (A) LA13-IIE3, (B) DF39-E1, (C & D) TOB5-D4. After coupling of the recombinant antibody onto the sensor chip and blocking with caseinate, different concentrations of CRP were applied and the respective frequency drop was measured. (D) multiple CRP detections (~40) 14 days after coupling of TOB5-D4 scFv.

For all used antibody fragments a linear relation between frequency drop and concentration of CRP could be shown (**Fig. 13**).

Most significantly, one recombinant antibody allowed more than 100 sequential measurements without unacceptable loss of sensitivity, thus providing a very useful feature on the way to an economically viable point of care device.

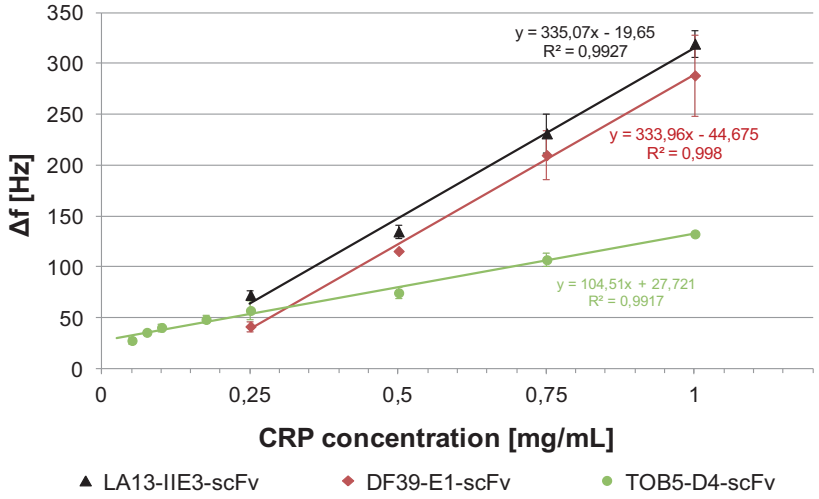

Fig. 13: Correlation of frequency drop with CRP concentration for different scFv fragments. Data assembled from different measurements.

Measurements in blood serum

CRP measurements were also tried with spiked fetal calf serum (FCS) as a surrogate for human blood serum. A correlation as shown above for the measurements in buffer could not be established. To test whether this is a general problem of the gold chip system, another antigen / antibody combination was used.

After coupling of recombinant antibody scFv D1.3 which recognizes lysozyme several sequential concentration dependent QCM measurements in serum could be performed (**Fig. 14**, B). Additionally, lysozyme specific detection using FCS instead of PBS as running buffer could also be shown (Fig. 14, B).

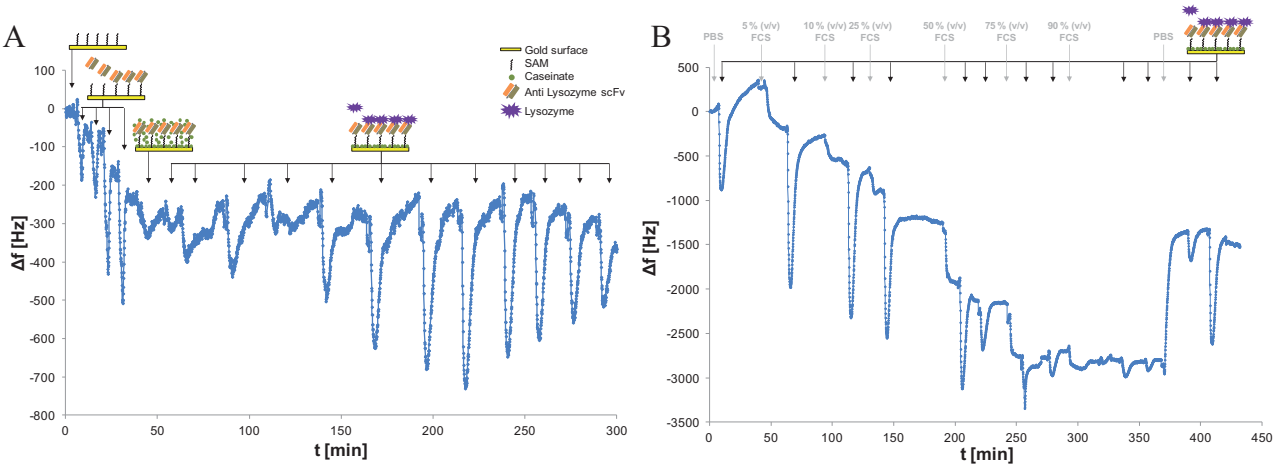

Fig. 14: Multiple concentration dependent lysozyme specific measurements with QCM using D1.3 scFv in buffer (A) and serum (FCS) (B).

The results demonstrate that the QCM system is compatible to measurements in serum, but further work has to be devoted to develop the biochemistry for CRP. A possible explanation for the observed effect would be a cross reactivity of the antibodies with cow-CRP.

Verification of the complete lab-on-chip system

The operational capability of the complete microfluidic system including the valve system and the automated measuring protocol has been tested using colored fluids. But there was not enough time for the final integration of the complete system with the biochemically optimized antibodies.

3.2.1.3 References to other works and collaborations in the SFB

CRP antibodies generated within this project were also already tested for their use in commercial diagnostic assays in cooperation with the Hong Kong University of Technology (HKUST). It became evident that the antibodies may need optimization of parameters which are different to those required for their application on the QCM chip – in particular in respect of their off-rate – but were shown to already compare well to the best available commercial antibody for the diagnosis of CRP.

3.2.1.4 Comparison with research outside the SFB

QCMs are widely used in the field of biosensors. A recent survey is given in [*Becker et al., 2011*]. Parallel to the present work, Kim et al. (*2009*) investigated the application of QCM to the detection of CRP as a cardiovascular biomarker. This application needs a much lower limit of detection as the use of CRP as a marker for inflammation. As capture molecules these authors used monoclonal anti-CRP antibodies. They were able to improve the detection limit of their system down to 0.1 pM by introducing streptavidin-coated gold nanoparticles during antibody-antigen complex formation [*Kim et al., 2010*]. In addition, CRP microsensors based on different measuring principles, for example Surface Plasmon Resonance, ELISA, and the use of magnetic nanoparticles as a label, have been explored (see section 3.2.1.1).

There are several methods for the separation of blood cells in microfluidic systems. Unfortunately, many authors do not give concrete hematocrit values of their samples, so that comparison is difficult. Nevertheless, an interesting review is given in Mukherjee et al. (*2009*). In ultrasonic micro flow-through cells the separation is based on the effect of a standing wave in the microfluidic channel. This principle has been scaled down to the microscale mainly by the group of Prof. Laurell, Lund, Sweden [*Pet, 2007*]. Several authors describe the use of filters [*Bercich et al., 2011; Nabatiyan et al., 2011; Sakamoto et al., 2010*]. However, realization of a continuous separation as well as cleaning of the filters between two samples proves to be particularly problematic. Centrifugal forces have also been used for blood separation. The centrifugal forces can be generated, for example, by use of curved microchannels [*Geng et al., 2010; Carlo, 2009; Russom et al. 2009*]. Separation systems based on the Zweifach-Fung effect are rarely found in the literature. One recent example is the system described by [*Kersaudy-Kerhoas et al., 2010*], who placed daughter channels alongside a main microchannel such that cells and plasma could be collected separately.

The results obtained in this study represent to our knowledge the first demonstration of an antibody based CRP assay which could be repeatedly run for more than 100 times using the same antibody-based detection chip in a flow through setup, thus being favorable for a point of care setup since it allows both quick measurement and calibration and promises significant economic advantages over single-use state of the art ELISA.

3.2.1.5 Literature

Aizawa, H.; Gokita, Y.; Park, J.-W.; Yoshimi, Y.; Kurosawa, S. (2006) Antibody Immobilization on Functional Monolayers Using a Quartz Crystal Microbalance. *IEEE Sensors Journal* 6 1052-1056

Aizawa, H.; Kurosawa, S.; Ogawa, K.; Yoshimoto, M.; Miyake, J.; Tanaka, H. (2001) Conventional diagnosis of C-reactive protein in serum using latex piezoelectric immunoassay. *Sensors and Actuators* B 76, 173-176

Ayala, V. C.; Michalzik, M.; Harling, S.; Menzel, H.; Guarnieri, F. A.; Büttgenbach, S. (2007) Design, Construction and Testing of a Monolithic pH-Sensitive Hydrogel-Valve for Biochemical and Medical Application. *Journal of Physics: Conference Series* 90, 012025

Becker, B.; Cooper, M. A. (2011) A survey of the 2006-2009 quartz crystal microbalance biosensor literature. *Journal of Molecular Recognition* 24, 754–787

Bercich, R.; Bernhard, J.; Larson, K.; Lindsey, J. (2011) Hand-held plasma isolation device for point-of-care testing. *IEEE Transactions on Biomedical Engineering* 58, 759–762

Bradbury, A., Sidhu, S., Dübel, S. & McCafferty, J. (2011) Beyond natural antibodies: the power of in vitro display technologies. *Nature Biotechnol. 29,* 245-254

Carlo, D. Di; Irimia, D.; Tompkins, R. G.; Toner, M. (2007) Continuous inertial focusing, ordering, and separation of particles in microchannels. *Proc. of the National Academy of Sciences of the United States of America* 104, 18892–18897

Carlo, D. Di (2009) Inertial microfluidics. *Lab on a Chip* 9, 3038–3046

Colwill, K.; Renewable Protein Binder Working Group & Gräslund, S. (2011) A roadmap to generate renewable protein binders to the human proteome. *Nature Meth.* 8, 551–558

Dübel, S.; Taussig, M.J.; Stoevesandt, O.; Hust, M. (2010) Generating antibodies to the complete human proteome. *Trends Biotec.* 28,333-339

Geng, Z.; Xu, Z.; Wang, W.; Su, W.; Li, Z. (2010) Separation of blood on a chip utilizing spiral micorchannel with fence and cofferdam as filtration structures. *Proc. 10th IEEE International Conference on Solid-State and Integrated Circuit Technology*, Shanghai, 1474–1476

Hosokawa, K.; Omata, M.; Sato, K.; Maeda, M. (2006) Power-free sequential injection for microchip immunoassay toward point-of-care testing. *Lab on a Chip* 6, 236-241

Hu, W. P.; Hsu H.-Y.; Chiou, A.; Tseng, K. Y.; Lin, H.-Y.; Chang, G. L.; Chen S.-J. (2006) Immunodetection of pentamer and modified C-reactive protein using surface Plasmon resonance biosensing. *Biosensors and Bioelectronics* 21, 1631-1637

Kersaudy-Kerhoas, M.; Dhariwal, R.; Desmulliez, M.; Jouvet, L. (2010) Hydrodynamic blood plasma separation in microfluidic channels. *Microfluidics and Nanofluidics* 8, 105–114

Kim, N.; Kim, D.-K.; Cho, Y.-J. (2009) Development of indirect-competitive quartz crystal microbalance immunosensor for C-reactive protein. *Sensors and Actuators B: Chemica* 143, 444–448

Kim, N.; Kim, D. K.; Cho, Y. J. (2010) Gold nanoparticle-based signal augmentation of quartz crystal microbalance immunosensor measuring C-reactive protein. *Current Applied Physics* 10, 1227–1230

Kurosawa, S.; Aizawa, H.; Tozuka, M.; Nakamura, M.; Park, J.-W. (2003) Immunosenors using a quartz crystal microbalance. *Measurement Science and Technology* 14, 1882-1887

Kurosawa, S.; Nakamura, M.; Park, J.-W.; Aizawa, H.; Yamada, K.; Hirata, M. (2004) Evaluation of a high-affinity QCM immunosensor using antibody fragmentation and 2-methacryloyloxyethyl phosphorylcholine (MPC) polymer. *Biosensors and Bioelectronics* 20, 1134-1139

Lee, H. J.; Yoon, K. H.; Hwang, K. S.; Park, J.; Ahn, S.; Kim, T. S. (2004) Label free novel electrical detection using micromachined PZT monolithic thin film cantilever for the detection of C-reactive protein. *Biosensors and Bioelectronics* 20, 269-275

Meyer, M. H. F.; Hartmann, M.; Keusgen, M. (2006) SPR-based immunosensor for the CRP detection-A new method to detect a well known protein. *Biosensors and Bioelectronics* 21, 1987-1990

Meyer, M. H. F.; Hartmann, M.; Krause H.-J.; Blankenstein, G.; Mueller-Chorus, B.; Oster, J.; Miethe, P.; Keusgen, H. (2007) CRP determination based on a novel magnetic biosensor. *Biosensors and Bioelectronics* 22, 973-979

Mukherjee, S.; Kang, T. G.; Chen, Y.; Kim, S. (2009) Plasma separation from blood: The lab-on-a-chip approach. *Critical Reviews in Biomedical Engineering* 37, 517–529

Nabatiyan, A.; Parpia, Z. A.; Elghanian, R.; Kelso, D. M. (2011) Membrane-based plasma collection device for point-of-care diagnosis of HIV. *Journal of Virological Methods* 173, 37–42

Petersson, F. (2007) On acoustic particle and cell manipulation in microfluidic systems. Dissertation, Lund University; Tryckeriet i E-huset, Lund, Schweden, ISBN: 978-91-628-7144-4

Sakamoto, H.; Hatsuda, R.; Miyamura, K.; Sugiyama, S. (2010) Design and fabrication of blood plasma separation PMMA chip using capillary phenomenon. *Proc. 21st Annual Int. Symposium on Micro-Nano Mechatronics and Human Science: Micro Nano Scale Syst. Rob. Mechatronics Syst.,* Nagoya, 35–40

Shen, Z.; Yan, H.; Parl, F. F.; Mernaugh, R. L.; Zeng, X. (2007) Recombinant antibody piezoimmunosensors for the detection of cytochrome P450 1B1. *Analytical Chemistry* 79,1283-1289

Shen, Z.; Mernaugh, R. L.; Yan, H.; Yu, L.; Zhang, Y.; Zeng, X. (2005) Engineered recombinant scFv antibody for Immunosensors. *Analytical Chemistry* 77, 6834-6842

Thie, H.; Toleikis, L.; Li, J.; von Wasielewski, R.; Bastert, G.; Schirrmann, T.; Esteves, I. T.; Behrens, C. K.; Fournes, B.; Fournier, N.; de Romeuf, C.; Hust, M.; Dübel, S. (2011) Rise and fall of an anti-MUC1 specific antibody. *PLoS ONE* 6, e15921; doi:10.1371/journal.pone.0015921

3.2.2 Project relevant own publications

a) Works that have appeared in publications of a scientific quality assurance at the time of application or final adoption

Balck, A.; Michalzik, M.; Al-Halabi, L.; Dübel, S.; Büttgenbach. S. (2011) Design and Fabrication of a Lab-on-a-chip for Point-of-care Diagnostics. *Sensors & Transducers Journal* 127, 102-111

Büttgenbach, S.; Balck, A.; Demming, S.; Lesche, C.; Michalzik, M.; Al-Halhouli A.T. (2009) Development of on Chip Devices for Life Science Applications. *International Journal of Engineering* 3, 148-158

Demming, S.; Balck, A.; Emeis, R.; Al-Halhouli, A. T.; Büttgenbach. S. (2009) PDMS Micro Components for Separation of Biomass in Lab-on-a- Chip Applications. *Proc. Mikrosystemtechnik Kongress* 2009, Berlin, 513-516

Michalzik, M.; Balck, A.; Ayala, C.; Lucas, N.; Demming, S.; Phataralaoha, A.; Büttgenbach, S. (2008) A Hydrogel-Actuated Microvalve for Medical and Biochemical Sensing. *Proc. Actuator 08*, Bremen, ISBN 3-933339-10-3, 803-806

b) Other publications

Al-Halabi, L. (2008) Rekombinante Antikörper für "Lab-on-chip". Dissertation, Technische Universität Braunschweig

Al-Halabi, L.; Fröde, D.; Balck, A.; Michalzik, M.; Hust, M.; Büttgenbach, S.; Dübel S. (2009) Recombinant Antibodies for Lab-on-Chip. *Proc. VAAM-Tagung* (Sonderausgabe der BIOSpektrum), Bochum, 217

Balck, A.; Michalzik, M.; Al-Halabi, L.; Dübel, S.; Büttgenbach, S. (2009) Surface modification of a quartz crystal microbalance sensor for detection of C-reactive protein. *Proc. EnFi-2009*, Hasselt, 55

Balck, A.; Al-Halhouli, A. T.; Büttgenbach S. (2009) Separation of Red Blood Cells in Y-Microchannels. *Proc. ICTEA09*, Abu Dhabi

Hust, M.; Steinwand, M.; Al-Halabi, L.; Helmsing, S.; Schirrmann, T.; Dübel, S. (2009) Improved microtitre plate production of single chain Fv fragments in *Escherichia coli*. *New Biotechnology* 25, 424-428

Michalzik M. (2009) Entwicklung eines mikrofluidischen Analysesystems zum immunologischen Proteinnachweis, Dissertation, Technische Universität Braunschweig, Berichte aus der Mikro- und Feinwerktechnik, Vol. 24, Aachen, Shaker-Verlag, ISBN 978-3-8322-8009-3

Michalzik, M.; Al-Halabi, L.; Balck, A.; Hust, M.; Dübel, S.; Büttgenbach S. (2008). A mass sensitive microfluidic immunosensor for CRP-detection using functional monolayers. *Biosensors 2008*, Shanghai, P1.72

Schirrmann, T.; Al-Halabi, L.; Dübel, S.; Hust, M. (2008) Production systems for recombinant antibodies. *Frontiers in Bioscience* 13, 4576-4594

3.3 Looking back on the promotion

The project has been funded since July 2004 in the SFB 578. It was completed on December 2010 (Büttgenbach) resp. December 2011 (Dübel).

3.3.1 Personnel in the project

	Name, acad. degree, service position	Narrower subject of the employee	Institute of University or non-university facility	Participation in the project in hours per week	Category
Basic staff					
Research associate (incl. auxiliary power)	1. S. Büttgenbach Prof. Dr. rer. nat.	Microsystem Technology	Institute for Microtechnology	3	Professorship
	2. S. Dübel Prof. Dr. rer. nat.	Biotechnology	Department of Biotechnology	3	Professorship
	3. M. Michalzik Dipl.-Chem. Dr.-Ing.	Microsystem Technology	Institute for Microtechnology	25	Ph.D. student, Post-doctoral
	4. M. Hust Dr. rer. nat.; PD	Biotechnology	Department of Biotechnology	20	Post-doctoral
Non academic staff	5. R. Kauf		Institute for Microtechnology	3	Administration secretary
	6. J. Büsing		Institute for Microtechnology	3	Technical staff
	7. B. Matheis		Institute for Microtechnology	4	Technical staff
	8. B. Thürmann		Institute for Microtechnology	4	Technical staff
	9. S. Schieseck		Institute for Microtechnology	2	Technical staff
	10. M. Wiegandt		Institute for Microtechnology	4	Technical staff
	11. D. Meier		Department of Biotechnology	4	Technical staff
Supportive staff					
Research associate (incl. auxiliary power)	12. A. Balck Dipl.-Ing.	Microsystem Technology	Institute for Microtechnology	40 resp. 20 during parental leave	PhD student
	13. D. Fröde Dipl.-Biotechnol.		Department of Biotechnology	40	
Non academic staff	14. N.N. Stud. assistants	Microsystem Technology	Institute for Microtechnology	10	Students

Responsibilities of employees (basic staff)

Position 1 - 11:

The involved employees in the subproject of the Institute for Microtechnology and the Department of Biotechnology supported the PhD-students and Post-doctorals in their micro- and biotechnological problems as well as in the development of microfluidic devices and anti-CRP antibody fragments.

Responsibilities of employees (supportive staff)

Position 12: Dipl.-Ing. A. Balck

Dipl.-Ing. Anne Balck was the responsible scientist at Institute for Microtechnology. She performed the main part of the microtechnological research and development tasks as described in section 3.2. In addition, she was responsible for the cooperation within the subproject as well as for the collaboration with other subprojects. Furthermore, she supervised the student assistants.

Position 13: Dipl.-Biotechnol. D. Fröde

Dipl.-Biotechnol. David Fröde was the responsible scientist in the Department of Biotechnology. He was responsible for the biological aspects of the project and performed the experiments including antibody fragments as described in section 3.2. In addition, he was responsible for the cooperation within the subproject as well as for the collaboration with other subprojects.

Position 14: Stud. assistants

The student assistants supported the extensive experimental work in the design, clean-room fabrication, characterization and test of microfluidic devices, as well as in the biochemical characterization of various recombinant antibodies.